Winter 2021

The Effect of Deep-Water Multibeam Mapping Activity on the Foraging Behavior of Cuvier's Beaked Whales and the Marine Acoustic Environment

Hilary Suzanne Curran Kates Varghese
University of New Hampshire

The Effect of Deep-Water Multibeam Mapping Activity on the Foraging Behavior of Cuvier's Beaked Whales and the Marine Acoustic Environment

By

Hilary Suzanne Curran Kates Varghese

Bachelor of Science in Biological Sciences with Distinction in Research,

Cornell University, 2011

Master of Science in Applied Mathematics,

Florida Gulf Coast University, 2017

DISSERTATION

Submitted to the University of New Hampshire

In Partial Fulfillment of

The Requirements for the Degree of

Doctor of Philosophy

In

Earth Science

December 2021

This dissertation was examined and approved in partial fulfillment of the requirements for the degree of Doctor of Philosophy in Earth Science by:

Jennifer Miksis-Olds, PhD

Research Professor

Dissertation Director

Thomas Lippmann, PhD

Professor

Kim Lowell, PhD

Research Scientist

Xavier Lurton, PhD

Research Scientist

Larry Mayer, PhD

Professor

On 11/23/2021

Approval signatures are on file with the University of New Hampshire Graduate School.

DEDICATION

This dissertation is dedicated to my family, who worked endlessly and lovingly to support me in this endeavor. Without each of them this dissertation would not exist. I am forever grateful to my team mate, best friend, and husband, Anuroop Jacob Varghese, who has supported me every step of the way and bolsters my well-being every single day. Without you, your love, and your teamwork, I could not have made it through. You deserve this dissertation just as much as I do. I also dedicate this dissertation to my daughter, Nila Isabelle Varghese, for unknowingly keeping me centered, focused, and giving me new purpose for completing this work-- and new purpose in general. To my mother, Susan Curran, I dedicate this to you for always being there for me in the most critical of times, and to my father, William Kates, for helping to relocate my family down the country during the middle of the final PhD countdown chaos! I should also say that if it were not for such a pair of role models, I may never have pursued a PhD in the first place. And finally to my sisters, Maggie Kates and Charlotte Bynum, for their unrelenting love and cheerleading. The completion of this dissertation --in this time and this space --would not have been possible without this family. I love you all tremendously.

ACKNOWLEDGMENTS

This dissertation would not have been possible without the support of my five incredible committee members and mentors. Thank you to my advisor, Dr. Jennifer Miksis-Olds, for helping me out of my comfort zone, pushing me intellectually, and always providing me with unexpected perspective. Thank you for giving me sea legs and the priceless oceanographic research experience. Thank you to Dr. Thomas Lippmann for your endless wisdom on time series analysis and your passion for providing your students with not just knowledge, but skills. Thank you to Dr. Kim Lowell for the extensive and enlightening conversations that moved thought exercises into published papers. Thank you to Dr. Xavier Lurton for your unique understanding of both engineering and biology, and your willingness to share that knowledge. I cannot tell you how grateful I am for your enthusiasm to discuss science with me at all hours of the day, and for your attention to detail. Thank you to Dr. Larry Mayer for asking the tough questions, and for personal, academic, and financial support throughout my time at CCOM.

The field work this dissertation was based on would not have been possible without the collaboration of many entities including Scripps Institute of Oceanography and the Office of Naval Research for ship time on the *R/V Sally Ride* and the U.S. Navy for the time on the range and use of the hydrophone data. Thank you to Nancy DiMarzio, with the U.S. Navy, for working with me over the last four years, from providing data to discussing research. Thank you also to Dr. Dave Moretti and Dr. Stephanie Watwood with the U.S. Navy, for their contributions to the work conducted at the SOAR. The field work would not have been possible without funding from both the National Science Foundation under Grant No. 1524585 and NOAA Grant NA15NOS4000200 provided to the Center for Coastal and Ocean Mapping at the University of New Hampshire. The work in this dissertation was also supported by the NOAA Grant NA15NOS4000200. This work and the presentation of it to the scientific community would not be complete without financial contributions from the Center for Acoustic Research and Education, the University of New Hampshire Graduate School, the School of Marine Science and Education, the Department of Earth Sciences, and the Acoustical Society of America.

I want to thank my colleagues and peers at the Center for Coastal and Ocean Mapping, particularly, Michael Smith and Liz Weidner for their endless hours of MATLAB mentorship, as well as their friendship. Also thank you to the CCOM administrative and IT teams. No graduate degree is complete without great friendships and experiences along the way. A special thank you to Tamer Nada, Tomer Ketter, Cris Seaton, and Aditi Tripathy. Thank you to my friends and peers at the University of New Hampshire: Kerri Sager, Dylan Wilford, Jennifer Johnson, Alex Padilla, Melissa Gloekler, Jess Steketee, Hadley Owens, Shannon Steele, Cassy Bongiovoni, Sam Reed, Annie Hartwell, Katie Kirk, Scott Loranger, Coral Moreno, and Shannon Hoy for making it a memorable experience. Thank you to the Grad to the Bones intermural teams as well. I would be remiss if I did not share my gratitude toward the faculty whose teaching left a particular impression on me: Dr. Lindsey Williams (Marine Policy), Dr. Joel Johnson (Geological Oceanography), Dr. Nathan Furey (Ichthyology), Jake Sullivan (International Policy), and Dr. Win Watson (Neurobiology). I also wish to acknowledge and pay respect to the Pennacook, Abenaki, and Wabanaki Peoples, whose traditional land the University of New Hampshire stewards today.

TABLE OF CONTENTS

LIST OF TABLES

LIST OF FIGURES

ABSTRACT

Sound can propagate great distances underwater and is an important mode for marine life to obtain information. Human activities in the ocean such as global shipping, coastal construction, gas and oil exploration, and mapping navigation routes intentionally and unintentionally emit sound into the ocean, potentially interacting with marine life. Therefore, it is essential that the effects of anthropogenic noise on marine life and the ambient marine acoustic environment be understood. Most of the work, to date, has focused on the impact of low-frequency (<1 kHz) sources such as shipping noise, which is ubiquitous in the ocean, and mid-frequency (1-10 kHz) sources such as naval sonar, to which many marine mammals have shown to be sensitive. The effect of these sources can be as salient as a mass stranding event or as benign as an animal swimming away from a source of noise with no other effect. Less work has focused on higher frequency sources (>10 kHz), including ocean-mapping sonar systems. However, most marine mammals, namely toothed whales (odontocetes), are capable of hearing mapping-sonar signals. The exposure of marine mammals to anthropogenic sound sources in the open ocean is regulated by the National Marine Fisheries Services through the Marine Mammal Protection Act (MMC 2015), the Endangered Species Act (DoI 2003), and the National Environmental Policy Act. Without a better understanding of the interaction of mapping sonar with marine mammals, the current guidelines imposed for marine mammal protection may not be protective enough, or alternatively, may be too conservative.

To gain a better understanding of the potential effect of mapping sonar and marine mammals, a scenario was examined that is possible to occur and has a high potential for a biologically meaningful interaction between mapping sonar and a sensitive marine mammal species: a 12-kHz multibeam echosounder (MBES) mapping survey and beaked whale foraging. This represents a possible interaction since 1) the relatively low frequency of the 12 kHz MBES

propagates further in the ocean environment than other mapping sonar frequencies (>30 kHz), and 2) beaked whales commonly reside in the deep-water environments where mapping with such a system would occur. Due to 1) the overlap of the frequency of this mapping system with beaked whales hearing, and 2) the life-sustaining nature of the behavior under consideration, this interaction has the potential to be biologically meaningful.

To understand the effect of deep-water multibeam mapping activity on beaked whale foraging, the temporal and spatial foraging behavior of beaked whales was assessed during two three-day ocean mapping surveys over the Southern California Antisubmarine Warfare Range hydrophone array (SOAR, featuring 89 bottom-mounted receivers over a 1800 km^2 area) utilizing a 12-kHz deep-water multibeam echosounder. Echolocation clicks recorded on the hydrophone receivers from foraging Cuvier's beaked whales were used as a proxy to assess their foraging behavior. In addition, a soundscape analysis was conducted using the acoustic data from the hydrophone array to provide context for the behavior study findings, as well as provide a more general perspective on the contribution of the deep-water mapping activity to the marine acoustic environment.

In the first phase of this work, passive acoustic monitoring data was used to identify foraging events of beaked whales. Four characteristics of the foraging events were used as proxies for foraging behavior and were subsequently compared *Before*, *During*, and *After* two deep-water ocean mapping surveys. These included 1) the number of foraging events (Group Vocal Periods, or GVPs), 2) the number of clicks per GVP, 3) GVP duration and 4) click rate per GVP. The findings of this effort revealed that only the number of GVPs increased during the deep-water mapping surveys, largely driven by the observations in just one of the survey years. This temporal analysis showed no impact on beaked whale foraging except for an increase in

foraging effort during mapping activity. In addition, this finding was a stark contrast to foraging behavior of beaked whales during MFAS activity, during which the number of foraging events decreased.

In the second phase of this work, an approach --the Global-Local-Comparison Approach (GLC)--was developed and tested that uses existing disparate spatial statistics and statistical hypothesis testing to assess whether a change in spatial behavior has occurred. Using three-prongs of assessment—global, local, and comparison—the approach provided knowledge about 1) the general distribution of observations over the entire area of study (i.e., clustered, random, dispersed), 2) identification of local hot and cold spots of activity, and 3) order-of-magnitude differences across distinct analysis periods, respectively. The approach was demonstrated on synthetic data and empirical case studies of marine mammal behavior to determine its effectiveness and limitations in assessing change in spatial observations across analysis periods. The results revealed that the approach was effective at identifying visually identifiable spatial changes, with robust statistical support.

The GLC Approach was then used to assess spatial change in beaked whale foraging behavior before, during, and after ocean mapping activity using the spatial data from the foraging events used in the first phase of work. The analysis revealed that for one of the years of study there was no obvious change in foraging behavior globally, locally, or in magnitude in response to the mapping activity, whereas a local change in beaked whale foraging effort was identified during the second mapping survey year. There were obvious differences in the spatial use of the array by foraging animals between the two years outside of the survey work, which in addition to the differences in results between the two years of study, provided little support that the local change identified was necessarily a response to the mapping activity.

The final phase of research was to characterize the contribution of one of the two ocean mapping surveys to the marine soundscape utilizing the acoustic data from the SOAR array, with a particular emphasis on understanding the contribution of the 12 kHz deep-water MBES. A comprehensive, multi-analysis approach focused on amplitude and frequency features of the changing soundscape across a nine-hydrophone subset of the array and across four analysis periods with respect to the survey activity: No Activity, Vessel Only, Vessel and MBES, and Mixed Acoustics was conducted. The analyses revealed that the contribution of the deep-water MBES to the acoustic environment was very stereotyped: contributing most substantially to the loudest sound levels in the soundscape, particularly in the 12.5 kHz decidecade band. These results aligned well with the physical characteristics of the system, i.e., nominal frequency, duty-cycle, transmission geometry, etc., suggesting these parameters can be reliably used to identify this source in subsequent soundscape studies. The assessment revealed that the MBES was the most consistent loud source throughout the survey period, but was intermittently present. There were other loud acoustic sources detected throughout the survey period, most frequently other vessels and biological activity. Several of the metrics used were weighted based on the hearing sensitivity of a mid-frequency cetacean, chosen specifically to provide context for what a Cuvier's beaked whale may have heard if in the area where the survey was conducted. The most important finding related to this aspect of the work was that the survey activity, particularly the MBES sound, did not contribute uniformly in space, time, or frequency to the SOAR soundscape of the mapping survey: it had a very local and transient effect.

In summary, at the resolution of the SOAR hydrophone array, this empirical work assessing beaked whale foraging during deep-water MBES mapping activity demonstrated:

1) no adverse changes in Cuvier's beaked whale foraging behavior, and

2) no clear response to the deep-water MBES mapping activity.

Deep-water MBES mapping activity contributed substantially to the change in sound levels at a finite scale around the survey vessel. This led to a temporally intermittent impact on the soundscape at a given location. Within these spatio-temporal bounds, deep-water MBES mapping activity has the potential to be detected by a Cuvier's beaked whale due to its spectral overlap with the frequencies of best hearing sensitivity of this species, as well as its loudness. However, no adverse effects on Cuvier's beaked whale foraging were observed here.

CHAPTER 1: INTRODUCTION AND BACKGROUND

Marine Mammal Protection Legislation

Until the 1970's, subsistence and commercial hunting of marine mammals was common practice around the world (Sahrhage and Lundbeck 1992). Many coastal communities relied on marine mammal harvesting for food, clothing, and fuel to survive (Hertz and Kapel 1986). Marine mammals that were harvested include seals, whales, manatees, walruses, and polar bears (Hertz and Kapel 1986). Initially, the impact to mammal populations due to harvesting for subsistence was small, but as technology and harvesting methods advanced, the harvesting of these animals was exploited for commercial use. Commercial exploitation included harvesting blubber, tusks, meat, oil, and skin of various mammals. The negative impact to marine mammal populations quickly became obvious as numerous stocks of marine mammals were hunted to depletion (Hertz and Kapel 1986).

Several attempts at regulating and protecting whale stocks were made in the early 1930's (Fitzmaurice, 2017), culminating in 1946 with a legal frame work set forth by the International Convention for the Regulation of Whaling and the establishment of the International Whaling Commission (ICRW 1946). Growing public concern about the environment and the effects of increased anthropogenic activities on both land and sea led to several major pieces of legislation during the 1970s, including the National Environmental Policy Act (1969), the Marine Mammal Protection Act (1972), and the Endangered Species Act (1973). The National Environmental Policy Act (NEPA) requires all groups with federally funded activities to prepare environmental assessments and impact statements detailing the potential effects of proposed activities on the environment. The Endangered Species Act was a domestic response to the Convention on International Trade in Endangered Species of Wild Fauna and Flora (CITES), which serves to protect species from extinction and recover populations that are threatened. The Marine Mammal

Protection Act mandates marine mammal management through an ecosystem-based approach. It also includes a moratorium on the take and import of all marine mammals in United States waters (MMPA 1972), with some permitted exceptions.

Take of marine mammals is defined as the harassment, hunting, capturing, collecting, or killing of marine mammals in US waters by U.S. citizens (MMPA 1972). There are some exceptions to the take of marine mammals through a permitting process of either direct or incidental take, which requires information on the specific activity, region, and potential species or stocks that will be affected. A large portion of incidental take authorizations are related to anthropogenic underwater noise activities such as sonar, gas exploration, construction, or scientific research. The effectiveness of these policies and permitting of incidental takes requires that the ocean user have a firm understanding of how the anthropogenic sounds they emit into the ocean impacts marine mammals. Thus, these acts necessitate research on marine ecosystems and species that may be vulnerable to such human activities.

Marine Anthropogenic Sound

Sound is an acoustic wave formed when an external force is applied to a medium, initially compressing and dilating it at the site of the perturbation. As the energy propagates outward from the site of disturbance the particles that make up the medium move back and forth in the direction of propagation; this is referred to as particle motion. The variation in hydrostatic pressure caused by particle motion is a pressure wave. As sound propagates through a medium, some of its intensity is lost due to spreading and absorption, where energy is converted to heat. High-frequency sound is more susceptible to absorption compared to low-frequency sound, thus the range of propagation will be different for different frequencies of sound. In an oceanic environment, lower frequency sound generally travels farther than higher frequencies. The speed

of sound is determined by the variation of oceanographic properties, such as temperature, salinity, and pressure. Changes in the sound speed of the medium can alter the path of propagation of an acoustic wave. One example of this is the SOFAR (Sound Fixing and Ranging) channel, which is a region of the water column defined by a sound speed minimum. In this channel, horizontally propagating sound refracts toward the layer of lower sound speed which allows the wave to propagate on great distances without losing energy to the seafloor or sea surface. Thus, sound can travel across ocean basins if the source level is loud enough, the frequency is low enough, and the oceanographic conditions are favorable.

Due to the complexities of underwater sound propagation, understanding and managing the effect of anthropogenic sounds on the marine environment can be challenging. Anthropogenic sounds in the ocean come from numerous sources ranging in loudness, frequency, repetition, prevalence, and location. These vary from high energy but short impulsive sounds, like pile driving and explosions, to continuous and persistent but lower energy sounds, like vessel engine noise. Most anthropogenic sounds are generated in coastal areas where human activity including recreational boating, marine development, and construction is at its highest. But there are anthropogenic activities including offshore construction, seismic exploration, and international shipping where large vessels transit across ocean basins, all of which bring sound to deeper offshore locations.

Several studies have stemmed from the desire to understand how noisy the oceans have become due to increasing anthropogenic activity in the oceans. Andrew *et al.* (2002) showed that sound pressure levels in the Pacific, measured at a California site, between 1963-1965 were 10 dB lower than during the period from 1994-2001 in the 20-80 Hz and 200-300 Hz bands. These findings were in agreement with McDonald (2006) who found a 10-12 dB increase in the

30-50 Hz band and 1-3 dB increase in the 100-300 Hz band at the same southern California site as the Andrew *et al.* (2002) study. These, as well as other early studies, led to the idea that global ocean noise levels were increasing with time. However, several other long term studies utilizing hydrophones distributed in multiple oceans (Miksis-Olds and Nichols 2016), and at multiple locations within an ocean (Andrew *et al.* 2011; Chapman and Price 2011), revealed that there is not a single global trend in ocean sound. The ambient noise floor of the Indian Ocean measured south of Diego Garcia, for example, increased during 2002-2012 in the 85-105 Hz band where sound from sources such as shipping, wind speed, and blue whale vocalizations dominate (Miksis-Olds *et al.* 2013). However, within the same decade, the ambient sound floor (5-115 Hz) in the South Atlantic decreased but at variable rates depending on the location of the hydrophones and the sound level metric under consideration (Miksis-Olds and Nichols 2016). Sirovic and Hildebrand (2016) compared sound pressure levels centered at 44 Hz south of Bermuda and found an increase of roughly 3 dB between the years of 1966 and 2013. These later studies suggest that where trends do exist, they are within a specific frequency band, a region, or a season, and have variable rates of change (Chapman and Price 2011; Miksis-Olds and Nichols 2016; Miksis-Olds *et al.* 2013; Sirovic and Hildebrand 2016).

Marine Mammals

Marine mammals include any mammals that rely solely on the ocean for at least one attribute of their existence (e.g., food, habitat). This group includes 1) amphibious animals such as walruses and pinnipeds (seals and sea lions), 2) animals that spend all of their time in water such as manatees, dugongs, and cetaceans (dolphins, porpoises, and whales), and 3) animals that rely on the ocean for food, such as polar bears and sea otters. The group of cetaceans can be

further broken down into odontocetes (toothed whales), which actively hunt for food using echolocation, and mysticetes (baleen whales), which filter feed.

Many marine animals, in particular social and sexually reproducing marine mammals, rely heavily on sound to communicate (Tyack 1986). Sound travels faster and farther in water (~1500 m/s) than it does in air (~350 m/s), making this a reliable mode of communication across large distances and in dark environments where visual communication is more difficult. Sound is used between conspecifics for foraging, attracting mates, communicating to young, or conveying other relevant information (Bradbury and Vehrencamp 1998). Environmental sound cues, like ambient sounds from a reef, are also used by animals to understand and navigate their environment (Tolimieri *et al.* 2000). Additionally, some animals produce sound to communicate information to themselves, such as echolocation signals for finding food or navigation (Madsen *et al.* 2013).

Effects of Marine Anthropogenic Sound on Marine Mammals

Research has shown there is an array of possible effects of anthropogenic noise on marine mammals. These can be broken down into two broad categories: acute and chronic effects (Williams *et al.* 2015). Acute effects range from behavioral changes, such as an abrupt change in swimming pattern away from a noise source (Miller *et al.* 2012; Sivle *et al.* 2015; Isojunno *et al.* 2016; Manzano-Roth *et al.* 2016), to physiological injuries ranging from permanent damages of the auditory system to death. Certain anthropogenic noises can also cause permanent (PTS) or temporary threshold shifts (TTS) (Kastelein *et al.* 2017), where an animal exposed to noise will temporarily or permanently be less able to detect signals at particular frequencies post-exposure. Chronic effects of anthropogenic noise pollution are harder to characterize but can include behavior changes that alter the natural history of a species, such as long-term changes in habitat

use (Richardson *et al.* 1987) that have the potential to cause population level changes. Other chronic effects may include acoustic masking, where effective acoustic communication is decreased due to raised background noise intensity at the same frequency of the acoustic signal used by an animal (Erbe *et al.* 2015), which can lead to a shift in the frequency at which an animal or population vocalizes (Parks and Clark 2007). If masking occurs for a long enough duration, it can result in the loss of critical information that may have individual or population level consequences. Chronic physiological effects can also arise due to an increase in noise-induced stress levels, which have the potential to impact life processes such as reproduction (Kellar *et al.* 2015; Rolland *et al.* 2017).

The effect that anthropogenic noise will have on marine life depends in part on the animal's ability to hear it and on the context for which the animal is exposed. An animal's physical ability to hear a sound depends on the sound being within the frequency range of hearing sensitivity of the species. This information is generally derived from either 1) behavioral response experiments where animals are trained to respond when they hear a sound, or 2) auditory evoked potential tests where the brain waves of an animal are monitored during exposure to pure-tone sounds at differing frequencies and amplitudes (Andre and Nachtigall 2007, Lucke 2008). This information is summarized into an audiogram, or a curve that shows the minimum sound intensity that an animal responded to for each frequency (Nedwell *et al.* 2004). In addition to the anatomical and hearing requirements of the animal to hear a sound, the animal must also be within an appropriate range of the sound to hear it (Richardson 1995). This range for an animal to be able to detect a sound is partly dependent on the properties of the sound (frequency, intensity, duration, direction of propagation) but will also depend on the ambient acoustic conditions at the time of exposure, or signal-to-noise ratio. Within the range of

detection, auditory injury is likely to occur at only very close distances, while behavioral affects may begin anywhere from the source out to the range of detection. The severity of the effect can also vary based on factors specific to the marine mammal, such as its previous exposures to noise, the biological significance of the noise to the animal (Tyack *et al.* 2011), the context of its exposure (e.g., foraging, mating, traveling, etc.), or its life stage (e.g., mother, calf).

The significant increase in our level of understanding about the acute effects of anthropogenic noise on marine life over the last several decades has led to the development of noise exposure criteria to regulate damaging sounds that can cause injury, PTS, and TTS. As such, the research priority has shifted to understanding the chronic effects of anthropogenic noise exposure, including questions related to behavioral effects, population level consequences, and how to predict their likelihood of occurring (Southall *et al.* 2007, Houser *et al.* 2013, Henderson *et al.* 2014, Southall *et al.* 2021).

Sonar and Multibeam Echosounders

There have been a number of government and private research programs created to study the impact of low (LFAS; <1 kHz) and mid-frequency (MFAS; 1-10 kHz) active sonar used in naval operations on marine mammals (Jarvis *et al.* 2014; Miller 2014; Harris and Thomas 2015), due to numerous marine mammal stranding events linked to these noisy activities (Hohn *et al.* 2006, Filadelfo *et al.* 2009, Ketten 2014). In comparison, little is known about how higher frequency (>10 kHz) active sonar, such as ocean-mapping multibeam sonar, impacts marine mammals despite the ability of some marine mammals to hear and communicate at these frequencies (Ketten 1998).

There are key differences between naval sonar and multibeam echosounders. Naval sonar was developed to detect submarines during times of warfare (D'Amico and Pittenger

2009). As a result, the ensonified area is broad, propagates horizontally, and due to the low frequencies (1-10 kHz) extends great distances (Figure 1.1). Multibeam echosounders (MBES) were developed to resolve fine-scale features in the ocean for seafloor mapping and natural resource exploration. The geometry of a multibeam echosounder's ensonified area is vertical below the vessel, with a wide across-track swath, but narrow along-track swath (Figure 1.1). The source levels of these systems are comparable but the radiated energy is on the order of 1000 times higher in MFAS due to longer pulse lengths and shorter duty cycles (Table 1.1). The exact ensonified area for both systems is a function of the water depth and frequency of the signal.

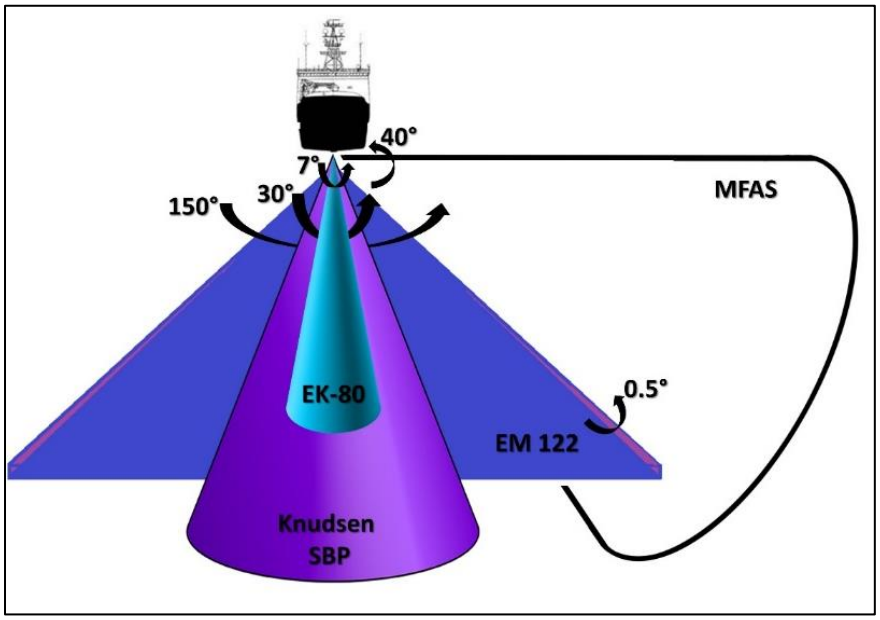

Figure 1.1. Simplified transmission beam geometries of the active acoustic systems used in the 2017 mapping survey, in addition to MFAS for comparison. Note the schematic depicts relative differences in length and width, where the length of the beam for each indicates, relative to one another, how far the signal could be detected based on the nominal frequency of the system. Although simplified here, the EM 122 can also be operated using two transmission swaths like the one shown here, i.e., *Dual-swath* mode, and/or with multiple transmission sectors in a swath.

Table 1.1. Comparison of mid-frequency active sonar (MFAS) signals used in naval operations to multibeam echosounder signals used for ocean mapping. The information in this table is generalized and may not be accurate for every system under every possible operational mode.

	MFAS	**MBES**
System example	AN/SQS-53	EM 122
Frequency range (kHz)	3-4	11-13
Maximum source level (dB re 1 µPa @ 1m)	235-239	241
Propagation loss rate due to absorption (dB/km)	0.15-0.2	1
Signal duration (s)	1	0.002-0.02 CW <0.05 FM
Time between pings (s)	20-30 (Subject to target range)	20 (Subject to water depth)
Signal content	Long pulses either CW and/or FM with broad bandwidth (ratio of about 0.3 to the center frequency)	Short pulses either CW and/or FM with narrow bandwidth (ratio about 0.04 to the center frequency)
Duty Cycle (on the order of)	1/10	1/1000
Typical Beam Pattern (vertical x horizontal)	40° x 120-360°	1° x 150°
Beam Direction	Generally horizontal, can be tilted	Generally vertical, can be tilted

The original MBES utilized advanced beamforming techniques to generate a narrow, angularly constrained swath of sound that propagates to the seafloor. Present day systems have undergone significant technological advancement in electronic and beamforming capabilities, resulting in the development of multi-swath and multi-sector capabilities which greatly complicate the transmission pattern of these systems. With respect to a multi-swath/multi-sector system, a single ping is comprised of a train of short independent pulses with non-overlapping, narrow bandwidths. Additionally, state-of-the-art multibeam systems are dynamic and can be operated under various permutations of several operating modes: 1) single/dual swath, 2) auto-ping mode/manually-selected mode (note: this feature does not impact the sound radiation

characteristics), 3) depth-specified modes, 4) with/without motion compensation, 5) various angular swath widths, 6) gated continuous-wave (CW)/frequency-modulated (FM) pulses, among other options which can further complicate the radiation pattern (Kates Varghese *et al.* 2019).

Most of these parameters are dictated by the need of the survey and the environment being mapped. Dual-swath coverage enables the user to obtain a higher density of pings in a fixed area, which can be important for the quality of data required for a survey and/or for the survey speed. Similarly, the use of various swath widths and motion compensation capabilities allow the ocean user to adapt to rough seas, survey at a faster or slower speeds, and still maintain or ensure quality data collection. Essentially the options available with state-of-the-art multibeam allow the ocean user to adapt to dynamic conditions in a variety of ways.

As an example, the Kongsberg EM 122, a deep-water MBES operates using either single or dual swath with 4-8 sectors per swath. The EM 122 can be manually or automatically changed to different operational modes as the depth of the water changes, which includes higher source levels, longer pulse lengths, more sectors, and frequency-modulated pulses at deeper depths. Pulse lengths may vary from 3 ms (CW) in the shallowest depths (i.e., <450 m water) to 100 ms (FM) in very deep water (i.e., up to 11,000 m). A typical deep-water survey (i.e., Deep mode is defined as 1000-2600 m depth) operates with 8 sectors ranging from 8-15 ms pulses and inter-ping interval of about 5-10 seconds.

In addition to military sonars and multibeam echosounders, there are other active acoustic sources commonly used and/or associated with ocean mapping and geophysical survey work (Masson 2003, Mayer 2006). These include systems designed specifically to identify acoustic scattering in the water column (e.g., scientific echosounders), to systems that are designed for

penetrating the seafloor (e.g., sub-bottom profilers), among others. Often classified together as scientific or geophysical sonar, there are differences between these active acoustic sources that certainly relate to the potential effects they may have on the marine acoustic environment and the life that inhabits it. Due to the rapid innovation in this field and the abundant and diverse systems, only generalities of the systems relevant to the work in this dissertation are discussed here, which include a scientific echosounder (e.g., Simrad EK-80), multibeam echosounders (MBES e.g., Kongsberg EM 122 and EM 712), and a sub-bottom profiler (SBP e.g., Knudsen 3260).

The main differences pertinent to the context of this work are their source levels, frequency range, pulse characteristics, and radiation patterns. Source levels are generally highest for MBES (~230-242 dB re 1 µPa @1 m), followed by the SBP (~199-208 dB re 1 µPa @1 m, Crocker *et al.* 2019) and the scientific echosounder (~188-226 dB re 1 µPa @1 m) (Crocker *et al.* 2019, Schuster *et al.* 2020). Frequencies for these systems also vary where SBP tend to be the lowest frequency (2 to 10 kHz) due to their need to penetrate the seafloor, followed by MBES and scientific echosounders (12 to 200 kHz and above). The frequency used for any one of these sources will be dictated by the purpose of the survey and the ocean depth, where a deeper depth requires a lower frequency. For identifying scattering in the water column, smaller targets require higher frequencies to resolve well. Pulse characteristics will also vary based on the purpose of the survey and ocean environment, but pulse durations tend to be longest for SBP. Although MBES tend to have the broadest swath, ~150° across-track, they are narrow along-track, 0.5-2°, whereas the other aforementioned sources have a conical radiation pattern with typical narrow apertures of 7° (scientific echosounder e.g., EK-80) to 30° (e.g., Knudsen SBP)

(Figure 1.1). All of these factors directly influence how the signal manifests in the marine acoustic environment.

Beaked Whales

Ziphiidae, or beaked whales, are pelagic deep-diving odontocetes, found in all oceans with the most studied populations in Hawaii, Southern California, and the Mediterranean (Baird *et al.* 2006, Aguilar Soto *et al. 2006,* DeRuiter *et al.* 2013). Beaked whales are the deepest and longest diving marine mammals known, diving to depths up to 3000 meters for over an hour at a time (Schorr *et al.* 2014). Beaked whales are commonly found in deep water habitats with complex topography, indicating dynamic oceanographic conditions such as strong currents, upwelling, and biological productivity (MacLeod *et al.* 2005, Mead 2009). Beaked whales prefer deep water habitats for foraging (MacLeod and Zuur 2005, Mead 2009). These animals show high site fidelity, as they are repeatedly sighted in the same area throughout the year (McSweeney *et al.* 2007, Aguilar Soto *et al.* 2006, DeRuiter *et al.* 2013).

Due to their deep-diving abilities, beaked whales have been difficult to study, as they do not spend much time at the surface, therefore little is known about their life history and behavior. A distinctive feature of beaked whales are the tusks on males of this family and on both sexes in the genus *Berardius*. Males are known to interact with other males in aggressive encounters that leave them covered with scars. Little is known about reproduction, but it is thought that it takes a decade to reach maturity. A single offspring is born at a time and likely remains with its mother for up to a year or more. Among the 22 species of beaked whales, two social structures exist: small groups of less than 10 individuals and larger groups of 5-20 individuals, with as many as 100. (Mead 2009)

Passive acoustic monitoring has been a primary method used for remotely studying the behavior of animals in the ocean that are difficult to observe directly, such as beaked whales (Zimmer 2011). Most of what is known about beaked whale behavior relates to their foraging behavior, since they are only known to emit sound while foraging. Beaked whales use echolocation to find prey, producing short, directional upsweeping clicks in frequencies ranging between 2-200 kHz, with the most energy between 20-60 kHz (Johnson *et al.* 2004). Inter-pulse intervals (ICI) last between 200-400 ms, click durations between 200-600 µs, and on-axis source levels range between 214-224 dB re 1 μPa @ 1 m (Baumann-Pickering *et al.* 2013, Baumann-Pickering *et al.* 2014, Gassmann 2015). Beaked whales forage in groups at depths greater than 200 meters (MacLeod and Zuur 2005) on prey consisting mostly of squid, fish, and occasionally crustaceans (Santos *et al.* 2001). Several studies have been conducted to determine diel variation in beaked whale foraging behavior, and have found that the exact foraging strategy (i.e., dive depth) may change from day to night (dive depth), while there is little difference in the amount of foraging that takes place between day and night (Baird *et al.* 2008, Arranz *et al.* 2011, Shearer *et al.* 2019). These studies hypothesized that the differences in diel foraging are directly related to region-specific prey distribution and behavior in the water column.

Few studies have assessed the hearing sensitivity of beaked whales due to the difficulty in capturing and safely containing a beaked whale (Cook *et al.* 2006, Finneran *et al.* 2009, Pacini *et al.* 2011). An auditory evoked potential (AEP) hearing measurement test on a live-stranded Blainville's beaked whale (*Mesoplodon densirostris*) revealed they can detect sounds between 5-80 kHz, with the strongest evoked potentials at modulation rates between 600-1200 Hz, though higher frequencies and modulation rates greater than 1800 Hz were not tested (Cook *et al.* 2006). Another AEP study of a stranded Blainville's beaked whale revealed that the animal produced

evoked potentials from 5 kHz up to about 160 kHz with best hearing sensitivity between 40-50 kHz (Pacini *et al.* 2011). Other studies have suggested that toothed whales, in general, have a broad range of hearing sensitivity, from about 10-120 kHz (Finneran *et al.* 2009, Pacini *et al.* 2011).

Soundscapes and Sound Source Characterization

The concept of a soundscape is used in a range of fields, including music, psychology, ecology, health care, etc. (Krause 2008), and in a variety of applications, such as environmental noise and quality of life in hospitals (Busch-Vishniac and Rhyerd 2019) to mitigating noise pollution in national parks (Olson and Reid 2013). Soundscape studies are often implemented in order to gain a better understanding of the acoustic environment from the perception of a sound receiver. Soundscapes are often thought of in the context of human perception but more recently have been applied with other animals in mind (Lindseth and Lobel 2018, Van Opzeeland *et al.* 2018). Although understanding the perception of sounds by other animals is arguably impossible, soundscape studies can provide insight about characteristics of an acoustic environment that may be relevant to a non-human receiver.

In the marine environment, many marine animals rely on acoustic cues as reliable sources of information, whether it be for communication with conspecifics (Sorensen *et al.* 2018), finding food (Johnson *et al.* 2004), finding suitable habitat (Lillis *et al.* 2014), among other reasons. Aside from the relatively greater distances that sound propagates underwater compared to on land, the geographical habitat of many marine animals coincides with areas of extensive anthropogenic and noise-generating activity. Accordingly, the likelihood that anthropogenic noise will interact with marine life is different compared with terrestrial environments and inherently more difficult to evaluate. Monitoring the marine acoustic environment and assessing

any changes is an important aspect of understanding an ecosystem's health as well as the health of the marine life within it.

In recognizing the importance of the marine acoustic environment on the ecology of marine mammals, an entire field of study has arisen to understand the information the acoustics represent (Lin and Tsao 2018), as well as to develop legislation to manage anthropogenic input to an acoustic environment (Van Opzeeland and Boebel 2018). Studies of the acoustic environment have been used to assess ecosystem health (Parks *et al.* 2014), identify and characterize acoustic sources present in an environment (Hatch *et al.* 2008), assess the effect of acute and chronic changes in the acoustic environment on acoustically active marine life (Wall Bell *et al.* 2016; Van Opzeeland and Boebel 2018), and monitor long-term changes in an environment (Andrew *et al.* 2011; Chapman *et al.* 2011; Miksis-Olds *et al.* 2013; Miksis-Olds and Nichols 2016).

Due to the infancy of soundscape ecology in marine studies, agreement on a robust, cohesive terminology, and set of comprehensive metrics to describe an acoustic environment has been a challenge (Erbe *et al.* 2016). For example, some studies take a more qualitative approach: identifying acoustic sources in long time series and characterizing them into anthrophony (human-generated), geophony (geology-related) and biophony (biology-related) categories (Putland *et al.* 2017a). Other studies take a quantitative approach: assessing overall sound levels across multiple sites (Putland, *et al.* 2017b) comparing trends in sound levels across seasons (Miksis-Olds *et al.* 2013), years, or decades (Andrews *et al* 2011; Miksis-Olds and Nichols 2016; Sirovic and Hildebrand 2016). Alternatively, marine researchers use adapted terrestrial ecoacoustic metrics as proxies for biodiversity, habitat complexity and habitat health in marine environments of interest (Parks *et al.* 2014; Harris *et al.* 2015). Aside from research-specific

reasons for such variable methodology, specific metrics at specific resolutions may be more valuable than others. There are a few common threads however, largely that soundscape metrics 1) tend to provide some information about space, time, or both, and 2) they are generally related to sound pressure amplitude and/or frequency.

With varying degrees of funding and resources, it can be challenging to acquire software and hardware that can meet a set of universal standards (e.g., minimum sample length or rate). Nonetheless, researchers and regulators recognize the need for an international set of standards to be able to compare and synthesize acoustic data across projects and environments (e.g., effect of noise on marine life, ecosystem health) (Southall *et al.* 2009, Boyd *et al.* 2011). An example of this recognition is that the International Organization for Standardization has now defined an underwater soundscape as, "the characterization of the ambient sound in terms of its spatial, temporal and frequency attributes, and the types of sources contributing to the sound field," and has defined numerous important terms frequently used in soundscape studies (ISO 2017). Additionally, the International Quiet Ocean Experiment (IQOE) successfully gained the approval of the United Nations project, Global Ocean Observing System, to add ocean sound to its Essential Ocean Variables, meaning it will be a sanctioned measurement for this global project (Jones, 2019).

The concept of a "soundscape," from the perception of a human (Schafer 1969; Yost 2015) has been adapted to other animals in terrestrial studies (Pijanowski *et al.* 2011), and now marine mammal studies by applying frequency-specific weightings, or auditory functions, to place sound measurements in the context of specific species or functional hearing groups (Houser *et al.* 2017). Auditory weighting functions are used to emphasize the frequency-range in which a specific species, or group of species is most sensitive. The range of frequencies is

rigorously determined either by psychophysical methods and auditory evoked potentials on individuals of a species, from behavioral studies, or modeled from assumptions about a species' auditory anatomy (Houser *et al.* 2017).

The current guidelines used by regulators to predict the impact of a sound on a marine life is to classify sound sources into distinct sound types based on the signal structure of the sound at its source and then to consider the functional hearing group of the animal and apply specific sound level thresholds based on both the functional hearing group and sound type (NMFS *et al.* 2018). Sound sources are categorized as impulsive (single pulse or multiple pulse) or non-impulsive (Southall *et al.* 2007; NMFS 2016). Characterizing a sound at its source is considered to be the most conservative approach since propagation effects typically cause a sound to be less damaging with greater distance from the source. This classification has repercussions on which regulatory criteria should be used for exposure assessment. For example, impulsive sounds, are regulated at lower threshold levels for the same metric relative to non-impulsive sounds due to the fact that these sounds are more likely to cause acoustic injury to an animal than non-impulsive sounds. In the current regulatory framework, marine mammals are divided into five functional hearing groups, based on the frequencies of sound to which they are most sensitive (NMFS 2018). These groups are low-frequency cetaceans, mid-frequency cetaceans, high-frequency cetaceans, phocid pinnipeds and otariid pinnipeds (NMFS 2018). Thus, existing law and recommended guidelines (NMFS 2018) necessitate the collection of information inherent to both the exposed animal, as well as the source to be able to predict exposure. It is worth noting that the latest scientific recommendation on this topic is to divide marine mammals into six functional hearing groups, including low-frequency cetaceans, high-frequency cetaceans (previously listed as mid-frequency cetaceans), very high-frequency

cetaceans (previously listed as high-frequency cetaceans), sirenians, phocids, and other carnivores (Southall *et al.* 2019). New science continues to inform these demarcations and is used to periodically update the regulatory guidelines.

The division of sound types into impulsive and non-impulsive sounds is based specifically on the premise that an impulsive sound is more likely to be physically damaging to an animal than a non-impulsive one. This delineation results in the application of a regulatory threshold 15-20 dB lower for a non-impulsive sound than for an impulsive sound (assuming all other delineations are kept equal, i.e., –functional hearing group and acoustic injury, e.g., TTS or PTS). Even with a simplified approach for such a specific application, there are challenges. In the regulatory framework, neither impulsive nor non-impulsive is explicitly or comprehensively defined (NMFS 2018), despite this important consequence in how the sound types are regulated. Impulsive is defined as a signal with high peak sound pressure, short duration, fast rise-time, and broad frequency content, whereas a non-impulsive sound is any steady-state sound (NMFS 2018). As such, even subject–matter experts have trouble placing certain sound sources into a specific category (Southall *et al.* 2007). For example, sonar signals, fall into both categories (Southall *et al.* 2007). This is largely because of the lack of a clear definition, but also because many sound sources can be operated in dynamic ways, resulting in variable signal characteristics such as pulse lengths, duty-cycles, and signal structure. The MBES, for example, can be operated in different modes based on the purpose of its use, or environmental factors, such as the weather or water depth. Consequently, MBES signals could be classified into more than one sound type category depending on how it is operated and on the impulsiveness definition (i.e., impulsive/non-impulsive) that is applied. It is also not clear whether the current demarcation of sounds into two sound types is appropriate or accurate beyond this very specific application in

the context of acoustic damage, such as extending its use for predicting the effect of a sound on the behavior of an animal. Understanding this will require substantial research about how a sound is perceived and integrated by an animal. This is a field of research that is ripe for advancement.

Despite this, in a majority of research reports looking at behavioral impacts of anthropogenic sounds on marine mammals, the noise sources are either not well described, or are reported only based on their source level, center frequency, and/or duration (Gomez *et al.* 2016, Southall *et al.* 2021). Several sound sources used in ocean exploration entail complicated systems with many sound producing parts that have dynamic operational modes and cannot be adequately described based on a few characteristics. For one, some systems are designed to operate within a specific frequency, but due to complicated and imperfect hardware designs can result in a wide bandwidth of spectral content. For example, the spectral ramp up of a 200 kHz echo sounder to its operational frequency within a short finite time period caused significant energy to be transmitted at sub-harmonic frequencies between 90 and 130 kHz (Deng *et al.* 2014). Secondly, the environment in which these sounds are transmitted can also have a significant impact on the propagation of the sound. For example, air gun sounds in a shallow environment have a high pass filter effect from the shallow water depth, whereas in a deep-water environment the higher frequencies are lost with greater propagation distances (Hermannsen *et al.* 2015). Current regulation is based on certain standards for reporting, such as root-mean-square (rms) pressure levels for exposure criteria (NMFS 2018). However, rms pressure levels do not represent short transient sounds well, such as sonar pulses, and relies heavily on the averaging window length used in its calculation (Madsen 2005). In defining safety criteria for exposure to low-frequency active sonar, Kastelein *et al.* (2014) showed that temporal patterning,

including the inter-pulse interval, and the energy of exposure (cumulative sound exposure level) of a sound had important repercussions on the likelihood of an animal to experience a threshold shift. Accordingly, sound sources are not well captured by reporting only the source level, duration, and center frequency. It can be difficult to report the characteristics of a sound source, especially when the study arises out of opportunity. For this reason, carefully characterizing commonly used and complicated anthropogenic sound sources with a comprehensive set of metrics is required to generate a first order understanding of how such sounds can influence an acoustic environment. This information is important for propagation modeling, which is often used in environmental impact assessments required by regulators.

Scientific Landscape and Significance of Dissertation Research

In 2008, a mass stranding of melon-headed whales occurred off of Antsohihy, Madagascar in an area that had been mapped a few weeks prior by a MBES 12 kHz system (Southall *et al.* 2013). This stranding event raised concern about the potential interaction of this source with marine mammals. Lurton (2016) along with DeRuiter (2011), modeled the radiation patterns of high-frequency sonar (seafloor-mapping echosounders), concluding that the risk of direct ensonification from MBES that can lead to auditory damage is low. Although the beam geometry of a single-beam echosounder is different from a multibeam (Figure 1.1), two recent field studies have shown high-frequency single-beam echosounders have a behavioral effect on some toothed whale species. In one study, significantly fewer beaked whale echolocation clicks were detected when a single beam EK-60 scientific echosounder was active compared to inactive (Cholewiak *et al.* 2017). Reduced echolocation clicks, produced when beaked whales forage, indicated that foraging behavior changed when the echosounder was active. In a study of tagged short-finned pilot whales, the animal's heading variance increased in the presence of an active

echosounder EK-60, suggesting the animals increased their vigilance to the sound (Quick *et al.* 2017). Two controlled experiments have been performed that assessed the impact of high-frequency multibeam sonar on marine mammal behavior in captivity (Hastie *et al.* 2014, Deng *et al.* 2014). In one study, grey seals in a tank where a 200-kHz sonar was actively transmitting spent more time hauled out than in the water compared to when the MBES was inactive (Hastie *et al.* 2014). The other study assessed the potential for MBES to impact marine mammals by looking at the spectral properties of MBES pulses, revealing that sub-harmonic sounds were also generated from three commercial echosounders with center frequency around 200 kHz, in addition to the nominal frequency sounds (Kongsberg SM2000 multibeam imaging sonar, BioSonics DT-X Digital Scientific Echosounder and Imagenex 965 multibeam imaging sonar) (Deng *et al.* 2014). These sub-harmonics are well within the hearing range of several marine mammal groups and at a level high enough to be detected by marine mammals. The combination of these field and opportunistic studies show that high frequency multibeam sonar has the potential to affect marine mammal behavior.

Hearing tests from select beaked whale species (Cook *et al.* 2006, Finneran *et al.* 2009, Pacini *et al.* 2011) show that the hearing sensitivity of beaked whales (5-160 kHz) has substantial overlap with the range of high frequency sources (> 10 kHz) typically used for ocean mapping (i.e., 10-400 kHz). Beaked whales are also known to inhabit environments where deep-water (12 kHz) MBES operate with bandwidths that intersect with the audible range of the whales. In addition, beaked whales are known to be sensitive to other anthropogenic sounds. Thus, beaked whales appear to be a particularly susceptible group to disturbance from such an anthropogenic sound source.

The extent of the effect of high-frequency echosounder sound on marine mammals, including beaked whales, is not well understood. It likely depends on a multitude of factors including those intrinsic to the exposed animal or species, as well as those relating to the operation of the sonar, the physical environment, and the interactions of all of these factors. In the few opportunistic field studies (Cholewiak *et al.* 2017, Quick *et al.* 2017), the exposure level and range from the source that elicited behavioral response were not well characterized, making it challenging to use these studies to predict future responses. Furthermore, due to the variable modes and frequencies used in operation, there is no consensus on what metrics should be used to characterize ocean mapping sound sources and their contribution to the ambient soundscape, or what aspects of their operation may elicit a response by a marine mammal (Southall *et al.* 2007).

Ocean mapping is necessary in coastal areas where routine surveying is needed for accurate charting of dynamic port bathymetries and identifying navigation hazards (Chiocci *et al.* 2011, Battista and O'Brien 2015). It is also needed for geological surveying of natural resources in offshore waters and will expand into underexplored areas, such as the Arctic as the climate changes. In addition, there is a global initiative to map the world's oceans by 2030 (Mayer *et al.* 2018). Thus, these sources will continue to be used at the same, or a greater capacity than they are today, and it is imperative that we understand how they may affect vulnerable marine life, if at all. With targeted research to assess the effect of ocean-mapping sonar on marine life and the ambient marine environment, we can begin to understand how this sound source fits in to existing regulation, and/or provide insight for how existing policy should be modified to further protect marine mammals from this sound source, if necessary at all.

To date, there have been no studies explicitly examining the effect of deep-water multibeam echosounder activity on free-ranging wild marine mammals. Hence, the broad aim of this research was to contribute to this gap in understanding by providing knowledge on the effect of ocean-mapping multibeam echosounder sounds on wild free-ranging marine mammals. The specific goal of this dissertation was to assess the effect of deep-water mapping activity, utilizing MBES, on the foraging behavior of Cuvier's beaked whales and the marine acoustic environment.

Study Site and System

On January 4-7th 2017 and again January 2-6th 2019, ocean-mapping surveys were conducted in order to characterize the radiation pattern of a Kongsberg EM 122 (12 kHz) deep-water multibeam echosounder. Each survey utilized the *R/V Sally Ride* and was conducted over the Southern California Antisubmarine Warfare Range (SOAR) of the United States Navy Southern California Offshore Range (SCORE), a multi-warfare training complex off of San Clemente Island, California in the San Nicolas Basin.

SOAR contains a hydrophone array containing 177 bottom-mounted omni-directional hydrophones covering an 1800 km^2 area. The area surrounding the hydrophone range varies from ~200 m deep near San Clemente Island to ~1800 m deep at the northwest part of the range. Acoustic features, including anthropogenic and biologic sounds, at frequencies below 48 kHz produced over the range can be recorded on the hydrophone receivers.

SOAR, used year-round for naval training exercises, is also home to a highly resident population segment of Cuvier's beaked whales (Schorr *et al.* 2019). An estimate for the number of animals utilizing the range is likely more than 100 animals. In one year, 88 animals were sighted through ship-based surveys, 23 were seen over multiple years, and several have been

sighted in the area for more than 10 years (Schorr *et al.* 2019). A more recent longitudinal study looking at the eleven years between 2007 and 2018 suggests that the number of animals present in a year is around 121 (Curtis *et al.* 2020). Much of what is known about this population segment is through experiments related to MFAS use on the SOAR (Falcone *et al.* 2017, Tyack *et al.* 2011, DiMarzio *et al.* 2010). Despite observed behavioral effects of the naval activity, the animals still show high site fidelity to the area (Schorr *et al.* 2019). Since Cuvier's beaked whales are known to produce sound when they forage, the 2017 and 2019 mapping survey over the SOAR hydrophone array provided an ideal opportunity to study the effect of MBES survey activity on the foraging behavior of the beaked whales.

Dissertation Outline

In order to provide knowledge on the potential effects of deep-water MBES activity on free-ranging marine mammals, this dissertation examines the effect of two mapping surveys, utilizing deep-water MBES, on beaked whale foraging behavior and the marine acoustic environment via three distinct perspectives. Chapter 2 provides insight on the temporal foraging behavior of Cuvier's beaked whales by assessing changes in four group vocal period characteristics across distinct analysis periods related to two ocean mapping surveys. Chapter 3 describes and demonstrates a robust and comprehensive statistical approach for assessing change in marine mammal behavior spatial observations with respect to distinct analysis periods which capitalizes on the use of a large-scale passive acoustic monitoring hydrophone array. Chapter 4 is an application of the statistical spatial approach presented in Chapter 3, and provides insight on spatial foraging effort of Cuvier's beaked whales during two ocean mapping surveys. Chapter 5 is a comprehensive documentation of the amplitude and frequency, spatial and temporal changes in sound pressure levels of a deep-water ocean mapping survey, which includes the identification

of sound sources attributing to those changes and a contextualization of the changing sound pressure levels to the hearing of a mid-frequency cetacean, such as Cuvier's beaked whales. Chapter 6 summarizes the work completed in this dissertation, including a discussion of the differing effect of deep-water MBES to the effect of MFAS on beaked whale foraging.

CHAPTER 2: TEMPORAL FORAGING BEHAVIOR OF CUVIER'S BEAKED WHALES DURING A DEEP-WATER MAPPING SURVEY

Preface

This chapter was published first in *The Journal of the Acoustical Society of America* and is reproduced here with the permission of the journal. The full citation for the published work is:

Kates Varghese, H., Miksis-Olds, J., DiMarzio, N., Lowell, K., Linder, E., Mayer, L., and Moretti, D. (2020). The effect of two 12 kHz multibeam mapping surveys on the foraging behavior of Cuvier's beaked whales off of southern California. *The Journal of the Acoustical Society of America* 147(6), 3849-3858.

The article in *The Journal of the Acoustical Society of America* may be found at https://doi.org/10.1121/10.0001385.

The author of this dissertation, Hilary Kates Varghese (HKV) was the lead author on this article and was responsible for all of the analysis, interpretation, drafting and editing the manuscript. Dave Moretti (D), Nancy DiMarzio (ND), Larry Mayer (LM), Jennifer Miksis-Olds (JM-O), and HKV were involved in the coordination of the field component of this study. ND processed the acoustic data and provided the GVP data for the analysis. HKV, through guidance from KL and Ernst Linder (EL), performed the reported analyses. JM-O, KL, and LM provided guidance to HKV on the interpretation and communication of the findings of this work. All authors discussed the results and contributed to the final manuscript. The supplementary work associated with this publication is contained in Appendix 2.1 as well as at https://doi.org/10.1121/10.0001385.

Abstract

The impact of multibeam echosounder (MBES) operations on marine mammals has been less studied compared to military sonars. To contribute to the growing body of MBES knowledge, echolocation clicks of foraging Cuvier's beaked whales were detected on the Southern California Antisubmarine Warfare Range (SOAR) hydrophones during two MBES surveys, and assembled into foraging events called group vocal periods (GVPs). Four GVP characteristics were analyzed *Before, During,* and *After* 12 kHz MBES surveys at the SOAR in 2017 and 2019 to assess differences in foraging behavior with respect to the mapping activity. The number of GVP per hour increased *During* and *After* MBES surveys compared with *Before.* There were no other differences between non-MBES and MBES periods for the three other characteristics: the number of clicks per GVP, GVP duration, and click rate. These results indicate that there was not a consistent change in foraging behavior during the MBES surveys that would suggest a clear response. The animals did not leave the range nor stop foraging during MBES activity. These results are in stark contrast to those of analogous studies assessing the effect of Naval mid-frequency active sonar on beaked whale foraging, where beaked whales stopped echolocating and left the area.

Introduction

Over the last 20 years there has been an increase in research focusing on mid-frequency (1-10 kHz) active sonar (MFAS) and its effect on toothed whales (McCarthy *et al.* 2011, DeRuiter 2013, Jarvis *et al.* 2014, Manzano-Roth *et al.* 2016, Falcone *et al.* 2017, DiMarzio *et al.* 2019). This is largely due to concerns raised after several mass stranding events were linked to naval activities using high intensity MFAS sources (Frantzis 1998, Evans and England 2001, Fernandez *et al.* 2004, D'Amico *et al.* 2009). Less research has focused on the effect of higher

frequency (>10 kHz) sonar (Vires, 2011, Cholewiak *et al.* 2017, Quick *et al.* 2017), such as multibeam echosounders (MBES), on toothed whales, despite similar source levels (216-245 dB re 1 µPa @1 m) to MFAS, and an overlap in frequency range (10-400 kHz) with the most sensitive hearing range of toothed whales (10-150 kHz) (Ketten 2004). In 2008, a stranding event of melon-headed whales in Antsihohy, Madagascar raised concern about the potential impact of MBES on marine mammals due to the temporal (< 24 hours) and spatial association (65 km away) of the stranding event with a 12 kHz ocean mapping survey (Southall *et al.* 2013). While no direct cause of the stranding was determined, the investigators concluded that the animals most likely changed their behavior in response to the mapping survey, indirectly leading to the stranding (Southall *et al.* 2013). This stranding event as well as other observational studies of wild marine mammal reactions to high frequency echosounders (Cholewiak *et al.* 2017, Quick *et al.* 2017) has warranted further investigation into the potential effects that MBES signals may have on toothed whales. Furthermore it raises the question, are MBES surveys any different than Naval sonar activity in terms of eliciting behavioral responses from toothed whales?

There are inherent differences in MFAS and MBES aside from operational frequency differences. MFAS are used to detect targets, like submarines, at distant ranges (10s of km). These systems generally have a wide vertical ensonification beam (40°) with 360° horizontal coverage, producing pings (1-2 s in length) for several minutes at intervals ranging from 6 to 15 min apart, and source levels in excess of 235 dB re 1 µPa @1 m (Hildebrand 2009, Falcone *et al.* 2017). MBES are primarily used for seafloor mapping, requiring precise beam positioning and high horizontal and vertical resolution. These requirements equate to narrow (0.5° to 2°) downward directed beams in the ship's along-track direction, wide swaths across-track (commonly, 120° to 150°), and short operational pulse lengths (10-100 ms) that vary based on

the ocean depth (Lurton and DeRuiter 2011, Lurton 2016, Kates Varghese *et al.* 2019). The resulting MBES geometry leads to a much smaller area of direct ensonification and orders of magnitude shorter pulses in comparison to MFAS, where exposure to harmful levels of sound are most likely to occur (Lurton 2016). While the effect of MFAS on wild marine mammal behavior has been studied for some species with a controlled experimental design (McCarthy *et al.* 2011, Martin *et al.* 2015, Manzano-Roth *et al.* 2016), the effect of MBES on wild marine mammal behavior has not. The goal of this study was to assess the effect of MBES activity on beaked whale foraging behavior with a controlled experimental design.

In an effort to better characterize the radiation pattern of a Kongsberg EM 122 (12 kHz) multibeam echosounder, two MBES mapping surveys utilizing this system were run over the Southern California Antisubmarine Warfare Range (SOAR) hydrophone array of the U.S. Navy Southern California Offshore Range (SCORE), a multi-warfare training complex off of San Clemente Island, California (Mayer 2017, Smith, 2019). A resident population of Cuvier's beaked whales (*Ziphius cavirostris*) are known to inhabit this region and produce sound when they forage (DiMarzio and Jarvis 2016). This provided an opportunity to collect complimentary beaked whale data to assess the foraging behavior of beaked whales during the echosounder characterization study. The design of this study was analogous to studies assessing the effect of MFAS on the foraging behavior of beaked whales on the same (DiMarzio *et al.* 2019) and other Navy hydrophone ranges (McCarthy *et al.* 2011, Manzano-Roth *et al.* 2016), informing discussion and allowing for the comparison of results.

Cuvier's beaked whales generally forage in groups of 1-4 animals generating groups of echolocation clicks, collectively referred to as group vocal periods (GVPs). Animals have been tracked to depths up to 2992 meters during foraging dives, foraging for an hour or more at a time

(Schorr *et al.* 2014). During these foraging dives, Cuvier's beaked whales produce frequency-modulated echolocation clicks to detect and capture prey (Tyack 2006). These highly directional clicks sweep through frequencies from 20 - 90 kHz, with most of the energy concentrated between 40-60 kHz, and which last between 200-600 µs. Inter-click intervals for this species range between 200-500 ms, and on-axis source levels for these clicks are between 214-224 dB re 1 μPa m (Johnson, *et al.* 2004, Zimmer, *et al.* 2005, Baumann-Pickering *et al.* 2013, Baumann-Pickering *et al.* 2014, Gassmann 2015).

In previous work at SOAR comparing beaked whale click detections with visually sighted groups, an estimated horizontal detection range of 6.3 km over the course of a foraging dive cycle was used for Cuvier's beaked whales (DiMarzio and Jarvis, 2016). This detection distance was similar to the 6.5 km detection distance measured for Blainville's beaked whales in the Bahamas (Ward *et al.* 2008, 2011), a species with similar foraging clicks and dive behavior (Johnson *et al.* 2004, Tyack *et al.* 2006), and was assumed to be true for this study on the SOAR range as well. Since beaked whales generally begin foraging below 200 meters and produce several thousand clicks in a foraging event, the spatial layout of the SOAR hydrophone range (<2000 m depth, < 6.5 km between adjacent hydrophones) was conducive for detecting a foraging event if it occurred on the range.

A previous review by DeRuiter (2010) suggests the hearing threshold of toothed whales is most sensitive between 10-150 kHz, indicating high sensitivity to the frequency range of deep-water MBES systems such as the one used in this study, which was the Kongsberg EM 122 with a 12 kHz center frequency. Understanding that Cuvier's beaked whales have been associated with MFAS-related stranding events on multiple occasions (Evans and England 2001, Cox *et al.*

2006, D'Amico *et al.* 2009), Cuvier's beaked whales were an appropriate species to assess the effect of MBES activity, as well as compare with the effects of MFAS.

Methods

In order to assess the effect of MBES activity on beaked whale foraging behavior, echolocation clicks from Cuvier's beaked whales were detected and classified into GVPs, and compared across three exposure periods (*Before, During,* and *After)* with respect to MBES activity on the SOAR. This was an analogous design to studies that looked at beaked whale foraging behavior in response to MFAS exercises (McCarthy *et al.* 2011, Manzano-Roth *et al.* 2016, DiMarzio *et al.* 2019). In the present study, the EM 122 (12 kHz) MBES surveys were conducted on the hydrophone range of the SOAR located off of San Clemente Island, California. The hydrophone array consists of 177 bottom-mounted hydrophones at depths ranging from 840-1750 m spanning an 1800 km^2 area (Figure 2.1). The hydrophones, spaced between 2.5 and 6.5 km apart, have a receive bandwidth between 50 Hz and 48 kHz (DiMarzio and Jarvis 2016), are sampled at 96 kHz, and are capable of receiving both the beaked whale clicks and the signals from the EM 122 MBES.

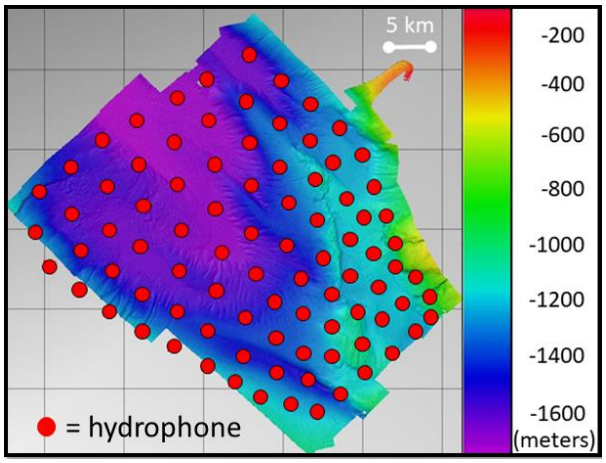

Figure 2.1. Bathymetry of the Southern California Antisubmarine Warfare Range hydrophone array. 88 hydrophones are shown, indicated by circles. The position of the other 89 hydrophones have a similar but offset arrangement to those shown here.

Sonar and Surveys

Two surveys, one in January 2017 (Mayer 2017, Smith 2019) and the other in January 2019, were conducted as part of a MBES characterization project, each utilizing the UNOLS vessel R/V *Sally Ride* and its Kongsberg EM 122, a deep-water MBES. According to the manufacturer's specification, the EM 122 has a maximum source level of 239-242 dB re 1 µPa @1 m and emits sound at center frequencies between 11 and 13.25 kHz. The EM 122 can be operated in single or dual swath mode, meaning each ping contains 8 or 16 pulses (Figure 2.2), respectively, which are either continuous wave (gated, single-frequency) or frequency-modulated. The exact signal depends on user-defined input as well as depth information, which will vary based on the survey design and location (Kates Varghese *et al.* 2019). For the SOAR surveys, pulse lengths were between 8-15 ms, and each ping was spaced roughly 6-7 seconds apart. These were typical parameters for a mapping survey in the deep-water environment at the SOAR.

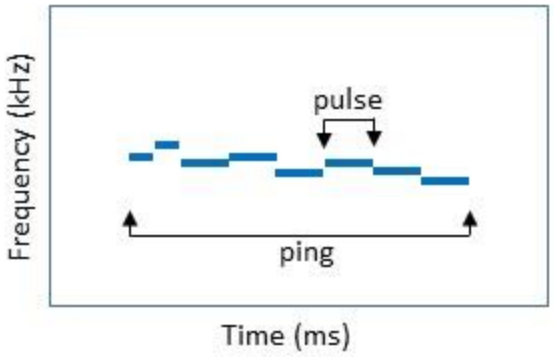

Figure 2.2. Simplified representation and nomenclature for the structure of a possible EM 122 single swath mode ping. Each of the eight lines represents a pulse, while the series of eight pulses together constitutes a ping. This ping example contains only continuous wave pulses. An EM 122 single swath ping produces pulses at discrete frequencies between 11 and 13.25 kHz. An individual pulse length is between 2-100 ms, where longer pulses are used for deeper depths. A complete ping can last between 8- 400 ms, again with longer ping durations associated with deeper depth modes.

The first MBES mapping survey was conducted 1/5/17 08:15-1/7/17 07:15 UTC. The majority of the survey was run in a 'mowing-the-lawn' fashion (Figure 2.3 Left) using the EM 122 in deep, dual swath mode with CW pulses only. The vessel's survey speed was 10 knots except when turning the ship, when the speed was dropped to 5 knots. This was followed by a shorter period when multiple acoustic sources were in use. These included the EM 122, a Kongsberg EM 712 MBES (40 kHz), a Simrad EK 80 wide-band echo sounder (18, 38, 70, 120, 200 kHz), and a Knudsen sub-bottom profiler (3.5 kHz).

The second MBES mapping survey was conducted 1/4/19 12:00-1/6/19 16:00 UTC during which the majority of the work was carried out in the southeastern corner of the range, restricting the EM 122 to single swath, CW only mode (Figure 2.3 Right). Following this, the EM 122 was set to operate in dual swath mode with FM pulses enabled and lines were run from the southeastern corner of the range to the center of the range and back twice before switching to

'mowing-the-lawn' type survey lines. To the best of our knowledge, no MFAS activity was taking place on the range during either of these surveys.

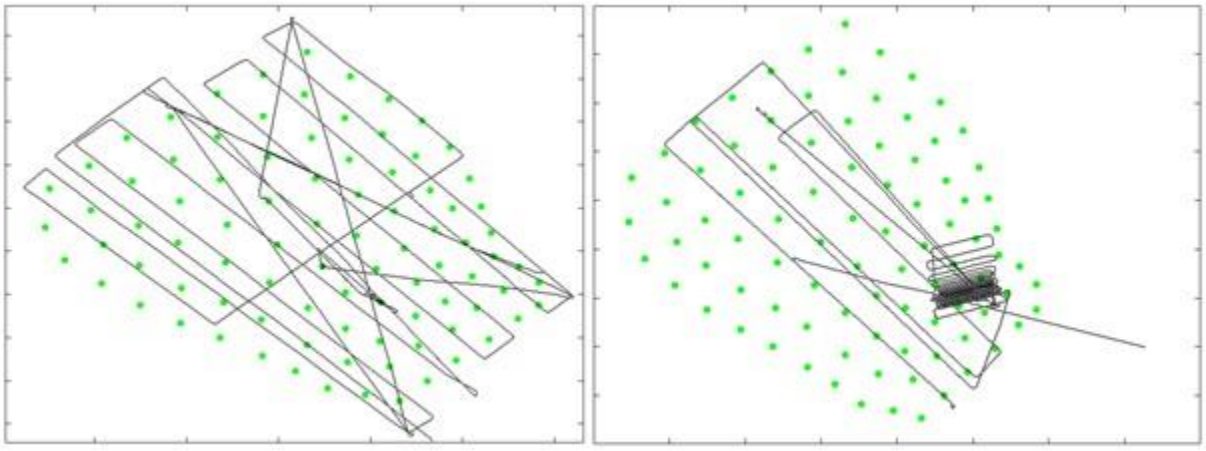

Figure 2.3. Hydrophone range overlaid with the ship track lines. Left: 2017, Right: 2019. Dots (green) indicate placement of the hydrophones. Lines (black) indicate track lines of the vessel.

GVP Detection on Hydrophones

The SOAR hydrophone data were processed at the Naval Undersea Warfare Center using a series of algorithms to obtain Cuvier's beaked whale group vocal periods (GVPs) (DiMarzio and Jarvis 2016). These were similar processing procedures used to analyze the impact of MFAS on marine mammals (McCarthy *et al.* 2011, DiMarzio *et al.* 2019). Cuvier's beaked whale foraging clicks were first detected and classified from the hydrophone data with a class-specific support vector machine (CS-SVM) classifier. The clicks were then formed into click-trains on a per hydrophone and per class basis using a Java-based click train processor (CTP) program. Clicks were added to each click train until at least three minutes passed without a click detection. If the click train had at least five clicks it was saved; otherwise it was discarded. The click trains were then used as input to a Matlab-based Autogrouper (AG) program which associated the click-trains into groups using a set of rules based on the time and location of the click trains

(Moretti 2019). The AG program was set to only use Cuvier's beaked whale click trains with inter-click intervals (ICIs) between 0.35 and 0.75 sec (Frantzis *et al.* 2002).

A group vocal period (GVP) is the time period from the first detected foraging click from the group to the group's last detected foraging click. The initial AG output was reformatted, filtered and summarized in R (R Core Team 2018) to produce a final AG output, which contained a list of Cuvier's beaked whale GVPs detected along with information about each detected GVP. The filtering removed GVPs with group click counts less than 300 or greater than 43200 clicks, and GVPs less than 5 min or greater than 90 min long. This was done to remove longer delphinid GVPs that may have been misidentified as Cuvier's beaked whales. 'Edge-only groups', or groups only detected on hydrophones on the edge of the range, were also removed. If an event was only detected on edge hydrophones, it was most likely from a group off the range and outside of the survey area. The detection statistics for the AG with the 'edge-only groups' removed are 0.759 for the probability of detection, 0.241 for the probability of false negatives and 0.185 for the probability of false positives (DiMarzio and Jarvis 2016).

For each GVP the output included 1) a timestamp for the start and end of each GVP, thereby providing the duration of the GVP; 2) 'center hydrophone,' or hydrophone with the most detected clicks; 3) number of clicks detected on the center hydrophone; and 4) the sum of all clicks detected on all hydrophones in the group ('group click count'). This dataset provided information on the number of GVPs that occurred on the range, as well as specific details about each GVP, but did not discern whether these events were made by unique foraging groups or individuals.

The GVP is defined as "a temporally and spatially unique set of vocalizations that represent a single group of beaked whales vocalizing during a deep foraging dive" (McCarthy *et*

al. 2011). Four GVP characteristics were used to assess foraging behavior: 1) number of GVP per hour, 2) number of clicks per GVP, 3) GVP duration, and 4) click rate. Click rate is defined as the number of clicks per minute of the GVP, whereas the 'number of clicks' is the total number of clicks for a single GVP event. Each GVP characteristic was computed by summing (number of GVP per hour) or averaging (GVP characteristics 2, 3, 4) the detections from all of the range hydrophones for each of the three exposure periods, *Before*, *During*, and *After*, with respect to each mapping survey. Therefore, these metrics provide information about the temporal but not spatial distribution of foraging on the range throughout the study period.

Experimental Design

The *During* period included the time when the EM 122 was first turned on until it was last turned off. The length of time of the *During* period in each year dictated how many hours of observation were selected for analysis *Before* and *After* the MBES activity to have a balanced analysis. So, for 2017 each of the three periods had 47 hours of observation and for 2019 the three periods were each 52 hours. To rule out potential diel foraging or diel differences in detectability (DiMarzio *et al.* 2019) as factors for differences between the time periods, each of the three periods started and ended at the same time of day, with respect to one another. The exposure periods were separated by approximately 24 hours to ensure appropriate comparison. For 2017, the *Before* period was 1/2/17 08:15-1/4/17 07:15 UTC and the *After* period was 1/8/17 08:15-1/10/17 07:15 UTC. The time separating each adjacent exposure period in 2017 was 25 hours. In 2019, the *Before* period was 1/1/19 12:00-1/3/19 16:00 UTC, and the *After* period was 1/7/19 12:00-1/9/19 16:00 UTC. The time separating each adjacent exposure period of 2019 was 20 hours.

Given that Cuvier's beaked whales forage on average for 40-60 minutes (Schorr *et al.* 2014, DiMarzio *et al.* 2019), an hour was chosen as the unit over which to average detections.

Therefore all detections within each hour of observation of a given exposure period were binned to compute each GVP characteristic hourly. Detections were binned based on the start time of each GVP, so that if a GVP started in a specific hour interval it was only accounted for once in that hour of observation, even if it lasted more than an hour. Using all hour observations in the analysis can increase the likelihood for temporal autocorrelation which increases the risk of a Type I error -- i.e., incorrectly concluding that there is a difference in foraging behavior across the *Before, During,* and *After* periods, when there is none. For this reason, a 99% confidence level for hypothesis testing was employed that is more stringent than the conventional 95% level.

The effect of MBES activity on foraging behavior of Cuvier's beaked whales was assessed by testing the following hypotheses with appropriate analysis of variance tests, either one-way ANOVA or, if the assumptions of the ANOVA were not met, a Kruskal-Wallis test:

$H0_1$- the number of GVP per hour was the same *Before, During,* and *After* MBES activity;

$H0_2$- the number of clicks per GVP was the same *Before, During,* and *After* MBES activity;

$H0_3$- the GVP duration was the same *Before, During,* and *After* MBES activity; and

$H0_4$- the click rate per GVP was the same *Before, During,* and *After* MBES activity.

In each case where the null hypothesis was rejected, a post-hoc multiple comparison test was used to determine which of the exposure periods were different from one another.

Based on previous information about the foraging behavior of this resident population of Cuvier's beaked whales, it was hypothesized that the two years of data would not be different from one another. To test this, independent t-tests were run to compare each of the three

exposure periods of 2017 to the respective exposure periods of 2019. Provided the two data sets were not different, they could be combined to add statistical power to the overall analysis.

Results

GVP detection reports including 141 hours of data were processed from 2017 and 156 hours from 2019: 47 hours for each of the three periods in 2017 and 52 hours for each of the three periods in 2019. For any hour increment in which no GVPs were detected, the other GVP characteristics could not be calculated, reducing the number of observations for analysis for those characteristics.

2017 Versus 2019

There were 575 GVP detections made over the course of the 2017 study and 394 GVP detections in 2019. In general, there were significantly ($p<0.01$) more GVPs per hour in 2017 (4.078 ± 2.36) than there were in 2019 (2.52 ± 1.95). Particularly in 2017, there were more ($p<0.01$) GVPs per hour both *During* and *After* MBES activity compared with 2019 (Figure 2.4 Center and Right), but no difference *Before* between the two years (Figure 2.4 Left). Compared across years, this metric may provide broader insight about foraging in this area, specifically, the inter-annual variability in animal presence on the range (DiMarzio *et al.* 2019). This could indicate that there were simply more animals overall on the range during 2017 in comparison to 2019. There was no difference between 2017 and 2019 in 1) the number of clicks per GVP, 2) GVP duration, or 3) click rate for any of the three exposure periods (Table 2.1). Since there were no differences in the other GVP characteristics, the two years of data were assumed to come from similar distributions and were combined into one data set for further analysis. Figure 2.5 shows the hourly binned data across the three exposure periods for each year for comparison. However, an additional analysis was performed separately for each survey year which assessed

the GVP characteristics across a finer-temporal scale with respect to the mapping activity that took place each year. These analyses are contained in Appendix 2.1.

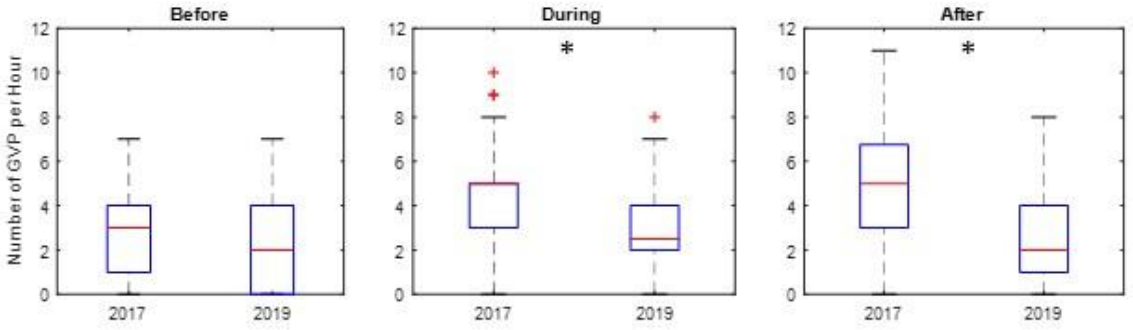

Figure 2.4. Boxplots of the number of GVP per hour for each exposure period by year. Left: *Before*, Center: *During*, Right: *After*. Center line indicates the median, top of the box indicates 75th percentile, bottom of box indicates 25th percentile, whiskers cover 99.3% of the data and plus signs indicate outliers. Presence of an asterisk on a plot indicates that the two years were significantly different at a 99% significance level for that period.

Table 2.1. Mean and standard deviation of each GVP characteristic for each year in each exposure period.

Exposure Period	***Before***		***During***		***After***	
Year	**2017**	**2019**	**2017**	**2019**	**2017**	**2019**
Number of GVP per hour	2.7 ± 1.56	2.21 ± 2.00	4.43 ± 2.26	2.87 ± 1.9	5.11 ± 2.51	2.5 ± 1.91
Number of clicks per GVP	2646 ± 1402	1903 ± 1046	2465 ± 1652	2327 ± 1197	3038 ± 1479	2853 ± 1889
GVP duration (min)	48.02 ± 14.25	35.85 ± 11.82	40.43 ± 12.35	37.81 ± 12.54	43.77 ± 10.35)	40.48 ± 16.28
Click rate (clicks/min)	58.39 ± 30.88	57.47 ± 42.57	58.90 ± 31.76	59.36 ± 25.92	68.04 ± 24.28	70.47 ± 42.30

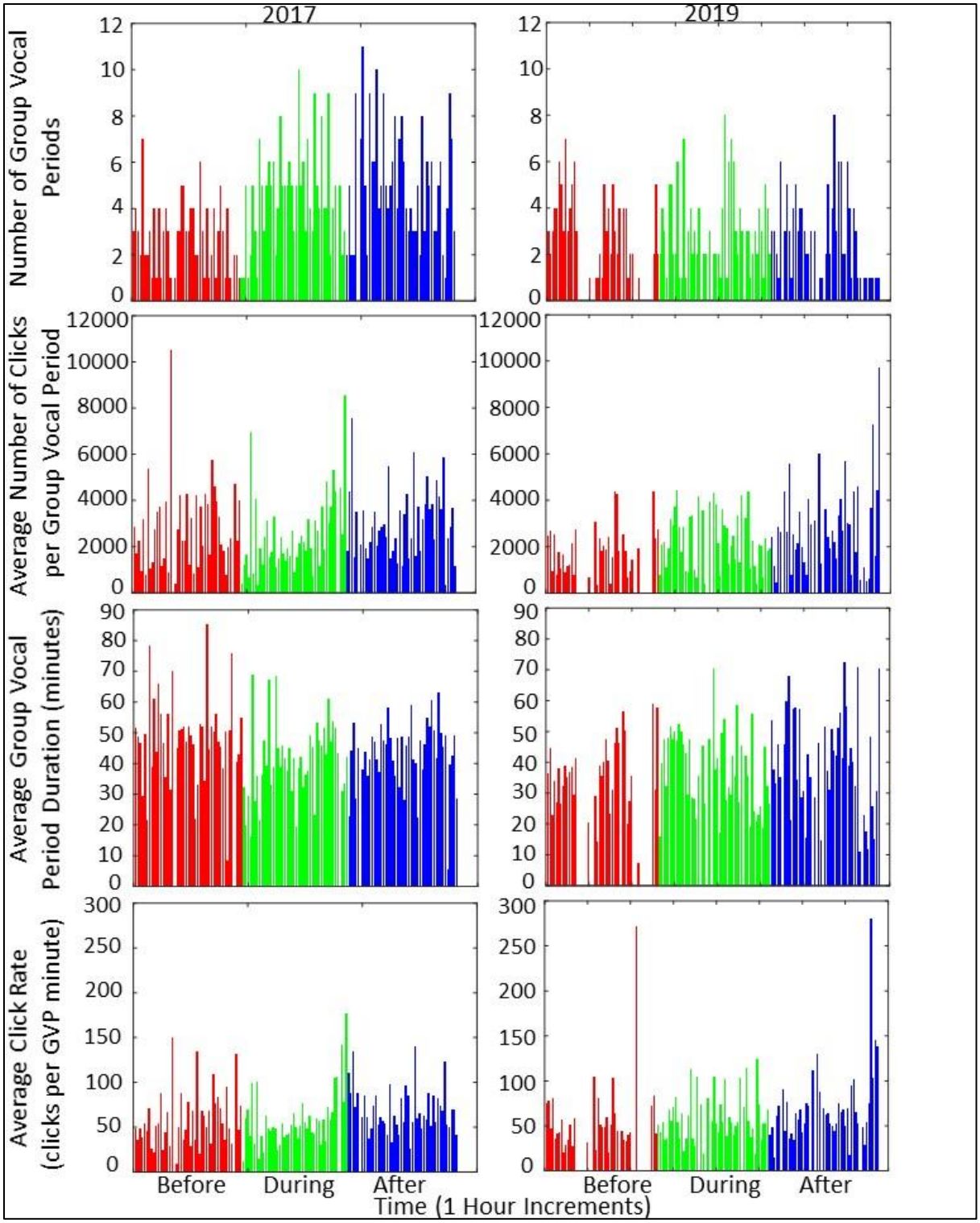

Figure 2.5. Barplots showing the hourly data of the four GVP characteristics across the three exposure periods of 2017, left column and 2019 right column. First row: number of GVP per hour; second row: number of clicks; third row: GVP duration in minutes; last row: click rate. Color transition across each plot on the x-axis shows transition between *Before, During* and *After* periods from left to right, respectively.

Number of GVP per Hour

The combined dataset contained 99 hours of observation for each of the three exposure periods. The average number of GVP per hour *Before* was 2.44 (SD=1.81), which increased to 3.61 (SD=2.21) *During,* and increased further to 3.74 (SD=2.56) *After* (Table 2.2). The data for this GVP characteristic met the assumptions of an ANOVA, so a one-way ANOVA was used to compare the exposure periods. The number of GVP per hour was not the same for the three exposure periods [F (2, 294) =10.18, p=0.00005]. There were more (p=0.00067) GVP per hour *During* and more (p=0.0001) GVP per hour *After* MBES activity than there were *Before* (Table 2.3).

There were several hours within the study when there were no GVPs detected. Since the remaining GVP characteristics could only be calculated if there were GVP detections within a given hour bin, there were fewer observation hours for the other three GVP characteristics compared to the number of GVP per hour. In particular, there were 81 hours with at least 1 GVP per hour *Before*, 94 hours *During*, and 92 hours *After* used to analyze the final three GVP characteristics. (Table 2.2)

Table 2.2. Descriptive statistics for the four GVP characteristics of the combined analysis, including the mean and standard deviation for each exposure period and number of samples used to compute those values in parentheses.

	Before	***During***	***After***
Number of GVP per hour	2.44 ± 1.81 (n=99)	1.61± 2.21 (n=99)	3.74 ± 2.56 (n=99)
Number of clicks per GVP	2312 ± 1301 (n=81)	2395 ± 1432 (n=94)	2946 ± 1690 (n=92)
GVP duration (min)	42.6 ± 14.49 (n=81)	39.1 ± 12.45 (n=94)	42.12 ± 13.67 (n=92)
Click rate (clicks/min)	57.98 ± 36.29 (n=81)	59.14 ± 28.77 (n=94)	69.26 ± 34.32 (n=92)

Table 2.3. ANOVA tables for the four GVP characteristics of the combined analysis, including post-hoc comparison p-values. SS= sum of squares, DF=degrees of freedom, MS= mean square, F= F-statistic, Chi-sq=Chi-square statistic, Prob > test statistic = the significance of the test.

Number of GVP per hour								
Source	**SS**	**DF**	**MS**	**F**	**Prob > F**			**Post-hoc p-values**
Groups	100.26	2	50.1313	10.18	0.00005		***Before vs. During***	0.00067
Error	1447.25	294	4.9226				***Before vs. After***	0.0001
Total	1547.52	296					***During vs. After***	0.91
Number of Clicks per GVP								
Source	**SS**	**DF**	**MS**	**Chi-sq**	**Prob > Chi-sq**			**Post-hoc p-values**
Groups	46523.5	2	23261.8	7.86	0.0196		***Before vs. During***	0.96
Error	1521879	264	5786.6				***Before vs. After***	0.034
Total	1568402.5	266					***During vs. After***	0.051
GVP Duration								
Source	**SS**	**DF**	**MS**	**F**	**Prob > F**			**Post-hoc p-values**
Groups	659.2	2	329.58	1.8	0.1665		***Before vs. During***	0.2
Error	48212.8	264	182.62				***Before vs. After***	0.97
Total	48872	266					***During vs. After***	0.28
Click Rate								
Source	**SS**	**DF**	**MS**	**Chi-sq**	**Prob > Chi-sq**			**Post-hoc p-values**
Groups	76023	2	38022.5	12.75	0.0017		***Before vs. During***	0.67
Error	1510135	264	5720.2				***Before vs. After***	0.002
Total	1586158	266					***During vs. After***	0.022

Number of Clicks per GVP

The average number of clicks per GVP *Before* was 2312 (SD=1301), 2395 (SD=1432) *During*, and 2946 (SD=1690) *After* (Table 2.2). A Kruskal-Wallis test was used to compare the number of clicks per GVP since the data for this metric did not satisfy the normality assumption of an ANOVA. The test showed no difference between the three exposure periods [H (2) =7.86, p=0.02] at the 99% significance level (Table 2.3).

GVP Duration

The average GVP duration *Before* was 42.6 minutes (SD=14.49), 39.1 minutes (SD=12.45) *During*, and 42.12 minutes (SD=13.67) *After* (Table 2.2). The data for this GVP

characteristic met the assumptions of an ANOVA, so a one-way ANOVA was used to compare the exposure periods. The test showed that there was no difference in GVP duration between the three exposure periods [F (2, 264) =1.8, p=0.1665] (Table 2.3).

Click Rate

The average click rate *Before* was 57.98 clicks per minute (SD=36.29), 59.14 clicks per minute (SD=28.77) *During*, and 69.26 clicks per minute (SD=34.32) *After* (Table 2.2). The Kruskal-Wallis test was used to compare the click rate data between exposure periods since the data did not satisfy the normality assumption of an ANOVA. There was a difference between the three exposure periods [H (2) =12.75, p=0.0017]. The click rate was higher (p=0.0021) *After* MBES activity than *Before* (Table 2.3).

Discussion

Of the four metrics used to assess beaked whale foraging behavior, only the number of GVPs per hour was statistically different *During* MBES activity versus a non-MBES period. In this case, there were more GVPs per hour *During* MBES activity than there were *Before.* This clearly shows that the animals did not stop foraging during the MBES surveys and did not leave the range since GVPs were still being detected on the range. More foraging events *During* the MBES survey is a stark contrast to the results of analogous studies assessing the effect of Naval sonar on foraging beaked whales (McCarthy *et al.* 2011, Manzano-Roth *et al.* 2016, DiMarzio *et al.* 2019). In the McCarthy study (2011), Blainville's beaked whales not only stopped echolocating, but left the hydrophone range as well during a multi-ship naval sonar exercise on the range (Tyack *et al.* 2011). A decrease in the number of GVPs during Naval MFAS exercises was also seen for groups of beaked whales from populations inhabiting waters on the Pacific Missile Range Facility in Hawaii (Manzano-Roth *et al.* 2016) and at the SOAR in southern California (DiMarzio *et al.* 2019).

The number of GVPs per hour and click rate both statistically differed between the *Before* and *After* periods, with more GVPs and an increased click rate occurring *After* than *Before*. The means of both of these GVP characteristics increased across the three exposure periods, while a similar trend was seen in the average number of clicks per GVP, although not statistically significant (Table 2.2). Of the four GVP characteristics, three increased over the time period evaluated, which implies an overall increase in foraging effort during this study. The increase in foraging effort over time, even after MBES activity, suggests that this trend is most likely a function of some other change in the environment, either on or off the range, rather than a response to the MBES survey itself. Alternatively, this result may be viewed as a lag in response by the foraging animals to the MBES survey. For example, in the McCarthy *et al.* study, though the number of GVPs decreased during the MFAS period, it was not until roughly 30 hours into the exercises that there was a pronounced decrease in the number of GVPs compared to pre-exposure numbers (2011). These surveys were operated as typical deep-water mapping efforts using surface-borne MBES, so the duration of MBES activity in this study represents a typical length survey for this type of environment (and perhaps even longer as other sources were used when the survey was completed). Conducting an even longer survey in a controlled study may provide insight into whether the increase in the number of GVPs per hour and click rate *After* compared with *Before* is a lagged response to MBES. However, performing a longer survey would also not be an accurate representation of exposure to this noise source under normal operating conditions.

Regardless of whether the results are from a lagged response to the MBES survey, or an effect of some other factor not studied here, it is valuable to explore what an increase in foraging effort may mean. One explanation is that the MBES survey may have affected the behavior of

the prey, squid, of the beaked whales. A recent study of squid abundance and distribution at the SOAR revealed large differences over small spatial scales that can have huge repercussions on a predator's decision to forage in a given area (Southall *et al.* 2018). Beaked whale foraging behavior is heavily dictated by prey abundance and distribution, so if MBES activity changed the dynamics of the prey, making them easier to hunt and/or capture, this could have led to the increase seen in foraging effort. Alternatively, it is possible that prey distribution at the SOAR, or the surrounding area, changed over the course of this study due to some external factor, such as the oceanographic conditions, that led to more favorable foraging conditions on the range. Local environmental conditions can affect prey densities and position in the water column. Due to the opportunistic nature of this work with the echosounder characterization study, only environmental parameters directly related to acoustic propagation were collected to support the source characterization work, which was not directly applicable to questions about prey dynamics. A third consideration is that the increase in foraging effort could represent unsuccessful or aborted foraging attempts, compensated for by an increase in the number and intensity of foraging attempts. One explanation for aborted foraging attempts could be that the signal from the MBES masks or jams the animal's ability to discern its own echolocation signal. This seems unlikely for two reasons: 1) the MBES signal frequency falls outside the octave band in which the echolocation signal of this species lies, and 2) by this argument, an individual GVP would be shorter in duration and contain fewer clicks, which was not observed. In the absence of tagging or tracking individual animals and prey dynamics, these hypotheses or any additional interpretations of the cause and/or effect of increased foraging effort cannot be verified.

There can be significant variability in marine mammal behavior at the species, group, and individual level that can confound comparing results across studies. Environmental and physical

conditions of the study site, such as the geometry of the seafloor, can affect how sound propagates and consequently how an animal will hear, perceive, and respond to a sound. Yet DiMarzio *et al.* (2019) showed a similar decreasing trend in the number of GVPs of Cuvier's beaked whales at the SOAR during MFAS activity as two other studies looking at a different species (Blainville's) of beaked whale (McCarthy *et al.* 2011, Manzano-Roth *et al.* 2016) at two other geographical locations (the Bahamas and Hawaii). Despite the potential for variability in marine mammal behavior, the equivalent results of the three MFAS studies (Manzano-Roth *et al.* 2016, McCarthy *et al.* 2011, DiMarzio *et al.* 2019) suggest a clear cessation of foraging response to MFAS activity by foraging beaked whales. Given the high site fidelity of Cuvier's beaked whales at the SOAR, it is likely that at least some of the animals in the DiMarzio *et al.* study (2019) were the same as those in the present study. Recognizing this, the decrease in all indicators (number of GVP and GVP duration) of foraging effort during MFAS activity in comparison to the lack of a statistical difference in three of the four foraging metrics and the increase in the number of GVP per hour *During* and *After* MBES activity is a notable difference in response by foraging Cuvier's beaked whales at the SOAR.

MFAS naval sonar had a clear measurable effect on beaked whale foraging (McCarthy *et al.* 2011, Manzano-Roth *et al.* 2016, Falcone *et al.* 2017, DiMarzio *et al.* 2019) in comparison to 12 kHz MBES mapping sonar despite comparable source levels and fairly similar frequencies (3-10 kHz for MFAS) from a toothed whale hearing sensitivity perspective. This is quite reasonable given the distinct differences between these two sonar types: the directivity of transmission, the limited area of ensonification, and the short pulse lengths of MBES as compared to MFAS. These differences have a profound impact on the likelihood of interaction of these sources with marine life, and are important to consider in an animal's ability to detect,

process, and potentially be affected by a signal (Southall *et al.* 2007). Additionally, the MFAS naval sonar exercises (McCarthy *et al.* 2011) involved multiple ships, sources, and occupied a specific location on the range for several days at a time. A typical ocean mapping survey includes one vessel with mapping sonar that continuously moves in a 'lawn-mowing' fashion over the survey area. Assuming the described operational paradigms are characteristic for these sonar types, along with the differences in pulse duration and ensonification volume, the two active sonar operations are inherently different which would factor into the different responses seen by foraging beaked whales.

Conclusion

This study took a coarse approach (1800 km^2 area) to assessing the effect of MBES mapping sonar on foraging behavior of Cuvier's beaked whales in order to compare to the approach taken in studies assessing MFAS (McCarthy *et al.* 2011, Manzano-Roth *et al.* 2016, DiMarzio *et al.* 2019). Therefore, this study did not elucidate changes within a particular group of foraging animals or responses by individuals. Individual responses are an important consideration when assessing the full impact of an anthropogenic noise source on marine life. A few studies have reported changes in individual (Quick *et al.* 2017) and group (Cholewiak *et al.* 2017) behavior of marine mammals in response to high frequency scientific echosounders, though there are none to date on individual response to MBES. The value of this study is a coarse look at how MBES activity affects groups of beaked whales in an area (i.e., the SOAR), a species known to be highly sensitive to other sonar types. The results of this study show an increase in the number of GVP *During* and *After* MBES, an increase in the click rate *After* MBES, and no change in the number of clicks or the duration of the average GVP for Cuvier's beaked whales *Before*, *During*, or *After* MBES activity at the SOAR. There was not uniform

change in the four GVP characteristics *During* MBES activity, and two of the significant differences were found in relation to GVP characteristics during non-MBES periods. Both of these findings highlight the large amount of variability found among foraging events on the range and through time, while the later result may suggest a lagged response to MBES activity. If the increase in foraging effort is in fact a response, albeit lagged, to MBES activity, this is the opposite response that beaked whales had to MFAS sonar. Since it is recognized that MFAS has a negative impact on beaked whale foraging, this result would suggest that there is not a negative impact of MBES activity on beaked whales foraging at the SOAR. If the significant differences in foraging behavior found in this study are due to the high variability seen in foraging activity, this would also suggest that there is no clear negative impact of MBES activity on beaked whale foraging at the SOAR. A finer temporal scale analysis of each year was conducted to assess some of these hypotheses and is provided in a supplementary section. This should be the first of many studies that take varying approaches (e.g., group/population versus individual, varying context and behaviors, environments, and mapping systems) to assessing the potential effects of MBES activity on marine mammals with a controlled experimental design.

CHAPTER 3: UNDERSTANDING MARINE MAMMAL SPATIAL BEHAVIOR BY APPLYING SPATIAL STATISTICS AND HYPOTHESIS TESTING TO PASSIVE ACOUSTIC DATA

Preface

This chapter was published in full as a Methods article in the Marine Megafauna section of the open access journal *Frontiers in Marine Science*. The full citation for the published material where this chapter has been reproduced from is:

Kates Varghese, H., Lowell, K., and Miksis-Olds, J. (2021). Global-Local-Comparison Approach: Understanding Marine Mammal Spatial Behavior by Applying Spatial Statistics and Hypothesis Testing to Passive Acoustic Data. *Frontiers in Marine Science* 8:625322. doi: 10.3389/fmars.2021.625322

The datasets generated for this study can be found in the supplementary material associated with the published material in *Frontiers in Marine Science*. The publication has been reproduced with the permission of *Frontiers in Marine Science*. Permission has been granted by *Aquatic Mammals* to reproduce Figure 3 contained herein from Manzano-Roth et al. (2016). Permission has also been granted to reproduce Figure 6 from McCarthy *et al.* 2011, by *Marine Mammal Science*, its publisher, John Wiley and Sons, and the publication authors.

The author of this dissertation, HKV, was the lead author on this article and responsible for all of the analysis, interpretation, drafting, and editing of the manuscript. HKV through the guidance of KL conceived of the presented idea and performed the reported analyses. JM-O provided guidance on the interpretation and communication of the findings of this work. All authors discussed the results and contributed to the final manuscript.

Abstract

Technological innovation in underwater acoustics has progressed research in marine mammal behavior by providing the ability to collect data on various marine mammal biological and behavioral attributes across time and space. But with this comes the need for an approach to distill the large amounts of data collected. Though disparate general statistical and modelling approaches exist, here, a holistic quantitative approach specifically motivated by the need to analyze different aspects of marine mammal behavior within a Before-After Control-Impact framework using spatial observations is introduced: the Global-Local-Comparison (GLC) approach. This approach capitalizes on the use of data sets from large-scale, hydrophone arrays and combines established spatial autocorrelation statistics of (Global) Moran's I and (Local) Getis-Ord Gi* (Gi*) with (Comparison) statistical hypothesis testing to provide a detailed understanding of array-wide, local, and order-of-magnitude changes in spatial observations. This approach was demonstrated using beaked whale foraging behavior (using foraging-specific clicks as a proxy) during acoustic exposure events as an exemplar. The demonstration revealed that the Moran's I analysis was effective at showing whether an array-wide change in behavior had occurred, i.e., clustered to random distribution, or vice-versa. The Gi* analysis identified where hot or cold spots of foraging activity occurred and how those spots varied spatially from one analysis period to the next. Since neither spatial statistic could be used to directly compare the magnitude of change between analysis periods, a statistical hypothesis test, using the Kruskal-Wallis test, was used to directly compare the number of foraging events among analysis periods. When all three components of the GLC approach were used together, a comprehensive assessment of group level spatial foraging activity was obtained. This spatial approach is demonstrated on marine mammal behavior, but it can be applied to a broad range of spatial observations over a wide variety of species.

Introduction

Studies investigating marine mammals in the wild have historically relied on human observers (Mann 1999, Acevedo-Gutierrez *et al.* 2000). Visual surveys are often conducted from land (Piwetz *et al.* 2018), or boats which limits the types of animals (e.g., coastal, amphibious) and/or behavioral states (e.g., hauled-out, surface-feeding, migrating, surface-swimming, etc.) that can be studied due to the limited range in which an observer can see an animal (e.g., distance from shore, at or near the surface of the water, etc.).

Over the past few decades, technological advancements have led to the ability to track animals further at or near the water's surface, at a wider range of depths and distances, in remote locations, and over longer periods of time than previously possible (Costa 1993). Technological developments have been used to enhance the study of marine mammals, including drones (Torres *et al.* 2018, Landeo-Yauri *et al.* 2020, Frouin-Mouy *et al.* 2020), telemetry devices and other biologgers (Fedak *et al.* 2002, Hart and Hyrenback 2009, Bograd *et. al.* 2010, McIntyre 2014, Joyce *et al.* 2019, Barlow *et al.* 2020), and gliders fitted with acoustic receivers (Johnson *et. al.* 2009, Baumgartner *et al.* 2013, Kowarski *et al.* 2020). Passive acoustic technology has also exploded with innovation (e.g., acoustics tags, autonomous acoustic receivers, towed hydrophone arrays) providing information at a range of scales on acoustically active marine mammals (Miller and Tyack 1998, Wahlberg 2002, Carstensen *et al.* 2006, Giraudet and Glotin 2006, Madsen *et al.* 2006, Wiggins and Hildebrand 2007, Miller *et al.* 2008, Barlow *et al.* 2008, Tyack *et al.* 2011, Southall *et al.* 2012, Gassman *et al.* 2013, Rettig *et al.* 2013, Sousa-Lima *et al.* 2013, Mate *et al.* 2016, DiMarzio *et al.* 2018, DiMarzio *et al.* 2019, Giorli and Goetz 2019, Caruso *et al.* 2020a, Caruso *et. al.* 2020b, Kates Varghese *et al.* 2020, Malinka *et al.* 2020, and countless more). Consequently, the potential to assess more challenging and complex questions

related to marine mammal behavior and population level impacts has also increased. For example, several U.S. Navy range hydrophone receiver arrays exist for tracking underwater vehicles (Moretti *et al.* 2016, DiMarzio *et al.* 2019) that house 10's of hydrophone receivers spread over a couple thousand square kilometers. These large arrays have been used to study the foraging behavior of groups of beaked whales during naval training exercises with mid-frequency active sonar (MFAS) and other noise-generating activities (McCarthy *et al.* 2011, Henderson *et al.* 2014, Manzano-Roth *et al.* 2016, Moretti *et al.* 2016, DiMarzio *et al.* 2019, Henderson *et al.* 2019, Jacobson *et al.* 2019, Kates Varghese *et al.* 2020).

With the ability to ask new and more complex questions related to marine mammal acoustic behavior comes the need to be able to analyze data collected to answer previously intractable questions. The goal of this work was to demonstrate a quantitative and comprehensive approach for examining and comparing group level marine mammal spatial behavior, the Global-Local-Comparison (GLC) approach. This approach was specifically developed for utilizing the spatial information derived from large-scale hydrophone receiver arrays and passive acoustic monitoring systems that receive, detect, and classify sounds emitted by marine mammals (e.g., Ward *et al.* 2000, Jarvis *et al.* 2014). This is not the introduction of a novel statistical method. Rather it is a novel bundling of existing and established statistical methods for an assessment of group level marine mammal spatial behavior. This approach includes a global (e.g., array-wide) and local (e.g., hydrophone) assessment, as well as an order-of-magnitude comparison of spatial observations across distinct analysis periods through the use of spatial-autocorrelation statistics (Moran's I, Getis-Ord Gi*) and hypothesis testing (Kruskal-Wallis).

The GLC approach was applied to 10 simulated pattern data sets to provide examples of the utility, limitations, and benefits of the approach. Datasets from large spatial arrays, like those

from navy ranges, set within a Before-After Control-Impact (BACI) framework, provided ideal empirical examples upon which to demonstrate this multi-faceted approach for assessing spatial change across analysis periods. Thus two BACI studies, McCarthy *et al.* (2011) and Manzano-Roth *et al.* (2016) assessing beaked whale foraging with respect to MFAS on U.S. Navy hydrophone ranges were used. Spatio-temporal data from these studies were visually extracted from heat map images produced in the original studies and the GLC approach applied.

While the aforementioned BACI studies incorporated coarse spatial modeling (i.e., edge versus inner hydrophone comparison), the focus of the original studies was on the temporal analysis of beaked whale foraging behavior. The GLC approach fills a need for a more comprehensive and quantitative approach for assessing the spatial aspects of group level marine mammal behavior. Other quantitative spatial methods have been used to examine specific study population attributes -- e.g., local decrease/increase of populations (McCarthy *et al.*, 2011, Manzano-Roth *et al.* 2016), or spatial re-distribution assuming no change in population numbers (Scott-Hayward *et al.* 2014)—but the three analyses combined in the GLC approach bring a comprehensive perspective to assessing spatial change in group level marine mammal observations.

Materials

This spatial analysis approach to assessing changes in marine mammal behavior capitalizes on the spatial detections representing a specific behavioral state of the study population –referred to here as group level behavior-- across distinct time periods. Group, here, refers to a number of animals (typically 10s of animals as opposed to a few individuals) of one species that occupy a local area. Group is used rather than population (Hammond 2002), as sufficient knowledge of what portion of a larger population a group of marine mammals

represents is often lacking. However, the use of group level does not exclude the study of an entire population, where that knowledge exists.

To demonstrate the GLC approach, spatial detections of acoustic signals consistent with foraging, or Group Vocal Periods (GVPs), were used as a proxy to assess beaked whale foraging behavior. A GVP is a vocal event of at least one, up to several, animals foraging together in close proximity to one another. During a GVP, beaked whales echolocate to find prey, producing several hundred species-specific echolocation clicks. If the animals are foraging within a sufficiently spaced hydrophone array, such as the U.S. Navy hydrophone arrays, there is a high probability that at least some of the thousands of highly directional echolocation clicks will be received on at least one hydrophone. Using detection and classification algorithms (e.g., Ward *et al.* 2000, Jarvis *et al.* 2014, DiMarzio *et al.* 2018) these clicks can be grouped into GVPs and assigned to a central hydrophone (e.g., the hydrophone that received the most clicks for a given timestamp) for the event, providing the basis of a GVP time series with associated spatial location information (McCarthy *et al.* 2011, Manzano-Roth *et al.* 2016, DiMarzio *et al.* 2019). The GLC approach does not provide detail for how to process hydrophone data but instead assumes the availability of such a data set prior to undertaking this protocol. In addition, some level of uncertainty exists with regards to the automated detection of species-specific GVPs and their corresponding assignment to a central hydrophone. It was assumed that the probability of detection of a GVP was constant over time and equal for all hydrophones.

Two types of data were examined: 1) simulated GVP data representing specific spatial patterns, and 2) extracted GVP data from two previously published exemplar marine mammal behavior studies (McCarthy *et al.* 2011, Manzano-Roth *et al.* 2016). For each data type, the total number of GVPs were summed by hydrophone for each analysis period. The total number of

GVPs per hydrophone served as the feature of interest for the spatial analysis, and the hydrophone location served as the spatial data of the feature. This information provided the necessary input for the spatial analysis.

GVPs were analyzed here, but the approach is not limited to the study of marine mammal foraging behavior. Any spatial feature could be studied assuming both a feature value and its spatial location information are available. In addition, the spatial layout of the observation array must be conducive to an examination of that feature. For example, a specific array with fixed and coarsely-spaced acoustic recorders may be appropriate for studying certain features over others, i.e., high frequency acoustic signals versus lower, or vice-versa.

Methods

The GLC approach entails calculating two spatial statistics, Moran's I and Getis-Ord Gi* for each analysis period, along with a data appropriate hypothesis test for comparing all analysis periods. The Moran's I statistic provides a global view of the spatial behavior over the entire region under study, i.e., the hydrophone receiver array, while the Getis-Ord Gi* statistic provides a more localized view of spatial behavior and spatial use, i.e., hot spots and cold spots of activity, within the array that would not otherwise be captured through the global statistic. Due to inherent differences in distributions and variances of observations across analysis periods, the spatial statistics cannot be directly compared across analysis periods. Thus, the statistical hypothesis test is required to provide insight about order-of-magnitude differences across analysis periods in the feature of interest.

Global Behavior/Spatial Autocorrelation

The Moran's I statistic is used to assess the global spatial pattern of the feature of interest, i.e., number of GVPs, over the entire array. The Moran's I statistic (Equation 3.1) characterizes spatial patterns by measuring the overall spatial autocorrelation of a data set,

producing a single value. The spatial correlation coefficient is normalized by the sum of the variance of the data so that the values of I range between (-1, 1) (Odland 1998, Goodchild 1986). A value of negative one corresponds to perfect dispersion, where very different values are found next to one another (Figure 3.1, *left*). A value of positive one corresponds to perfect clustering, where similar values are found next to one another (Figure 3.1, *right*). A value of zero represents no spatial autocorrelation and describes a perfectly spatially random distribution of values (Figure 3.1, *middle*). The variance of the expected value of Moran's I, under an assumption of a random spatial distribution (Odland 1998, Goodchild 1986), is calculated to test for statistically significant clustering or dispersion.

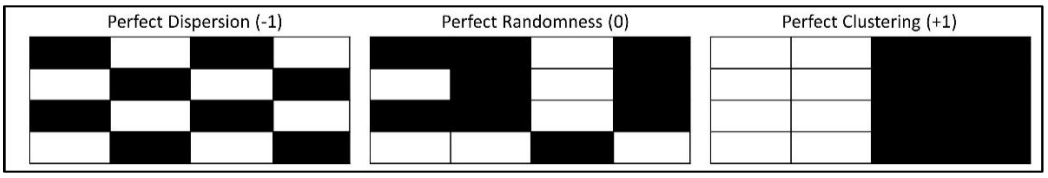

Figure 3.1. Spatial depiction of ideal Moran's I values: *left*- perfect dispersion, Moran's I value=-1; *middle*- perfect randomness, Moran's I value=0; *right*- perfect clustering, Moran's I value=+1.

The Moran's I statistic is given by the formula (Odland 1998, Goodchild 1986):

$$I = \frac{N}{W}\frac{\sum_i\sum_j w_{i,j}(x_i - \overline{x})(x_j - \overline{x})}{\sum_i (x_i - \overline{x})^2} \qquad \text{Equation (3.1)}$$

where $W = \sum_{i=1}^{n}\sum_{j=1}^{n} w_{i,j}$, $w_{i,j}$ is the weighting between the ith and jth spatial units, and w represents the weighting matrix with i rows and j columns. x_i refers to the ith feature value, (e.g., the total number of GVP of the ith spatial unit (e.g., hydrophone)), and $\overline{x}$ is the mean of all of a feature's values (e.g., the mean number of GVP across all hydrophones).

The weighting matrix (w) is a contiguity matrix representing the relationship between each pair of spatial units, e.g., hydrophones (the i^{th} row and j^{th} column). The weighting ($w_{i,j}$) determines the contribution that each set of hydrophones (the ith and jth) makes to the final spatial

autocorrelation value. For example, a "Queen's case" (Figure 3.2) contiguity weighting scheme considers all hydrophones (j) that are directly perpendicular, horizontal, and diagonal to a particular hydrophone (i) to be adjacent neighbors to that hydrophone, while the other hydrophones are not, i.e., $w_{i,j} = \begin{cases} 1, & if\ j\ adjacent\ i \\ 0, & if\ j\ not\ adjacent\ i \end{cases}$. Those hydrophones that are not adjacent neighbors therefore do not contribute ($w_{i,j}$=0) to the Moran's I statistic. The "Bishop's case" (Figure 3.2) only considers hydrophones that are directly diagonal to be adjacent neighbors, while the "Rook's case" (Figure 3.2) only considers hydrophones directly perpendicular or horizontal to be adjacent neighbors. In open ocean beaked whale habitat, it was not expected that there would be any restrictions in how a whale would move so the "Queen's case" was determined to be the most realistic representation of hydrophone adjacency and was employed when testing both the simulated pattern and exemplar data sets. The use of this specific criterion also assumes that the hydrophones are omnidirectional and therefore able to fully capture this expectation. To ensure the Moran's I values fall within the (-1, +1) scale, the weighting matrix is row-standardized by dividing each row value by the row sum so that the sum of values in each row totals to one.

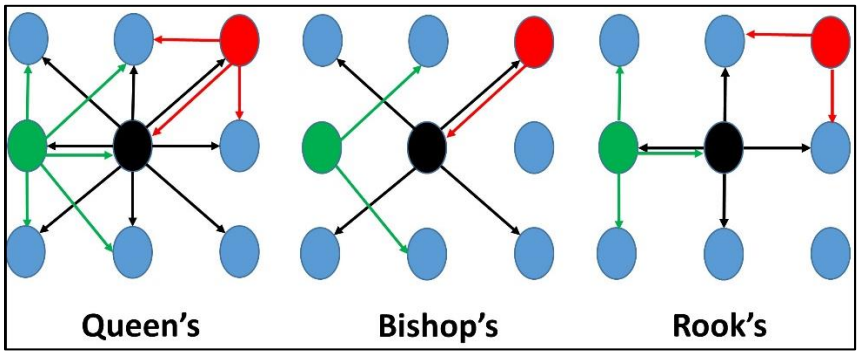

Figure 3.2. Three examples of contiguity weighting schemes for generating weighting matrices. "Queen's case" (*left*) was used in this study, while "Bishop's case" is in the middle, and "Rook's case" is on the right. Colored arrows indicate which hydrophones would be considered an adjacent neighbor to the same colored hydrophone. Notice: not all hydrophones will have the same number of neighbors.

To determine if the observed spatial pattern deviates significantly from random (i.e., I=0) the Moran's I statistic is converted to a z-statistic (z_I) (Equation 3.2) with a standard normal distribution upon which significance is determined. The formula for this is given by:

$$z_I = \frac{I - E[I]}{\sqrt{V[I]}} \qquad \text{Equation (3.2)}$$

where $E[I] = \frac{-1}{(n-1)}$ is the expected value for a spatially random distribution and $V[I] = \frac{A-B}{C}$ is the variance of the expected value. Note that the variance of Moran's I can be calculated based on an assumption of normality, or randomization (Odland 1998, Goodchild 1986). The former is appropriate when data follows a normal distribution, but in cases where the distribution is not normal or is unknown, the less restrictive randomization assumption can be used. For skewed data-- as is often the case with marine mammal detections and was true in this study-- the randomization assumption is more appropriate. This should be reconsidered for the specific application of this statistic. The formula for variance when normality is assumed can be found in Odland (1998). The variance under the randomization assumption is calculated by the following set of equations (Odland 1998, Goodchild 1986) (Equations 3.3-3.8):

$$A = n[S_1(n^2 - 3n + 3) - nS_2 + 3W^2] \qquad \text{Equation (3.3)}$$

$$B = D[S_1(n^2 - n) - 2nS_2 + 6W^2] \qquad \text{Equation (3.4)}$$

$$C = W^2(n-1)(n-2)(n-3) \qquad \text{Equation (3.5)}$$

$$D = \frac{\sum_{i=1}^{n}(x_i - \overline{x})^4}{\left(\sum_{i=1}^{n}(x_i - \overline{x})^2\right)^2} \qquad \text{Equation (3.6)}$$

$$S_1 = \frac{1}{2}\sum_{i=1}^{n}\sum_{j=1}^{n}(w_{i,j} + w_{j,i})^2 \qquad \text{Equation (3.7)}$$

$$S_2 = \sum_{i=1}^{n}\left(\sum_{j=1}^{n} w_{i,j} + \sum_{j=1}^{n} w_{j,i}\right)^2 \qquad \text{Equation (3.8)}$$

A p-value is obtained by matching the z-statistic to a standard normal distribution look-up table for the designated level of significance. A 5% significance level (95% confidence level) was used here. The analysis conducted with the Moran's I statistic is a hypothesis test, where the test hypothesis is that the spatial distribution of the observations is no different from "perfectly" random (I=0). If the p-value associated with the Moran's I statistic is less than 0.05, then the distribution is interpreted as statistically different from random: either significantly clustered (I=+1) (Figure 3.1, *right*), or significantly dispersed (I=-1) (Figure 3.1, *left*).

In the demonstration of the GLC approach, a change in significance of the Moran's I z-statistic from one analysis period to another is interpreted as a change in mammal behavior globally – e.g., from spatially random to spatially clustered. However, no change would be detected if, for example, all mammals were on the east side of the array as in Figure 3.1 (*right*) at time t_1 and moved to the west side at time t_2. Hence, a coupled analysis of behavior at a local scale is necessary.

Local Behavior/Spatial Autocorrelation

The Getis-Ord Gi* statistic (Getis and Ord 1992) is used to identify pockets of high spatial association, e.g., clustering of similar feature values, or in this demonstration, the number of GVPs. For the remainder of the paper this analysis will be referred to as Gi*. The Gi* z-statistic is computed for each spatial unit, or hydrophone, using the following formula (Getis and Ord 1992):

$$G_i^* = \frac{\sum_{j=1}^{n} w_{i,j}x_j - \overline{X}\sum_{j=1}^{n} w_{i,j}}{S\sqrt{\frac{n\sum_{j=1}^{n} w_{i,j}^2 - (\sum_{j=1}^{n} w_{i,j})^2}{(n-1)}}} \qquad \text{Equation (3.10)}$$

where $S = \sqrt{\frac{\sum_{j=1}^{n} x_j^2}{n} - (\overline{X})^2}$ and $\overline{X} = \frac{\sum_{j=1}^{n} x_j}{n}$ and all other variables are as described for the Moran's I statistic. Note that the use of the Gi* statistic assumes that the data examined are asymptotically normal (i.e., as the number of observations increases the distribution approaches normality) (Getis and Ord 1992). When using a binary adjacency weighting, such as the queen's criterion used here, 'as long as the distance is not too small and the weights are not too uneven, approximate normality is a reasonable assumption' (Ord and Getis 1995). Thus in using a contiguity weighting scheme, it is recommended that the number of adjacent sites per feature location be eight or more (Ord and Getis 1995). This was achieved for interior hydrophones in the array.

Using a two-tailed test, a p-value is determined and used to identify and interpret areas of either high and/or low feature values, e.g., number of GVPs. In particular, a significant hot spot – a non-random cluster of high feature values--will be identified if any hydrophone has a very high z-statistic (>+1.96, or 2 standard deviations) and associated p-value ≤0.025, while a significant cold spot –a non-random cluster of low values--will be identified if any hydrophone has a very

low z-statistic (<-1.96, or 2 standard deviations) and associated p-value ≥0.975. Clusters of high and low feature values are used to track how spatial behavior changes on the array through subsequent analysis periods.

Examining locational changes of areas of clustering from one analysis period to the next, provides insight into spatial behavior not captured by the global Moran's I result. In the exemplars, if all mammals move from the east to the west from one period to the next, as described earlier, a clear change in the location of hot and cold spots would be observed which would not have been detected by using only the global Moran's I statistic.

Comparison Analysis

Each spatial statistic takes into account the distribution and variance of only a single set of observations from one unit of time, or analysis period. Since the distribution and variance of a feature (e.g., number of GVPs) can change across analysis periods, it is not appropriate to compare the spatial statistic (i.e., Moran's I or Gi*) values across analysis periods (i.e., a comparison of a Moran's I value of 0.2 for one period to a Moran's I value of 1.2 in another period is meaningless if the distribution and variance of each period is different). In addition, the Gi* z-statistic is scale-invariant (Ord and Getis 1995), meaning the same results may occur for a similar pattern despite a different range of feature values for two or more analysis periods. For example with beaked whale foraging behavior, neither Moran's I nor Gi* will detect that there has been a substantial change if there are two analysis periods where the hot spot cluster remains in the western corner of the array. But if one cluster has 30 GVPs, while in the next analysis period the cluster only has one GVP, a substantial change has occurred. This would be detected by comparing the order-of-magnitude across analysis periods. A comparison test is necessary for determining if the number of observations across analysis periods has changed (i.e., do the two samples come from a similar population or not). It is recommended that statistical test-specific

assumptions be evaluated to decide the most appropriate statistical hypothesis comparison test to use for a specific data set.

Here, the non-parametric Kruskal-Wallis test (Kruskal and Wallis 1952) was used to compare the data sets of spatial observations (i.e., the number of GVPs per hydrophone) in the different analysis periods. The test hypothesis in the Kruskal-Wallis test is that the samples come from similarly shaped distributions (Kruskal and Wallis 1952). However, the test does not assume that the data are normally distributed, which is the primary driver for its use here. The distribution of the number of GVPs per hydrophone was skewed, with many hydrophones having zero observations. One other assumption of the Kruskal-Wallis test is that the samples compared are independent (i.e., both in and across analysis periods). The exemplar data sets were assumed to be independent as both temporal and spatial autocorrelation were tested and found to be low or non-existent in the original studies (McCarthy *et al.* 2011, Manzano-Roth *et al.* 2016).

The Kruskal-Wallis test works by ranking the observations in each analysis period and comparing the mean ranks of each (Kruskal and Wallis 1952). A significance level is used to statistically identify the compatibility between the observed data and what is expected under the test model and its assumptions (Greenland *et al.* 2016). For ease in interpretation, a 5% significance level ($\alpha = 0.05$) was used here. A p-value smaller than 0.05 suggests that the data are rare under the model, in other words, that the samples come from different distributions, while a p-value larger than 0.05 suggests the data are not unusual under the model, or that the samples come from similar distributions. If differences in the number of spatial observations (i.e., number of GVPs) across analysis periods are detected, a post-hoc multiple comparison test is used to determine which analysis periods are different from one another. Here, Tukey's honest significant difference criterion was used due to its effectiveness with data of equal sample sizes

(i.e., there were 89 observations, one for each hydrophone, per analysis period) (The MathWorks 2020). A significance level of 5% was used again to interpret which analysis periods differed from one another.

Finally, difference plots are generated to show the relative change (e.g., increase, decrease, or no change) in the number of observations on a per hydrophone basis between consecutive analysis periods. It is worth noting that the difference plots are based on binary rather than continuous values; a hydrophone that has a change of positive 1 between two periods will be represented the same as a hydrophone that has a change of positive 0.1 from one period to the next. Thus, these plots, as well as visualizing the original data, are only used to aid in the interpretation of the spatial statistics.

Note that the choice of statistical hypothesis test and post-hoc test may vary depending on the nature of the data. For example, if the data follow a normal distribution and satisfy the other assumptions of a parametric test, a test such as the analysis of variance (ANOVA) can be more powerful, although Andrews (1954) found the Kruskal-Wallis test to have a power efficiency of 0.955 relative to the parametric ANOVA's *F* test.

Data

Simulated Data Sets

Several patterned GVP data sets were created and tested to reveal how this approach would perform on known types of spatial distributions. The types of spatial distributions tested were chosen because they represent simple but realistic patterns of what might be expected of marine mammal foraging. This was conducted on a mock 50 "hydrophone" (10 row by 5 column) equi-spaced array. The simulated GVP data sets included seven patterned data sets (Alternate, Diagonal, Striped, Steep Grade, Graded, Cluster, and Graded Cluster) and three randomly generated data sets (Random 1-3). The ten simulated data sets tested are shown in

Figures 3.5 & 3.6, column 1. These figures will be introduced in full in the Results section. The Alternate, Diagonal, Striped, and Cluster pattern data were all generated using hydrophone values of zero (to represent a low value) or ten (to represent a high value) only to ensure the pattern was clear and not confounded by varying degrees of low and high values. For the Alternate pattern, every other hydrophone was either a zero or a ten so that no two hydrophones next to one another in the horizontal or vertical direction would have the same number, though they would diagonally. The Diagonal pattern consisted of three diagonal rows of zeros while the values of the remaining hydrophones were ten. The Striped pattern consisted of five alternating columns of ten hydrophones with a value of either zero or ten. The Steep Grade pattern consisted of five columns with values of ten, seven, four, zero, five, moving from left to right, while the Graded pattern consisted of five columns with values of ten, nine, eight, seven, eight, from left to right. The Cluster pattern consisted of a set of three by three hydrophones each with a value of ten in the center of the array and zeros for the remaining hydrophones. The Graded Cluster pattern included the same cluster pattern in the center of the array with a surrounding ring of hydrophones around this cluster with value of five and the remaining hydrophones with value zero. The three random data sets were randomly generated integer values between zero and ten for each of the 50 hydrophones.

Specific to the Moran's I statistic, the Alternate design was hypothesized to represent a scenario of dispersed foraging (i.e., $I<0$), while the remaining simulated patterns were hypothesized to represent different configurations of clustered foraging (i.e., $I>0$). The random data sets were hypothesized to show spatial patterning no different from random (i.e., $I=0$). The Gi* results were hypothesized to statistically identify the areas of high and low GVP activity (hot and cold spots, respectively) intentionally designed into each of the simulated spatial patterns.

For example, it was expected that the Diagonal pattern, consisting of low values in a diagonal pattern across the array would lead to a diagonal pattern of cold spot hydrophones in the same location as the low GVP values. It was expected that the cluster of high values in the center of the Cluster and Graded Cluster patterns would be identified as a cluster of hot spots in the Gi* analysis. It was also hypothesized that there would be a noticeable difference in the resulting Gi* values and significance, for the Steep Grade versus the Graded patterns, as well as the Cluster versus Graded Cluster patterns due to differences in grading, despite the similar overall pattern within these two sets of patterns. The random patterns were expected to show no significant hot or cold spots.

Exemplar Studies

The data from two previously published marine mammal behavior studies were extracted and tested to demonstrate how the GLC approach performed on empirical spatial behavior data. One study assessed Blainville's beaked whale foraging behavior during mid-frequency active sonar (MFAS) Naval exercises in 2007 on the Atlantic Undersea Test and Evaluation Center (AUTEC) in the Bahamas (McCarthy *et al.* 2011). The AUTEC study compared foraging intensity *Before*, *During*, and *After* MFAS activity on an 82 hydrophone array. The second study involved the same species and MFAS exposure between 2011 and 2013 on the Pacific Missile Range Facility (PMRF) off of Hawaii (Manzano-Roth *et al.* 2016). The PMRF study compared foraging intensity *Before*, *During Phase A, During Phase B*, and *After* navy sonar activity on a 62 hydrophone array. The difference between the two *During* phases of the PMRF study was that *Phase A* only included submarine-on-submarine activity without MFAS, while *Phase B* used surface ship MFAS, sonobuoys, and dipping sonars (Manzano-Roth *et al.* 2016). The length of and timing between analysis periods of the two studies was on the order of hours to days. For more specific details on the activities and characteristics of the analysis periods in these studies,

see the respective publications (McCarthy *et al.* 2011, Manzano-Roth *et al.* 2016). In both studies, the authors performed a visually quantitative spatial assessment generating the heat maps of GVP activity reproduced in Figure 3.3. The intention in using the McCarthy *et al.* (2011) and Manzano-Roth *et al.* (2016) data was not to serve as a reanalysis of those efforts, but rather specifically to demonstrate the GLC approach on an empirical data set. If one is explicitly interested in the effect of MFAS on beaked whale behavior, the McCarthy *et al.* (2011) and Manzano-Roth *et al.* (2016) papers should be reviewed.

Since the original data from the McCarthy *et al.* (2011) and Manzano-Roth *et al.* (2016) studies were not available for use in this study due to military data access, foraging intensity values were visually extracted from the heat maps (Figure 3.3). Note that both studies display the foraging intensity, but the AUTEC metric units (McCarthy *et al.* 2011) were GVPs per hour, whereas the PMRF metric units were GVPs normalized by the total hours of effort (Manzano-Roth *et al.* 2016). Thus, there was an order of magnitude difference between the data values of the two studies. In this study, white grid lines were overlaid on the AUTEC and PMRF data images (Figure 3.4), and the value at each grid intersection was visually extracted. Values at the white grid locations indicated by a yellow 'x' were ignored to achieve a similar number of hydrophone observations as the original studies (Figure 3.4). These grid patterns were designed to provide a representative sampling of the original study area. However, the heat maps in the original studies were generated using interpolation between hydrophones, so the extracted values do not necessarily align with the hydrophone data values of the original studies. The extracted values were then associated with a mock hydrophone array with 84 hydrophones for the AUTEC exemplar (Figure 3.4 - *top*) and 62 for the PMRF exemplar (Figure 3.4 - *bottom*). The mock arrays were designed to mimic the original array designs, with staggered rows and a similar

number of rows and columns to the original hydrophone arrays. The actual layouts of the AUTEC and PMRF hydrophone arrays deviate from this simplified design. Rather than matching the precise layouts of the AUTEC and PMRF arrays, the simplified designs were chosen because the purpose of this study was a proof-of-concept and demonstration of the GLC approach rather than definitively quantifying the spatial behavior of beaked whales on AUTEC and PMRF during those studies. The extracted data and neighbor-weighting matrices generated for both the AUTEC and PMRF exemplars can be found in the supplementary material. It was hypothesized that for the AUTEC exemplar, the Moran's I analysis would show spatial clustering for all three periods (*Before, During, After*), but that the Gi* analysis would reveal a cluster of hot spot hydrophones in the southwest corner of the array *Before,* a cluster of cold spot hydrophones in the middle of the array *During,* and a hot spot cluster again in the southwest corner of the array *After* navy MFAS activity. For the PMRF exemplar, it was hypothesized that the Moran's I analysis would show spatial clustering for all four analysis periods (*Before, Phase A, Phase B, After*), but that the Gi* analysis would reveal a change in where the clustering took place on the array. In particular, *During Phase B* and *After* the hot spot of activity would shift southward on the array, and a cold spot of activity would be located in the center of the array *During Phase B.*

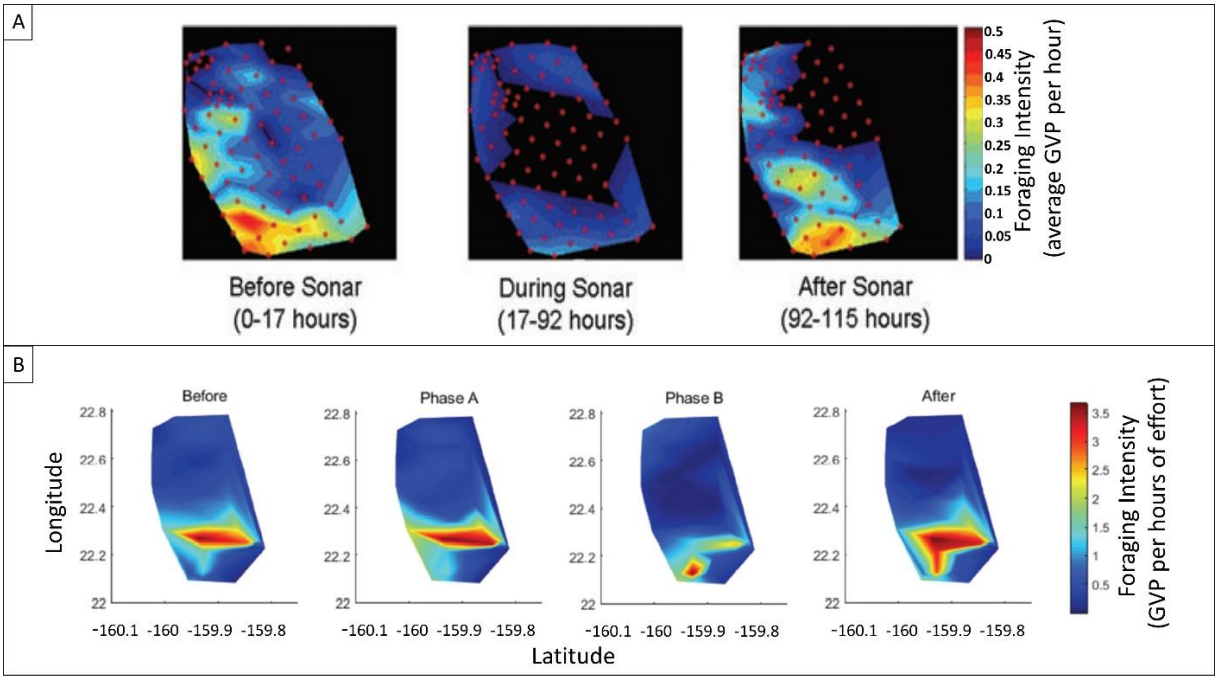

Figure 3.3. A) Reproduced from Figure 5.3.1 in McCarthy *et al.* 2011, which shows the foraging intensity, as the average number of GVPs per hour, of Blainville's beaked whales on the AUTEC hydrophone array *Before*, *During*, and *After* MFAS activity. Red circles indicate positions of the hydrophones in the McCarthy *et al.* 2011 study. Color bar values and label have been rewritten for legibility from original figure. B) Reproduced from Figure 3 in Manzano-Roth *et al.* 2016, which shows the foraging intensity in GVPs per hours of effort of Blainville's beaked whales on the PMRF array *Before*, *during Phase A, during Phase B*, and *After* naval sonar activity. Color bar label has been added and was not present in original figure.

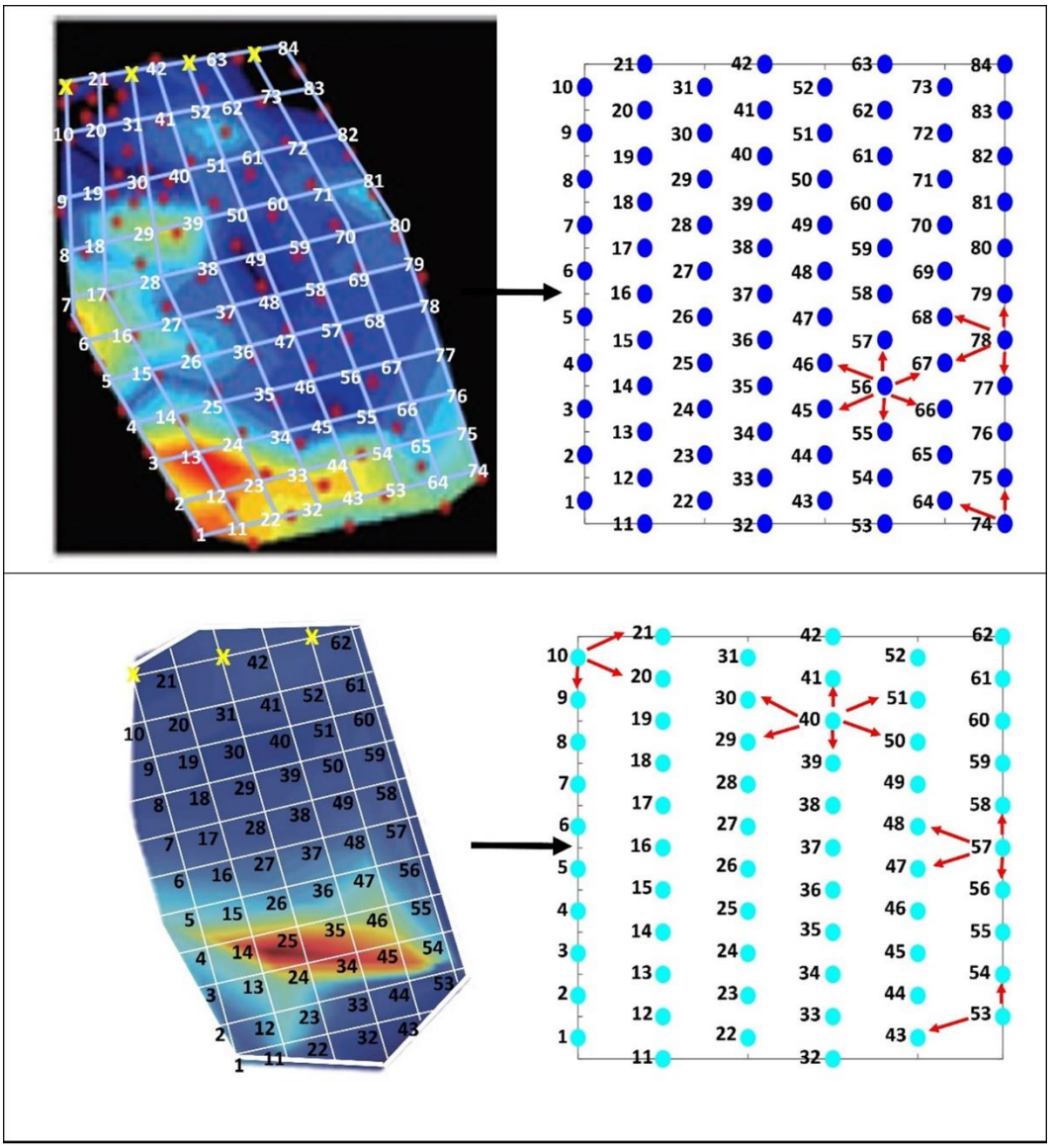

Figure 3.4. Schematic of how the data were extracted from the heat maps in the original studies (left figures) --AUTEC (top) and PMRF (bottom)-- and mapped onto the mock hydrophone arrays (right figures). For this study the white grid lines were added to each of the analysis period data images in Figure 3.3. The values at the grid intersections were extracted to create the exemplar data sets. Gridlines marked by a yellow 'x' indicate values that were not extracted. Each circle on the right represents the location of a hydrophone on the mock arrays. The numbers in the left figures correspond to the same number in the right figures and show where the value on the heat map was extracted from and to. In addition, the right figures provide examples of adjacent neighbor assignments for each of the hydrophone array layouts. Red arrows point to hydrophones that would be considered an adjacent neighbor to the respective hydrophone centered within the arrows.

Results

Simulated Data Sets

The Moran's I analysis results including the Moran's I value, z-statistic, and p-value are shown for the seven patterns and three randomly generated data sets in Table 5.3.1. The Diagonal, Steep Grade, Graded, Cluster, Graded Cluster, all exhibited significant spatial clustering as expected. In addition Random 2 was also significantly clustered, contrary to expectation, while Random 1 and Random 3, as expected, could not be statistically differentiated from a random spatial distribution. The Alternate and Striped patterns were statistically no different from random, which was also not expected.

Table 3.1. Moran's I analysis results by exposure period for the patterns and random data sets, including Moran's I value (I), the z-statistic (z_I), and the associated p-value.

Exposure Period	Moran's I (I)	Z-statistic (z_I)	p-value	Spatial Distribution
Alternate	0.053	0.9818	0.1635	random
Diagonal	0.583	8.0393	<0.001	clustered
Striped	-0.222	-2.687	0.9803	random
Steep Grade	0.638	8.7665	<0.001	clustered
Graded	0.705	9.6615	<0.001	clustered
Cluster	0.494	6.8501	<0.001	clustered
Graded Cluster	0.773	10.5593	<0.001	clustered
Random 1	0.0459	0.8823	0.189	random
Random 2	0.241	3.4836	<0.001	clustered
Random 3	0.039	0.7852	0.218	random

Despite some of the unexpected Moran's I results, with all ten simulated data sets the Gi* analysis corroborated the findings of the Moran's I analysis (Table 5.3.1) and provided further insight into the results. The spatial pattern of the Gi* z-statistics and significance results (Figure

3.5 and 3.6, columns 2 and 3) matched intuitively to the values in the original pattern. For every clustered pattern, clusters (i.e., several hydrophones next to one another) of hot spots and/or cold spots were identified, while for every random pattern only a few or no hot/cold spot hydrophones were detected. As an example, in the graded patterns (i.e., Steep Grade and Graded) the highest number of GVPs were on the western hydrophones and lowest were on the eastern hydrophones of the array. The Gi* analysis identified a column of hot spots in the western-most column and cold spot hydrophones in the eastern-most two columns.

The results of the Gi* analysis of the Alternate and Striped patterns provided further insight into the unexpected result of the Moran's I analysis that showed these patterns had a random distribution. These patterns had low z-statistic variability with values that deviated little from the mean (Figure 5.4B and H, respectively). Because of the narrow range of z-statistic values, both patterns were non-significant and no hot or cold spots were identified (Figure 5.4C and I). The lack of z-statistic variability can be explained by the fact that each hydrophone was surrounded by roughly the same number of high and low value neighbors and there was no variability in what those high and low values were (either ten or zero). The exception to this was the middle column in the Striped pattern that was surrounded by high values on either side thereby producing a larger z-statistic for the middle hydrophones of the pattern. A random result for Moran's I and non-significant result for the Gi* analysis suggest that the observable patterns in these examples were not sufficiently pronounced to be detected statistically with this analysis.

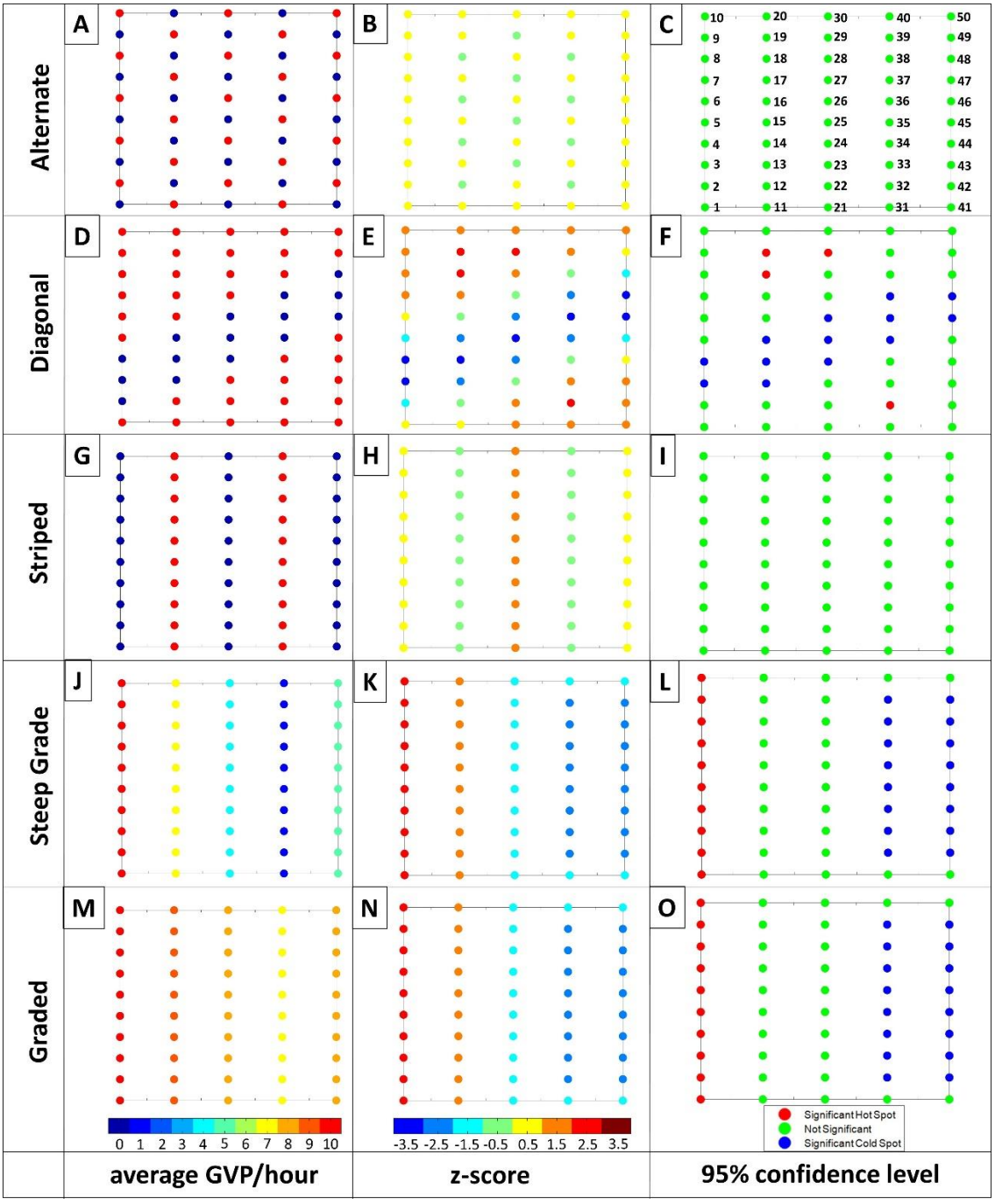

Figure 3.5. Visualization of the Gi*results for the Alternate, Diagonal, Striped, Steep Grade and Graded Patterns (top to bottom). From left to right: first column: average GVP per hour with color bar ranging from 0 (dark blue) to 10 (red); second column: Gi* z-statistic with color bar ranging from -3.5 (dark blue) to 3.5 (dark red); third column: 95% confidence level, where red indicates a significant hot spot and blue indicates a significant cold spot, while green is not significant. Note: For ease in displaying, individual hydrophone values were rounded to the closest number on the color bar for columns one and two. The numbers provided on Figure 3.5C correspond to hydrophones discussed in the Results.

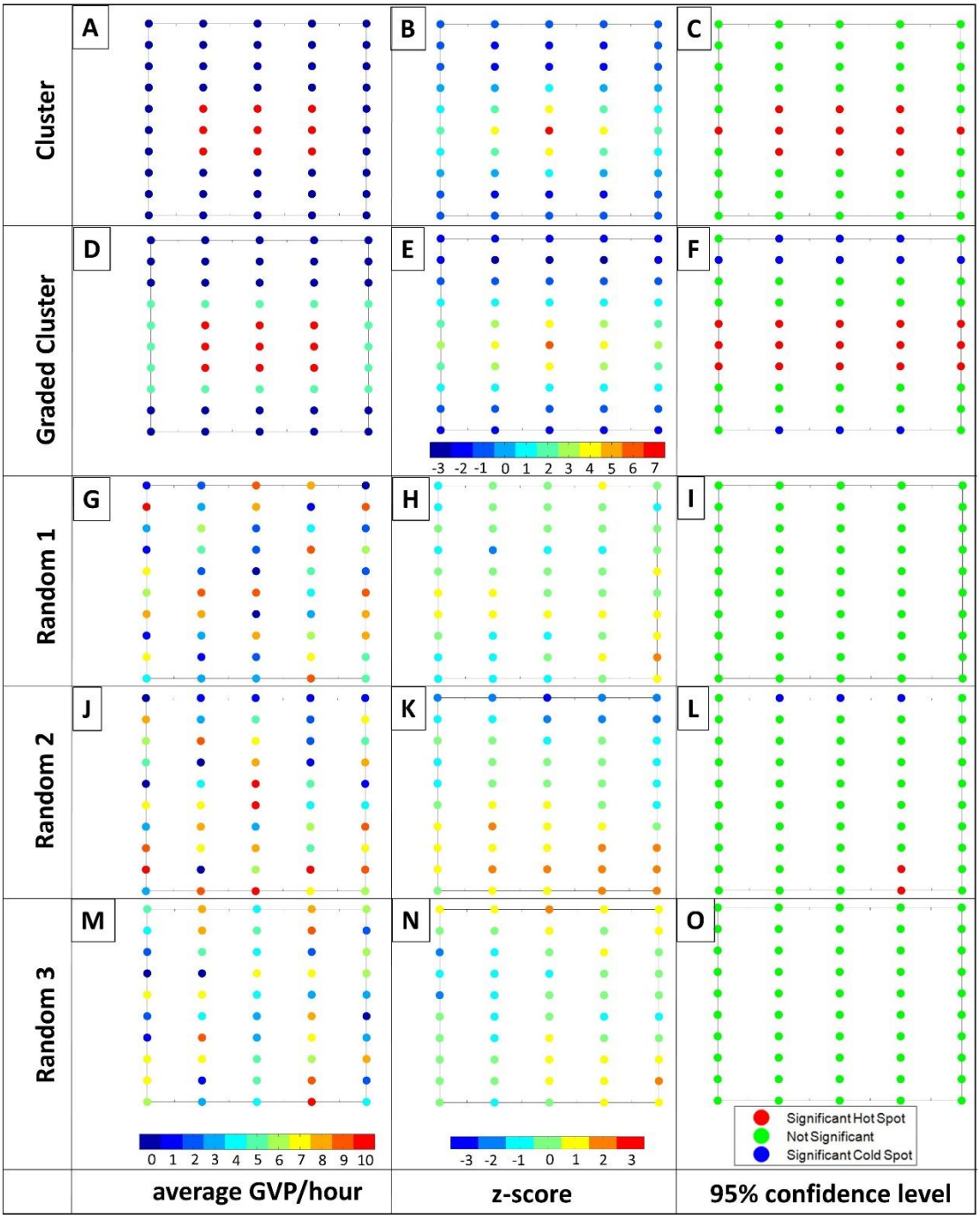

Figure 3.6. Visualization of the Gi* results for the Cluster, Graded Cluster, Random 1, Random 2 and Random 3 patterns (top to bottom). From left to right: first column: average GVPs per hour with color bar ranging from 0 (dark blue) to 10 (red); second column: Gi* z-statistic with color bar ranging from -3 (dark blue) to 7 (red) for the Cluster and Graded Cluster patterns and from -3 (dark blue) to 3 (red) for the random arrangements; third column: 95% confidence level, where red indicates a significant hot spot and blue indicates a significant cold spot, while green is not significant. Note: For ease in displaying, individual hydrophone values were rounded to the closest number on the color bar for columns one and two.

The results of the Gi* analysis of the Alternate and Striped patterns provided further insight into the unexpected result of the Moran's I analysis that showed these patterns had a random distribution. These patterns had low z-statistic variability with values that deviated little from the mean (Figure 3.5B and H, respectively). Because of the narrow range of z-statistic values, both patterns were non-significant and no hot or cold spots were identified (Figure 3.5C and I). The lack of z-statistic variability can be explained by the fact that each hydrophone was surrounded by roughly the same number of high and low value neighbors and there was no variability in what those high and low values were (either ten or zero). The exception to this was the middle column in the Striped pattern that was surrounded by high values on either side thereby producing a larger z-statistic for the middle hydrophones of the pattern. A random result for Moran's I and non-significant result for the Gi* analysis suggest that the observable patterns in these examples were not sufficiently pronounced to be detected statistically with this analysis.

The spatial distribution of the hot/cold spot hydrophones in the simulated patterns that were identified by the spatial analysis as clustered (i.e., Diagonal, Cluster, Graded Cluster, Steep Grade, and Graded) generally overlapped the designed observable pattern (e.g., a diagonal pattern of cold spot hydrophones was indeed present on the hydrophone array in the Diagonal example). However, with each pattern there were a few exceptions. For example in the Diagonal pattern, there was a cold spot cluster of hydrophones almost entirely overlapping the area of the zero-valued diagonal pattern (Figure 3.5F), with the exception of two perimeter hydrophones (hydrophones 3 and 48) which were not identified as cold spots, despite being a part of the original diagonal pattern. As another example, the entire cluster plus the two middle hydrophones on the lateral edges of the cluster (hydrophones 5 and 45) were identified as significant hot spots in the Cluster pattern (Figure 3.6C). There were similar cases of this in the

other clustered patterns where some hydrophones were or were not identified as being significant hot/cold spots, despite what one may expect based on visual expectation. This was an effect of the neighbor-weighting aspect of the Gi* z-statistic calculation. Edge hydrophones generally have fewer neighbors, meaning the value of those neighbors has a greater weight in comparison to the neighbors of hydrophones in the center of the range and therefore a different contribution to the z-statistic calculation.

The matching Gi* spatial distribution of hot and cold spots for the Steep Grade and Graded patterns (Figure 3.5L and O) exemplified the scale-invariant nature of the Gi* analysis. There were no obvious differences between the two patterns upon which the magnitude difference between the two patterns could be differentiated, supporting the need for the comparison analysis when comparing two data sets or analysis periods.

For the three random patterns the spatial distribution of the Gi* z-statistic values appeared random, except for Random 2 which had a more graded pattern with high Gi* z-statistic values toward the south and southeast corner and a row of low values along the northern perimeter of the hydrophone array (Figure 3.6K). As a result, two hot spot hydrophones were identified in Random 2 near the southeast corner of the array and three cold spot hydrophones were identified along the northern perimeter of the array (Figure 3.6L). There were no hot or cold spot hydrophones identified in Random 1 or 3 (Figure 3.6I and O, respectively), matching the Moran's I result that these patterns were random.

To further explore the likelihood of the Random 2 results, an ad hoc simulation test was run to compute the Moran's I analysis on 1000 randomly generated data sets. On average, the Moran's I value was 0.1283, the z-statistic was 2.0583 (SD=±0.88), and the p-value was 0.0587 (SD=±0.09). Based on a 5% significance level, a random data set would, on average, not result

in statistical significance and therefore would be interpreted as no different from random. However, implicit in the use of a significance level to detect statistical significance, is the acceptance that there may be times when the data do not match the underlying model. Thus on an array of 50 hydrophones and a 5% significance level, it is acceptable that 5%, or 2.5 hydrophones, may be identified as hot or cold spots despite an underlying random distribution, which the Random 2 pattern demonstrates.

Exemplar Studies

AUTEC Exemplar

Visual interpretation of the GVP data (Figure 3.7, column 1) indicated that *Before* MFAS activity the most GVPs occurred on hydrophones in the southwest corner of the array. *During* MFAS activity there were very few GVPs on the array compared to the *Before* period and the few GVPs that were present appeared highest along the edges of the array. After MFAS activity the level of activity appeared to match the *Before* period, with a shift toward the south-center of the array.

The Moran's I, z-statistic, and p-value component of the GLC approach for *Before*, *During*, and *After* in the AUTEC study are listed in Table 3.2. The Moran's I values all suggest clustering of GVP activity on the array in each analysis period. From an array-wide perspective, there was no clear change in global foraging behavior.

Table 3.2. Moran's I analysis results by analysis period for the AUTEC exemplar, including Moran's I value (I), the z-statistic (z_I), and the associated p-value.

Exposure Period	**Moran's I (I)**	**Z-statistic (z_I)**	**p-value**	**Spatial Distribution**
Before	0.77	12.37	<0.001	Clustered
During	0.7	11.24	<0.001	
After	0.83	13.28	<0.001	

The Gi* portion of the GLC analysis corroborated the results of the Moran's I test since both hot and cold spot hydrophone clusters were found in all analysis periods. In particular, a cluster of hot spot hydrophones were identified by the Gi* analysis in the southwest of the array for each analysis period (Figure 3.7C, F, I). The exact location and number of hot spot hydrophones did vary from period to period, but drawing upon the results of the simulated patterns, some variation is expected due to the neighbor-weighting component of the analysis. The GLC approach consistently identified a cluster of hot spot hydrophones in the southwest of the array that accords with a visual assessment, suggesting that the animals continued to forage predominantly in the same area throughout all analysis periods. The significance test of the Gi* analysis also revealed a cluster of cold spots in each of the analysis periods, which clearly changed location on the array from one analysis period to the next. *Before*, there were only a few cold spot hydrophones along the northern perimeter of the array; *During*, there was a large cluster of cold spot hydrophones in the center of the array; *After* there was a large cold spot cluster in the northeastern corner of the array (Figure 3.7C, F, I). In both the *During* and *After* periods there were roughly double the number of cold spot hydrophones compared to the *Before* period. These cold spots were also all clustered together, unlike in the *Before* period where they were more spaced out along the northern perimeter (Figure 3.7C). The results of the Gi* portion of the GLC approach suggest there was a change in where GVP activity was absent on the array *During* MFAS activity. It also shows that there was an increase in the number of hydrophones upon which no GVP activity took place.

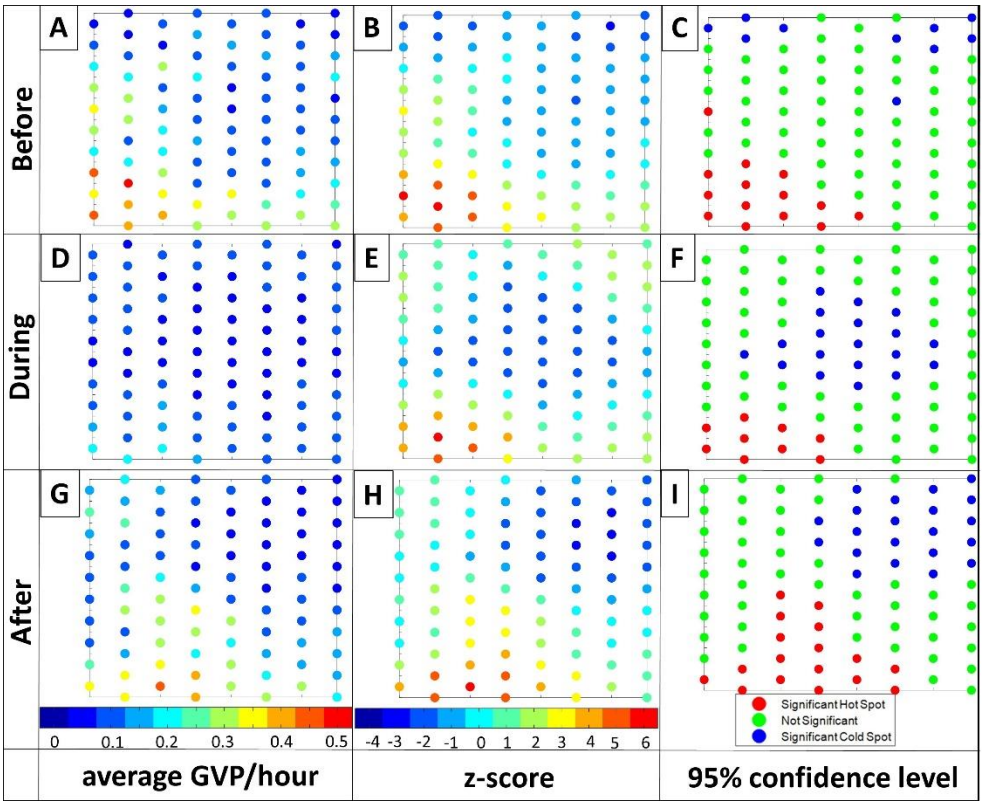

Figure 3.7. Visualization of the Gi* results for the AUTEC exemplar: *Before*, *During*, and *After*, from top row to bottom row, respectively. From left column to right: 1) the average GVP/hour with color bar ranging from 0 (dark blue) to 0.5 (red) GVP/hour, 2) the Gi* z-value with color bar ranging from -4 (dark blue) to 6 (red), and 3) hot (red) and cold spots (blue) at a 95% confidence level. Note: For ease in displaying, individual hydrophone values were rounded to the closest number on the color bar for columns one and two.

As discussed, the Moran's I and Gi* statistics alone do not confirm the change in overall activity. Hence the ability to detect changes in the global level of activity through the comparison test is an integral part of the GLC. The Kruskal-Wallis test showed that there was a difference across the mean ranks of the analysis periods [H (2) =48.48, $p=2.97 \times 10^{-11}$]. The post-hoc test showed that there were fewer ($p< 0.001$) GVPs on the array *During* MFAS activity than *Before* or *After*. So although the location on the array with the highest foraging activity (i.e., hot spot cluster) relative to a particular analysis period did not change, the absolute number of foraging events within a period did change. The difference plots supported this finding; there was a

decrease in the number of GVPs on most of the hydrophones from *Before* to *During* and an increase or no change in the number of GVP from *During* to *After* (Figure 3.8). Due to the scale-invariant nature of the Gi* statistic and the global nature of the Moran's I analysis, this overall understanding about the spatial behavior and magnitude of change was not completely realizable through the spatial statistics alone. This emphasizes the importance of considering each of the three parts to the GLC approach in interpreting and understanding spatial behavior change.

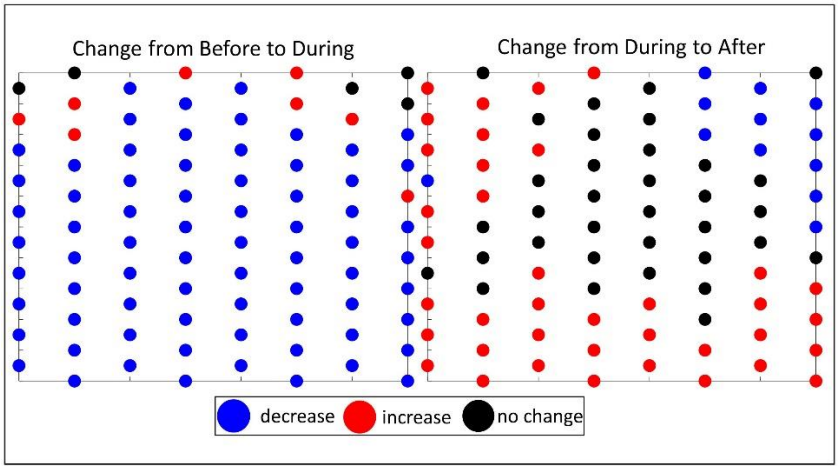

Figure 3.8. Spatial layout of mock AUTEC hydrophone array, where the circles represent the hydrophones of the array, and the color represents the change in the number of GVP on each hydrophone from one analysis period to the next: blue=decrease, red= increase, black=no change. *Left*- the change from *Before* to *During* MFAS activity, and *Right*- the change from *During* to *After* MFAS activity.

PMRF Exemplar

A visual analysis of the PMRF exemplar revealed that the most GVP activity appeared in the top part of the southern half of the array. During *Phase B* and *After*, there was a shift southward in where the most activity occurred in comparison to the earlier periods (i.e., there was also high GVP activity along the bottom southwest edge of the array). The least amount of GVP activity appeared to be along the southern edge of the array *Before*, but then shifted to the northern edge of the array during *Phase A*, and then to the center of the array during *Phase B* and *After* (Figure 3.9, column 1).

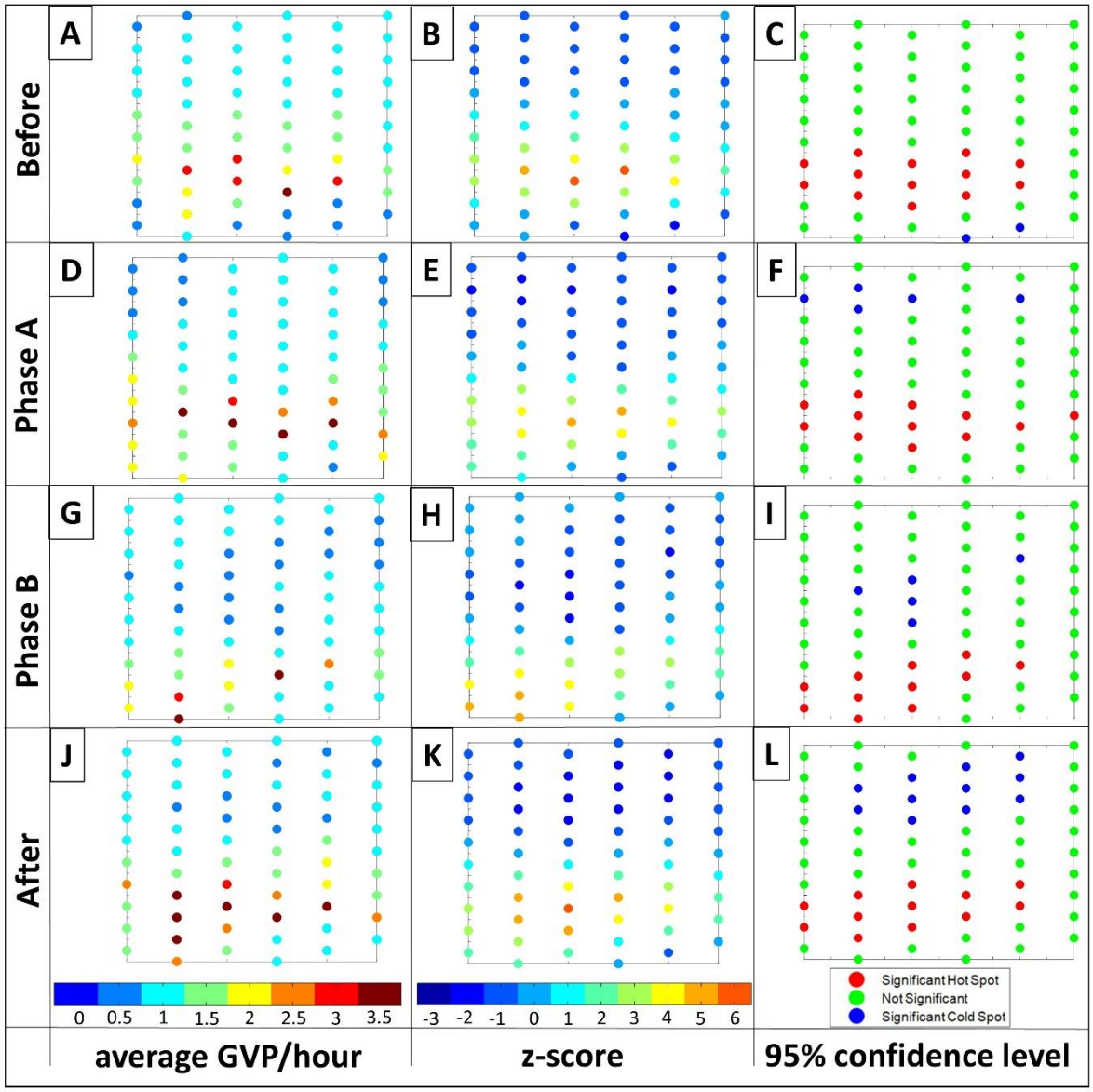

Figure 3.9. Visualization of the Gi* results for the PMRF exemplar: *Before*, *Phase A*, *Phase B*, and *After*, from top row to bottom row, respectively. From left column to right: 1) the average GVP/hour standardized to total time where the color bar ranges from 0 (dark blue) to 3.5 (red) GVP/hour) the Gi* z-value with color bar ranging from -3 (dark blue) to 6 (red), and 3) hot (red) and cold spots (blue) at a 95% confidence level. Note: For ease in displaying, individual hydrophone values were rounded to the closest number on the color bar for columns one and two.

The Moran's I values, associated z-statistics, and p-values for *Before*, *Phase A*, *Phase B*, and *After* are listed in Table 3.3. For all analysis periods of the PMRF study, the Moran's I

results suggested significant spatial clustering of GVP activity, or lack of activity, on the array. From the Moran's I analysis alone there was no indication that the beaked whales changed their global foraging behavior on the array.

Table 3.3. Moran's I analysis results by analysis period for the PMRF exemplar, including Moran's I value (I), the z-statistic (z_I), and the associated p-value.

Exposure Period	**Moran's I (I)**	**Z-statistic (z_I)**	**p-value**	**Spatial Distribution**
Before	0.60	8.3	<0.001	Clustered
Phase A	0.65	8.9	<0.001	
Phase B	0.66	9.09	<0.001	
After	0.73	10.03	<0.001	

The Gi* analysis provided further insight about the clustering result of the Moran's I portion of the GLC approach analysis. There were clusters of hot and cold spot hydrophones identified in each of the analysis periods. In all four periods there was a large cluster of hot spot hydrophones that spanned across nearly all columns in the southern half of the array (Figure 3.9, column 3). However, the *Phase B* period was the only period in which hot spots were identified on some of the southern perimeter hydrophones. Though there were differences in the exact hydrophones that were identified through the GLC analysis as hot spots, based on this information alone, there was no compelling reason to suggest these differences were outside of the variation expected due to natural variation in behavior, or due to the sensitivity in the GLC analysis, discussed previously.

Overall the Gi* z-statistic plot for each period had a similar appearance: lower values dominated the northern half of the array (Figure 3.9, column 2), suggesting this area was consistently not used for foraging. There were subtle differences in how far this low-value space extended. In particular, it was confined mostly to the northern half of the array *Before* (Figure

3.9B), but extended further south in *Phase B* (Figure 3.9H). In terms of significance, the GLC approach identified five or fewer hydrophones as cold spots in the first three analysis periods, while in the *After* period a more substantial cluster of 11 cold spot hydrophones was identified. In addition, the cold spots moved from the southern perimeter of the array *Before* to a more northern location during *Phase A*, and a more central location of the array during *Phase B* and *After*. These results closely matched the visual assessment and suggest that the animals may not have used the middle of the array as widely during these periods as they did *Before*.

Using the spatial statistics of the GLC approach alone, it was difficult to tell whether the small changes in location of hot spots were an actual change in spatial behavior over the array or within the natural variation to be expected in marine mammal behavior. It is also possible that the resolution of the hydrophone spacing was not fine enough to fully capture the potential spatial behavior change – a danger present in all spatial studies. However, the comparison analysis provided further insight. The Kruskal-Wallis test revealed that there was a difference in the mean ranks of the four analysis periods [$H(3) = 9.53$, $p = 0.0231$]. The post-hoc test showed that there were fewer GVPs on the array overall during *Phase B* compared to *Phase A* ($p = 0.043$) and *After* ($p = 0.035$). This finding was also corroborated visually in the difference plots which showed the center of the array had an overall decrease in GVP activity from *Phase A* to *Phase B*, but had an increase again from *Phase B* to *After* (Figure 3.10). The results of the comparison portion of the GLC approach provided support that a change in spatial behavior did occur. There were fewer animals foraging and the location of foraging shifted southward during *Phase B*. This exemplar of the GLC approach further highlights the value of using all three analyses of the GLC approach together to fully understand group level spatial behavior change. It also draws attention

to the importance of having the correct spatial resolution to be able to identify spatial behavior patterns.

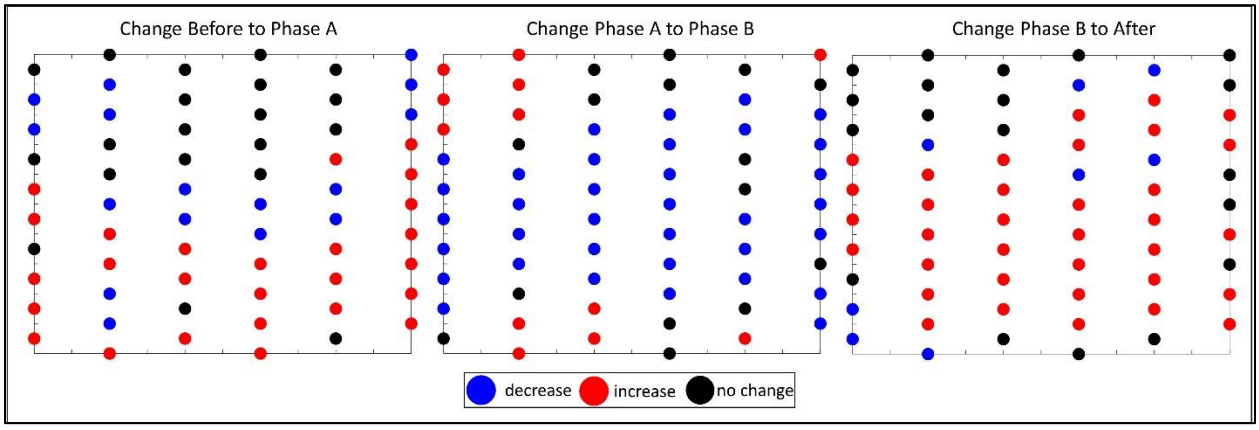

Figure 3.10. Spatial layout of PMRF hydrophone array, where the circles represent the hydrophones of the array, and the color represents the change in the number of GVPs on each hydrophone from one analysis period to the next: blue=decrease, red= increase, black=no change. *Left*- the change from *Before* to *Phase A*, *Middle*-the change from *Phase A* to *Phase B*, and *Right*- the change from *Phase B* to *After*.

Discussion

The results of the spatial analysis for the simulated data sets offered unique insight into how the GLC approach performed and provided guidance on how to interpret the more complex results of the empirical exemplars of group level marine mammal spatial detections representing foraging behavior. The results of the exemplar data sets conveyed the importance and necessity of using all components of the GLC approach together to achieve a comprehensive understanding of spatial behavior patterns. Moreover, the weakness of examining individual statistics in isolation of the others was demonstrated. When the underlying mechanism of the spatial pattern is not known, the insight gained in this three-pronged approach, along with knowledge of the context, can help support or refute potential hypotheses explaining the observations.

Several instances arose within the simulated data sets where edge hydrophones were either non-intuitively identified or not identified as being significant by the Gi* analysis of the

GLC approach in comparison to the visual assessment of the original data. For example, the Gi* analysis of the Diagonal pattern did not identify some perimeter hydrophones that made up the diagonal pattern as significant, while in the Cluster pattern some hydrophones outside of the cluster pattern were significant. This is because edge hydrophones have fewer neighbors than center hydrophones, so the contribution of each neighbor in the edge hydrophone case, has a larger weight in the Gi* statistic calculation than in the case of a center hydrophone (Ord and Getis 1995). This has important implications in analyzing hydrophone arrays that are long and narrow rather than square or circular. This is also an important aspect to keep in mind when choosing the number of hydrophones in the array. For example, in a square array of only four hydrophones the weighting contribution of all neighbor hydrophones would be the same, but in a square of 16 hydrophones, all but the center four would be considered "edge" hydrophones. The edge hydrophone effect will occur with any of the contiguity weighting schemes shown in Figure 2. However, if the weighting scheme is more constrained (i.e., choosing "Rook's" over "Queen's"), the edge hydrophone calculation will be different (i.e., a more constrained neighbor scheme means less neighbors and less neighbors equates to a higher weight for each neighbor in the overall calculation) in comparison to a center hydrophone, than if the weighting is less constrained (i.e., "Queen's" over "Rook's") (Ord and Getis 1995). This is an important aspect of the calculation to consider when interpreting the outcome of the GLC Gi* significance test using an adjacent neighbor weighting scheme. When using a similar weighting scheme it is recommended that the general area of hot/cold spot hydrophone clusters be compared rather than scrutinizing differences between individual hydrophones. Alternatively, a distance weighting scheme can be used, where every pair of hydrophones within some distance of the hydrophone of interest is represented in the Gi* calculation for that hydrophone. As the distance from the

hydrophone of interest increases, the contribution of other hydrophones (i.e., the weighting coefficient) toward the Gi* value decreases. It is therefore possible to minimize the edge effect (i.e., ensure all hydrophones have the same number of neighbors) using this scheme, since the number of weights is no longer a function of edge versus non-edge hydrophone, but rather a function of distance. Whether this is realized would depend on the exact parameter (i.e., distance threshold) and array layout used. A distance weighting scheme is especially appropriate for observations that change on a gradient. This was not assumed to be the case for beaked whale foraging behavior, which is strongly linked to--often patchy and heterogeneous--prey distributions (Benoit-Bird *et al.* 2013, Southall *et al.* 2018).

The type of neighbor-weighting rule can also have significant implications on the overall outcome of the Moran's I statistic. The Moran's I analysis of the simulated pattern data sets revealed that it was difficult to attain a perfectly dispersed pattern (i.e., I=-1). The only pattern for which a negative Moran's I value was achieved was the Striped pattern, though it was not statistically different from random. This is understandable given the "Queen's case" neighbor-weighting rule, which takes into account all adjacent hydrophone values. The more hydrophones that are considered a neighbor to a particular hydrophone, the more dependence the result for that particular hydrophone will have on surrounding values. To achieve a truly dispersed pattern a particular hydrophone either has to have less dependence on neighboring values, which can be achieved with a more constrained neighbor-weighting rule (i.e. "Rook's" or "Bishop's"), or the array needs to be larger so that similar values are more separated. The array sizes used in the exemplars were already quite large, rare in reality, and resource intensive. Given these challenges, the ability to detect perfect dispersion (I=-1) may not be possible without modifying certain parameters of the GLC approach, such as the neighbor-weighting rule. However, the

neighbor –weighting rule should be chosen based on the specific assumptions of the research question. In the exemplars, the "Queen's case" most accurately described hydrophone adjacency with respect to beaked whale foraging. If, for example, the more restrictive "Rook's case" neighbor-weighting rule was used for the Alternate pattern it would have likely elicited a dispersed Moran's I result. The hydrophones in only the perpendicular directions would have been considered adjacent neighbors to a particular hydrophone. This would have resulted in adjacent neighbors with a value that was always opposite to the center hydrophone, characteristic of a dispersed pattern.

In the case of beaked whale foraging, these animals have been shown to consistently forage in the same areas where aggregations of their prey exist (Henderson *et al.* 2016, Southall *et al.* 2018, Baird 2019). Hence a clustered distribution for beaked whale foraging was expected, and any change from this was seen as a deviation from typical behavior. When looking for a spatial change using the Moran's I analysis with the parameters described here, one is primarily testing to see whether the distribution shifts from clustered to random between analysis periods, or vice-versa. Despite the limitation in detecting dispersion, it would have been possible to detect a change in global (i.e., array-wide) behavior, should there have been any.

Many marine mammals forage on organisms, such as fish and plankton, that tend to aggregate either based on favorable environmental conditions (Quetin *et al.* 1996, Davis *et al.* 1999), or as a survival mechanism (Castro *et al.* 2002). Marine mammal foraging behavior is often closely associated with the distribution of these aggregations (Piatt and Methven 1992, Bowen *et al.* 2002, Maxwell *et al.* 2011, Benoit-Bird *et al.* 2013), so a clustered distribution to describe foraging behavior seems probable. However, marine mammals employ diverse foraging strategies (e.g., in groups versus individually) and/or social strategies (e.g. may demonstrate site

fidelity) that regardless of prey distribution may lead to different patterns in global spatial behavior than as seen in these examples with foraging beaked whales. Hence a critical part of extending the GLC approach to other species, and/or other behaviors is a thorough understanding of the behavioral strategies employed by the species under study, research-specific assumptions, and an appropriate choice of a contiguity rule based on those assumptions.

For hydrophone arrays that are regularly spaced, the binary neighbor-weighting rules (e.g., Queen's, Bishop's and Rook's), which do not require a distance measure, is appropriate. However, a neighbor-weighting rule that takes distance into account may be more fitting for other applications, such as irregularly spaced data where the spatial distribution between hydrophones is not uniform. Different neighbor-weighting rules and irregular hydrophone spatial arrangements were not addressed in this study. Scott-Hayward *et al.* (2014) address this type of data by using spatial interpolation to convert irregularly spaced tracks to persistent grid locations. Nonetheless, because the GLC approach is not constrained to grids, it can be applied to other hydrophone patterns with minor modification. Future work should investigate the use of other neighbor-weighting rules, e.g., distance-weighting, other binary weighting schemes, etc., along with various hydrophone arrangements for studying spatial behavior with the GLC approach.

The observed significance of a few of the hydrophones in the Gi* analysis of the Random 2 data recalls the need to understand the assumptions made in the hypothesis test. One way to interpret the use of a 95% confidence level is that if the study were repeated over and over again, the results may match the underlying model 95% of the time (Greenland *et al.* 2016). It is therefore important not to strictly use the statistical results, rather use them to guide the interpretation of the underlying data within the full context of the study. As a consequence, it is

most appropriate to interpret the statistical designation of hot and cold spots more holistically than on an individual hydrophone level. The precise hydrophones that are identified as significant should be emphasized less compared to the general pattern or area of significance, such as a cluster of several hydrophones. The number of hydrophones, their spatial resolution, and the expected scale of change one might expect to find are all important considerations when determining the appropriate design for this type of spatial analysis.

Synthesizing these findings from the simulated patterned and random data sets, the exemplars of marine mammal spatial behavior were more easily understood. For example, the issue of scale-invariance with the Gi* analysis (Ord and Getis 1995) was evident when the same spatial significance pattern resulted for the Steep Grade and Graded patterns, despite their differing values. This highlighted the need for the additional comparison analysis to identify order-of-magnitude differences undetectable by the spatial analyses. In the AUTEC exemplar, a hot spot cluster was found in the same general area in all three analysis periods, suggesting no spatial change in foraging activity. But after applying the comparison analysis it became clear that there were statistically fewer GVPs *During* MFAS activity. Thus an overall change had occurred, which would have been missed if the comparison analysis had not been applied.

Though this approach provides a way to view group level behavior over a large spatial scale, the ability of the test to identify spatial patterns is constrained to the resolution and layout in which the data are sampled. If a hypothesis test leads to the conclusion that no spatial autocorrelation exists, this only means that a spatial pattern does not exist at the resolution the data were sampled, but it does not mean spatial patterns at a smaller scale do not exist. The PMRF exemplar serves as a good case to this point. Though a spatial change was detected, it might have been more obvious with a finer spatial sampling resolution. Tagging efforts and other

approaches (Houser 2004, Gallagher *et al.* 2021) that focus on individual behavior can provide vital information about disturbance at finer scales that can complement these larger-scale efforts. Not detecting spatial autocorrelation may also mean that the sample size is too small, either not enough observations on individual hydrophones (i.e., too many zeros) or not enough hydrophones in the area where the spatial change is occurring to provide adequate resolution. These design constraints should be considered when drawing conclusions about whether spatial behavior has been affected or not.

Observations of marine mammals can be limited, which raises the question of whether a statistical test applied to such data has enough power to detect an effect (Hawkins *et al.* 2017). The exemplar data sets were chosen in part because the original analyses demonstrated there was an effect. Thus, the simulated data sets and mock arrays were designed to represent array sizes and observation numbers with a similar magnitude to the exemplars to be confident that there were a sufficient number of degrees of freedom to provide enough statistical power to detect meaningful differences without a formal analysis. However, tools exist (e.g., G*Power and MRSeaPower) for determining effect size and statistical power (Faul *et. al.* 2007 and MacKenzie *et al.* 2017, respectively) and should be used when relevant for a particular research question.

It is worth reiterating that the purpose of this paper was strictly to introduce and demonstrate the GLC approach on empirical data, and not to reassess the spatial effect of the MFAS activities on beaked whale foraging behavior in the McCarthy *et al.* (2011) and Manzano-Roth *et al.* (2016) studies. Though the intention of visual extraction of the data from the original studies was to obtain as similar a data set as possible, it is not the same data set. The use of similar but not identical data would lead to unknown differences, which would make a

comparison misleading. As such, a comparison of the results presented here was not made to the original results of the exemplar studies.

Inherent in any analysis is the need to interpret the results. The spatial analyses of previous studies assessing marine mammal spatial behavior using hydrophone arrays during noise-generating activities heavily relied on heat maps to visually assess differences in the spatial distribution of animals across analysis periods (McCarthy *et al.* 2011, Manzano-Roth *et al.* 2016). This has been a powerful tool for easily communicating the results of the research. However, visual results can be very subjective. A certain color bar theme may make the results appear more stark than the value of the color bar implies, or vice-versa. Spatial modelling has also been used to assess marine mammal spatial behavior, sometimes in conjunction with heat maps (McCarthy *et al.* 2011, Manzano-Roth *et al.* 2016) or as a stand-alone (Thompson *et al.* 2013). Generalized linear models, generalized additive models, and mixed models are commonly used (Thompson *et al.* 2013, McCarthy *et al.* 2011, Manzano-Roth *et al.* 2016, Henderson *et al.* 2019, Jacobson *et al.* 2019). These models consider factors such as spatial site (e.g. hydrophone location), distance to the activity of interest, received sound level, and identifying differences with respect to perimeter versus center hydrophones in an array to assess and characterize spatial change. But the results of statistical models by themselves can be non-intuitive to interpret.

Henderson *et al.* (2019) and Jacobson *et al.* (2019) have made parallel efforts to those presented here to assess local spatial changes in marine mammal behavior with respect to noise-generating events. A multi-stage generalized additive model was used to quantify the spatial response of beaked whales to various periods related to naval mid-frequency active sonar. The modelled results were also visualized by using tessellation of a non-uniform hydrophone array. Scott-Hayward *et al.* (2013) designed an approach for marine mammal detection data collected

along a line transect, which was used in an environmental impact assessment in wind-farm construction (Scott-Hayward *et al.* 2014). Their approach used a spatial smoothing model (CReSS) to identify spatial differences in animal densities from one period to another. This approach is especially fitting for data that is not tied to a geographically fixed position, whereas the GLC approach was designed for data that is geographically fixed. Data in either form could easily be modified to fit either approach. If an interpolation approach is adopted, however, it is imperative that the observations of the study species are spatially continuous within the resolution upon which the data were collected (e.g., this may be more difficult for animals that move in pods or are aggregated heterogeneously across space). One of the benefits of establishing a spatial model instead of testing empirical data (like that of the GLC approach) is that, if well-supported by empirical evidence, it can be used to predict or forecast changes (Redfern *et al.* 2013, Scott-Hayward *et al.* 2014). With any approach there are advantages and disadvantages, depending on the specific research question. As such, several approaches should be considered when deciding the optimal way to answer a given research question.

The significance of establishing the GLC approach is that it combines many of the strengths of existing methods (visual and statistical, global and local) in an organized manner, providing a comprehensive assessment of empirical spatial observations of marine mammals and objective descriptions of different group level animal behaviors. It builds off approaches that use visual representations of quantitative data by statistically quantifying patterns that can be illustrated through visual representations. The Gi* analysis essentially performs the same job as our eyes when looking at a heat map: it identifies spatial patterns and changes to those patterns, but without subjectivity. In evaluating the effects of anthropogenic noise on marine mammal behavior, visuals can be extremely intuitive, providing a powerful tool for communicating the

statistics to policy makers and other stakeholders. Thus the GLC approach incorporates visualizations of the local results. Other efforts largely focus on the local scale. But the global analysis provides a quick way to assess whether a broad-scale change has occurred, which is one way of assessing whether animal behavior in the system under study was disturbed. Finally, the comparison analysis brings another dimension to the spatial question providing insight about the degree of change identified, or standalone knowledge when spatial change is not identified. Together, the three-prongs of the GLC approach provide a reliable, objective, and standardized approach to assessing spatial change in marine mammal behavior. It ensures a robust statistically-backed analysis without compromising on the ability to effectively communicate the findings.

Not only is this approach applicable to a BACI data set-- for which it was originally designed and demonstrated here-- but a final strength of the GLC approach is that it is not limited to the study of marine mammal behavior, or the assessment of anthropogenic noise impact. For example, the value of spatial autocorrelation analyses has been demonstrated in other applications, such as marine spatial planning (Redfern *et al.* 2013, Jossart *et al.* 2020). Within a large-scale hydrophone receiver array framework, some examples of ways the GLC approach can be extended could include spatially analyzing sound levels over different periods of time in a changing soundscape, or assessing changes in marine mammal vocalizations that are not directly linked to behavior. In addition, there are many ways in which this three-pronged approach of established statistical methods can be extended or modified to answer other spatially-driven research questions by using different observation types and observation platforms.

Conclusion

The GLC approach serves as a tool to quantitatively measure spatial patterns, or lack thereof, allowing for the identification of changes in group level spatial behavior on large observational arrays. Within the approach are two scales of spatial assessment: global and local. The global statistic, Moran's I, provides a coarse overview of the type of spatial distribution of a set of features which can be used to quickly evaluate whether an array-wide change in behavior has occurred when comparing two or more analysis periods. The local statistic, Getis-Ord Gi*, provides the visual and spatial detail about change within an array by identifying local hot and cold spots of activity. An additional statistical hypothesis test (e.g., Kruskal-Wallis test) and difference plots, are used to detect potential differences in the overall level of activity on the array not identified by the spatial statistics alone.

The GLC approach was demonstrated using simulated patterned data sets that revealed the global analysis, utilizing a Queen's case neighbor-weighting, would be most effective at detecting a shift from clustered to random distributions, or vice-versa. The exemplar data sets provided two empirical examples of how to use this spatial analysis approach to evaluate spatial change in group level marine mammal behavior *Before-During- After* anthropogenic noise events. Overall the GLC approach provides a quantitative and intuitive way to assess group level spatial behavior change, but with careful consideration of the assumptions discussed herein, its use can be much broader than just this application.

CHAPTER 4: SPATIAL FORAGING EFFORT OF CUVIER'S BEAKED WHALES DURING A DEEP-WATER MAPPING SURVEY

Preface

This chapter was published as part of a Research Topic in the Marine Ecosystem Ecology section in *Frontiers in Marine Science* on 'Before-After Control-Impact (BACI) Studies in the Ocean.' The article is reproduced here with the permission of *Frontiers in Marine Science*. The complete citation of the published work is:

Kates Varghese, H., Lowell, K., Miksis-Olds, J., DiMarzio, N., Moretti, D., and Mayer, L. (2021). Spatial Analysis of Beaked Whale Foraging During Two 12 kHz Multibeam Echosounder Surveys. *Frontiers in Marine Science* 8:654184. doi: 10.3389/fmars.2021.654184

The author of this dissertation, HKV, was the lead author on this article and responsible for all of the analysis, interpretation, drafting, and editing of the manuscript. DM, ND, LM, JM-O, and HKV were involved in the coordination of the field component of this study. ND processed the acoustic data and provided the GVP data for the analysis. The GVP data which was further processed for this study is contained in the supplementary section associated with the published work. HKV, through guidance from KL, performed the reported analyses. All authors discussed the results and contributed to the final manuscript.

Abstract

To add to the growing information about the effect of multibeam echosounder (MBES) operation on marine mammals, a study was conducted to assess the spatial foraging effort of Cuvier's beaked whales during two MBES surveys conducted in January of 2017 and 2019 off of San Clemente Island, California. The MBES surveys took place on the Southern California Antisubmarine Warfare Range (SOAR), which contains an array of 89 hydrophones covering an area of approximately 1800 km^2 over which foraging beaked whales were detected. A spatial

autocorrelation analysis of foraging effort was conducted using the Moran's I (global) and the Getis-Ord Gi* (local) statistics, to understand the animals' spatial use of the entire SOAR, as well as smaller areas, respectively, within the SOAR *Before, During,* and *After* the two MBES surveys. In both years, the global Moran's I statistic suggested significant spatial clustering of foraging events on the SOAR during all analysis periods (*Before*, *During,* and *After*). In addition, a Kruskal-Wallis (comparison) test of both years revealed that the number of foraging events across analysis periods were similar within a given year. In 2017, the local Getis-Ord Gi* analysis identified hot spots of foraging activity in the same general area of the SOAR during all analysis periods. This local result, in combination with the global and comparison results of 2017, suggest there was no obvious period-related change detected in foraging effort associated with the 2017 MBES survey at the resolution measurable with the hydrophone array. In 2019, the foraging hot spot area shifted from the southernmost corner of the SOAR *Before*, to the center *During,* and was split between the two locations *After* the MBES survey. Due to the pattern of period-related spatial change identified in 2019, and the lack of change detected in 2017, it was unclear whether the change detected in 2019 was a result of MBES activity or some other environmental factor. Nonetheless, the results strongly suggest that the level of detected foraging during either MBES survey did not change, and most of the foraging effort remained in the historically well-utilized foraging locations of Cuvier's beaked whales on the SOAR.

Introduction

It is well understood that underwater anthropogenic sound can impact marine life (Hildebrand 2005, Wright *et al.* 2007, Gomez *et al.* 2016). The exact effect will vary based on a multitude of factors (NRC 2003) including but not limited to, characteristics inherent to the animal, the specific characteristics of the source of noise (Southall *et al.* 2007), the proximity of

the animal to the source (Richardson *et al.* 1995, Erbe and Farmer 2000, Falcone *et al.* 2017), whether the source and/or the animal is moving, and the behavioral state of the animal (Isojunno *et al.* 2016). The effect may also vary with different species (Miller *et al.* 2012) and among individuals of the same species (Sivle *et al.* 2015). Therefore, carefully controlled studies are necessary (Popper *et al.* 2020) to build an understanding about which species, behaviors, contexts, and interactions are most vulnerable to negative impacts during exposure to various anthropogenic underwater sound sources. Significant work has focused on understanding factors that lead to acute injury and death (Kastelein *et al.* 2017, Ketten 2014), but arguably an equally concerning effect is behavioral change to a group or population that may ultimately lead to injury, death, or population decline (Johnson 2012). This would include potential changes to important behaviors for an animal's livelihood such as foraging (Croll *et al.* 2006, McCarthy *et al.* 2011, Manzano-Roth *et al.* 2016), mating (Blom *et al.* 2019), and migrating (Malme 1984).

Much of the work addressing the effect of anthropogenic noises on marine life has focused on marine mammals, for which the research has been heavily motivated by the protection of marine mammals under the Marine Mammal Protection Act (MMC 2015). One of the most vulnerable groups of marine mammals to anthropogenic noise appears to be beaked whales, as evidenced by the numerous strandings often linked to naval training exercises (Frantzis 1998, Evans and England 2001, Fernandez *et al.* 2012, D'Amico and Pittenger 2009). As a result, there have been several studies investigating beaked whale foraging behavior during exposure to mid-frequency active sonar (MFAS) used during naval training exercises (McCarthy *et al.* 2011, Tyack *et al.* 2011, DeRuiter *et al.* 2013, , Manzano-Roth *et al.* 2016, Falcone *et al.* 2017, DiMarzio *et al.* 2019). Several of these studies capitalized on the use of expansive hydrophone arrays found on United States Navy training ranges that are capable of receiving the echolocation

clicks of foraging beaked whales (Jarvis *et al.* 2014). A Group Vocal Period (GVP), which represents a group of beaked whales foraging together in time and space, is a set of species-specific echolocation click trains associated to a central hydrophone of the foraging event (McCarthy *et al.* 2011). The GVP has been used as a proxy to assess foraging behavior across different time periods related to MFAS activity (McCarthy *et al.* 2011, Manzano-Roth *et al.* 2016, DiMarzio *et al.* 2019).

The spatial extent of the U.S. Navy hydrophone arrays extends over a couple thousand square-kilometer area. The MFAS and beaked whale foraging studies utilizing these arrays has included a temporal analysis (DiMarzio *et al.* 2019) in addition to a spatial analysis in some cases (McCarthy *et al.* 2011, Manzano-Roth *et al.* 2016). In the McCarthy *et al.* (2011) and Manzano-Roth *et al.* (2016) MFAS studies, heat maps of where the foraging events took place *Before*, *During*, and *After* MFAS activity were generated to provide insight into how the spatial use of the hydrophone arrays changed during the analysis periods. The lack of a more robust spatial analysis was likely the result of a clear temporal and spatial change in beaked whale foraging effort due to MFAS activity that did not require statistics to validate the obvious visual response reflected in the heat maps. The temporal analyses showed that the number of foraging events decreased on the array *During* MFAS activity, while the spatial analyses showed that most of the foraging effort shifted toward the edge (Manzano-Roth *et al.* 2016) or completely off the hydrophone array (McCarthy *et al.* 2011).

While it is clear that MFAS has an impact on beaked whales, the question has arisen as to the potential impact of other sonar signals on marine mammals, in particular, scientific echosounders. There have been several observational studies that suggest marine mammals react to high frequency scientific echosounders, either ceasing echolocation transmissions (Cholewiak

et al. 2017), or increasing their heading variance (Quick *et al.* 2017). In 2008, there was a stranding event of melon-headed whales off of Madagascar that was associated in time with an offshore deep-water multibeam echosounder (MBES) mapping project 65 km away from the stranding site, though it was never conclusively determined to be the cause of the stranding (Southall *et al.* 2013). The increase in prevalence of these systems due to their expanding use in scientific work, geophysical surveys, and ocean mapping efforts has warranted further investigation of the potential effects echosounders may have on marine mammals.

This paper builds off of a recent study investigating the effect of deep-water MBES (12 kHz) activity on Cuvier's beaked whale foraging behavior (Kates Varghese *et al.* 2020), of which the analysis was modeled after similar MFAS work (McCarthy *et al.* 2011). Kates Varghese *et al.* (2020) presented a temporal assessment of foraging behavior *Before, During,* and *After* two MBES surveys conducted over the Southern California Antisubmarine Warfare Range (SOAR) hydrophone array of the U.S. Navy Southern California Offshore Range (SCORE). The temporal assessment of beaked whale foraging *During* MBES did not show a clear change in behavior with regards to MBES activity like that of the MFAS studies. Only one of the four metrics (number of GVPs, number of clicks per GVP, GVP duration, and click rate per GVP) used to assess foraging behavior changed *During* MBES activity; there was an increase in the number of GVPs per hour. A finer temporal analysis of each survey showed that the increase in the number of GVPs occurred during only one of the two surveys (Kates Varghese *et al.* 2020). And the number of GVPs increased again after the survey was complete, thereby providing no clear indication that the change was associated with the anthropogenic activity like that of the MFAS studies. Moreover, the increase in the number of GVPs during the MBES survey was a stark contrast to the decrease in the number of GVPs seen during the MFAS exercises.

In the MBES study, it was unclear through the temporal analysis alone whether the increase in the number of GVPs during one of the two MBES survey periods was associated with the MBES activity. In order to provide a more complete picture of the potential effect of deep-water MBES as a sound source on beaked whale foraging behavior, a spatial analysis of beaked whale foraging behavior was conducted herein for the same two MBES surveys as the Kates Varghese *et al.* study (2020). In the MFAS studies, spatial distribution maps of foraging events were used and provided another perspective on the effect that MFAS had on beaked whale foraging behavior. Not only did many of the animals decrease vocalizations but they visibly changed where they were predominantly foraging (McCarthy *et al.* 2011, Manzano-Roth *et al.* 2016), and sometimes left the U.S. Navy range where the MFAS was actively transmitting, clearly indicating a response to the MFAS activity. Here a robust spatial analysis, beyond spatial distribution maps, was conducted to provide greater insight and to complement the temporal results in a comprehensive understanding of the potential impact of MBES on beaked whale foraging. In particular, the Global-Local Comparison (GLC) method described in Kates Varghese *et al.* (2021a) was used, which was developed to robustly assess spatial marine mammal behavior across large-scale hydrophone arrays using spatial statistics and analysis of variance tests.

Materials and Methods

This work utilized data from 89 hydrophones from the SOAR hydrophone array. The bottom-mounted hydrophones placed two to six km apart are found at depths ranging from 840 to 1750 m over an area of approximately 1800 km^2 off of San Clemente Island, California. The SOAR is shallowest along San Clemente Island in the southeast region, near which a shallow canyon is found before dropping off to 1500 m or greater over most of the rest of the range

(Figure 4.1). The omnidirectional hydrophones were sampled at 96 kHz, and had a receiver bandwidth between 50 Hz and 48 kHz (DiMarzio and Jarvis 2016). Due to their high site fidelity at the SOAR (Falcone *et al.* 2017), Cuvier's beaked whales and echolocation clicks from these animals, transmitted during foraging events, are routinely detected on the SOAR hydrophones.

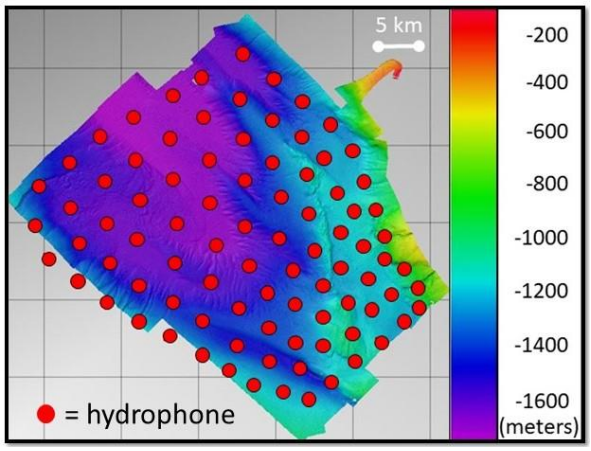

Figure 4.1. Bathymetry of the SOAR with overlaid 89 hydrophone (red circles) sensors in the array. Depth scale is in meters. (Published first in Kates Varghese, H., Miksis-Olds, J., DiMarzio, N., Lowell, K., Linder, E., Mayer, L.A., Moretti, D. (2020). The Effect of Two 12 kHz Multibeam Mapping Surveys on the Foraging Behavior of Cuvier's Beaked Whales Off of Southern California. *J. Acoustic. Soc. Am.* 147(6), 3849-3858, reproduced with the permission of the Acoustical Society of America.)

As a follow-on to earlier work assessing the effect of MBES activity on the temporal aspects of Cuvier's beaked whale foraging behavior (Kates Varghese *et al.* 2020), the same detection and data processing schemes used in that study were used here. Echolocation clicks from several marine mammal species at the SOAR were detected using a class-specific support vector machine. Those that were classified as Cuvier's beaked whale foraging clicks were formed into click trains on a per hydrophone basis. Then a MATLAB-based auto-grouper program used a set of rules based on the time and location of the click trains to form the GVPs (DiMarzio *et al.* 2018, Moretti 2019). A GVP may be detected on multiple hydrophones, but the hydrophone that records the highest click density is defined as the center hydrophone of the

event. The center hydrophone was used as the location of a GVP in this study. The maximum detection range of Blainville's beaked whale clicks was measured at 6.5 km at a U.S. Navy range in the Bahamas by cross-correlating the pattern of clicks identified on a DTAG, produced by the tagged animal, against the click patterns on surrounding bottom-mounted range hydrophones (Ward *et al.* 2008). These animals have a similar click source level and dive behavior to Cuvier's beaked whales (Johnson *et al.* 2004, Tyack *et al.* 2006). Previous studies at the SOAR have used an estimated horizontal detection distance of 6.3 km in defining a spatial range for Cuvier's beaked whale clicks detected from a single group (Kates Varghese *et al.* 2020). This detection range was assumed to be true for this study as well. The number of GVPs, per hydrophone, was used as a proxy to assess spatial foraging effort. For complete details on the detection and processing of GVPs see DiMarzio *et al.* (2018) and for its application to this work see the Materials and Methods section of Kates Varghese *et al.* (2020).

The method and data of this research study provide the opportunity to assess the change in overall spatial foraging behavior amongst Cuvier's beaked whales on the SOAR i.e., the "foraging effort." This broad-stroke term is used because it emphasizes that this approach is agnostic to group size and composition, as both attributes can be ephemeral, in addition to other unknown factors such as foraging rates. Past studies of Cuvier's beaked whales have shown that this species is known to forage in small groups that can vary in composition (Moulins *et al.* 2007) and change in size (McSweeney *et al.* 2007). Animals may leave one foraging group and begin foraging with another. A group of animals may leave an area, while another group arrives, and numerous groups could be foraging simultaneously in a particular location (Falcone *et al.* 2009). Frequently at SOAR it appears that multiple small groups are foraging in the same general area, ensonifying some common hydrophone. Therefore it is important to note that a GVP

represents a single detected period of a group of beaked whales foraging, but a GVP is not tied to a specific group of animals. The formation of GVPs is an automated process based on a fixed set of rules, but the group of individuals it represents may differ. Thus this is not an assessment of specific individuals or the behavior of a specific group, rather overall group-level foraging effort.

Two MBES surveys were conducted, one in January 2017 (Mayer 2017, Smith 2019) and the other in January 2019 (Mayer 2019), as part of a MBES characterization project for the Kongsberg EM 122, a deep water MBES. Both surveys utilized the UNOLS research vessel R/V *Sally Ride* and its hull-mounted EM 122 (12 kHz center frequency) operating with typical parameters used for mapping a deep-water environment such as the SOAR (Table 4.1). The survey in 2017 followed a characteristic mowing-the-lawn pattern across the entire SOAR (Figure 4.2 *left*), whereas the efforts of the 2019 characterization survey required a tighter mowing-the-lawn pattern confined to the canyon in the southeastern corner of the SOAR in addition to a few cross-range lines (Figure 4.2 *right*). These surveys served as an opportunity to assess the effect of MBES on the spatial foraging effort of Cuvier's beaked whales. Because the exact movement of a vessel and hull-mounted MBES will vary from survey to survey based on the needs of the operation, the assessment of the two surveys provided a chance to observe potential variability in beaked whale spatial foraging effort during two separate MBES surveys.

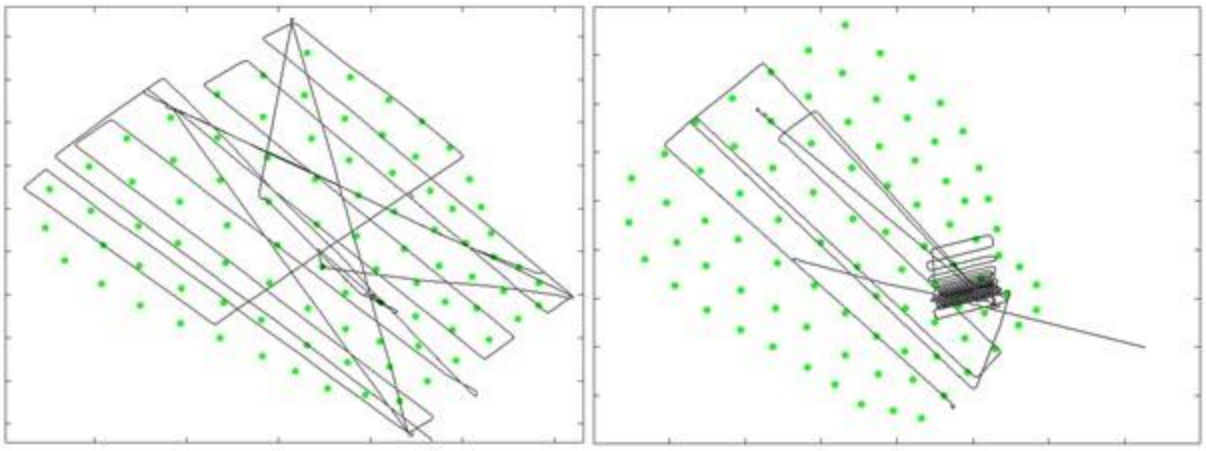

Figure 4.2. Track lines from the 2017 (left) and 2019 (right) MBES surveys. (Published first in Kates Varghese, H., Miksis-Olds, J., DiMarzio, N., Lowell, K., Linder, E., Mayer, L.A., Moretti, D. (2020). The Effect of Two 12 kHz Multibeam Mapping Surveys on the Foraging Behavior of Cuvier's Beaked Whales Off of Southern California. J. Acoustic. Soc. Am. 147:6, 3849-3858, reproduced with the permission of the Acoustical Society of America.)

Table 4.1. MBES signal attributes and the estimated value for the 2017 and 2019 MBES surveys.

MBES Signal Attribute	**Estimated value**
Source Level (SPLrms)	239-242 dB re 1 µPa @1 m
Center Frequency of Transmission	11-13.25 kHz
Transmission length	on the order of 100 ms
Time between pulses	6-7 s
Beam width (-3dB relative to reported source level) and geometry	1º along-track by ~150 º across-track; directed vertically toward seafloor

In order to assess the effect of MBES activity on the spatial foraging effort of Cuvier's beaked whales, the number of GVPs were summed by hydrophone over each analysis period: *Before*, *During*, and *After* for each of the two MBES surveys. The same analysis periods assessed in the temporal analysis (Chapter 2, published in Kates Varghese *et al.* 2020) were used here for consistency (Tables 4.2 and 4.3 for the 2017 and 2019 surveys, respectively). In the 2017 survey, each analysis period was 47 hours long, whereas in 2019, each analysis period was 52 hours long. These analysis periods were based on and equivalent to the length of time that the MBES was operating in each year.

Table 4.2. Analysis period times and details of the 2017 data set.

Analysis Period	**Date Time**	**Details**
Before	1/2/17 08:15-1/4/17 07:15	47 hour period ending 25 hours before MBES activity started on the array
During	1/5/17 08:15-1/7/17 07:15	47 hours, MBES activity on the array
After	1/8/17 08:15-1/10/17 07:15	47 hour period starting 25 hours after MBES activity ended on the array

Table 4.3. Analysis period times and details of the 2019 data set.

Analysis Period	**Date Time**	**Details**
Before	1/1/19 12:00-1/3/19 16:00	52 hour period ending 20 hours before MBES activity started on the array
During	1/4/19 12:00-1/6/19 16:00	52 hours, MBES activity on the array
After	1/7/19 12:00-1/9/19 16:00	52 hour period starting 20 hours after MBES activity ended on the array

Though it was not explicitly addressed in this study, previous research has shown that environmental and oceanographic conditions can affect prey availability on various spatiotemporal scales, impacting marine predator-prey relationships (Sims *et al.* 2006, Thayer and Sydeman 2007, Embling *et al.* 2012, Santora *et al.* 2014, Cox *et al.* 2018). Based on this knowledge, it was expected that environmental conditions and prey distributions that could drive the beaked whales' spatial use of the SOAR would vary on a timescale of less than two years (the time between the two surveys). Thus each survey year was assessed individually.

The Global-Local-Comparison (GLC) Approach (Chapter 3, published in Kates Varghese *et al.*, 2021a), a spatial assessment for analyzing marine mammal behavior on large hydrophone arrays, was used here. This method included two statistical spatial analyses: a global and local approach, as well as comparison analysis of variance tests and visualization tools for interpreting the statistical results. The global analysis used the Moran's I statistic (Moran 1948) to provide a coarse assessment of the type of spatial distribution, i.e., clustered, random, or dispersed, of the

foraging events over the SOAR as a whole. The local approach used the Getis-Ord Gi* statistic (Getis and Ord 1992), a local indicator of spatial association (Anselin 1995), which identifies where relative hot and cold spots of foraging activity occurred on a per hydrophone basis. The comparison analysis used the Kruskal-Wallis test (Kruskal and Wallis 1952) to identify order-of-magnitude differences in the number of GVPs per hydrophone among analysis periods.

Global Analysis

In order to assess the spatial distribution of the foraging events over the entire SOAR, the global statistic, Moran's I, was used. Moran's I measures the overall spatial autocorrelation of a data set, producing a value between (-1, 1). A value of negative one corresponds to perfect dispersion (Figure 4.3 *left*), a value of positive one corresponds to perfect clustering of like values (Figure 4.3 *right*), and zero represents no autocorrelation, or a perfectly random distribution (Figure 4.3 *middle*).

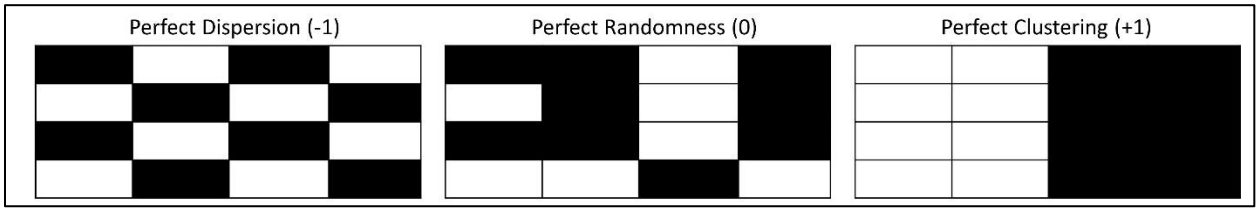

Figure 4.3. From Kates Varghese *et al.* (2021a, also Chapter 3). Spatial configurations that would result in ideal Moran's I values: *left*- perfect dispersion, Moran's I value=-1; *middle*-perfect randomness, Moran's I value=0; *right*-perfect clustering, Moran's I value=+1.

Moran's I is given by the formula:

$$I = \frac{N}{W}\frac{\sum_i\sum_j w_{i,j}(x_i-\overline{x})(x_j-\overline{x})}{\sum_i(x_i-\overline{x})^2} \qquad \text{(Equation 4.1)}$$

where $W = \sum_{i=1}^{n}\sum_{j=1}^{n} w_{i,j}$ with $w_{i,j}$ being the weighting between the i^{th} and j^{th} hydrophone and *w* represents the neighbor weighting matrix of *i* rows and *j* columns. x_i refers to the i^{th} hydrophone value, in this case the number of GVP of the i^{th} hydrophone and $\overline{x}$ is the mean number of GVPs over all of the hydrophones. A queen's contiguity neighbor weighting rule was

used here as was recommended for similar data in Kates Varghese *et al.* (2021a, also Chapter 3). The queen criterion defines neighbors as spatial units that share a boundary with the hydrophone of interest (i.e., all hydrophones immediately horizontal, vertical, or diagonal). Thus, the maximum number of neighbors an interior hydrophone could have is eight, whereas edge and corner hydrophones will have fewer.

The Moran's I statistic for each analysis period was converted to a z-score. To aid in the interpretation of the global results, p-values were computed for each z-score. The smaller the p-value, the greater the discrepancy between the observed data and the null hypothesis being tested (Tanha *et al.* 2017). The null hypothesis for the Moran's I analysis was that the spatial distribution of GVPs under consideration, for any of the analysis periods, was no different from random (I=0). Alternatively, it was hypothesized that the spatial distribution was clustered (I=+1) during each analysis period, *Before, During,* and *After*, since beaked whales are known to primarily forage in the deepest part of the SOAR (Falcone *et al.* 2009, Schorr *et al.* 2014, DiMarzio *et al.* 2019, Southall *et al.* 2019). The Moran's I statistic, along with the p-value, was used to make a statement about whether the GVPs were clustered or not.

Local Analysis

If global spatial correlation – clustering or dispersion -- was detected, the Getis-Ord Gi* (Gi*) local statistic was also computed. The Gi* statistic was found for each hydrophone using the formula:

$$G_i^* = \frac{\sum_{j=1}^{n} w_{i,j}x_j - \overline{X}\sum_{j=1}^{n} w_{i,j}}{S\sqrt{\frac{n\sum_{j=1}^{n} w_{i,j}^2 - (\sum_{j=1}^{n} w_{i,j})^2}{(n-1)}}} \qquad \text{(Equation 4.2),}$$

where $S = \sqrt{\frac{\sum_{j=1}^{n} x_j^2}{n} - (\overline{X})^2}$ and $\overline{X} = \frac{\sum_{j=1}^{n} x_j}{n}$ and the remaining variables were the same as described for the Moran's I statistic. This statistic was used to understand where, i.e., on which

specific hydrophones, the spatial correlation (relative hot or cold spots) occurred within the SOAR. For example, to be a relative hot spot, a hydrophone must be surrounded by other hydrophones that also exhibit a high number of GVPs and vice-versa for a relative cold spot. What constitutes a high or low number of GVPs will change depending on the specific set of data, their distribution and variance, which are all considered in the Gi* calculation.

P-values associated with each Gi* statistic, which is itself a z-score, were computed to help understand how the observed Gi* results differed from the null hypothesis. The null hypothesis was that GVPs were randomly distributed and thus that there were no relative hot or cold spots of foraging activity. A small p-value indicated a greater discrepancy from this null hypothesis suggesting a spatial anomaly – i.e., an area of congregation or absence. Since there are 89 hydrophones on the SOAR, alternative hypotheses were not made about individual hydrophones. However, it was hypothesized that the northwest part of the SOAR, which has the deepest depths, and where the animals are historically known to forage (Falcone *et al.* 2009, Schorr *et al.* 2014, DiMarzio *et al.* 2019, Southall *et al.* 2019), would be an area of high foraging activity (i.e., hot spots), while the shallow area in the southeast along San Clemente Island would have low foraging activity (i.e., cold spots). It was hypothesized that the relative hot and cold spots, with respect to foraging, would remain in these respective areas throughout the three analysis periods, which would indicate the spatial distribution of GVPs did not change during MBES activity.

Comparison Analysis

Although the spatial statistics provided insight into spatial changes on the SOAR, they did not provide information about differences in scale, i.e., the average number of GVPs per hydrophone occurring on the SOAR in the various analysis periods. In addition to, or in the absence of a spatial change, understanding potential order-of-magnitude differences in the number of GVPs detected provided further information about the extent of change. Following the

GLC method from Kates Varghese *et al.* (2021a, also Chapter 3) for similar data, the Kruskal-Wallis test was used to compare the magnitude of observations among different analysis periods. For both years of study, the null hypothesis was that there was no difference in the number of GVPs per hydrophone on the SOAR among the analysis periods. Difference plots of the hydrophone array were also generated to show spatially what the relative change (e.g., increase, decrease, or no change) was in the number of GVPs between consecutive analysis periods.

The GLC approach is further developed and described in more detail in Kates Varghese *et al.* (2021a, also Chapter 3).

Results

2017

Of the 47 hours analyzed for each of the three analysis periods in 2017, there were 127 GVPs detected across the 89 hydrophones *Before,* 135 *During,* and 148 *After.* The results of the global analysis are provided in Table 4.4. For all analysis periods of 2017, the Moran's I value suggested strong spatial clustering of GVPs on the SOAR.

Table 4.4. Global analysis results by analysis period for 2017, including Moran's I value (I), the z-score (z_I), and the associated p-value. A positive I indicates a clustered distribution, a negative I represents a dispersed distribution, and the p-value associated with each.

Analysis Period	**Moran's I (I)**	**z-score (z_I)**	**p-value**	**Conclusion**
Before	0.2472	4.6851	<0.001	Clustered
During	0.2108	4.0260	<0.001	
After	0.3706	6.9217	<0.001	

The total number of GVPs detected and the respective Gi* z-score for each hydrophone was calculated and is shown in the map presented in the first and second columns, respectively, of Figure 4.4 for each analysis period of 2017. To aid in the designation and interpretation of hot

and cold spots in the Gi* results, p-values equal to or less than 0.1, or equal to and more than 0.9 were mapped along-side the Gi* results (Figure 4.4, *column 3*). Hydrophones with p-values of 0.1 or less provided the strongest evidence of hot spots on the Gi* plot, while a p-value of 0.9 or more provided the strongest evidence of a cold spot on the Gi* plot. Exact Gi* and p-values for all hydrophones are provided in the data section of this publication. Ultimately, a critical alpha level of 0.05 was used to guide the final interpretation of the Gi* results. Because of the two-tailed nature of this analysis (hot and cold spots), the authors focused on areas with p-values less than or equal to 0.025 (hot) or greater than or equal to 0.975 (cold) in the descriptive interpretation of the Gi* results that follows.

In each analysis period, there was a clustering (i.e., a group of several adjacent hydrophones) of hot spots in the northwest corner of the SOAR (Figure 4.4, *column 3*), overlapping the deeper waters of the SOAR (Figure 4.1). This result matched expectations since this area has historically been noted as favorable foraging grounds for these animals due to the deep-water conditions (Falcone *et al.* 2009, Schorr *et al.* 2019), providing ideal habitat for the squid that Cuvier's beaked whales prey upon (Santos *et al.* 2001). The exact cluster of hot spot hydrophones shifted slightly between analysis periods. However, based on the recommendation of Kates Varghese *et al.* (2021a, also Chapter 3) in the development of the GLC method, the general area of hot/cold spot clusters should be compared rather than employing a precise comparison of individual hydrophones. Since many of the hydrophones in the hot spot cluster were the same across analysis periods and remained in the same general area in the deepest part of the SOAR, this result suggested no obvious change occurred in spatial foraging effort in the 2017 study.

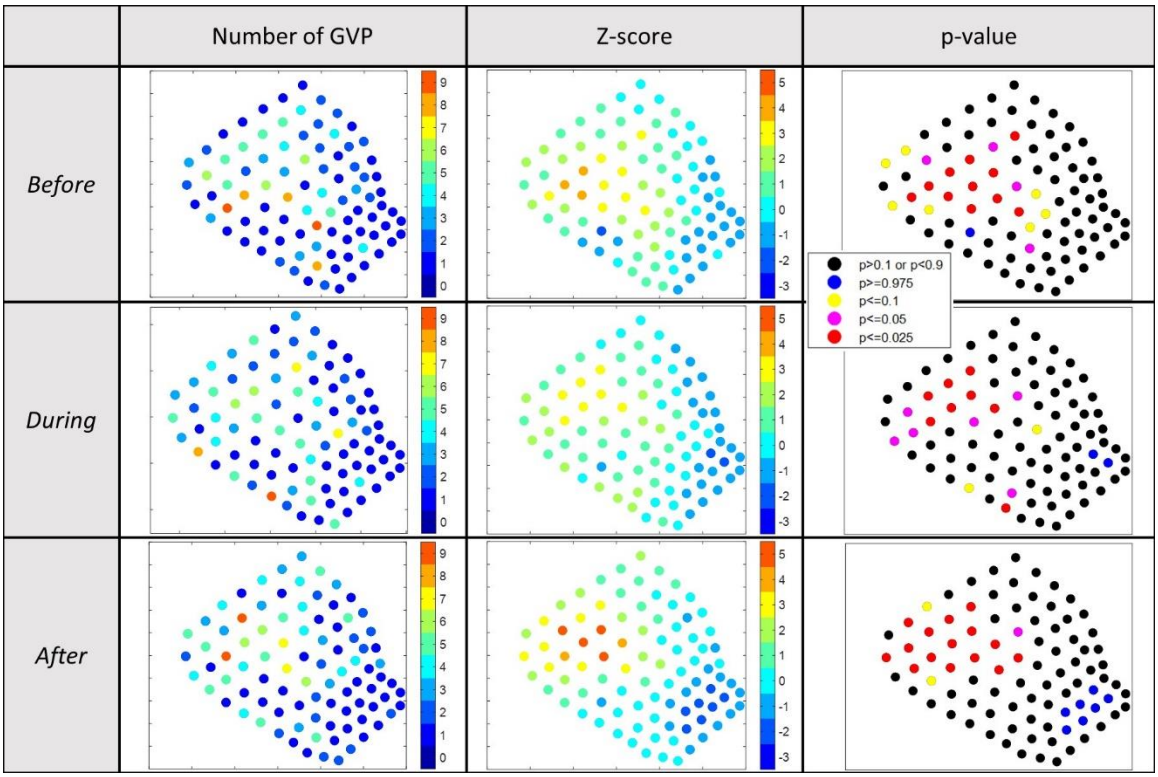

Figure 4.4. Results of the 2017 Gi* analysis for local hot/cold spots. Column 1: visual depiction of the number of GVP by hydrophone; column 2: visual depiction of the Gi* z-values by hydrophone; column 3: visual depiction of the p-values associated with the Gi* results by hydrophone. $p<0.025$ were considered relative hot spots, whereas $p>0.975$ were considered relative cold spots. Each row represents a different analysis period: top-*Before;* middle-*During*; bottom-*After.*

With respect to where there were very few GVPs, there was one cold spot hydrophone in the central-western part of the SOAR in the *Before* period and a small cluster of hydrophones signifying cold spots in the southeast corner of the SOAR *During* and *After*. Overall the southeastern corner – the relatively shallow and historically least-used area (Falcone *et al.* 2009, Schorr *et al.* 2014) -- was not a high-use area for foraging beaked whales (Figure 4, column 1). Thus, the Gi* analysis further suggested no obvious spatial change occurred in beaked whale foraging effort among analysis periods in 2017 at a local level. This finding was supported by the

difference plots for which the spatial distribution of hydrophones that exhibited no change, increase, or decrease in the number of GVPs appeared random (Figure 4.5).

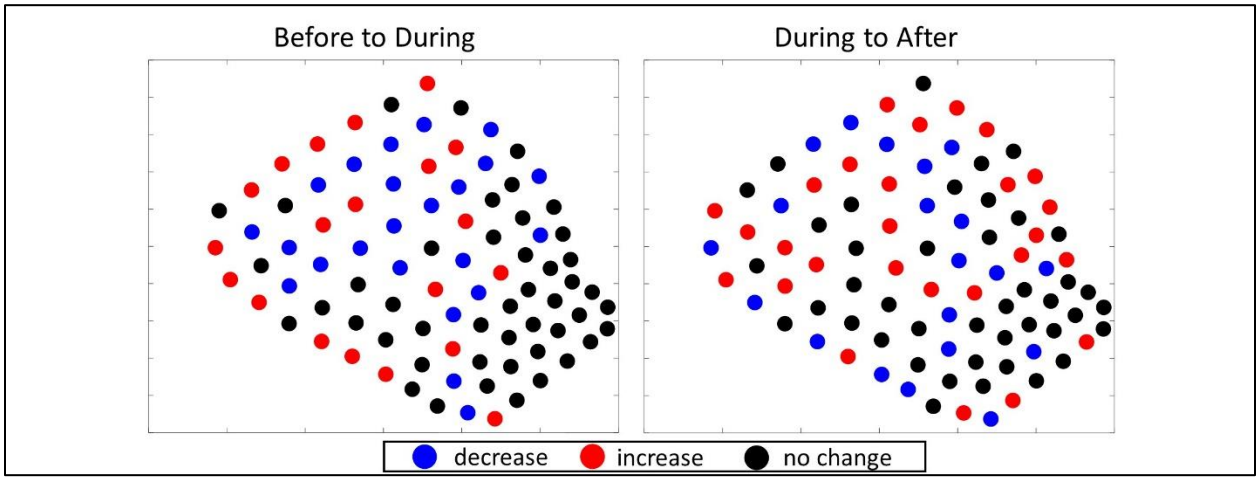

Figure 4.5. Difference plots showing the direction of change in the number of GVPs per hydrophone from one period to the next of the 2017 survey. *Left:* difference plot showing change from *Before* to *During*; *Right:* difference plot showing change from *During* to *After*.

Not only was there no overall change in the spatial location of relative hot/cold spots among analysis periods, but the Kruskal-Wallis comparison test revealed that the total number of GVPs per hydrophone among the three analysis periods were similar [H (2) =1.24, p=0.5369].

Overall the GLC spatial analysis of the 2017 study showed a consistent pattern, both globally and locally, in spatial clustering of GVPs and a similar number of GVPs for non-MBES and MBES analysis periods.

2019

52 hours of hydrophone data were analyzed for each of the three analysis periods in 2019. There were 60 GVPs detected *Before*, 93 *During*, and 77 *After*. The global analysis results are provided in Table 4.5. For each of the three analysis periods the Moran's I value strongly suggested GVPs were spatially clustered on the SOAR.

Table 4.5. Global analysis results by analysis period for 2019, including Moran's I value (I), the z-score (z_I), and the associated p-value. A positive I indicates a clustered distribution, a negative I represents a dispersed distribution, and the p-value associated with each.

Analysis Period	**Moran's I (I)**	**z-score (z_I)**	**p-value**	**Conclusion**
Before	0.1105	2.2082	0.0139	Clustered
During	0.2078	3.9711	<0.001	
After	0.1265	2.4991	0.0064	

The total number of GVPs detected, the Gi* z-score, and associated p-values were calculated and are shown by hydrophone in Figure 4.6, *columns 1-3*, respectively. Exact Gi* and p-values for all hydrophones are provided in the data section of this publication. A similar interpretation of Figure 4.6 was conducted as described for the interpretation of the 2017 local results. There were no obvious cold spots identified in the 2019 analysis periods, suggesting widespread use of the SOAR by foraging beaked whales in 2019 (Figure 4.6). There were distinct hot spot clusters identified in each analysis period. In the *Before* period the hot spot cluster was in the southwestern corner of the SOAR, *During* MBES activity the hot spot cluster was in the center, and *After* MBES activity there were several hot spot hydrophones in the center and a cluster of hot spot hydrophones in the southwestern corner of the SOAR (Figure 4.6). These results suggested that local spatial foraging effort did change during the 2019 study, a finding that was supported by a distinguishable spatial pattern visible in the 2019 difference plots (Figure 4.7). That is, there was a cluster of hydrophones in the center of the SOAR that all recorded an increase in GVPs from *Before* to *During* (Figure 4.7 *left),* while from *During* to *After* (Figure 4.7 *right*) there was a cluster of hydrophones in the center that all decreased in the number of GVPs.

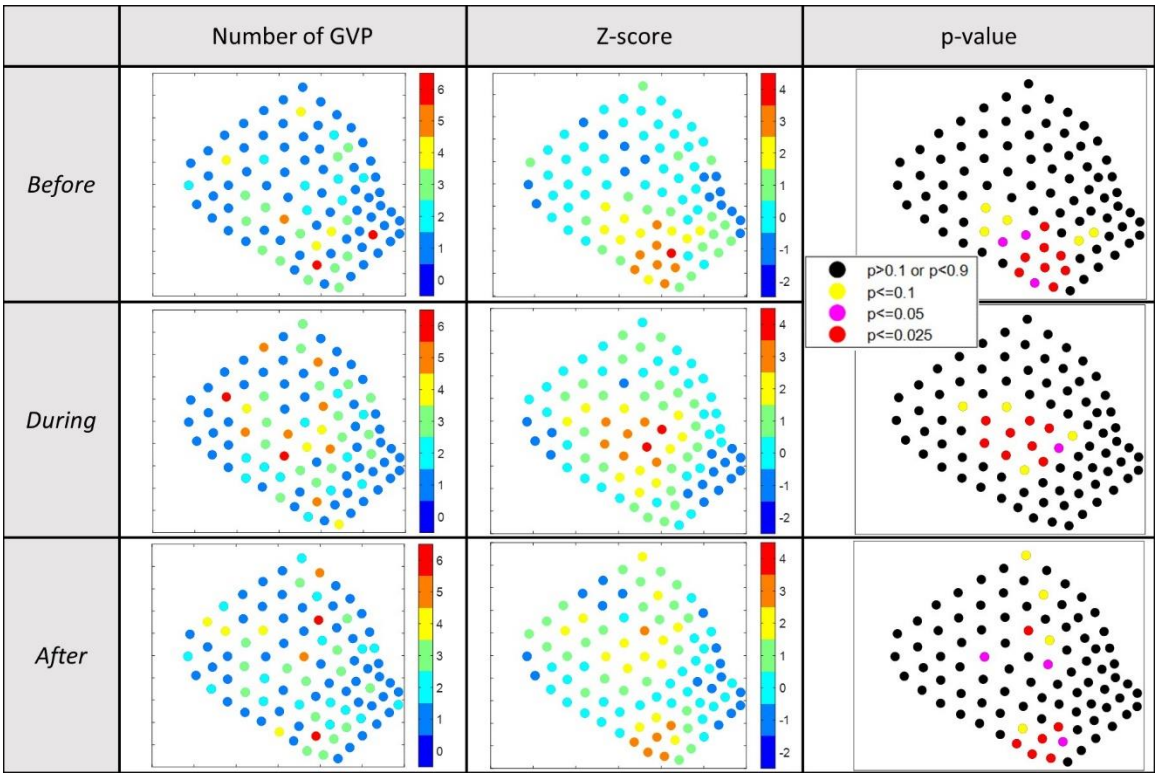

Figure 4.6. Results of the 2019 Gi* analysis for local hot/cold spots. Column 1: visual depiction of the number of GVP by hydrophone; column 2: visual depiction of the Gi* z-values by hydrophone; column 3: visual depiction of the p-values associated with the Gi* results by hydrophone. $p<0.025$ were considered relative hot spots, whereas $p>0.975$ were considered relative cold spots. Each row represents a different analysis period: top-*Before;* middle-*During*; bottom-*After*.

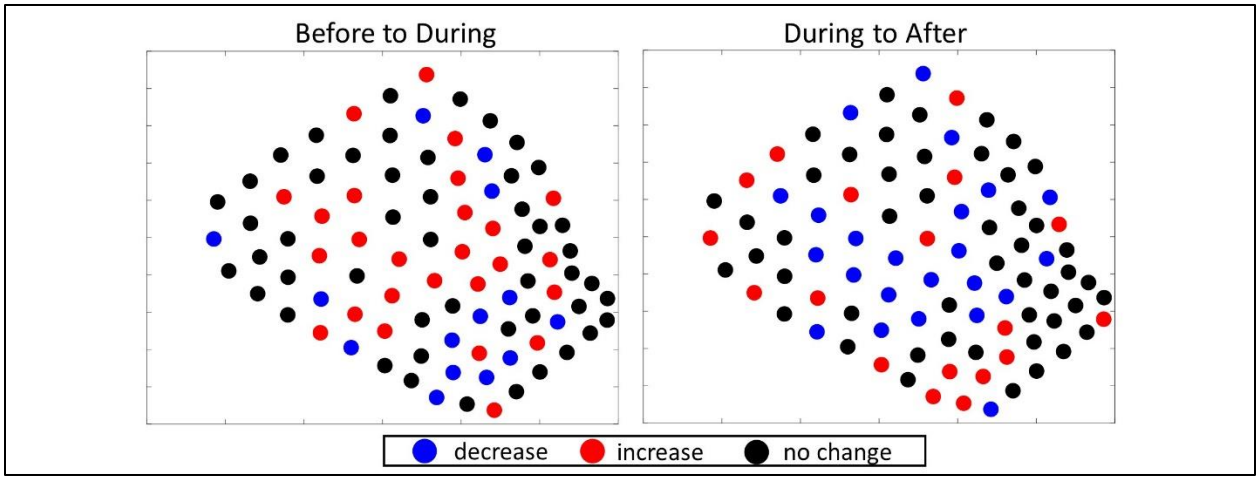

Figure 4.7. Difference plots showing the direction of change in the number of GVPs per hydrophone from one period to the next of the 2019 survey. *Left:* difference plot showing change from *Before* to *During*; *Right:* difference plot showing change from *During* to *After*.

The Kruskal-Wallis comparison test showed that the number of GVPs per hydrophone were similar between the three analysis periods [H (2) =3.95, p=0.1387].

Overall the GLC spatial analysis of the 2019 study showed foraging effort was consistently clustered, and the overall magnitude of foraging effort was similar throughout the 2019 analysis periods. But, the location of the foraging hot spot cluster changed through time.

Discussion

The global analysis revealed that GVPs on the SOAR were notably clustered spatially in all analysis periods in both 2017 and 2019. In addition, the comparison tests for both years revealed that the overall number of GVPs detected per hydrophone was equivalent among analysis periods within each year. These results suggest that no obvious range-wide change in foraging effort occurred during MBES activity. The local results for the two surveys were not the same. In 2017, foraging hot and cold spots were respectively identified in the same general area of the SOAR during all three analysis periods. In 2019, foraging hot spots were identified in each analysis period, but the location shifted through time. Like the temporal analysis of foraging

behavior during the two MBES surveys (Chapter 2, also Kates Varghese *et al.* 2020), the difference in local spatial results between the two years brings in to question whether the MBES activity (i.e., different spatial usage of the SOAR) could have contributed to the differences identified, or if the differences were related to variability in some other factor, such as prey distribution during the two years of study.

The results of the 2017 local analysis identified relative hot and cold spots in the same general area of the SOAR, but during each period on a slightly different set of hydrophones in the array. There are likely multiple interacting reasons for the slight difference in cluster locations. Firstly, even if the animals tend to forage in the same area throughout time, it is within reason to expect some amount of variation due to the natural variability in behavior (e.g., the animals are mobile, peaks and lulls in foraging are observed even in the absence of anthropogenic activity) (Falcone *et al.* 2017, Schorr *et al.* 2014), and because a cluster likely represents numerous groups foraging, each with their own movements over the wider area. Additionally, there may have been small changes in the distribution of prey, due to varying environmental conditions, which could have affected exact foraging locations. Lastly, the Gi* statistic, the statistic used in the local analysis, is a function not only of the number of GVPs at a specific hydrophone, but of its neighboring hydrophones as well. This can lead to a slightly different spatial z-score pattern, despite a generally very similar spatial data set. For this reason Kates Varghese *et al.* (2021a, also Chapter 3) recommended that it is most appropriate to interpret change in spatial behavior using the GLC method more holistically than on a single hydrophone basis to account for some of the sensitivity in the Gi* statistic. Most of the GVPs occurred in the northwest and north-central parts of the array and were lacking in the southeast. Since many of the hot spot hydrophones overlapped from one period to the next, there was no

indication from this analysis that the area used for foraging had changed in an obvious way that would suggest the 2017 MBES survey had an effect.

The interpretation of the local analysis result for 2019 was less clear. *Before* the MBES survey, a distinct cluster of foraging hot spots was identified in the southwestern corner of the SOAR, *During* the survey a distinct cluster of foraging hot spots was identified in the center, and *After* there was a distinct hot spot cluster in the southwestern corner and potentially another hot spot cluster in the center of the SOAR. In general, the hot spot clusters had minimal overlap across abutting analysis periods, suggesting there was a change in foraging effort at the local level. But the pattern of two potential hot spot clusters identified in the *After* period was perplexing. Specifically, the potential cluster in the center of the array *After* was not as obvious as other clusters, raising the question of whether the center of the SOAR was in fact a highly used area by the animals during this period. Whether it was or not would provide information that could help in ruling out certain potential drivers of the 2019 result.

Referring to the spatial distribution of the 2019 raw data, z-scores, and difference plots provided further insight in interpreting the local result. The spatial distribution of high versus low GVP values *After* appeared random in the center area, suggesting it was only a few hydrophones where many GVPs occurred and not the entire area. In addition, the z-scores of hydrophones in the center in the *After* period were lower in comparison to all of the other hot spot clusters from any of the 2019 analysis periods -- i.e., the center area hydrophones of the *After* period had a z-score value of mostly twos, while all other hot spots had z-scores of mostly threes or fours. This suggests that although there were a high number of GVPs in the center, it was not the most highly used area relative to the rest of the SOAR. In fact, the southwestern corner had higher z-score values during the same period. In examining the difference plots, none

of the center hot spot hydrophones increased in the number of GVPs from *During* to *After*, and most of the GVP values on surrounding hydrophones in the center either decreased or stayed the same, whereas those in the southwestern corner had an increase in GVPs detected. Again, this result suggests that the center was not as active as the southwestern corner of the SOAR *After* the survey. Together, these results best support the interpretation that the center area was no longer as favored by the animals for foraging as it was in the *During* period.

If the spatial change was due to the MBES survey, one would expect a more discrete difference between each set of analysis periods, and thus a clear change back to the southwestern corner *After*. For example, in the McCarthy *et al.* study (2011) in which the analysis periods abutted temporally, there was a distinct spatial change between the *Before, During,* and *After* analysis periods. In a finer temporal analysis of the spatial data, the researchers found that the animals returned to their normal spatial use of the range after 35 hours. In the study herein, there were 20 hours between each set of analysis periods in 2019, and each analysis period lasted 52 hours. If the MBES was the cause of spatial change, assuming a similar response time as in the MFAS study, the temporal spacing in this study (i.e., time between analysis periods plus the duration of an analysis period) should have been more than adequate to capture distinct differences in foraging effort location. If the spatial change was due to a factor that was primarily a function of time rather than related to the MBES survey, one might expect a more gradual spatial change across all three analysis periods. But what occurred was a distinct change in foraging effort (i.e., relative hot spots) location from *Before* to *During* and a spatial pattern suggestive of a gradual change from *During* to *After*, a response somewhere in between the two scenarios that were expected. Thus, it is not readily obvious what the cause of the shift was.

There is no standard definition of what constitutes a meaningful shift in habitat use, especially in the context of response to anthropogenic activity or some other external factor. A meaningful shift in habitat use depends on a number of factors including the behavioral or ecological context for which the shift occurs, the species, suitable habitat connectivity, among many other factors. In the case where a group of animals is negatively affected by a disturbance, there may exist circumstances where either no suitable alternative habitat exists for the animals to move to, or the animals endure the disturbing activity despite potential and realized biological consequences (Claridge 2013, Moretti 2019). In addition the degree to which an easily observable response, such as behavior change, correlates with a meaningful effect, such as biological or physiological change, is not often known (Beale 2007). Our ability to understand the degree to which a measured behavioral response is indicative of something meaningful requires comprehensive integration of the information available regarding the factors under which the behavioral change took place, as well as consideration of other known analogs. With this in mind, potential explanations for the observed shift in spatial use of the SOAR by beaked whales were explored.

Since the 12 kHz MBES sound is within the hearing range of beaked whales (Cook *et al.* 2006, Pacini *et al.* 2011), one explanation for a shift in foraging location is that the whales were disturbed by the anthropogenic activity on the SOAR, e.g., vessel presence, vessel noise, or MBES activity. In the case of a disturbance, movement would be expected away from the disturbing activity. This was the case with beaked whales in response to other sources within their hearing range, such as MFAS (McCarthy *et al.* 2011, Manzano-Roth *et al.* 2016) and acoustic pingers (Carretta *et al.* 2008). In both the McCarthy *et al.* (2011) and Manzano-Roth *et al.* (2016) studies, where a clear negative response to MFAS activity was concluded, the number

of GVPs of Blainville's beaked whales was reduced and the majority of foraging shifted to the edge or off the range during MFAS activity. In the case of the acoustic pingers (10-12 kHz), bycatch of several beaked whale species was reduced to zero after the implementation of the pingers on gillnets in the California drift gill net fishery (Carretta *et al.* 2008). Neither of these were similar to the result seen here.

Alternatively, a shift in foraging effort location could also be due to attraction of the whales to the anthropogenic activity. During the first 24 hours of the 2019 MBES survey (i.e., roughly half of the *During* period) the MBES survey was confined to the southeast corner of the SOAR (see Figure 2 and the supplementary results of Kates Varghese *et al.* 2020 for a detailed description of the MBES surveys—also Figure 2.2 and Appendix 2.1 in this dissertation). Therefore, one might expect if the whales were attracted to the MBES sound that they might move to the southeast corner. Yet, this was not where the foraging hot spots were found. The remainder of the *During* period involved lines that ran across the center of the SOAR in a "mowing-the-lawn" pattern. Given that the MFAS study results (McCarthy *et al.* 2011, Manzano-Roth *et al.* 2016) are viewed as an avoidance response, where many of the animals moved to the edge or off the range, one might view a shift in foraging effort to the center of the SOAR during anthropogenic activity as movement toward, or an attraction to, the activity. In this case it is worth considering the sound propagation of the deep-water MBES on the SOAR. MBES transmit sound toward the seafloor in a beam that is narrow along-track (1º) and broad (~150 º) across-track (Lurton 2016, Kates Varghese *et al.* 2019a). As a result, most of the energy is directed toward the seafloor directly below the vessel as lines are run over the survey area, reducing the acoustic footprint relative to an omni-directional or horizontally transmitting source (Lurton and DeRuiter 2011, Lurton 2016). A preliminary examination of some of the acoustic

data from the hydrophone array from the 2017 survey revealed that the signal from the MBES was only detectable above the noise floor when the vessel was within 10-15 kilometers, or roughly 2-3 hydrophones, from a given hydrophone (Mayer 2019, Kates Varghese *et al.* 2019b). The acoustic data from the array was not available for the 2019 survey as of the writing of this paper, but it is reasonable to expect that the sound propagation during the 2019 survey was similar to the 2017 survey since the survey utilized the same vessel, MBES, and was conducted in a similar sea state (Mayer 2019). Since the MBES was not stationary during the survey, a distance of 10-15 km or less between the vessel and a group of foraging whales was likely only met a small portion of the time. Based on this, one might expect that if the whales heard and were attracted to the MBES that the spatial pattern of their foraging would more closely follow the track lines. This would likely lead to the detection of a more random spatial pattern in the local results than the clustering in the center seen here. Thus it does not seem probable that an attraction to the sound was the cause of the spatial change. However, a full analysis of the soundscape with respect to the distribution of GVPs would be needed to rule this out completely.

Another explanation for a shift in foraging location is due to a change in prey distribution, since foraging behavior in beaked whales is heavily driven by prey dynamics (Benoit-Bird *et al.* 2016, Southall *et al.* 2019, Benoit-Bird *et al.* 2020). The anthropogenic activity could have disturbed or attracted the prey, leading to a change in their distribution (Fewtrell & McCauley 2012), followed by a change in where the whales foraged. Beaked whales primarily forage on deep-water squid (Santos 2001) and some fish, both of which are thought to primarily detect low-frequency (<1 kHz) acoustic signals (in addition to particle motion) (Mooney *et al.* 2010, Popper and Hawkins 2018). Thus it seems unlikely that such prey species would respond to the 12 kHz MBES signal. It is possible that the prey could detect and respond

to vessel noise, which is lower in frequency (<1 kHz). Prey distribution and patchiness can also vary naturally due to normal prey movement over time and/or in response to spatially variable and temporally changing environmental conditions (Benoit-Bird *et al.* 2020). In fact, recent work has shown that within the SOAR, prey fields are heterogeneous over small distances (Southall *et al.* 2019). It is also possible that a specific prey patch was depleted by foraging whales, resulting in their movement to another prey patch elsewhere on the SOAR. Backscatter data from sonar systems can be used to identify squid and other prey items in the water column (Moline and Benoit-Bird 2016, Southall *et al.* 2019), and be used to explore these prey distribution hypotheses. However, the signal needed to achieve an adequate estimate of biological organisms at the depths relevant to beaked whale foraging is not feasible from a traditional hull-mounted MBES (Moline and Benoit-Bird 2016), like the one used in this study. Given the results of this study and the hypotheses explored here, the most probable explanation of the 2019 result is linked to the strong relationship between foraging behavior and prey field dynamics. Without complementary prey field information this cannot be concluded with certainty.

Although there was a change in the spatial use of the array in 2019 and the cause remains unclear there are a few key observations to take away from the 2019 survey. First, the most highly utilized location by the foraging animals (i.e., relative foraging hot spot) remained in the deeper area of the SOAR during all analysis periods. Despite the deeper waters being identified in past studies as the area where these animals forage (Falcone *et al.* 2009, Schorr *et al.* 2014), there may still be negative implications for a shift within this area (i.e., from the southwest to the center). Southall *et al.* (2019) found that even within small areas of the SOAR (the west versus the east for example) prey density can be quite different, which can have huge repercussions on the energetic costliness of an induced spatial change from favorable to unfavorable foraging

grounds (Moretti 2019). However, the number of GVPs detected during the MBES survey period was no different than the non-survey periods. Assuming there was no change in the number of animals foraging, this would suggest that there was not an overall change in foraging effort. Furthermore, the fine-scale temporal analysis of the 2019 survey showed no difference in two other GVP characteristics (i.e., number of clicks per GVP, and click rate per GVP) during the MBES survey versus non-MBES periods (Kates Varghese *et al.* 2020, also Chapter 2 of this dissertation). These results further suggest that there was little change in how the animals were foraging. If there were obvious differences in the number of GVPs and intrinsic characteristics (i.e., number of clicks, click rate) of the GVP, this might suggest there was a change in the quality of the prey field with respect to foraging. In the absence of prey distribution data for this study, these results suggest that the spatial change identified may not be associated with a high energetic cost to the animals. Future studies assessing MBES impact should integrate prey field assessments to verify this. This is extremely important in being able to assess the biological and ecological relevance of a change in behavior.

The spatial change in the 2019 study and absence of change in 2017 raises the question, why was there a difference between the two years? Both surveys were conducted in January, removing potential seasonal differences in beaked whale ecology that might affect behavior. The surveys were also conducted using the same vessel and 12 kHz MBES, and occurred for similar lengths of time (47 hours in 2017 versus 52 hours in 2019). The only known difference between the two surveys were the line plans. The 2017 survey was conducted in a mowing-the-lawn pattern across the full length of the array, whereas the 2019 survey used a tighter mowing-the-lawn pattern confined to the southeast corner of the SOAR before conducting a few full-length passes across the middle of the SOAR. As discussed previously, the spatial change found in the

2019 study does not appear to be driven by MBES activity, so it would seem unlikely that the different line plans were the reason for the inter-annual differences. However, without further evaluation of some or all of the hypotheses posed here, this hypothesis should not be disregarded. It should be noted though that while the "mowing the lawn" survey conducted in 2017 is representative of a typical MBES mapping survey, the localized MBES survey in 2019 was conducted particularly to assess the beam pattern of the MBES system and is not at all representative of the use of MBES in deep-water ocean mapping work.

It is worth drawing attention to the spatial distribution of GVPs in the non-MBES periods before the surveys were conducted. These were also dissimilar between the two years. In 2017, there was relatively minimal GVP activity in the southeast portion of the SOAR, whereas in 2019 there was more widespread use of the entire SOAR. These patterns were seen throughout each respective year, suggesting that there was simply variation in the use of the SOAR by the animals from one year to the next. If the spatial distribution *Before* MBES activity was different between the two years, one cannot therefore assume that the difference between the two years was related to the anthropogenic activity or differences related to the operation of the MBES. Again, since prey distribution heavily dictates where these animals forage, there were very likely differences between prey patches in the two years that led to differences in use of the range both during and outside of periods of anthropogenic activity. Though, this may not be the only possible explanation for differences in spatial use of the SOAR between the two years. Finally, it is important to keep in mind that the spatial statistics used here can only detect patterns at the resolution of the hydrophone array. Any potential changes in the spatial use of the array that happened on a scale finer than the hydrophone spacing of two to six kilometers were not detected. Spatial change in foraging behavior may occur on a different spatial resolution than

was measured here and may have a different consequence on foraging animals. Animal tagging studies and those that focus on individual behavior provide a necessary understanding of finer-scale changes in behavior and potential impacts of anthropogenic noises and should be undertaken with respect to MBES impact where possible in the future.

Conclusion

The overall findings of this spatial analysis align with the conclusions of the temporal assessment (Kates Varghese *et al.* 2020, also Chapter 2 of this dissertation): foraging effort did not change in a stereotyped way that would suggest that the MBES surveys had a clear negative effect. In both years of study, neither the range-wide or order-of-magnitude comparisons revealed any obvious differences in beaked whale foraging during the MBES surveys. In the 2017 MBES survey there was no indication that the overall foraging effort changed spatially on a local level. *During* the 2019 MBES survey there was a change detected in the local spatial use of the SOAR. The change was a shift in the most foraging activity toward the center of the range, which was unlike the typical avoidance response seen several times in studies assessing beaked whale foraging response to MFAS. It was also a shift that remained in the deep-water area of the SOAR, thought to be favorable foraging grounds for beaked whales. This best supports the prey-dependence hypothesis as the cause of spatial change. However, the cause of this change and its overall impact cannot be stated with certainty. Future studies targeting the hypotheses posed here are needed to understand the 2019 result completely and should integrate animal tagging, prey field, and soundscape assessments to establish a more comprehensive picture.

CHAPTER 5: SOUNDSCAPE ASSESSMENT OF THE MARINE ACOUSTIC ENVIRONMENT DURING A DEEP-WATER MAPPING SURVEY

Introduction

In the context of anthropogenic noise and marine life, soundscape studies can provide insight into how, and the extent to which, an acoustic environment changes due to anthropogenic noise-generating activity. When possible, baseline assessments are made to provide a foundation upon which to assess the extent of change beyond expected natural variation. Soundscape studies are imperative for providing context to our understanding of the interplay between anthropogenic activity and marine life, in addition to understanding and assessing changes due to natural phenomena.

The goal of this chapter was to understand how the activity of the 2017 mapping survey impacted the overall marine soundscape of the Southern California Antisubmarine Warfare Range (SOAR). The motivation for this was two-fold. While modelling efforts (Lurton and DeRuiter 2011, Lurton 2016) show that the EM 122 multibeam echosounder - the primary system used in the 2017 mapping survey - has a finite impact on the acoustic environment, a thorough assessment of its impact on the marine acoustic environment in the field during typical operations had not been undertaken prior to this work. And in fact, parallel work characterizing the radiation pattern of the Kongsberg EM 122 system (Smith 2019) showed that this particular model produced grating lobes due to an error in the firmware (which has since been corrected). The presence of unintended grating lobes in the acoustic environment further justifies the need to assess acoustic sources *in situ*, which provides important ground-truthing of modelling efforts and theoretical expectations. This is especially necessary when such unintended outcomes (i.e., grating lobes) may have consequences on vulnerable marine life. Thus, the first motivation for

this chapter was to provide empirical observations of the spatial, temporal, and frequency impact on the marine soundscape of the acoustic sources (vessel sound and active acoustic sources) associated with a typical deep-water multibeam mapping survey. Although multiple active acoustic systems (EM 122, EM 712, Knudsen SBP, and EK-80) were used at different times during the 2017 survey, the primary mapping system was the EM 122 MBES. As such, the emphasis of this soundscape chapter was on characterizing the impact of this system on the marine acoustic environment. However, where possible, the impact of the other systems was examined and discussed. The second motivation for understanding the impact of the mapping survey on the acoustic environment was to provide context and inform the interpretation of results of the earlier behavior chapters, in particular, to understand how the acoustic environment evolved through the various survey-related activities. However, the results of this and the former behavior chapters will not be synthesized here, rather they will be synthesized in the final chapter.

Much of the concern surrounding the relationship between marine life, often marine mammals, and anthropogenic noise is with respect to hearing damage that certain sounds may cause. Significant knowledge has been gained on this topic over the last several decades, helping to determine which aspects of sound are physically most damaging to an animal. These signals tend to be high-amplitude, impulsive, and broadband sounds. Thus, many soundscape studies focus heavily on characterizing and analyzing the changes in sound pressure level amplitudes (Sanchez-Gendriz and Padovese 2016, Putland *et al.* 2017). Research has also shown that the mechanism of marine mammal hearing functions is an energy detector rather than an intensity detector (Tougaard and Beedholm 2018). Thus, the total amount of sound energy contained in a signal over a specified time period, i.e., the sound exposure level, is particularly relevant when

assessing the impact on marine mammals (Martin 2019). More recently, research has shed light on other metrics that can be used to identify physically damaging sounds, such as kurtosis, uniformity, and other measures of impulsiveness (Martin 2019, Wilford *et al.* 2021), although the mainstream use of these for assessing soundscapes has yet to be adopted.

Sounds can have non-injurious impacts on marine life as well, including direct and indirect behavioral and/or ecological effects. For example, anthropogenic sounds can mask important signals such as in conspecific communication, or in auto-communication. These communication signals tend to be species-specific based on the frequencies of best hearing (most sensitive) and overlap with frequencies the animals are able to produce. Thus, another aspect of soundscape studies often focuses on frequency-specific metrics most relevant to the species or acoustic sources under study (Codarin and Picciulin 2015, Haver *et al.* 2019). Octave bands or decidecade bands are commonly used in soundscape assessments motivated by understanding impacts on marine mammals, as this way of summarizing frequency content into bands aligns with how mammals hear (Merchant *et al.* 2012, Erbe *et al.* 2016). Research has shown that there may be other features of sound that make it more or less salient to a specific group of animals (Gotz and Janik 2010, Mikkelsen *et al.* 2017), including the ecological relevance of the signal, how long the sound is present in the soundscape, or its periodicity (Sanchez-Gendriz and Padovese 2016, Wilford *et al.* 2021). For example, marine mammals, that are often the prey of killer whales, respond quite drastically to the sounds of killer whales versus other sounds of similar amplitude (Harris *et al.* 2017); the signals used in acoustic deterrent devices have been optimized to be aversive to particular marine mammal groups, thus deterring them from an area (Mikkelsen *et al.* 2017). Although these attributes of acoustic signals have been identified as

relevant in the discussion of how sound will affect marine life, the specific features that cause such responses are still not fully understood.

One of the most rudimentary and fundamental ways of understanding a soundscape is to review the acoustic data in detail using tools such as spectrograms, long-term spectral averages, and spectral probability density plots, to help contextualize the results (Kaplan and Mooney 2015, Erbe *et al.* 2016, Haver *et al.* 2019). When it comes to comparing soundscapes, large comprehensive data sets must be distilled to a few practical and representative metrics, such as percentiles, medians, and averages (Erbe *et al.* 2016, Haver *et al.* 2019). Many soundscape studies involve manually or automatically identifying contributing sources (Haver *et al.* 2019, Lin, *et al.* 2019) and classifying or quantifying them into categories such as biophony, geophony, and anthropophony (Erbe *et al.* 2016, Putland *et al.* 2017). The specific analyses employed are generally driven by the project-related goals and context, many of which are motivated by a specific time or spatial dimension of interest, or a combination of both (Kaplan and Mooney 2015, Bertucci *et al.* 2015). Statistical hypothesis testing using ANOVA or non-parametric tests is commonly employed (Kaplan and Mooney 2015, McWilliam and Hawkins 2013, Bertucci *et al.* 2015) to identify differences across temporal or spatial metrics that describe the soundscape, such as sound level amplitude metrics, or across acoustic indices such as those that describe biodiversity, complexity, and entropy (Sueur *et al.* 2018, McWilliam and Hawkins 2013, Parks *et al.* 2014). (For a more complete picture of the field of underwater soundscape studies, metrics, and shortcomings, see the review paper by Lindseth and Lobel, 2018.)

Although there are several metrics and types of analyses commonly used in underwater soundscape analyses, including statistical comparisons, there is no defined standard today for processing or reporting soundscape parameters, leaving room for innovative ways to examine

and compare acoustic data. Distilling and comparing large and rich data sets is not unique to the field of underwater acoustics. As such there is a lot to be gained by stepping outside the field and bringing in tools that work elsewhere. As a secondary objective in this chapter, additional analysis tools--beyond those commonly used in underwater soundscape studies-- were explored and used to assess the impact of the mapping survey on the acoustic environment. The strengths and limitations of these tools in addition to more traditional approaches will be discussed.

To achieve the project goals, a comprehensive soundscape study was pursued that provided both temporal and spatial information through amplitude and frequency-based sound level analyses applied to characterize the acoustic environment. The amplitude assessment--which was also considered with respect to frequency (i.e., decidecade bands levels and the application of frequency-weighting)-- was divided into four parts beginning with a time series annotation which provided the most local and detailed perspective of the evolution of sound levels at the SOAR array across the entire study period. To characterize the changing sound pressure levels, several metrics --identified in the time series annotation as clearly changing with respect to the multibeam mapping activity --were examined further in period-specific sound level percentile and sound level distribution comparisons. The sound levels were also considered with respect to acoustic impact on marine mammals and anthropogenic noise regulation thresholds. And finally, a frequency-based correlation analysis was performed providing insight into the how sound pressure levels varied across the frequency domain.

The specific metrics used in the aforementioned analyses were tailored to their relevance to the acoustic sources used in the mapping survey and what may be considered most detectable to a foraging beaked whale. Specifically, peak sound pressure levels, sound exposure levels, and selected decidecade band levels were used. The sound level metrics were also weighted using the

National Marine Fisheries Services (NMFS) marine mammal weighting (M-weighting) curve for mid-frequency cetaceans, the functional hearing group to which beaked whales belong (NMFS 2018). The weighting serves as a filter over the acoustic data, which de-emphasizes frequencies that are outside the range of best hearing sensitivity of a functional marine mammal hearing group. In addition, the temporal window for which the sound pressure level metrics were computed was chosen to closely match the hearing integration time of marine mammals. Finally, the sound level metrics used to assess noise impact on marine mammals with respect to marine anthropogenic activities were calculated and compared to marine mammal noise impact thresholds used by regulators in the United States. It is also worth noting that the acoustic observations used in this soundscape study were collected on hydrophone receivers mounted to the seafloor, which makes this assessment especially relevant to beaked whales that generally forage near the seafloor.

While the time series annotation and sound level percentile comparison components of the amplitude analyses are methods frequently used in characterizing and comparing soundscapes, the probability distribution and frequency correlation analyses are not and warrant further background information. The probability distribution analysis utilized statistical hypothesis testing based on the Wasserstein Distance as a test metric. The Wasserstein Distance (*W*), also known as the Earth Mover's Distance in computer science (Rubner *et al.* 2000), can be thought of as the minimum cost of transforming (i.e., location, size, and shape) one pile of dirt into another. In other words, the value of *W* indicates how different two distributions are. The Earth's Mover's Distance has been used in computer science to compare images and in-pattern recognition applications (Rubner *et al.* 2000), as well as in optimal transport problems (Li *et al.* 2016). It has also recently been used to examine the distribution of RNA sequencing data

(Schefzik 2020). This metric is particularly useful for comparing complex distributions, such as those that are not unimodal. When a distribution is unimodal, the mean and variance are often adequate descriptors, but when multimodal, the mean may not change despite other clear differences between the two distributions. The squared version of the Wasserstein Distance, the 2-Wasserstein Distance, can be decomposed into location, size, and shape terms, providing further information about how two distributions differ. The 2-Wasserstein Distance decomposition was used here to holistically characterize the distribution of sound pressure level observations during the multibeam mapping activity and determine whether the distributions significantly differed between distinct analysis periods with and without survey activity. If there were differences, the decomposition provided insight into how they differed. In terms of a soundscape, the location term (difference of means) indicates whether one distribution consists of sound levels that are louder or quieter than the other. The size term, represented by the difference in standard deviation, indicated how dispersed the sound level data were. If one distribution was more dispersed than the other, that analysis period could be considered dynamic, whereas a less dispersed distribution would be considered static. The shape term, or correlation coefficient of the two distributions, describes the skewness and/or modality of the distributions. For example, a left-skewed sound level distribution is mostly quiet, with intermittent loud periods, whereas a right-skewed distribution is mostly loud, with intermittent quiet periods. The use of this approach for comparing sound levels therefore was not in assessing the absolute sound levels, but in how the distributions of the different analysis periods compared to one another.

The frequency analysis of this work focused on frequency correlation of sound levels. Frequency correlation has been used to interpret ocean ambient sound (Nichols and Bradley

2019) and understand changes in source contributions to a soundscape (Miksis-Olds and Nichols 2016). Frequency correlation is therefore not new to underwater acoustics, but its utility has not been fully captured. Frequency correlation matrices are a tool that can be used to understand how different frequencies relate to one another (Miksis-Olds and Nichols 2016, Nichols and Bradley 2019). If two frequencies are highly correlated, it means the sound levels at both frequencies vary at the same times, either increasing or decreasing, which can indicate that they are being driven by the same source mechanism (e.g., vessel noise, MBES signal, biological acoustic activity, etc.). To identify changes, two frequency correlation matrices representing distinct periods are subtracted and compared. The resulting matrix shows how the periods differ. Frequency correlation matrices and difference matrices were generated for distinct analysis periods and used here to understand the frequency contribution of the EM 122 and other active acoustic sources to the soundscape.

Common Methodology

SOAR Hydrophone Array

The SOAR hydrophone array spans an approximately 1800 km^2 area and contains a subset of 89 bottom-mounted hydrophones that were used in the work presented in this chapter. These hydrophones range in depth from 850 to 1750 meters, and are sampled at a rate of 96 kHz. The omnidirectional hydrophones have a roughly flat sensitivity response between 50 Hz and 48 kHz (Smith 2019). The acoustic data from all 89 hydrophones were collected from January 04, 2017 20:13 until January 07, 2017 06:55 UTC, a time period that spanned before until the end of the 2017 deep-water MBES mapping survey of the SOAR.

Acoustic Data Processing

The raw acoustic data were extracted in a duty cycle of 5 minute ON/10 minute OFF to reduce processing time and memory. The acoustic data were then converted to various

frequency-specific and broadband sound level metrics. This was generally done by taking the raw voltage time series data and converting it to the frequency domain using MATLAB®'s fft function. Then the amplifier gain (*gn*) and frequency-specific sensitivity of the system (*ocr(f)*) were applied (Equation 5.1).

$$P(f) = V(f) \times \frac{1}{ocr(f)} \times \frac{1}{gn} \times W(f) \quad \text{(Equation 5.1)}$$

where $ocr(f) = 10^{OCR(f)}$, $gn = 10^{\frac{Gn}{20}}$, $V(f)$ is the frequency-dependent voltage after taking the Fourier transform (fft function in MATLAB®); *OCR*(*f*) is the open circuit response curve; the amplifier gain (*Gn*) of the system was 66 dB; and the *OCR*(*f*) curve for frequencies between 2-50 kHz was provided by the Naval Undersea Warfare Center and is roughly flat between these values. The curve was extended to 10 Hz by assuming a constant response from 10 Hz to 2 kHz. Worth noting, the dynamic range of the hydrophones was limited, resulting in maximum recordable level of 138 dB re 1µPa; all signals above this limit value were clipped. For broadband metrics, the frequency components were summed in the frequency domain to a broadband value based on Parseval's Theorem, which says that the sum of energy in the time domain equals the sum of energy in the frequency domain (Lurton 2002). This holds true for both power and energy metrics and was used consistently here to avoid unnecessary processing to convert the acoustic data back to the time domain (Smith *et al.* 2021).

The exception to this process was the conversion of voltage data to unweighted peak sound pressure levels (*SPLpk)* (discussed further below), which was handled in the time domain by applying a single average open circuit response value (ocr_{mean}), instead of using the frequency-specific response curve (Equation 5.2).

$$p(t) = v(t) \times \frac{1}{gn} \times \frac{1}{ocr_{mean}} \quad \text{(Equation 5.2)}$$

where *v(t)* is the voltage value in the time domain, and ocr_{mean} is the average value of the OCR curve. This estimate of *SPLpk* resulted in a difference of no more than 1 dB from the precise value (Michael Smith, *personal communication*) and was an acknowledged trade-off to reduce processing time. Note: the calculation of weighted *SPLpk* followed the process of Equation 5.1 and required conversion back to the time-domain using the inverse Fourier transform.

W(f) refers to either *W(f)* =1 for unweighted sound levels, or the frequency-specific weighting function coefficient derived from Equation 5.3 (NMFS 2018) for weighted sound levels:

$$W(f) = C + 10\left\{\frac{\left(\frac{f}{f_1}\right)^{2a}}{\left[1+\left(\frac{f}{f_1}\right)^2\right]^a\left[1+\left(\frac{f}{f_2}\right)^2\right]^b}\right\} \quad \text{(Equation 5.3)}$$

where $a = 1.6, b = 2, C = 1.2, f_1 = 8.8,\ f_2 = 110$. These are the low- and high-frequency cut-off exponents (dimensionless), weighting function gain (dB), and low- and high-frequency cutoff frequencies (kHz), respectively; these values correspond with the mid-frequency cetacean functional hearing group (NMFS 2018). For specific details on these parameters, the NMFS Technical Guidance should be referenced (2018).

Multiple sound level metrics across the entire study period were generated with the acoustic data including:

- Weighted and unweighted peak sound pressure levels (*wSPLpk* and *SPLpk*, respectively)
- Weighted and unweighted sound exposure levels (*wSEL*, *SEL*)
- Weighted and unweighted decidecade band levels (*BL*) with center frequencies between 50 Hz and 40 kHz.*

* Broadband metrics for this study included frequency content inclusive of the 50 Hz to 40 kHz decidecade *BL*s.

These metrics were generated using the following definitions and formulas:

The peak sound pressure level, *SPLpk* (dB re 1 μPa), identifies the maximum pressure amplitude in a given time window. This was calculated by taking 10 times the log of the maximum of the absolute value of the instantaneous squared pressure $p^2(t)$ in a specified time window:

$$SPLpk = 10\log(\max(|p(t)|^2)/p_0^2) \quad \text{(Equation 5.4)}$$

where p_0^2 refers to the reference square pressure value.

Sound exposure level, *SEL* (dB re 1 μPa^2 s), measures all of the energy within a specific time window (*T*), in other words, integrating the squared signal over the time window of interest. In the discrete case, *SEL* was computed by summing the absolute value of the squared pressure observations (normalized to p_0^2) contained in a specific time window with respect to a reference duration of 1 second (Equation 5.5). The value in decibels therefore is:

$$SEL = 10log\left(\sum_{k=0}^{N-1}\left|P_{dft}(k)\right|^2/p_0^2 * \frac{\Delta t}{N}\right) \quad \text{(Equation 5.5)}$$

where $P_{dft}(\mathrm{k})$ represents the spectral output of the fast Fourier transform with *N* samples contained in the time window analyzed.

Lastly, the decidecade band levels (*BLs*) represent the mean square sound pressure spectral density level in each decidecade, or one tenth of a decade band (ISO 18405) with units of μPa^2/Hz. These were computed by summing the squared sound pressure over each decidecade band and accounting for the bandwidth of the spectral content contained in the band (Equation 5.6). The *BL*s were chosen to directly align with the Atlantic Deepwater Ecosystem Observatory Network (ADEON) project, as one of the primary objectives of that project was to develop standardized measurement and processing methods for underwater acoustic projects (Ainslie *et*

al. 2017). There, decidecade bands were aligned with the 1 kHz band (band index *n*=0). The same banding was used here.

$$BL\_f_{c,n} = 10\log(\frac{1}{N^2}\sum_{k_{min,n}}^{k_{max,n}}|P(k)|^2/p_0^2) - 10\log(bw) \quad \text{(Equation 5.6)}$$

where $k_{max,n}$ and $k_{min,n}$ are the indices of the upper and lower frequencies of each band, which are 0.5 decidecade above and below the center frequency of the band ($f_{c,n}$), i.e., $f_{max,n} = f_{c,n}10^{\frac{1}{20}}$, $f_{min,n} = f_{c,n}10^{-\frac{1}{20}}$, $f_{c,n} = (1\text{ kHz})10^{\frac{n}{10}}$, and *bw* represents the bandwidth of the decidecade band in Hz (Ainslie *et al.* 2017). As no formal standard exists yet for computing and reporting broadband quantities, a decision was made to maximize the spectral observations available with this data set. Consequently, broadband was defined here as the 30 bands inclusive of the 50 Hz through 40 kHz center frequency decidecade bands (i.e., $n = -13$ to 16).

A purposeful selection of the *BL*s were chosen for detailed analysis, which represented specific acoustic source expected to contribute to the SOAR soundscape. These were the *BL*s with center frequencies of 50 Hz, 500 Hz, 3.2 kHz, 12.5 kHz, and 40 kHz. The 12.5 kHz band (11.2-14.1 kHz) was selected because it encompasses the majority of the frequency content of the EM 122 MBES signal (11-13.25 kHz). This band also contains biological sounds, such as from vocalizing marine mammals. The 40 kHz band (35.5-44.7 kHz) was chosen as it contains the peak frequency of beaked whale foraging clicks (Baumann-Pickering *et al.* 2013). It also contains the signal of the EM 712 used during the Mixed Acoustic period of the mapping survey (40 kHz). The 50 Hz (44.7-56.2 Hz), 500 Hz (447-562 Hz), and 3.2 kHz (2.8-3.5 kHz) bands were chosen as they each represent a distinct regime of the low-frequency signals that often dominate a soundscape. The 50 Hz band represents vessel engine sound, the sound from propellers, as well as the low frequency harmonics of these sources (Hildebrand 2009). The 500 Hz band includes other ship-radiated sound, as well as other natural and ambient sources such as

marine mammals that communicate at low frequencies (Wenz 1962). The 3.2 kHz band was selected because it can contain higher frequency radiated vessel noise, as well as significant energy from the SBP (center frequency of 3.5 kHz, with bandwidth up to 12 kHz) used during the Mixed Acoustic period of this study.

The aforementioned metrics were computed using a 100-ms time window, which was motivated by the need to interpret the sound levels with respect to marine mammal hearing and the MBES signals. Several temporal windows for hearing integration times of marine mammals have been reported, including 35, 50, and 125 ms, as well as the conjecture that some, if not all, marine mammals may have frequency-dependent hearing integration (Johnson 1991, Kastelein *et al.* 2010a, Kastelein *et al.* 2010b, Tougaard *et al.* 2015). Due to the uncertainty around the exact integration time of marine mammal hearing and in recognition of the time-frequency resolution trade-offs of this specific data set (i.e., shorter time windows equates to coarser frequency resolution), a 100-ms time window was chosen as the primary temporal window upon which to assess sound levels with respect to beaked whale hearing. The MBES signal duration is on the order of 10's of milliseconds (due to the multisector transmission), thus the 100 ms temporal window was relevant in consideration of the MBES signals as well. Thus, the 100 ms window was primarily used throughout this work, but did vary in a few circumstances (i.e., computation of 24-h cumulative sound exposure levels). Where it diverged from this, the choice of temporal window will be further explained. The acoustic data processing was done in collaboration with Michael Smith at the Center for Coastal Ocean Mapping who performed the essential MATLAB processing of the acoustic data set into the sound level time series used in the rest of this work.

Mapping Activity and Designation of Analysis Periods

The goal of this chapter was to examine sound level metrics and compare them across time and space in order to characterize the anthropogenically-modified and natural sound levels

of the marine soundscape. Thus, the sound level metric time series were partitioned into four analysis periods based on the anthropogenic activities during those periods. These included 1) No Activity (NA), a time immediately preceding the mapping survey when no activity related to the mapping survey was occurring on the SOAR array, 2) Vessel Only (VO), a period when only the survey vessel was known to be on the array and all active acoustic systems related to mapping were off, 3) Vessel and MBES (VM), a period which included the presence of the survey vessel and the active EM 122 MBES on the SOAR array, and 4) Mixed Acoustics (MA), a period that included the survey vessel on the array with transmitting Kongsberg EM 122, Kongsberg EM 712 MBES (40 kHz), Simrad EK 80 wide-band echosounder at various frequencies (18 kHz), and a Knudsen sub-bottom profiler (3.5 kHz) at various times throughout the period. More detail will be provided on the nature of the activities conducted during each of these periods in the Results section.

Aside from the known active acoustic sources used during the three-day survey, there may have been other acoustic sounds incidentally recorded on the array hydrophone receivers. These may have included sounds inherent with the safe operation of the research vessel, sounds from other vessels transiting near the array, and/or biological, mechanical, or geophysical activity. Additionally, there may have been sounds related to any activity occurring on or near San Clemente Island, the U.S. Navy base, directly adjacent to the SOAR. However, it is worth noting that the survey took place during the first week of January when activity at the SOAR was very limited, if at all. As such, there was no way of excluding other potential sound sources from the soundscape assessment of the survey activity. But the presence of other sounds to some degree—anthropogenic or natural—would be a reasonable expectation for the SOAR soundscape. Due to the sporadic and intermittent use of the various active acoustic systems

together and separately throughout the MA period, a thorough characterization and comparison of all active acoustic sources in this period was not undertaken. The emphasis of the soundscape study was on characterizing the contribution of the 12-kHz EM 122 MBES, the system primarily used for the mapping survey.

Spatially, analyses were conducted either from an array-wide perspective, utilizing all of the sound level data from all 89 hydrophones, or individually by assessing the sound levels from nine select hydrophones, which provided perspective about the variability in sound levels across the array, due to the bathymetry, depth of the hydrophones, and exposure of the hydrophones to the various anthropogenic activities related to the mapping survey. The nine hydrophones were selected to provide a representative spatial coverage of the array, while avoiding peripheral (or edge) hydrophones. The hydrophones examined were numbers 14, 16, 19, 22, 45, 57, 63, 70, and 85 (Figure 5.1), with roughly 5-15 km horizontal distance between two adjacent hydrophones examined. Hydrophone 14 is located in the northeast, hydrophone 16 in the north center, hydrophone 19 in the northwest, hydrophone 22 in the center-east, hydrophone 45 in the center, hydrophone 57 in the west center, hydrophone 70 in the southeast, hydrophone 63 in the south center and hydrophone 85 in the southwest (Figure 5.1). A closer inspection and comparison of each of the 89 hydrophones individually was beyond the scope of this study.

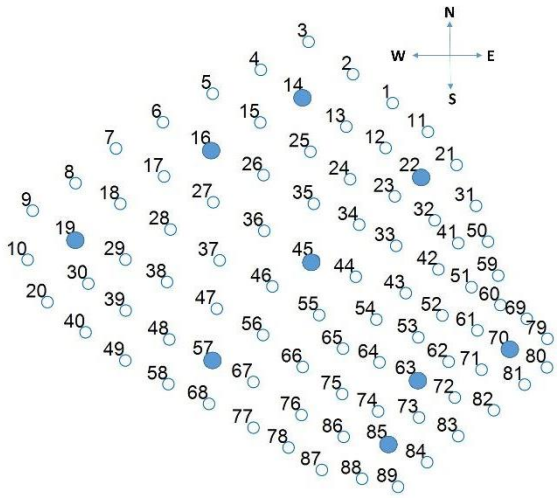

Figure 5.1. SOAR hydrophone array and the 9 hydrophones selected (blue filled circles) for examination.

Amplitude Analyses

Time Series Annotation

Analysis-specific Methodology

In order to understand how the MBES mapping survey impacted the local soundscape, the sound level metric time series were examined to identify acoustic events during the study period. This was done on a per hydrophone basis for each of the nine selected hydrophones. Because of its location in the center of the SOAR and proximity to repetitive passes of the survey vessel during the mapping survey, the sound level time series of hydrophone 45 were annotated first. Sound level percentiles, i.e., 1, 5, 10, 25, 50, 75, 90, 95, and 99th, were computed for the following sound level metrics for the hydrophone 45 acoustic data set: *SPLpk*, *SEL*, 50 Hz, 12.5 kHz, 40 kHz *BL* for each analysis period, i.e., NO, VO, VM, and MA. An acoustic event was defined *a priori* as a point in the *SPLpk* time series when the 95th percentile was exceeded in a given analysis period. The *SPLpk* time series had to return to or below baseline conditions -- defined here as the 50th percentile of the *SPLpk* metric for a given analysis period --before another acoustic event was triggered. Changes in the other sound level metrics were discussed with respect to the 50th percentile level value for the same metric being discussed for a specific

analysis period. The 50th percentile level value was referred to throughout as the baseline sound level. For those *BL* metrics where the percentiles were not calculated, changes in the sound levels were discussed relative to a local baseline, defined here as the approximate static sound level value for a given metric before and/or after an acoustic event.

Acoustic events were identified across the entire study period and described. Several animations of the sound levels were generated and visually referenced for interpreting the nature (source, amplitude, duration, spatio-temporal characteristics) of the acoustic event. In particular, animations iterating through the spectral probability density (SPD) of every minute, spatial animations iterating through the one-minute broadband and individual decidecade *BL*s (Smith *et al.* 2021), and spectrograms of specific events were generated. The SPD plots provided a temporal and frequency perspective of how the sound levels varied over time by showing the empirical probability density of the spectral level observations across all decidecade bands in each one-minute window. To obtain the empirical probability density, the 100-ms temporal observations of each minute, in each of the 30 decidecade bands were partitioned into 1/10th dB bins constituting each SPD plot. Broadband and decidecade band spatial animations were created by Michael Smith at the Center for Coastal and Ocean Mapping and were used to understand if the acoustic event was present only on the hydrophone under assessment, or if the event was a more spatially broad phenomenon (e.g., elevated sound levels on all hydrophones or over a larger vicinity). Spectrograms corresponding to the time of the acoustic events were created in Audacity® and were examined to aid in the identification of the sound-generating source and the nature of each acoustic event.

In addition, sound level metric time series plots were generated to clearly display the acoustic events and summarize the time series annotation effort for each hydrophone. The 100

ms sound level time series were smoothed over each 5-minute window and plotted. To provide context for and aid in the interpretation of the source of the acoustic events with respect to the mapping activity, the oblique range (*R*) of the survey vessel to each hydrophone (Equation 5.7), and the expected transmission loss (*TL* in dB) at those ranges (Equation 5.8) were also plotted, based coarsely on spherical spreading loss and frequency-specific attenuation with the same time resolution as the sound level time series.

$$R = \sqrt{(se - he)^2 + (sn - hn)^2 + (depth)^2} \quad \text{(Equation 5.7)}$$

$$\text{TL} = 20logR + \alpha R \quad \text{(Equation 5.8)}$$

where the variables in Equation 5.7 refer to the ship and hydrophones' easting (*se*, *he*, respectively) and northing (*sn*, *hn*, respectively) location in the Universal Transverse Mercator coordinate system (UTM). Depth corresponds to the hydrophone depth (mean sea level), with the unit of each variable and the resulting oblique range in meters. The attenuation coefficient (α) used in Equation 5.8 for each *BL* was determined based on the center frequency of the respective *BL* (Francois and Garrison 1982). These were $\alpha = (0, 2.4 \times 10^{-5}, 1.92 \times 10^{-4}, 1.5 \times 10^{-3}, 1.12 \times 10^{-2}$ in dB/m) for the 50 Hz, 500 Hz, 3.2 kHz, 12.5 kHz, and 40 kHz *BL*s, respectively.

Based on the results of the initial, detailed annotation of hydrophone 45, a more efficient procedure was established for annotating the acoustic data from the other hydrophones with respect --specifically--to the survey activity. It was expected that there would be obvious features in the sound level time series that could be used to identify the acoustic events related to the mapping activity (e.g., distinct peak or extended elevated levels in the 12.5 kHz *BL*). Sound level percentiles (1, 5, 10, 25, 50, 75, 90, 95, and 99th) for the *SPLpk*, *SEL*, 50 Hz, 12.5 kHz and 40 kHz *BL*s were also computed for each analysis period for each of the other eight hydrophones

and used in subsequent analyses. However, the sound level percentiles for the other hydrophones were not used for the identification of acoustic events, as they were for hydrophone 45.

Results

Chronological summary of study activities

The No Activity (NA) period was based on the amount of time prior to the survey vessel's presence on the SOAR array for which acoustic data could be obtained. This was an approximately 3 hour and 40 minute period from 1/4/17 20:13-23:51 UTC (note: all times presented in UTC).

The Vessel Only (VO) period, which began 1/4/17 23:51 and ran until 1/5/17 08:16 for a total of 8.5 hours, consisted of two across the array lines by the survey vessel from the south center to the north center of the array and back to the south. The survey vessel was operated at roughly 10 knots throughout this period. All other active acoustic sources were off. The track lines of the VO period are shown in blue in Figure 5.2.

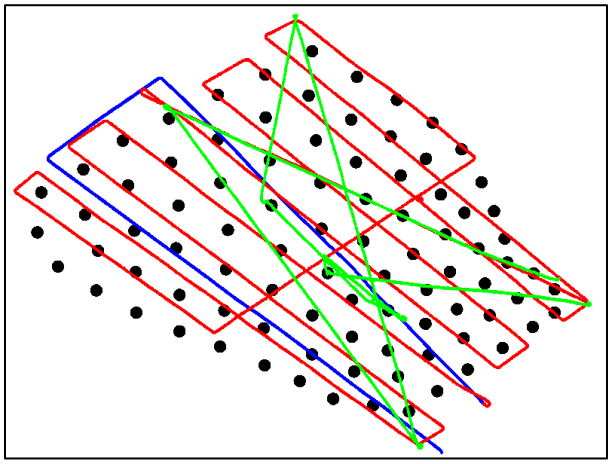

Figure 5.2. Track lines of the vessel during the analysis periods containing anthropogenic activity: blue lines correspond to the Vessel Only period, red with the Vessel and MBES period, and green with the Mixed Acoustics period.

The Vessel and MBES (VM) period consisted of the primary mapping survey utilizing the hull-mounted Kongsberg EM 122, a MBES with a 12-kHz center frequency. The VM period

began at the end of the VO period on 1/5/17 at 08:16, and ran until 1/6/17 13:48, for a total of approximately 29.5 h (Table 5.1). The survey was conducted as a typical mapping survey in a 'mowing-the-lawn' fashion (Figure 5.2, red lines) using the EM 122 in *Deep*, *Dual Swath* mode with continuous wave pulses only -- i.e., not frequency-swept. The survey was conducted in a calm sea state with 1–2-foot swells. Generally, the swath width of the EM 122 transmission was fixed to 130° for each swath. However, there were times when it was decreased to 90° or increased to 144° to optimize data collection for mapping purposes. The vessel's survey speed was 10 knots except when turning the ship, during which the speed was dropped to 5 knots.

The Mixed Acoustics (MA) period lasted from 1/6/17 13:48- 1/7/17 06:55, approximately 18.33 h (Table 5.1) and included a few diagonal lines across the array, as well as a few shorter lines (Figure 5.2, green lines). This period consisted of multiple acoustic sources which were in use intermittently. The acoustic sources included the Kongsberg EM 122, a Kongsberg EM 712 MBES (operating frequency of 40 kHz), a Simrad EK 80 wide-band echo sounder (with operating frequency of 18 kHz), and a Knudsen sub-bottom profiler (3.5 kHz).

Table 5.1. Extraction times (UTC) and duration of each analysis period.

Analysis Period	Start Time	End Time	Total Time
NA	1/4/17 20:13	1/4/17 23:51	3 h 38 min
VO	1/4/17 23:51	1/5/17 08:16	8 h 25 min
VM	1/5/17 08:16	1/6/17 13:48	29 h 32 min
MA	1/6/17 13:48	1/7/17 06:55	18 h 17 min

The detailed events of the MA period that were logged in the cruise report are provided here. The EM 712 was turned on auto mode at 1/6/17 13:48, initially turning on in *Very Deep* mode with a single 112° swath. *Auto-ping* mode was turned off 1/6/17 14:32 and fixed in *Extra*

Deep mode with a 90° swath until 1/6/17 15:16 when it was turned off for a series of calibration exercises with the EM 122 in the center of the array (Hydrophones 36, 55, and 65 in Figure 5.1) that lasted until 1/6/17 19:20. At this time, the EK-80 was turned on and run intermittently from 1/6/17 19:33-20:17, and again from 21:19-22:36. When the EK-80 was operational, the 18-kHz frequency was used with 8-ms pulse lengths, 2000 W power, and a 5-s interval between pings. At 20:56, the EM 122 was turned back on and operated in Deep, *Dual Swath, CW Only* mode with 144° swaths. At 22:41, the EM 122 was switched to *Very Deep, FM-enabled* mode, which forces the system into single swath only with a reduced swath width of 108°. The EM 122 was turned off at 1/7/17 1:42, when simultaneously the Knudsen Chirp 3260 SBP was turned on. There were some issues initially that led to its intermittent use until 02:20, at which time it was operated continuously until 1/7/17 06:55 (i.e., the end of the survey activity). At, 04:29 the EK-80, EM 122 (*Very Deep, FM* mode), EM 712 (*Extra Deep* mode), and the Knudsen SBP were all operated together until 1/7/17 6:55 when the survey was considered complete. At this point, the survey vessel transited off the SOAR array and continued to survey along nearby San Clemente Island using the EM 122 and EM 712 in *Auto-ping* mode. A summary of this narrative is provided in Figure 5.3.

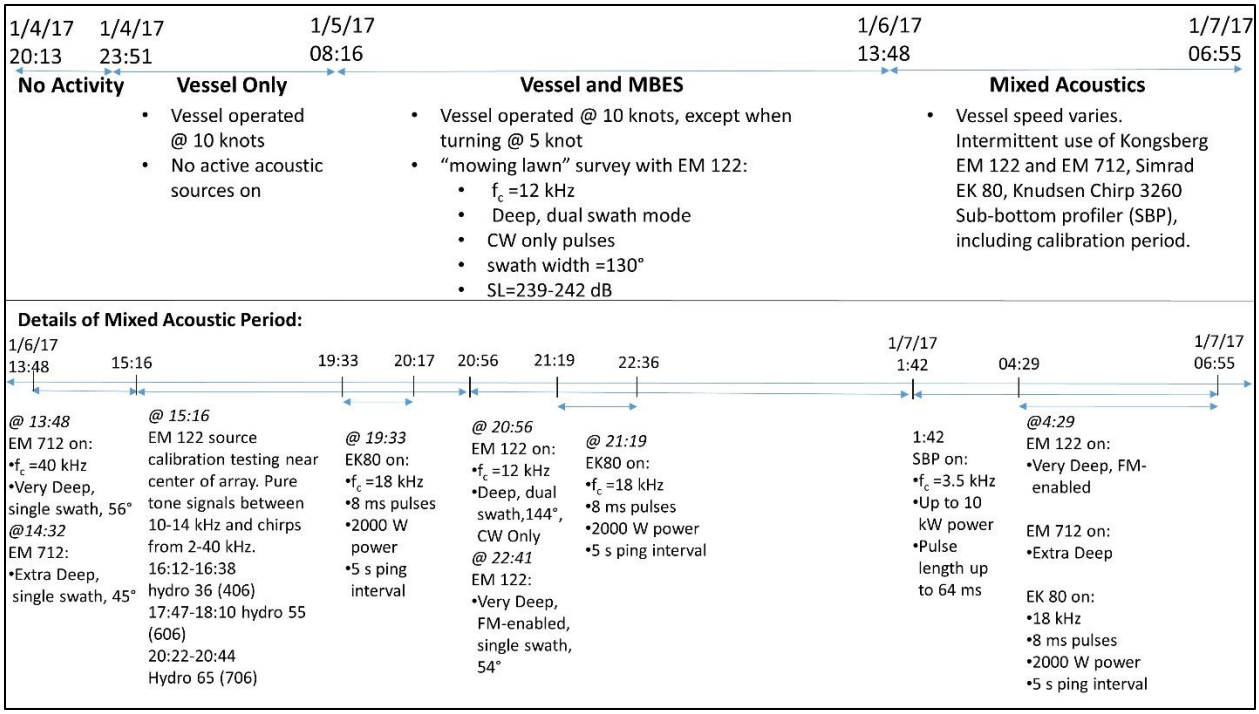

Figure 5.3. *Top.* Timeline of four temporal analysis periods and description of acoustic sources related to mapping activity. *Bottom.* Finer-temporal timeline of the operation of active acoustic sources during the Mixed Acoustic Period.

SPD animations (archived in the soundscape folder share drive repository in RES2019SCORE housed at the Center for Coastal and Ocean Mapping at the time of dissertation publication, henceforth termed the repository), spatial animations iterating through the one-minute broadband and individual decidecade band levels (located in the repository, created by Michael Smith), and spectrograms of specific events were generated and saved (Appendix 5.1). Audio files (.wav) of a selection of the acoustic events from each hydrophone were also archived (located in the repository).

Hydro 45

The results of the hydrophone 45 annotation follow. Acoustic events were identified when the 95th percentile *SPLpk* was exceeded for each analysis period (Table 5.2). Where possible, changes in the sound level metrics were discussed with respect to the baseline sound

level i.e, the 50th percentile level, for a given metric. These values are contained in Table 5.2. For those *BL* metrics where the percentiles were not calculated, changes in the sound levels were discussed relative to the local baseline, defined here as the approximate static sound level for a given metric before and/or after an acoustic event.

Table 5.2. *SPLpk* percentile values (dB re 1 µPa) for each analysis period used for annotating the sound level time series on hydrophone 45, and select baseline decidecade band levels (dB re 1 $\mu Pa^2/Hz$). These values are also contained in Appendix 5.2.

	Percentile Value			
Percentile	**NA**	**VO**	**VM**	**MA**
SPLpk 50th (baseline)	101	99	103	102
SPLpk 95th (i.e., threshold for triggering an acoustic event)	111	113	112	117
50 Hz band 50th (baseline)	68	60	55	56
12.5 kHz band 50th (baseline)	19	21	31	24
40 kHz band 50th (baseline)	13	14	16	14

NA period

The *SPLpk* of the NA period was higher than the baseline sound level (i.e., the 50th percentile of 102 dB re 1 µPa) of the entire study period over much of the NA period (Figure 5.4, *first plot*). Two acoustic events in *SPLpk* were detected in this period, one of 116 dB re 1 µPa (event 1, Figure 5.4) and the other of 113 dB re 1 µPa (event 2, Figure 5.4). An examination of the recreated *SPLpk* through time and space on the entire array (online repository) revealed that event 1 was an array-wide phenomenon, whereas the second event appeared to be isolated to the western edge of the array. Based on the spectrograms, the greatest spectral energy corresponding to these events was represented as spectral lines at very low frequencies (10's of Hz) (event 1 and 2, hydro 45, Appendix 5.1), suggesting the elevated levels may be driven by a passing vessel

(see corresponding peaks in the 50 Hz and 500 Hz time series--Figure 5.4, *second plot*). The survey vessel, the *Sally Ride*, seems an unlikely source given it was more than 30 km away from the SOAR at these times. However, the array-wide nature of event 1, in particular, raises uncertainty about whether a passing vessel was the source of this event.

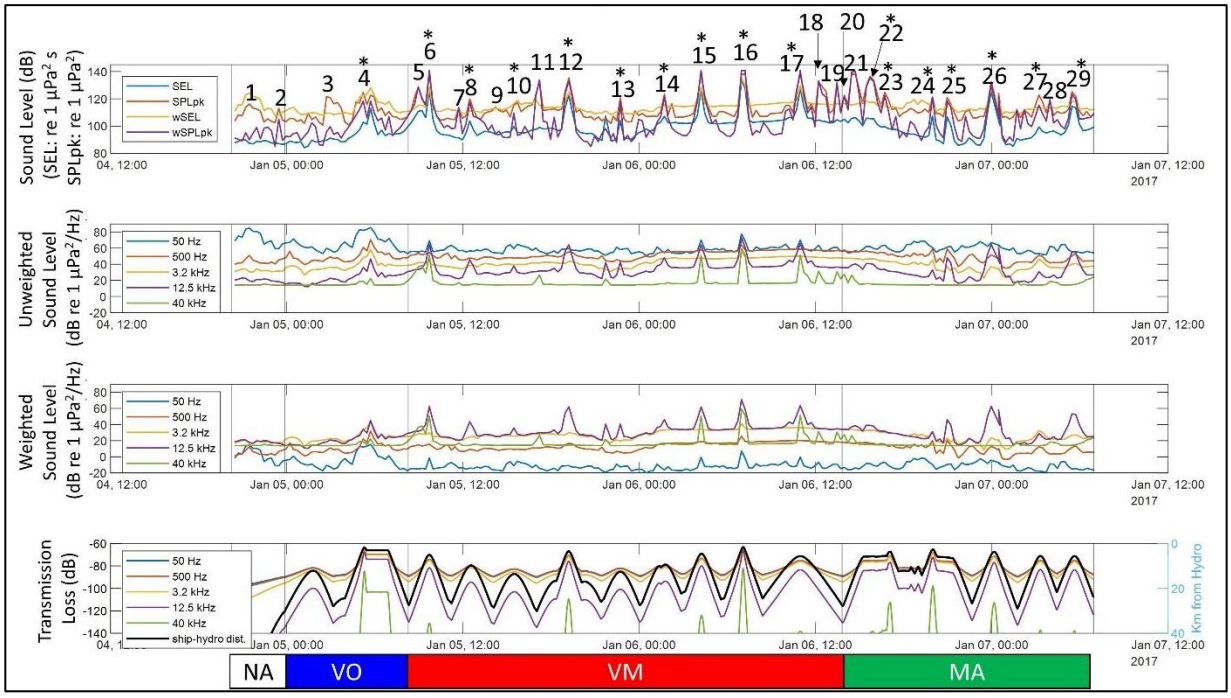

Figure 5.4. Sound level time series for hydrophone 45. *First plot*- Broadband sound level time series: *SEL* (blue), *SPLpk* (orange), *wSEL* (yellow), and *wSPLpk* (purple). Numbers indicate acoustic events identified in annotation. Asterisks indicate that the acoustic event was most likely attributed to the survey activity. Perpendicular lines on all graphs delineate the four analysis periods, NA, VO, VM, and MA, shown at the bottom of the figure, respectively. *Second plot*- Select unweighted BL time series: 50 Hz (blue), 500 Hz (orange), 3.2 kHz (yellow), 12.5 kHz (purple), and 40 kHz (green). *Third plot*- Weighted decidecade BL time series. Line colors and frequencies are the same as in the second plot. *Fourth plot*-Time series of modelled frequency-specific transmission loss (left axis) and range from hydrophone in kilometers (black line, right axis). Color of frequency-specific transmission loss corresponds to colors of frequencies described for the second plot.

VO Period

During the VO period, the first acoustic event (i.e., *SPLpk* > 113 dB re 1 µPa) corresponded with an increase in the 50 Hz, 500 Hz, and 12.5 kHz *BL*s (event 3), suggesting the event may be related to a passing vessel. The *Sally Ride* was over 20 km away from hydrophone

45 at this time and was unlikely to be the cause, especially as the sound levels decreased again despite a continuously decreasing distance between the survey vessel and hydrophone. An examination of the spatiotemporal animations of the *SPLpk* revealed that this phenomenon occurred across the array. Inspection of a spectrogram of this event (Appendix 5.1, hydro 45, event 3) suggested this event was largely driven by increased energy at frequencies of 5 kHz and below, noticeably centered around 400 Hz, 1.2 kHz, and 5 kHz. The cause for such a spatially broad phenomenon was unclear.

The *Sally Ride* made its first relative closest point of approach (RCPA) during the VO period to within 2 km of the hydrophone, corresponding with a peak in *SPLpk* (event 4, 125 dB re 1 μPa). There was a clear rise in all of the *BL*s examined (Figure 5.4, event 4), suggesting this event was very likely associated with the proximity of the survey vessel to the hydrophone. Although the levels fluctuated in each band prior to this event, there was a steady monotonic increase in the *BL*s starting when the vessel was approaching from ~ 15 km away. The levels did not return to baseline (i.e., <99 dB re 1 μPa^2/Hz) until the *Sally Ride* was again ~ 15 km away. There was a similar increase in all of the *BL*s examined, correlated with the increase in *SPLpk*. The peaks in the various *BL* time series were consistently narrower as the frequency increased. Narrower peaks corresponded to shorter time periods that the particular *BL* was elevated, which makes sense given that lower frequency signals attenuate less over the same distance compared with higher frequency signals (see Figure 5.4, *fourth plot* for frequency-specific estimates of transmission loss). In other words, the lower frequency components of a signal are elevated for a longer time period than the higher frequency components as the source moves away from the hydrophone because the high frequency sounds attenuate more rapidly as they propagate. For event 4, the 50-Hz band varied by 26 dB from baseline levels (i.e., 60 dB re 1 μPa^2 /Hz median

vs a peak in this band of 86 dB re 1 μPa^2 /Hz), while the 40-kHz band increased by only 8 dB (i.e., 14 dB re 1 μPa^2 /Hz median vs a peak in this band of 22 dB re 1 μPa^2 /Hz). It is worth noting that a second, albeit smaller peak, occurred when the vessel was approximately 3 km away conducting a CTD cast to approximately 1600 meters, which took just over an hour to perform. The vessel changed orientation throughout this time, despite staying relatively stationary, with respect to hydrophone 45. This peak in the sound levels may be an artifact of the ship thrusters trying to hold position during the CTD cast when using dynamic positioning. Alternatively, this secondary peak in the sound levels could be due in part to differences in directivity of vessel-radiated sound (Mitson 1993, Arveson and Vendittis 1999, McKenna *et al.* 2011, Gassman *et al.* 2017). It is worth noting that differences in directivity are more pronounced at higher frequencies. For example, McKenna *et al.* (2011) showed that ship noise from several commercial ship types radiates asymmetrically, with louder noise from the stern versus the bow. The activity of the survey vessel was distinguishable in the time series for about 3.5 hours of the VO period, which was generally when the vessel was within 8 km of the hydrophone.

VM Period

The first acoustic event during the VM period (i.e., *SPLpk* of 129 dB re 1 μPa, note: the acoustic event trigger for the VM period was 112 dB re 1 μPa) visually correlated with a peak in the 40 kHz band (Figure 5.4, event 5). Because the survey vessel was ~15 km away and the transmission loss in this band at that range was over 140 dB, this event was very unlikely related to the survey vessel. Rather it was likely related to a source much closer to the hydrophone. Upon reviewing a spectrogram of the event (Appendix 5.1, hydro 45, event 5) it appeared to be clicks potentially from foraging beaked whales, known to produce signals at this frequency (Baumann-Pickering *et al.* 2013). There was also significant energy centered around 1 and 5

kHz, but with no discernable temporal pattern, that likely also contributed to the high *SPLpk* value. The next acoustic event (event 6) was visible as elevated levels in all of the metric time series. This event corresponded with when the survey vessel was transiting from the south to the north by hydrophone 45, with the closest approach to hydrophone 45 at 5.3 km. At the peak, the sound levels were 25-35 dB over baseline (Table 5.2) for the 12.5 kHz, 40 kHz, *SEL*, and *SPLpk* metrics (e.g., for the 12.5 kHz band the peak was 64 dB re 1 μPa^2/Hz and the median for the period in this band was 31 dB re 1 μPa^2/Hz). For the lower frequency *BL*s, the respective peak magnitudes of the event were ~15 dB or less over baseline (e.g., in the 50 Hz band the peak was 69 dB re 1 μPa^2/Hz and the 50^{th} percentile, i.e., baseline, was 55 dB re 1 μPa^2/Hz). The maximum *SPLpk* reported at this time was likely conservative, as the hydrophone clipped (i.e., *SPLpk* 138 dB re 1 μPa). This acoustic event very clearly correlated with the vessel and MBES activity due to the strong response in the 12.5 kHz band, which was noticeably different than the sound level signature of event 4 in the VO period when the MBES was not on.

Event 7 (*SPLpk* peak of 114 dB re 1 μPa) corresponded with a peak in the 40 kHz band (17 dB re 1 μPa^2/Hz), and appeared to be related to clicks near the hydrophone, potentially from a marine mammal (Appendix 5.1, hydro 45, event 7). The next RCPA of the survey vessel was ~ 10 km from the hydrophone, which corresponded with another peak in *SPLpk* (120 dB re 1 μPa) and the 12.5 kHz band (31 dB re 1 μPa^2/Hz median vs 46 dB re 1 μPa^2/Hz peak) (event 8). There were not clear peaks in the other select frequency bands at this time. During event 9, *SPLpk* reached 114 dB re 1 μPa. The only obvious signal in the corresponding spectrogram was a very loud low frequency signal (around 50 Hz) that occurred roughly every twenty seconds for a duration of one second (Appendix 5.1, hydro 45, event 9). The source of this event is unknown,

but appears unrelated to the survey vessel which was beyond 30 km from the hydrophone at this time.

Event 10 corresponded with the next RCPA of the survey vessel to the hydrophone at ~14 km. The MBES signal was again noticeable in the spectrogram of this event (Appendix 5.1, hydro 45, event 10). There was simultaneously a very loud signal present between 50-100 Hz (likely in-part related to the low frequency ship-radiated sounds), which also contributed to the peak observed in *SPLpk* (i.e., 115 dB re 1 μPa). The same peak in the 12.5 kHz band (38 dB re 1 $\mu Pa^2/Hz$), corresponded with a level 7 dB above baseline (Table 5.2). A similar low frequency signal also seemed to be the driving mechanism of peak event 11 (*SPLpk* 133 dB re 1 μPa), but at this time the survey vessel was more than 25 km away making it unlikely to be the only source (i.e., the low frequency ship-radiated sound) for such a loud event. There were also short regularly repetitive pulses in the 40 kHz band (Appendix 5.1, hydro 45, event 11) that contributed to this acoustic event.

Event 12 very clearly correlated with the next RCPA of the survey vessel passing from west to east by the hydrophone at ~3.5 km (*SPLpk* of 135 dB re 1 μPa). The event was dominated by energy in the 12.5 kHz band (64 dB re 1 $\mu Pa^2/Hz$ peak), but there were smaller peaks in the lower frequency *BL*s. Similarly, event 13 (*SPLpk* peak of 121 dB re 1 μPa) corresponded with a peak in the 12.5 kHz *BL* (43 dB re 1 $\mu Pa^2/Hz$) when the vessel was 12.5 km away. Between 1:15 and 1:35 on 1/6/17, position data were lost for the survey vessel. While these were restored, the vessel spun around roughly in the same position about 10 km to the east of hydrophone 45. The timing of this activity corresponded with the pattern in the 12.5 kHz *BL* time series just before event 14 (Figure 5.4). Event 14 corresponded with the next RCPA of the survey vessel to 9.3 km from hydrophone 45, characterized by a peak in *SPLpk* of 123 dB re 1

μPa and in the 12.5 kHz band of 48 dB re 1 μPa^2/Hz, which were above baseline levels (Table 5.2) for the period by 20 and 17 dB, respectively. Events 15, 16, and 17 all corresponded to RCPAs of the survey vessel to under 6 km (4.7 km, 1.6 km, and 5.7 km, respectively) of the hydrophone, where each time the *SPLpk* peak recorded was 138 dB re 1 μPa, the receiver's clipping threshold. These events corresponded with peak values in the 12.5 kHz band of 64, 73, and 66 dB re 1 μPa^2/Hz, respectively (i.e., 33, 42, and 35 dB above baseline (Table 5.2, respectively). At each of these times, there were also peaks in the 50 Hz and 40 kHz band (i.e., local increases of 12-45 dB), with a visible increase in the other bands (i.e., local increases of 3-12 dB). In fact, the change at these time points (events 15, 16, and 17) in the 40 kHz band sound levels was more relative to the change in the 12.5 kHz *BL*s. An examination of the spectrograms of these events (Appendix 5.1, hydro 45, events 15-17) revealed the most clipping occurred during event 16, which is when the vessel was closest to the hydrophone, 1.6 km away, and clipping occurred the least during event 17 when the vessel was 5.7 km away from the hydrophone. There were also clicks present during event 17, centered around 40 kHz, but not during events 15 and 16. Therefore, at least part of the peak in the 40 kHz band was attributed to a source other than the mapping activity, most certainly marine mammal clicks.

It is also worth noting that immediately preceding and following event 17, there were smaller peaks in *SPLpk* and the 12.5 kHz *BL* when the vessel was ~ 9 km away approaching hydrophone 45 obliquely rather than straight on (as in event 15 and 16). These peaks were of 115 and 116.5 dB re 1 μPa in *SPLpk*, and 45 and 44 dB re 1 μPa^2/Hz in the 12.5 kHz *BL*, before and after event 17, respectively. One hypothesis for these peaks in the time series is that they were due to grating lobes, or replicas with comparable intensity to the main transmission beam of the

EM 122. This artifact, which is not normally present, has since been fixed in the latest version of the 12-kHz Kongsberg system, i.e., the EM 124 (Kongsberg, *personal communication*).

Events 18 and 19 (*SPLpk* of 132 and 131 dB re 1 μPa, respectively) both corresponded with peaks in the 50 Hz and 40 kHz bands. These events did not appear to be correlated with the vessel activity, as the 40 kHz peaks were practically of identical levels despite the survey vessel constantly moving away during these times (i.e., 9 km away during event 18 and 24 km away during event 19), in addition to the transmission loss at these distances being extremely severe, i.e., >140 dB. Spectrograms of these events revealed presumably marine mammal clicks centered around 40 kHz, as well as a longer, louder, and more irregular signal around 50 Hz (Appendix 5.1, hydro 45, events 18-19).

MA Period

The first acoustic event of the MA period (event 20, *SPLpk* of 122 dB re 1 μPa; note the *SPLpk* 95th percentile for this analysis period was 117 dB re 1 μPa) corresponded with a peak in the 40 kHz band (27.5 dB re 1 μPa^2/Hz) when the vessel was more than 25 km away. Due to the transmission loss at this range (>>140 dB), it is implausible that it could have been the 40 kHz signal of the EM 712 transmitting at the time. The spectrogram revealed that the source was most likely clicks near the hydrophone, presumably from a marine mammal (Appendix 5.1, hydro 45, event 20). Event 21 (*SPLpk* of 138 dB re 1 μPa) also corresponded with a peak in the 40 kHz (26.5 dB re 1 μPa^2/Hz) and 12.5 kHz band (40 dB re 1 μPa^2/Hz, 16 dB over baseline, see Table 5.2). This, again, seemed unrelated to the survey vessel which was still over 17 km away (TL >>140 dB for 40 kHz and >110 dB for 12.5 kHz). An examination of the spectrogram of event 21 and the SPD animation revealed elevated levels related to regularly spaced pulses with spectral content between 3-20 kHz, which lasted about 30 milliseconds each. Additionally, there

were clicks centered around 40 kHz, which appeared to be similar to those presumed to be marine mammal clicks in other instances (Appendix 5.1, hydro 45, event 21). The source of the broader pulses was not identified, as no known signal at these frequencies was being transmitted in relation to the survey activity at this time. Event 22 (*SPLpk* of 135 dB re 1 µPa) also contained pulses of an unidentified source. These were more broadband, between 200 Hz and 40 kHz, but with the highest energy below 2 kHz. These pulses occurred every 400-600 ms and lasted approximately 50 ms (Appendix 5.1, hydro 45, event 22). This event occurred when the vessel was stationary about 6 km away and just before the calibration tests with the EM 122 were conducted. It is possible that there were signals transmitted during the calibration testing that were not comprehensively noted in the survey report.

During the calibration tests, pure tones at 500 Hz steps between 10-14 kHz, as well as a 2-20 kHz and 2-40 kHz chirps were transmitted from the EM 122. These tests were performed first over hydrophone 55, then hydrophone 65, and finally over hydrophone 36. There were breaks between each of the hydrophone tests as the vessel transited to the next location. Event 23 (*SPLpk* of 125 dB re 1 µPa) appeared to be related to the calibration event 5.5 km away on hydrophone 55, as there were noticeable pulses in the spectrogram of this event that match the signals being transmitted at this time (Appendix 5.1, hydro 45, event 23). There were no peaks in the *SPLpk* that coincided with the second calibration event 12 km away from hydrophone 45. Between the second and third calibration events the EK-80 (18 kHz) was turned on and the vessel made a close pass by hydrophone 45 to within 2.6 km. This was visible as a peak (event 24, *SPLpk* of 121 dB re 1 µPa) across all of the selected frequencies (Figure 5.4, *second plot*), characteristic of other very close passes by vessels in this annotation. The EK-80 signal was also clearly visible in the spectrogram of the event, and manifested as an elevated 99th percentile

around 18 kHz in the SPD animation at this time. A distinct acoustic event was not triggered at the time of the third calibration event occurring ~6 km from hydrophone 45, although there was a very small peak in *SPLpk* between events 24 and 25 that may be attributed to this event. Immediately after the last calibration test the EM 122 was turned on again while the vessel was 6 km away, corresponding with a peak of 121 dB re 1 μPa in *SPLpk* (event 25). This event was especially prominent in the 12.5 kHz band (48 dB re 1 μPa^2/Hz peak, 24 dB above baseline), and at frequencies of 500 Hz and lower (Appendix 5.1, hydro 45, event 25).

The next acoustic event (event 26, *SPLpk* of 132.5 dB re 1 μPa) was closely associated with the next RCPA of the survey vessel to the hydrophone at ~3.7 km (event 26). At this time the EM 122 was on in Very Deep, FM-enabled single swath mode, which corresponded most prominently with an elevated 12.5 kHz *BL* (65 dB re 1 μPa^2/Hz, 34 dB over baseline). There were also elevated lower frequency *BL*s, most likely corresponding to vessel noise from the close approach. Immediately following event 26, there was a strange spike in both the *SPLpk* and 12.5 kHz *BL* time series. It is unclear what this may be, but one hypothesis is that it may be related to the EM 122 grating lobes, which may have resulted in clipped signals at the receiver as the survey vessel was approximately 8 km from the hydrophone. The next acoustic event (*SPLpk* of 123 dB re 1 μPa) occurred when the vessel made another RCPA to hydrophone 45 at 5.8 km while the Knudsen SBP was on (event 27). This event was associated with peaks in the 500 Hz, 3.2 kHz (i.e., 46 dB re 1 μPa^2/Hz peak, 10 dB over the local baseline), and 12.5 kHz *BL*s (i.e., 31 dB re 1 μPa^2/Hz peak, 7 dB over baseline), although the EM 122 was not on at this time (Figure 5.4, second plot, event 27). Event 28 (*SPLpk* of 120 dB re 1 μPa) was characterized by small peaks in the 50 Hz and 40 kHz *BL*s. Inspection of the spectrogram of this event revealed high amplitude clicks centered around 40 kHz (Appendix 5.1, hydro 45, event 28). This event was not

correlated with the survey activity as the vessel was 14 km away and transmission loss at this range was greater than 140 dB. The final peak event detected (event 29, *SPLpk* 125 dB re 1 µPa) occurred when the survey vessel passed within 5.6 km of hydrophone 45 with all active acoustic sources turned on (EM 122, 712, EK 80 and SBP). This corresponded with peaks in the 12.5 kHz band (55 dB re 1 μPa^2/Hz, 31 dB over baseline), the 500 Hz band (~10 dB over the local baseline), and the 3.2 kHz band (~5 dB over the local baseline). It is worth noting that all of the acoustic sources had been turned on an hour prior to this peak event when the vessel was >20 km away from hydrophone 45 and remained on for the remainder of the study period. The levels in all bands decreased by the time the vessel was beyond 15 km, suggesting even this loud event was local in nature.

In the unweighted time series, the 50 Hz band was the dominant signal for all but the west-to-east RCPA (event 12) when the 12.5 kHz band was elevated more than the 50 Hz band. After weighting the sound levels, the 3.2 kHz band and 12.5 kHz band were similarly the most distinguishable across the entire study period (i.e., all analysis periods), except during the majority of the events identified as related to the survey activity when the 12.5 kHz band dominated. During event 27, the 3.2 kHz levels, presumably related to the SBP, were slightly elevated over the 12.5 kHz levels. There were also a few times when the 12.5 kHz band was elevated over the other bands, but not because of the survey activity. In addition, there were times when the 40 kHz band also exceeded the 3.2 kHz band, coinciding with events related to RCPAs of the survey vessel and MBES under 5 km of the hydrophone (i.e., events 6, 15, 16, and 17). The elevated 40 kHz band in this context, may be related to harmonics from the EM 122 in this band, which are generally much lower than the main signal in the 12.5 kHz band, but at this

distance may still be detectable. Lastly, the 50 Hz band signals were the least distinguishable with respect to the weighted sound level metrics.

Hydrophone 45 Annotation Summary

Several patterns were revealed through the annotation of hydrophone 45. First, there were times of elevated low frequency levels during the NA period, which was an array-wide phenomenon of unknown origin. The close approach of the survey vessel during the VO period corresponded with maximum increases in *SPLpk* and the 50 Hz band of 26 dB, however, this event also coincided with another array-wide increase in these levels. Local increases of 8-23 dB were observed in the other select bands that did not seem influenced by the array-wide phenomenon. During the VM period, close passes (i.e., ≤6 km) of the vessel by the hydrophone were characterized by maximum increases of 25-35 dB in the 12.5 kHz and *SPLpk* metrics, and maximum increases of 15 dB in the lower frequency bands. During these close passes, clipping did occur at times. Up to 10 km from the hydrophone, survey vessel passes with the active EM 122 were characterized by increases of 15-20 dB over baseline in the 12.5 kHz band and *SPLpk* metrics. Up to 15 km away these maximum increases were between about 7-12 dB over baseline. During the MA period, the EK-80 signal was visible in spectrograms within only a few kilometers of the hydrophone, but did not seem to affect the overall *SPLpk*. When the SBP was on and the vessel was around 5 km from the hydrophone, the 3.2 kHz band levels were about 5-10 dB over baseline for that analysis period. The signal of the EM 712 was not identified in the hydrophone 45 time series. This is most likely because even at its closest point while the EM 712 was on, the survey vessel was still 5 km away. Aside from the directivity of the signal, at this range the 40 kHz signal also has an estimated transmission loss of about 120 dB. There was not a discernible difference in the broadband levels when all of the active acoustic sources were on

versus when only one system was on. Furthermore, the elevated levels corresponding to acoustic events associated with the survey activity decreased again to baseline conditions within a similar time frame as when only one system was on. For example, with a 10-knot speed, even the closest RCPA of the vessel to the hydrophone was only visible in the sound level time series for about two hours, whereas some of the furthest RCPAs detected in the time series were only visible for a half an hour. In total, during the VM period, the activity of the survey vessel was clearly discernable on hydrophone 45 for about 11 hours and 45 minutes (i.e., about one third of the VM period), which was when the survey vessel was observed to be roughly within 17 km of the hydrophone. Of the 29 acoustic events detected in the hydrophone 45 *SPLpk* time series, 17 were identified as related to the survey activity. During the VM period all of the acoustic events associated with the mapping activity clearly corresponded with a peak in the 12.5 kHz band.

Focused Annotation

In the hydrophone 45 annotation, the 12.5 kHz *BL*s were reliably indicative of the survey activity. Thus distinct peaks in the 12.5 kHz *BL*s were used to guide a more focused annotation of the other eight hydrophones, i.e., 14, 16, 19, 22, 57, 63, 70, 85, with respect to the mapping activity. Due to the highly detailed nature of the annotation exercise and the repetitiveness of similar findings across hydrophones, the focused annotation results are contained in Appendix 5.3. A summary of the annotation work, incorporating the findings from all nine hydrophones, follows here.

Time Series Annotation Summary

The detailed time series annotation of the nine hydrophones provided useful insight about how the various anthropogenic activities related to the mapping survey contributed to the sound levels of the SOAR soundscape. It also provided awareness about other sound sources present in

the acoustic data. In particular, during the NA and VO periods, there were epochs of low frequency sound present across the array, as demonstrated by a similar peak in the 50 Hz band on all nine hydrophones during both periods. There were also instances where vessels, other than the survey vessel, passed nearby to the array. These events were routinely detected on the northern and western edge hydrophones (i.e., hydro 14, 16, 19, 57, and 85) (which made sense given standard vessel traffic routes). There was also a lot of biological activity interspersed throughout the acoustic data on all of the hydrophones, particularly prominent in the 12.5 and 40 kHz band levels. And finally there were many unknown sources and signals identified, some of which were equally as loud as some of the closest passes of the survey vessel to the hydrophones (e.g., hydro 22, event 3).

The NA period, during which the survey vessel was not on the array, was meant to provide information about the background SOAR soundscape without anthropogenic acoustic activity. However, there were several events on many of the hydrophones that indicated closely passing vessels, i.e., anthropogenic activity, during this period. For example, there seemed to be a vessel transiting across the north of the array visible on hydrophone 14 (event 2) and 19 (event 1), and another event reminiscent of ship-radiated sound on hydrophone 85 (event 1). It was also expected that this period would be stable and quiet in comparison to the other periods. However, there was a high amplitude, low frequency (visible in 50 Hz band) signal detected across the entire array over much of the NA period. Because the assumptions about this period were not met, a comparison of the NA period with the other periods with these attributes in mind may be misleading. The assumption that the NA period was not influenced by substantial anthropogenic activity appears to hold better for hydrophones 22, 45, 63, 57, and 70 in comparison to the other hydrophones. Ultimately, the characterization of the NA periods on each hydrophone and

comparison to the survey activity periods provides understanding of what the added input of a mapping survey would be on top of the typical SOAR background soundscape.

The other analysis periods served to provide understanding about how the sound levels were influenced by the various anthropogenic activities and how those activities differed from one another (i.e., vessel-related sound versus vessel and multibeam signals). Although the survey vessel was distinguishable in most of the selected hydrophone time series, it was not readily distinguishable on all (i.e., hydrophones 14, and 70), and in the case of hydrophone 85 the survey vessel made close approaches (i.e., <5 km) more than once. In addition to the different exposure each hydrophone had to the VO activity, there were also instances where other suspected anthropogenic sources influenced the sound levels. For example, there were three events on both hydrophone 16 (events 2, 3, and 4) and 57 (events 2, 3, and 4) that appeared to be vessels transiting nearby, while only one of these events was the survey vessel. Similarly during the VM period, there appeared to be additional anthropogenic sources (i.e., transiting vessels) that influenced the sound levels. This included at least one documented event on hydrophone 19 (event 7), 57 (event 9), and two on hydrophone 85 (events 6 and 7). In terms of anthropogenic sources, the MA period seemed to be largely influenced by only the survey activity. However, there was a lot of biological activity identified during this period that appeared solely responsible for some of the changing sound levels (e.g., hydrophone 16, event 13; hydrophone 70, event 12), or was identified in addition to an anthropogenic source (e.g., hydrophone 85, event 14).

The time series annotations revealed that the various anthropogenic activities related to the survey had different and distinguishable sound level signatures. For example, events 4 and 16 on hydrophone 45 represent the closest approach of the survey vessel during the VO and VM periods, respectively. In the VO period, the elevated sound levels in the five decidecade *BL*s

scaled similarly (i.e., the increase in levels parallel each other), whereas in the VM period, the close approach of the vessel and the actively transmitting EM 122 manifests as severely steep peaks in the high frequency bands (i.e., 12.5 kHz and 40 kHz) which surpass the peaks in the lower frequency bands (i.e., 3.2 kHz and 500 Hz). The 12.5 kHz band and the 50 Hz bands were similarly loud. This matches expectation since the EM 122 signal is a known sound source in the 12.5 kHz band.

The peak in the 40 kHz band was unexpected but could be related to harmonics in the 40 kHz band produced unintentionally from the transmission of the MBES. Harmonics are generally about 30 dB less than the fundamental frequency, and harmonics at 40 kHz should attenuate much more at the same distance as a 12.5 kHz signal. Thus a harmonic in the 40 kHz band should only be detected at very short distances from the source, so the presence of such a large peak in the 40 kHz band may be a function of some other phenomenon. One hypothesis is that it is a measurement artifact related to the times when the EM 122 signal clipped. This is reasonable given that the peak in the 40 kHz band is only visible when the survey vessel comes within close range of the hydrophone, which would be the times when the EM 122 signal clipped. If this is related to the clipping it would be a pure measurement artifact, and would not correspond to anything real in the soundscape. The increase in the 40 kHz band will need to be explored further to fully understand this phenomenon.

Nonetheless, the sound level signature of the survey vessel and EM 122 varies with distance from the vessel to the hydrophone. During VM events where the vessel was ~6 km or less from the hydrophone the signature described above was visible (e.g., hydrophone 22, events 4, 5, 6). For RCPAs that were closer to 10 km or greater, the 12.5 kHz peak was the only *BL* that was pronounced (e.g., hydrophone 45, events 8, 13, and 14). And at distances greater than 15 km

the sound levels were not clearly impacted by the survey and EM 122 activity (e.g., see the second half of the VM period on hydrophone 57, or event 7 on hydrophone 16). However it was not always so clear. For example, the signal did not clip during event 3 on hydrophone 85 when the vessel was 4 km away, but it did during event 5 when the vessel was 6 km away. In both cases the survey vessel was transiting in the same direction from south to north, though, on the western side of the hydrophone in event 5, and on the eastern side during event 3. Undoubtedly, orientation of the vessel to the hydrophone also plays a role since the transmission beam of the MBES is strongly directional (0.5° aperture), downward-propagating and fan-like (i.e., not omnidirectional), which likely accounts for many of the inconsistencies identified here based on a range-only explanation. Not only is the transmission directional, but there are multiple beams that make up the transmission pattern. The main lobe of the transmission is the loudest and is generally directed vertically toward the seafloor, whereas side lobes are transmitted at oblique angles to vertical and are typically on the order of 20-30 dB lower in amplitude than the main beam. In addition, the EM 122 used in this survey had a flaw that caused grating lobes to occur (see hydrophone 45, event 17 as a possible example) at a level comparable to the nominal transmitted sector. Thus, some of the variability in the detection of the EM 122 signal in the sound level time series was related to 1) the orientation of the survey vessel as it approached and/or departed the hydrophone, and 2) whether the hydrophone was exposed to the main transmission beam, a side lobe, or a grating lobe. Thus, there was not a consistent range at which the EM 122 signal was present in the acoustic record at a particular level. However, the signal of the EM 122 was most consistently distinguishable in the 12.5 kHz band sound level time series at ranges less than 17 km in this annotation (observed once, albeit faintly, in a spectrogram at a time when the vessel was up to ~20 km away).

With regard to the changes in the sound levels, clipped peaks in *SPLpk* (i.e., 138 dB re 1 µPa) occurred when the EM 122 was in use 6 km away or less from the hydrophones. These events had corresponding peaks in the 12.5 kHz band of 50-75 dB re 1 μPa^2/Hz that were 19-42 dB over baseline, and the 40 kHz band was elevated by a similar magnitude. It is worth noting that the peaks in the 40 kHz band identified with these very close approaches of the EM 122 were puzzling. Although harmonics are produced with the MBES transmission, they typically account for only a few percent of the transmitted power and are commonly 20-30 dB lower than the intended signal when it is not clipped. This is a finding that needs further exploration. The lower select decidecade *BL*s were generally 10-15 dB over local baselines at close distances (i.e., < 6 km). At distances of 6-10 km, peaks in *SPLpk* ranged between 107-127 dB re 1 µPa and the 12.5 kHz peaks were 30-54 dB re 1 μPa^2/Hz, or 6-23 dB over baseline. At this range, the other decidecade *BL*s were only elevated by about 3-6 dB and there was no longer a similar magnitude peak in the 40 kHz band (though some events may have this because there were biological clicks present at the same time). Distinguishable peaks in the 12.5 kHz band time series that were clearly associated with the vessel and EM 122 activity were identified up to ranges of 13.5-17 km between the vessel and hydrophone (although EM122 pulses were visible in spectrograms out to 20 km). At this range, *SPLpk* varied from 107-134 dB re 1 µPa with peaks in the 12.5 kHz band of 35-44 dB re 1 μPa^2/Hz, or 2-14 dB over baseline. And fluctuations in the other decidecade bands were less than 3 dB. However, at this range, the peaks in *SPLpk* were not reliably indicative of solely the survey activity. For example, *SPLpk* was 134 dB re 1 µPa on hydrophone 70 during event 4, and although the EM 122 signal was present in the acoustic record while the survey vessel was 11.75 km away with an associated peak in the 12.5 kHz band

of 2 dB over baseline, there was also a very loud sound below 2 kHz recorded on the hydrophone receiver.

Although other active acoustic sources were used in the survey and identified in the annotation, their presence in the acoustic record was less pronounced. This is in part because they were used only intermittently during the MA period, but also because their source levels and duty cycles contributed to a much smaller impact. Thus, the acoustic contribution of these systems appeared to be even less than the EM 122. For example, the activity of the EM 712, the 40 kHz MBES, was detected only once during event 10 on hydrophone 70 and was only distinguishable in the sound level time series for a half hour while the survey vessel was within 5 km of the hydrophone. At its maximum, *SPLpk* was observed at 131 dB re 1 µPa and the 40 kHz band peak was 50 dB re 1 $\mu Pa^2/Hz$ when the survey vessel and hull-mounted EM 712 was within 1 km of the hydrophone. Though this most certainly was not the only hydrophone with sound levels that were elevated due to the use of this system, it suggests that this source had a very local acoustic impact due to the substantial transmission loss of the high frequency signal, and its non-omnidirectional radiation pattern. Using the elevated 3.2 kHz sound levels as a proxy for the presence of the SBP, the SBP was detected on six of the nine hydrophones (16, 22, 45, 57, 70, and 85) when the survey vessel was within 8 km of the hydrophones. This was associated with levels 5-10 dB over the local baseline. At most, the SBP was documented as distinguishable in the 3.2 kHz time series of hydrophone 16, which covered an hour and 45 minutes while the survey vessel was within 7 km of the hydrophone. Since the EK-80 is not a source primarily used for mapping deep-water environments, it was only used intermittently. Consequently, a comprehensive assessment of its contribution to the sound levels could not be made and the decidecade band most relevant to the EK-80 signal was not examined. Anecdotally, the EK-80

signal was detected during events when the vessel was within 3 km of a hydrophone (e.g., event 24 on hydro 45; event 12 on hydro 14; event 15 on hydro 16) and the *SPLpk* levels were not noticeably different during these times, compared to when the EK-80 was not in use. Because the other systems were only in use during the MA period and used intermittently, it was difficult to make a complete assessment about their realized contribution to the marine acoustic environment beyond that which is known about propagation loss of these system's signals. Despite comparable source levels, the EM 712 (40 kHz) and EK-80 (18 kHz) signals were of higher frequency than the EM 122, and thus attenuated more quickly in the acoustic environment, making them harder to observe. The SBP has a slightly lower source level of about 225 dB re 1 µPa @ 1m than the EM 122 and also a lower nominal frequency (3.5 kHz center frequency), meaning its signal attenuates less quickly. However, this part of the frequency spectrum was often quite loud, potentially masking the SBP signal.

The close passes of the survey vessel alone had a very characteristic sound level signature indicative of ship-radiated sound, i.e., elevated levels across a broad range of frequencies. A spectral analysis of the specific signature of the *Sally Ride* in comparison to other vessels present in the acoustic data was not made. However, based on the few decidecade band levels examined, the sound level signature of the survey vessel was quite similar to other passing vessels. When the survey vessel alone was within 3 km of a hydrophone, the peaks in the 50 Hz, 500 Hz, 3.2 kHz, and 12.5 kHz bands were all about 15-25 dB over their respective local baselines, and this was similar for *SPLpk*. Beyond 10 km, it was difficult to distinguish just the survey vessel in the sound level time series, and there was only one hydrophone upon which to characterize the sound levels at intermediate distances (hydrophone 85). The first passage of just the vessel to within 5 km of hydrophone 85 was not easily identifiable, while the second instance was. At this

later time, the 50 Hz-12.5 kHz *BL*s were between 5-10 dB over the local baseline and *SPLpk* was about 12 dB over baseline (although *SPLpk* may have also been influenced by other active acoustic sources higher in frequency at the same time since there was also a peak in the 40 kHz band).

Thus, the EM 122 signal appeared to be the most dominant source related to the survey activity. But there were other loud events of similar magnitude (e.g., hydrophone 45, event 11, *SPLpk* of 134 dB re 1 µPa) to the closest passes of the survey vessel with the EM122, frequently of unknown origin, although not attributed to the survey. It was unclear whether these were loud events far from the hydrophone, or potentially something brushing up against the hydrophone (e.g., hydrophone 22, event 3; hydrophone 70, event 4). There were also other repetitive pulses and clicking (e.g., hydrophone 45, event 21). Biological activity--often dolphin whistles and beaked whale clicks—was also routinely detected at *SPLpk* in the 115-125 dB re 1 µPa range (e.g., hydrophone 45, event 18 and 20), as well as in the 12.5 kHz band (e.g. hydrophone 16, event 11 and 13).

Despite other signals and periods of elevated levels from non-survey activity detected on the hydrophones, the survey activity was by far the most common source of acoustic events identified through the annotations. The survey vessel alone was detected on seven of the nine hydrophones (not on hydrophones 14 or 70), and discernible for 1 (hydrophones 63 and 85) to 3.5 hours (hydrophone 45) of the VO period. The survey activity during the VM period was intermittently discernable in the sound level time series for 7.33 hours on average, ranging from as few as 5 hours (hydrophone 19) to at most 11.75 hours (hydrophone 45). The survey activity during the MA period was also intermittently distinguishable for 3.6 hours on average, ranging from zero hours (hydrophone 19) to 8.75 hours (hydrophone 45).

From a weighted perspective, the contribution of the five decidecade band levels examined could generally be subdivided into three groups: the 3.2 kHz and 12.5 kHz bands as the most discernable (i.e., loudest), the 50 Hz band as the least discernible (i.e., quietest), and the 40 kHz and 500 Hz bands as intermediaries. This was unlike the unweighted levels in which the 50 Hz band was the most discernible. The extremely loud events (i.e., >> 40 dB re 1 $\mu Pa^2/Hz$) in the weighted levels aligned with when the survey vessel was within 5 km of the hydrophone and when the EM 122 was transmitting. At these times, the 12.5 kHz and 40 kHz bands dominated. It is worth noting that there were also other discernible acoustic events in the 12.5 kHz band that were not attributed to the EM 122 signal. These were generally much smaller peaks (i.e., 10 dB or less above the other bands), associated with biological activity and far less common. There were also times when either the 40 kHz band or 3.2 kHz band were most dominant, again, generally by no more than 10 dB more than the other bands. These events were often identified as marine mammal clicks (regarding the 40 kHz band) or a passing vessel nearby (regarding the 3.2 kHz band). The 50 Hz band was consistently at least 30 dB lower than the intermediary bands (i.e., 500 Hz and 40 kHz), except during the two events that appeared to be array-wide phenomenon—one in the NA period and the other in the VO period—as well as different times in the MA period on certain hydrophones.

Major Findings

- The time series annotation was an essential step for understanding the complex acoustic data from the deep-water MBES mapping survey. The exercise revealed the strong temporal and spatial dependence of the survey activity to the soundscape. In other words, the change in the sound levels was closely tied to a finite spatial radius around the mobile survey vessel, which meant the temporal impact at any given location was also confined to the brief time period that the vessel was in the respective area.

- The EM 122 signal was detectable in the acoustic record (i.e., discernable peaks in the sound level time series data) only when the survey vessel was within 17 km of a hydrophone receiver (visibly faintly in spectrograms up to 20 km from a hydrophone receiver).
- The EM 122 signal most clearly and consistently manifested in the elevated 12.5 kHz decidecade band levels, and was often—but not always-- associated with the peaks in the peak sound pressure level of the sound level metrics examined.
- The other active acoustic systems were detected substantially less often in the annotation than the EM 122, suggesting that the EM 122 had the largest contribution to the soundscape of the active acoustic sources in the 2017 mapping survey.
- The EM 122 was not the only detected source. There was consistently biological activity, other vessels passing on or near the array, as well as unidentified acoustic sounds.
- Clipping occurred at times when the survey vessel and transmitting EM 122 were 6 km or less away from a hydrophone, which meant the true sound level could not be recovered at those times.

Sound Level Percentiles

Analysis-Specific Methodology

Differences in the analysis period sound level percentiles (i.e., 1, 5, 10, 25, 50, 75, 90, 95, and 99th, Appendix 5.2) were computed both array-wide and on a per hydrophone basis for all of the sound level metrics (i.e., weighted and unweighted *SPLpk* and *SEL*, 50 Hz, 12.5 kHz, and 40 kHz *BL*s) and used to understand the variability in the sound levels recorded across the array. The array-wide sound level percentiles were calculated for each analysis period by considering all of the sound level observations averaged over all 89 hydrophones. Array-averaged sound level percentile differences were then generated by subtracting the same percentile of two

different analysis periods. Local sound level percentile differences were similarly calculated on a per hydrophone basis for the nine select hydrophones but by only considering the observations from a particular hydrophone.

Although sound level percentile differences were computed for each of the sound level metrics, the times series annotation findings (see Time Series Annotation section) were used to identify the most relevant metrics with respect to the survey activity, i.e., *SPLpk* and the 12.5 kHz *BL*s. These were the focus of interpretation, whereas only broad stroke trends were gleaned for the other metrics, i.e., *SEL*, 50 Hz, and 40 kHz *BL*s. The difference results were interpreted by partitioning the results into four relative magnitude classes based on the findings of the time series annotation: 1) < 3 dB (*negligible*), 2) 3-10 dB (*small* change), 3) 10-20 dB (*moderate* change), 4) >20 dB (*extreme* change). The fourth class, 20 dB or more, corresponded to the most extreme changes identified in the annotation, which were primarily identified in association with the survey activity at very close distances, under a few kilometers. The third class, 10-20 dB, often corresponded with survey activity within 10 km of a hydrophone, but there were other acoustic sources that also contributed to this level of change. The second class, 3-10 dB, corresponded to the smallest amount of change in the sound levels that was possible to associate with distinct acoustic events—survey or non-survey acoustic activity. Although a change of 3 dB indicates a doubling or halving of energy, it was difficult to clearly associate this magnitude of change with a distinct acoustic event. Thus, changes less than 3 dB were considered *negligible* for the purpose of this study. The higher magnitude changes were assumed to be most indicative of survey activity as changes of 20 dB or more were almost always associated with events corresponding with survey activity. Whereas for classes of lesser magnitude, the confidence that the survey activity was driving the observed change was expected to decrease

step-wise. It is worth reiterating that these difference classes and their descriptors i.e., *negligible, small, moderate, extreme* are used to describe the --relative --change in sound levels, as even a change of 3 dB represents a substantial change in acoustic intensity.

Within each of these broader categories the weighted and unweighted results are described with respect to the four classes of relative difference examined. General trends were described rather than descriptions of what occurred on each hydrophone. As the nine hydrophones were selected to represent a homogenous spatial sampling of the entire array, the trends were described from a spatial perspective. Therefore, the top row of hydrophones (i.e., 19, 16, 14) were described as the northern hydrophones, the middle row (i.e., 57, 45, 22) as the center hydrophones, and the bottom row (i.e., 85, 63, 70) as the southern hydrophones, whereas the left column (i.e., 19, 57, 85) were categorized as the western hydrophones, the middle column (i.e., 16, 45, 63) as the central hydrophones, and the right column (i.e., 14, 22, 70) as the eastern hydrophones.

Results

The 1st, 5th, 10th, 25th, 50th, 75th, 90th, 95th, and 99th percentile differences for *SPLpk* and the 12.5 kHz *BL*s were computed for each metric and are contained in Figure 5.5-Figure 5.8. The percentile difference results for the *SEL*, and other *BL* metrics are contained in Appendix 5.4. The individual hydrophone results are presented first, followed by the array-wide results.

By hydrophone

SPLpk

There were mostly *negligible* changes in the unweighted *SPLpk* percentiles across the analysis periods and hydrophones, with some *small* differences, commonly at the 75th or higher percentiles, and a few *moderate* changes, but only in the 95th or 99th percentiles (Figure 5.5, left). Only *small* differences were detected between the VO and NA periods, and these were mainly in

the central (16, 45, and 63) or eastern side (14, 22, and 70) of the array, most consistently in the 99th percentile. The lack of difference between these two periods on the western hydrophones was likely attributed to two factors, 1) there were vessels on/near the array documented in the sound levels during both periods, and 2) these hydrophones are bottom-mounted in the deepest part of the array where many high frequency signals generated close to the sea-surface are likely to attenuate to a great degree before reaching the receivers in comparison to the depth of some of the more shallow hydrophones.

There were also only *small* differences detected in *SPLpk* between the VM and NA periods, most ubiquitously in the 99th percentile levels. Although the northern hydrophones (19, 16, and 14) had *small* differences in *SPLpk* from the 75th percentiles and up-- the NA period was louder, whereas the VM period was louder in the 99th percentiles on the central and southern hydrophones. Between the MA and NA periods, the results varied by hydrophone, but differences were most consistently found in the 95th and 99th percentiles with the MA period louder. The lack of consistent differences found in lower percentiles (50th and below) suggests that it was really only for a short duration in the loudest levels that the anthropogenic periods differed from the NA period. Among the anthropogenic activity periods, there were fewer consistent changes across space. For example, the northern and southern hydrophones were slightly louder in the VO period than the VM period, while there was little difference in the center hydrophones. The MA/VO and MA/VM comparison results seemed even more random, with most differences detected in the 95th and 99th percentiles, but the period that was louder depended on the specific location. This suggests that the anthropogenic periods were not reliably different from one another in terms of unweighted *SPLpk*, and in what way the periods differed really depended on the hydrophone and likely its spatial location with respect to the survey lines.

Overall, the differences identified in *SPLpk* were *small* and the most consistent differences were in the 99th percentile between the NA period and the periods of anthropogenic activity. (Figure 5.5, *left*)

wSPLpk

The trends in w*SPLpk* differed from the unweighted results (Figure 5.5, *right*). When unweighted, the sound levels in the NA period had a substantial contribution from low frequency sound (e.g., long periods of elevated levels in the 50 Hz band) which seemed to dwarf the other higher frequency signals present. The weighting process de-emphasized the very low frequency, and emphasized the higher frequency content, for which the multibeam mapping survey contributes. For w*SPLpk*, there were very few percentiles with *negligible* differences between NA and survey activity periods (i.e., VO, VM, and MA). There were many more *moderate* differences identified between periods and *extreme* differences, again, with respect to periods with and without survey activity. The survey activity periods were consistently louder, as expected. Between the VO and NA periods, the central and eastern side of the array had the most *moderate* and *extreme* differences, which were commonly in the 75th, 90th, and 95th percentiles. Between the VM and NA periods, the most *extreme* differences were in the 99th percentiles on the central hydrophones, albeit there were *moderate* differences in several percentiles on all but the northern corner (19, and 14) and southwestern corner (85) hydrophones. This is unsurprising as it correlates well with where the most activity occurred during the VM period. This was generally true for the MA and NA comparison too, where the hydrophones that were the furthest from the survey lines run during the MA period (hydrophones 19, 22, 57) had *small* differences relative to the other hydrophones closer to the survey activity. Although, there were only *small* differences with respect to hydrophone 85 between these two periods despite the survey vessel

closely passing this hydrophone during the MA period. There were *small* differences detected among the various periods of survey activity, with respect to w*SPLpk*. But again, there were not clear and consistent delineations in how the periods were different. This very likely reflects the other acoustic activities present that were not survey activity. The northern and southern hydrophones were generally slightly louder during the VO period than they were in the VM period. However, the center hydrophones were slightly louder in the VM period than they were in the VO period. There were far fewer differences in w*SPLpk*, even *small* ones, between the VO and MA periods with no consistent patterns other than that the southeast corner (hydrophones 63 and 70) of the array was slightly louder in the lower 75th percent of the data during the VO period. This was not expected, given the survey activity during the VO period was mostly confined to the central or western side of the array. However, a closer inspection of the sound level time series of these two periods revealed extended periods of elevated levels in the 40 kHz band (see Time Series Annotation section), which was associated with substantial biological activity, i.e., marine mammal clicks.

The comparison of w*SPLpk* between the MA and VM period was also telling. Albeit not consistently, the lower 50th percent of the data were slightly louder in the VM period, whereas the upper 50th percent of the data were slightly louder in the MA period. This suggests that the ambient conditions of the VM period were slightly elevated (i.e., 3-6 dB) in comparison to the MA period, but the loudest times (i.e., upper 25%) of the VM period were generally slightly quieter than the MA period. This matches expectation since the EM 122 was consistently on during the VM period and the track lines comprehensively covered the array spatially. In the MA period, multiple loud acoustic sources were used, which elevated levels locally and slightly more than the VM period, but the track lines of the survey vessel during this period were not

comprehensive. Although there were other sound sources present during both periods that may have contributed to this result in an unknown way, this finding suggests that the additional acoustic sources, beyond just the EM 122, may have contributed to the changing sound levels in a noteworthy way. However, the differing spatial coverage of the survey activity during these two periods is a confounding factor in fully understanding this result. (Figure 5.5, *right*)

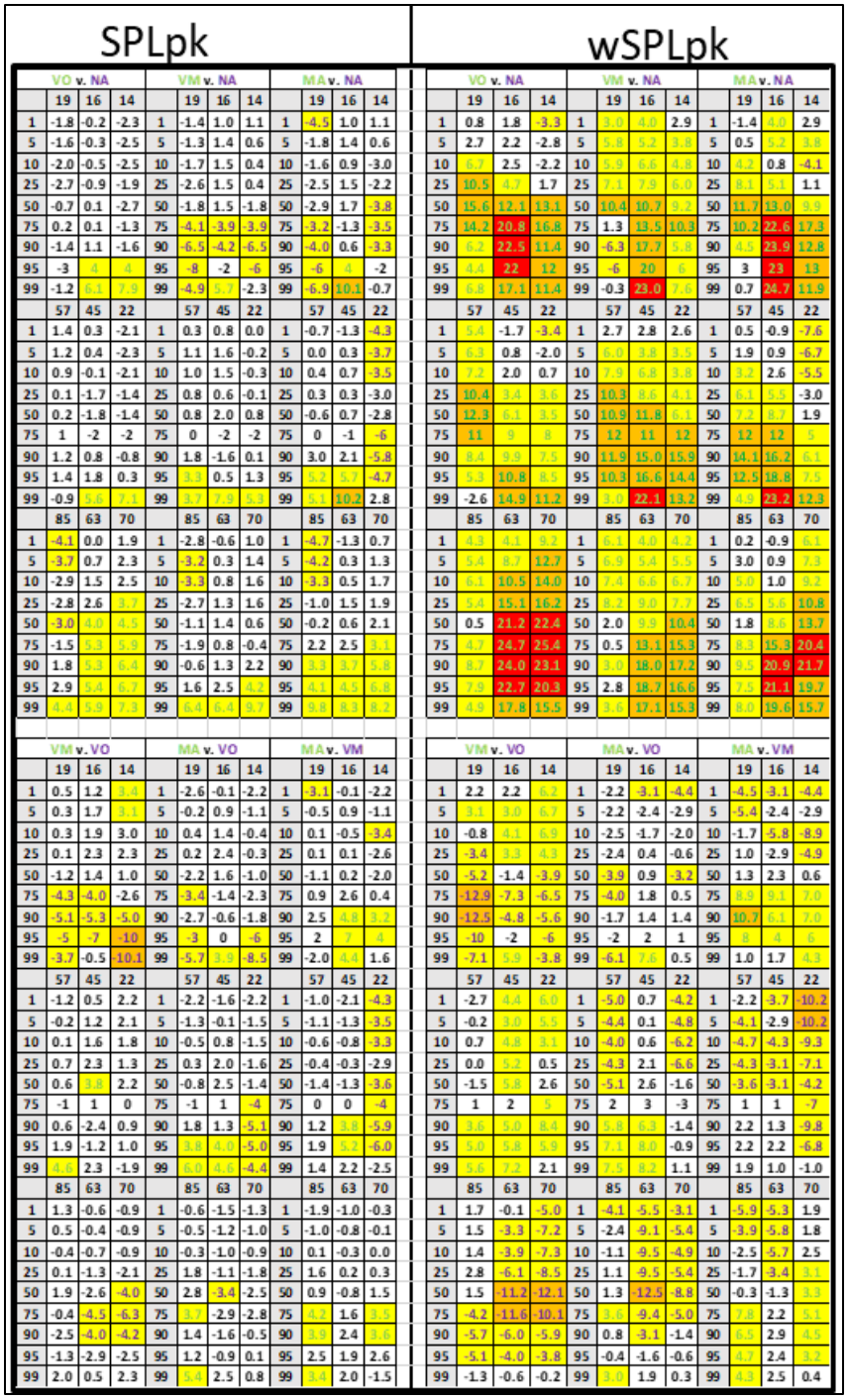

Figure 5.5. Sound level percentile differences for *SPLpk* (left) and *wSPLpk* (right) across analysis periods. Each cell represents the specific percentile (grey row headings) difference by hydrophone (grey columns headings) between two analysis periods (white column headings): VO (Vessel Only), NA (No Activity), VM (Vessel and MBES), MA (Mixed Acoustics). Differences were identified in four classes: 1) < 3dB (white), 2) 3-10 dB (yellow), 3) 10-20 dB (orange), 4) >20 dB (red). Where differences were identified, the color (green/purple) of the value represents which analysis period was louder, corresponding with the color of the two specific analysis periods being compared.

12.5 kHz BLs

There were mostly *small* and *moderate* differences between analysis periods in the 12.5 kHz band level percentiles (Figure 5.6). *Moderate* differences were commonly found between periods with and without survey activity mostly in the upper 50 % of the data, whereas *smaller* differences were more commonly found between the different periods of survey activity (VO, VM, and MA). *Extreme* differences were found, mostly between the NA period and those when mapping sonar was in use (i.e., VM and MA). However, the 99th percentile was much louder in the VO period than the NA period on hydrophone 45. This was likely because of its location in the center of the array, which makes it 1) less susceptible to changes due to off-range activity, and 2) exposed to the VO activity more than any of the other select hydrophones. Between the VM and NA period, *moderate* or *extreme* differences were identified in the 99th percentile on all but hydrophone 19, which suggests the biggest differences were really only in about 1% of the sound level data. However, most of the percentile differences between these two periods were at least *moderate* on the western and central part of the array, while the eastern side had mostly *small* differences, except at the 99th percentile. Because the survey lines during the VM period were generally spatially comprehensive over the entire array, it does not seem likely that this difference was related specifically to the spatial pattern of the survey activity. However, the differences in the MA/NA comparison may be attributed to the difference in exposure of the select hydrophones to the MA activity since the track lines during the MA period were not spatially comprehensive. Hydrophones 14, 16, 45, 63, and 85, which all had *extreme* differences in the 99th percentile levels, were all exposed to very close passes of the survey vessel during the MA period, whereas the other hydrophones were not. (The only exception to this was hydrophone 70 which also was within a very close distance to the survey vessel during the MA period, but only had *moderate* differences in the 99th percentile levels.) This result further

confirms the localized impact of the survey activity, i.e., the spatial impact is at a scale smaller than the spacing between the select hydrophones, and the most pronounced differences at the highest percentiles suggests a very finite, i.e., short and transient, temporal impact. In other words, for hydrophones that were not within a very close distance of one of the MA survey lines, the sound level percentile differences were *small* to *negligible*.

The pattern in the percentile differences between the VM and VO periods generally mirrored the VM/NA results, but at a lesser magnitude. There were mostly *small* differences identified between the two periods in all of the percentiles, except at the 99th percentile, which were mostly *moderate* differences. This suggests that the signals from the EM 122 only made a *moderate* difference to the 12.5 kHz band levels beyond the presence of the survey vessel alone. There were not clear patterns that came out of the comparison of the MA/VO periods in the 12.5 kHz band, likely because the vessel had a very different spatial coverage during each of the two periods, making it difficult to tease apart interacting factors such as the amount of exposure to the anthropogenic activities and the actual anthropogenic activities themselves. The central hydrophones and hydrophone 85 were all within at least one track line of each the MA and VO periods, which generally all showed that the upper 5-10% of the data was *slightly* (i.e., small difference) or *moderately* louder in the MA period with largely *negligible* differences in the lower 50% of the data. The biggest differences in the MA/VM periods in the 12.5 kHz band were in percentiles 50 and lower, where the VM period was *moderately* louder. This was least pronounced on the central hydrophones, likely because of their centralized location to the survey activities during each period. (Figure 5.6)

	VO v. NA				VM v. NA				MA v. NA			
	19	16	14		19	16	14		19	16	14
1	-1.5	0.7	-4.3	1	3.8	5.3	2.8	1	-6.2	5.3	2.8
5	-0.8	1.0	-4.0	5	6.6	5.9	3.8	5	-6.2	5.9	3.8
10	0.4	1.3	-3.1	10	6.9	6.2	4.5	10	-5.9	-0.1	-11.1
25	2.0	2.1	-0.9	25	6.9	8.7	5.1	25	-1.0	2.4	-5.4
50	2.7	3.9	3.0	50	10.9	9.7	7.1	50	3.7	5.2	-0.5
75	4.4	4.3	4.5	75	10.4	9.9	8.5	75	4.5	7.2	3.8
90	-1.6	8.7	3.0	90	2.8	10.8	6.2	90	-1.0	13.3	3.9
95	-2.6	10	6	95	1	14	5	95	-3	16	6
99	-3.2	12.4	10.0	99	8.4	26.7	14.9	99	-3.0	23.6	20.5
	57	45	22		57	45	22		57	45	22
1	0.6	-3.0	-6.2	1	3.8	6.4	0.6	1	-1.7	-0.8	-13.7
5	1.6	-3.4	-5.9	5	9.4	6.6	2.5	5	-1.6	-0.1	-13.5
10	3.0	-2.0	-5.0	10	11.0	7.2	3.0	10	-1.3	-0.1	-13.0
25	4.0	-1.2	-1.0	25	12.9	9.8	4.2	25	2.7	1.7	-8.4
50	7.3	1.9	2.3	50	16.9	12.3	7.3	50	6.7	4.5	-4.7
75	9	5	3	75	17	15	9	75	10	10	-1
90	9.1	9.2	1.5	90	16.2	15.5	6.8	90	12.1	12.3	1.8
95	12.1	12.1	4.5	95	17.4	18.4	9.3	95	12.6	17.3	1.9
99	15.0	21.3	14.7	99	29.6	27.9	21.3	99	10.7	25.4	6.2
	85	63	70		85	63	70		85	63	70
1	0.6	-1.5	4.5	1	6.6	3.0	5.5	1	-1.4	-0.8	2.6
5	1.2	-0.5	6.1	5	8.5	6.1	6.1	5	-1.4	-0.1	4.6
10	2.2	1.3	5.8	10	9.2	6.9	5.8	10	-1.0	-2.7	4.9
25	4.4	8.0	5.8	25	12.6	13.3	7.4	25	5.4	1.4	6.3
50	5.4	10.4	6.5	50	14.6	15.7	8.4	50	9.0	10.2	7.8
75	3.6	11.6	5.7	75	9.5	17.6	7.5	75	6.1	14.0	9.7
90	4.6	13.0	5.6	90	8.9	17.3	7.9	90	5.6	14.6	12.5
95	5.0	13.7	6.2	95	11.0	19.4	11.4	95	10.4	18.2	13.8
99	8.3	15.0	7.2	99	23.2	27.8	21.7	99	30.1	25.7	15.7

	VM v. VO				MA v. VO				MA v. VM		
	19	16	14		19	16	14		19	16	14
1	5.3	4.6	7.0	1	-4.6	-5.2	-10.1	1	-10.0	-5.2	-10.1
5	7.4	4.9	7.8	5	-5.4	-2.7	-9.7	5	-12.8	-2.7	-9.7
10	6.5	5.0	7.7	10	-6.2	-1.4	-7.9	10	-12.8	-6.3	-15.6
25	4.9	6.6	6.0	25	-3.0	0.3	-4.6	25	-7.9	-6.3	-10.6
50	8.2	5.7	4.1	50	1.0	1.2	-3.4	50	-7.2	-4.5	-7.6
75	6.0	5.6	4.0	75	0.1	2.8	-0.7	75	-5.9	-2.7	-4.7
90	4.4	2.1	3.2	90	0.6	4.5	1.0	90	-3.8	2.4	-2.2
95	3	4	0	95	0	6	0	95	-4	2	1
99	11.6	14.4	4.9	99	0.3	11.2	10.4	99	-11.3	-3.2	5.6
	57	45	22		57	45	22		57	45	22
1	3.2	9.4	6.8	1	-2.3	2.2	-7.5	1	-5.5	-7.2	-14.3
5	7.9	10.0	8.4	5	-3.2	3.3	-7.6	5	-11.1	-6.7	-16.0
10	8.0	9.2	8.0	10	-4.2	1.9	-8.0	10	-12.2	-7.3	-16.0
25	8.9	11.0	5.2	25	-1.3	2.9	-7.4	25	-10.3	-8.1	-12.6
50	9.6	10.4	5.0	50	-0.6	2.6	-7.0	50	-10.2	-7.8	-12.0
75	9	10	6	75	2	6	-3	75	-7	-4	-9
90	7.1	6.3	5.3	90	2.9	3.1	0.2	90	-4.2	-3.2	-5.1
95	5.3	6.3	4.8	95	0.5	5.2	-2.6	95	-4.8	-1.1	-7.4
99	14.6	6.7	6.6	99	-4.3	4.1	-8.5	99	-18.8	-2.6	-15.1
	85	63	70		85	63	70		85	63	70
1	6.0	4.6	0.9	1	-2.0	-1.4	-1.9	1	-8.0	-5.9	-2.9
5	7.3	6.6	0.0	5	-2.5	-2.4	-1.5	5	-9.8	-9.0	-1.5
10	7.0	5.6	0.0	10	-3.2	-4.0	-0.9	10	-10.2	-9.6	-0.9
25	8.1	5.3	1.5	25	1.0	-6.6	0.5	25	-7.2	-11.9	-1.1
50	9.2	5.3	1.9	50	3.7	-0.1	1.3	50	-5.6	-5.4	-0.6
75	5.9	6.1	1.8	75	2.5	2.5	4.0	75	-3.4	-3.6	2.3
90	4.4	4.3	2.3	90	1.0	1.6	6.9	90	-3.4	-2.7	4.7
95	5.9	5.7	5.2	95	5.4	4.5	7.5	95	-0.5	-1.2	2.3
99	14.9	12.8	14.5	99	21.7	10.7	8.5	99	6.9	-2.1	-6.0

Figure 5.6. Sound level percentile differences for 12.5 kHz BL across analysis periods. Each cell represents the specific percentile (grey row headings) difference by hydrophone (grey columns headings) between two analysis periods (white column headings): VO (Vessel Only), NA (No Activity), VM (Vessel and MBES), MA (Mixed Acoustics). Differences were identified in four classes: 1) < 3dB (white), 2) 3-10 dB (yellow), 3) 10-20 dB (orange), 4) >20 dB (red). Where differences were identified, the color (green/purple) of the value represents which analysis period was louder, corresponding with the color of the two specific analysis periods being compared.

The sound level percentile difference figures for the 50 Hz *BL*, 40 kHz *BL*, and *SEL* metrics are contained in Appendix 5.4.

50 Hz BL

As expected, the NA period was *slightly* (VO) or *moderately* louder (VM and MA) than any of the anthropogenic periods in the 50 Hz *BL*. This makes sense given the extended time of elevated levels identified in this period and band. The periods with active acoustics (i.e., VM and MA) were generally *slightly* louder than the VO periods, but *moderately* louder in the top 10% of the data. There were only *small* differences between the two active acoustic periods (MA/VM),

for which the MA period was *slightly* louder than the VM period in the 50 Hz band. (Appendix 5.4, Figure 5.4.1)

40 kHz BL

The differences identified in the 40 kHz *BL* were almost exclusively in the upper 25th percent of the data (i.e., percentiles 75 and above). In comparing periods with and without survey activity, the most pronounced differences were in the south or north of the array, with the most *extreme* differences on hydrophones at the southern end of the array. The survey periods were always louder (*moderately* or *extremely*), in this respect, compared to the NA period. But again, this was primarily in the upper –loudest--quarter of the data with little (i.e., *small*) difference in the quieter levels (i.e., 50th percentile and below). Between periods of survey activity, *small* and *moderate* differences were identified at the 75th and higher percentiles. For example, between the VM and VO periods, the VO period was *slightly/moderately* louder on northern and southern hydrophones, but the VM period was *slightly* louder on center hydrophones. It is unclear why this was the case. There were few and inconsistent differences in the percentiles between the MA and VO periods. This is reasonable given 1) the EM 712 was the only intentional survey signal transmitting at this frequency during the MA period, and its signal was expected attenuate rapidly in the environment, and 2) there were known biological sound sources contributing to this frequency band all across the array and throughout the entire study period (i.e., all analysis periods). Thus no consistent patterns were expected for this frequency band. The results for the 40 kHz band further support the conclusion that the impact of the survey activity was localized—with respect to space, time, and—as the results of this band show--frequency. (Appendix 5.4, Figure 5.4.2)

SEL

The trends in the *SEL* results (Appendix 5.4, Figure 5.4.3) mimicked the *SPLpk* results, albeit smoothed, as expected based on the definitions of these two metrics. In terms of unweighted *SEL*, there were mostly only *negligible* to *small* differences detected in any of the percentiles, largely in the upper 25th percent of the data and mostly restricted to the comparisons of the NA period with the periods with active acoustics, or between the VO period and the periods with active acoustics. There were hardly any differences between the NA and VO periods, and the two periods of active acoustics, suggesting there were two groupings with respect to *SEL*. One might hypothesize that this has to do with the prominent acoustic events of the NA and VO periods being more continuous (i.e., general quiet in the NA period and continuous vessel sound in the VO period), whereas the acoustic events of the VM and MA periods were more transient and pulsed (i.e., active acoustics in both periods). For the weighted *SEL* there was a distinguishable difference between periods of survey activity (i.e., VO, VM, and MA) and those without (i.e., NA). For analysis periods with survey activity, there were generally *small* percentile differences among the periods. The VM period clearly contained the most energy of the three periods (i.e., higher *wSEL* in VM compared to both VO and MA). (Appendix 5.4, Figure 5.4.3)

Array-wide

Array-wide comparisons were made between each of the analysis periods for each of the sound level metrics (Figure 5.7-Figure 5.8; Appendix 5.4, Figure 5.4.4-5.4.7). The results generally corroborated the findings from the individual hydrophone comparisons. For example, only the 99th percentiles of *SPLpk* were *slightly* elevated in the survey activity periods, i.e., VO, VM, and MA (3.5, 3.7, and 3.6 dB, respectively) over the levels of the NA period (Figure 5.7). For *SEL*, the main differences (up to 6 dB) were largely between the NA period and the active

acoustic periods, or between the VO period and the active acoustic periods (Figure 5.4.7). In either case, the sound level percentiles of the active acoustic periods were lower, again, likely because of the persistent and ubiquitous very low frequency energy in both the NA and VO periods. This trend was flipped for *wSEL*, where the sound levels in periods with survey activity were all elevated over the NA period. When comparing *wSEL* across the three periods of survey activity, the VM period was loudest, followed by VO, then MA. But in terms of w*SPLpk*, the VO period was relatively loudest, followed by VM, then MA (Figure 5.7, right). As expected, the largest differences in w*SPLpk* were between periods with and without survey activity, with generally similar trends despite differences in the particular survey activity. There were *small* differences between the 25^{th}-99^{th} percentiles, and *moderate* differences between the 75^{th}-95^{th} percentiles in comparing the NA period to all periods of survey activity. The VM period had *small* differences in comparison with the NA period at the other percentiles (i.e., 1-10^{th}), whereas there were *negligible* differences between the MA/NA periods at these same percentiles. The VO/ NA comparison had a similar trend as the comparison of VM/ NA, with *moderate* differences at the 50^{th} percentile and *negligible* differences in the 1^{st} percentile. These differences are likely largely due to the difference in spatial coverage of the various survey activities during these two periods.

SPLpk							wSPLpk						
Percentiles	VO v NA	VM v NA	MA v NA	VM v VO	MA v VO	MA v VM	Percentiles	VO v NA	VM v NA	MA v NA	VM v VO	MA v VO	MA v VM
1	-0.2	0.5	-1.2	0.7	-0.9	-1.6	1	2.7	5.3	-0.2	2.6	-2.9	-5.5
5	-0.1	0.4	-1.0	0.5	-0.9	-1.4	5	4.4	6.7	0.8	2.3	-3.5	-5.9
10	-0.3	0.4	-1.0	0.7	-0.7	-1.4	10	5.5	7.5	2.3	2.0	-3.2	-5.2
25	-0.2	0.3	-0.9	0.5	-0.7	-1.2	25	8.0	8.2	4.5	0.2	-3.5	-3.7
50	0.3	0.0	-1.1	-0.3	-1.4	-1.1	50	12.4	9.1	7.3	-3.3	-5.1	-1.8
75	1.2	-1.1	-1.2	-2.3	-2.4	0.0	75	15.6	10.1	11.3	-5.4	-4.3	1.1
90	1.9	-1.1	0.1	-3.0	-1.8	1.2	90	14.7	11.1	12.5	-3.6	-2.2	1.4
95	2.5	0.2	1.3	-2.2	-1.2	1.0	95	12.6	10.0	10.9	-2.6	-1.7	0.9
99	3.5	3.7	3.6	0.2	0.1	-0.1	99	6.0	6.4	6.2	0.4	0.2	-0.2

Figure 5.7. Array-wide *SPLpk* (left) and *wSPLpk* (right) percentile differences between each set of analysis periods. Differences were identified in four classes: 1) < 3dB (white), 2) 3-10 dB (yellow), 3) 10-20 dB (orange), 4) >20 dB (red). Where differences were identified, the color (green/purple) of the value represents which analysis period was louder, corresponding with the color of the two specific analysis periods being compared.

Percentiles	VO v NA	VM v NA	MA v NA	VM v VO	MA v VO	MA v VM
1	0.1	6.7	-1.3	6.7	-1.4	-8.1
5	1.4	8.7	-1.5	7.3	-2.9	-10.2
10	2.2	9.7	-1.3	7.5	-3.4	-11.0
25	4.0	10.8	0.9	6.9	-3.1	-10.0
50	4.2	10.0	2.9	5.9	-1.2	-7.1
75	4.0	9.6	4.4	5.6	0.3	-5.3
90	3.4	8.0	5.1	4.6	1.8	-2.9
95	1.0	5.7	4.4	4.7	3.5	-1.2
99	-3.2	7.3	4.8	10.5	8.0	-2.5

Figure 5.8. Array-wide percentile differences in the 12.5 kHz band between each set of analysis periods. Differences were identified in four classes: 1) < 3dB (white), 2) 3-10 dB (yellow), 3) 10-20 dB (orange), 4) >20 dB (red). Where differences were identified, the color (green/purple) of the value represents which analysis period was louder, corresponding with the color of the two specific analysis periods being compared.

From an array-wide perspective, two patterns were clear in the 12.5 kHz band percentile differences: 1) the VM period was loudest relative to the other periods of survey activity, and 2) all periods of survey activity were louder relative to the NA period. Across the array, the VM period was louder at every percentile, in comparison to the same percentiles in either the NA or VO periods (Figure 5.8). There were *small* differences between the VO and NA periods in the upper 75th percent of the data, whereas there were *small* differences between the MA and NA period in only the upper 25th percent of the data. The MA and VM periods differed in *small* and

moderate ways in all but the 90th and higher percentiles which were not different. The difference in spatial coverage of the two survey periods (i.e., more survey lines in the VM period) likely contributes to these observed differences. Whereas for the MA and VO periods, the MA period was *slightly* louder at the 95th and 99th percentiles while the VO period was higher at the 10th and 25th percentiles. As there were few survey lines in both periods, this difference is more likely attributed to the difference in acoustic activity rather than the difference in survey lines.

The differences detected in the 50 Hz band (Appendix 5.4), again, confirm that the NA and VO periods were loudest and this can be attributed to the array-wide phenomena identified in the time series annotation. The differences in the 40 kHz band from an array-wide perspective were in the upper 25th percentile, suggesting the observations in this frequency band were largely unchanged by the survey activity (Appendix 5.4). Because there were multiple known sources contributing to this band (i.e., EM 122 harmonics, EM 712, beaked whale clicks, unknown pulses), an interpretation beyond this with respect to the survey activity was unclear. It is worth noting that the results of the array-wide analysis do not provide further insight about the contribution of the survey activity beyond that of the select hydrophone analysis. This 1) further confirms the local scale (spatial, temporal, and frequency) of impact that the survey had on the soundscape, and 2) suggests that an investigation of the changing sound levels at a scale smaller than the resolution of the nine select hydrophones would be more meaningful.

Major Findings

- The differences identified in *SPLpk* were small (<10 dB) and most consistently in the 99th percentile between the NA period and the periods of anthropogenic activity (i.e., VO, VM, and MA). The lack of consistent differences found in lower percentiles (50th and below) for *SPLpk* suggests that it was really only for a short duration in the loudest levels that the anthropogenic periods differed from the NA period.

- For the 12.5 kHz band, *moderate* (10-20 dB) or *extreme* (>20 dB) differences were only identified in the 99th percentile between the VM and NA period, suggesting the biggest changes related to the MBES mapping activity occurred in only a small portion of the observations and at the loudest sound levels.
- The survey activity had a local impact. There was clear variation across hydrophones, indicating that the spatial impact was on a scale smaller than the spacing between the select hydrophones examined. The most pronounced differences occurred only at the highest percentiles (99th), indicating the limited temporal impact of the mapping activity. The clearest patterns in the sound level differences were observed in the 12.5 kHz band, reflecting the narrow frequency contribution of the MBES mapping activity.

Probability Distribution Comparison

Analysis-Specific Methodology

In order to better characterize the impact of the primary mapping system, the EM 122, on the marine acoustic environment, the cumulative distribution functions (CDFs) of the 12.5 kHz decidecade band sound level observations were compared across space and time on a per hydrophone basis for the nine select hydrophones, as well as an array-wide average (i.e., using observations from all 89 hydrophones).

A statistical hypothesis test using the Wasserstein Distance (W) as a test metric was used to compare distributions by testing whether the two samples, i.e., analysis period CDFs, came from a similar population. The Wasserstein Distance is defined as follows:

$$W = \left(\int_0^1 \left(F_A^{-1}(u) - F_B^{-1}(u)\right)^2 du\right)^{1/2} \quad \text{(Equation 5.9)}$$

where F_A and F_B represent the continuous CDFs of the two samples representing two different conditions, i.e., analysis periods. The 2-Wasserstein Distance (W^2) was used to understand how the two analysis periods differed and is defined as:

$$W^2 = \left(\int_0^1 \left(F_A^{-1}(u) - F_B^{-1}(u)\right)^2 du\right) = (\mu_A - \mu_B)^2 + (\sigma_A - \sigma_B)^2 + 2\sigma_A\sigma_B(1 - \rho^{A,B}) \quad \text{(Equation 5.10)}$$

which can be decomposed into location, size, and shape terms. The location term is a function of the means (μ), the size term is a function of the standard deviations (σ), and the shape term is a function of both the standard deviations and the Pearson correlation coefficient (ρ). (Schefzik *et al.* 2021)

Here, discrete, empirical CDFs were used to approximate the distributions of the continuous CDFs. First, the empirical PDFs of the 12.5 kHz *BL*s of the four analysis periods were computed by partitioning the respective (i.e., for a given analysis period and hydrophone/array-wide) sound level observations, *y* (dB), into discrete sound level bins in 1-dB increments, i.e., $y \in bin_x \; if \; x_a \leq y \leq x_b$, where x_a and x_b are 0.5 dB less or more, respectively, than the center point of the bin, x. The center points therefore were defined at 0.5 dB re 1μPa^2/Hz values. For example, if the first three bin center points were 0.5, 1.5, and 2.5 dB re 1μPa^2/Hz, then the range of the respective bins were from 0-1, 1-2, 2-3 dB re 1μPa^2/Hz, and so on. The observations were summed by bin and divided by the total number of samples contained in the entire distribution to obtain the probability of a specific sound level in a sound bin for a specific analysis period. The minimum and maximum sound level bin magnitudes were defined based on the minimum and maximum sound levels over the entire study 12.5 kHz band level time series for the respective observations assessed. The data were then rearranged to form CDFs, i.e., $y \in bin_x \; if \; y \leq x_b$ where x_b is as defined previously.

The R package 'waddR' (Schefzik, 2020), was used to compute and compare the 2-Wasserstein Distances due to its reported versatility across other fields (Schefzik *et al.* 2021). The 'waddR' package is based on a semi-parametric testing procedure, in which a series of permutations of the original data are computed and compared. The default number of permutations-- 10,000-- was used. The permutation procedure is based on a random sampling of the data. The semi-parametric procedure incorporates a generalized Pareto distribution approximation, which is optimal for modeling the tail of another distribution (MathWorks, R2021a). The null hypothesis of the test was that the two samples came from the same distribution. If the null hypothesis was rejected, the 2-Wasserstein decomposition provided information about the percent of the difference that was explained by the location, size, or shape of the distribution. Here, an alpha critical value of 0.1 was used to guide the interpretation of the results. For test results with a p-value <0.1, the two distributions were interpreted as different from one another.

It was hypothesized that the sound level distributions of all of the select hydrophones and an array-wide average would differ between the NA and VM period, since the 12.5 kHz *BL* was specifically used to identify changes with respect to the survey activity during the VM period and because the survey activity was distributed fairly homogenously over the array during this period. By similar reasoning, it was expected that at least some of the hydrophone-specific sound level distributions would differ between the NA and MA period since the EM 122 was also used at times during this period, although the activity was not as spatially homogenous as in the VM period. It was also hypothesized that there would be differences between the VO period and the VM and MA periods since there was also no known source transmitting in the 12.5 kHz band in the VO period. However, because of the nuanced spatial coverage of the survey during

both the VO and MA periods, it was not expected that the results would be as clear as in the NA and VM comparisons.

Results

The 795,000 100-ms sound level observations (for each hydrophone) of the 12.5 kHz decidecade band spanned from 1 to 100 dB re 1 $\mu Pa^2/Hz$ and were binned by 1 dB into 100 bins. The sound level distributions of the 12.5 kHz band were compared across the four analysis periods. The significant results of the hypothesis test for each of the nine hydrophones, as well as all of the array-wide results, are provided in Table 5.3 and Table 5.4, respectively, whereas the non-significant findings by hydrophone are contained in Appendix 5.5. Although the cumulative distribution functions were the input that were compared in the hypothesis testing, figures of the probability distributions are provided as they were more intuitive for interpreting the hypothesis test results.

By hydrophone

Table 5.3. Summary of 12.5 kHz decidecade band level probability distribution comparisons with significant results. The two distributions compared are listed, followed by the p-value of the comparison test, the 2-Wasserstein distance (W^2), and its decomposition into location, size, and shape terms, each as a percentage of the difference explained.

Analysis periods compared, Hydrophone number	**P-value**	**W^2**	**Location (%)**	**Size (%)**	**Shape (%)**
NA vs. VO, Hydro 63	0.0711	0.0529	15.62	3.32	81.06
NA vs. VM, Hydro 16	0.0842	0.0524	17.79	4.73	77.48
NA vs. VM, Hydro 45	0.0328	0.0772	19.77	3.63	76.6
NA vs. VM, Hydro 57	0.0063	0.1044	21.82	6.36	71.82
NA vs. VM, Hydro 63	0.0079	0.0974	22.04	4.58	73.37
NA vs. VM, Hydro 85	0.0373	0.0552	24.93	9.56	65.52
NA vs. MA, Hydro 63	0.0613	0.0404	16.77	0.25	82.98
VO vs. VM, Hydro 45	0.0803	0.0407	22.84	10.69	66.47
VM vs. MA, Hydro 22	0.0512	0.0554	23.33	11.58	65.09

Of the nine hydrophones, only the hydrophone 63 sound level distributions differed between the NA and VO periods (W^2 =0.0529, p<0.0711). This was not surprising since there were no known sound sources active in this band related to the survey activity. The shape of the distributions was predominantly driving this result: the NA distribution was mostly symmetrical, whereas the VO period was left-skewed. The central tendencies of the two distributions were also clearly different (Figure 5.9); the VO period was shifted to the right of the NA period. The annotation of hydrophone 63 (Appendix 5.3, Figure 5.3.6) corroborates this, the 12.5 kHz band was quite stable in the NA period, whereas the VO period levels were noticeably elevated over the NA period and with larger fluctuations. Although the survey vessel did come within a few kilometers of hydrophone 63 during this period, it was only at the end and for a short period.

This hydrophone had a lot of biological activity during this period that likely was the driving mechanism for the difference between these two periods.

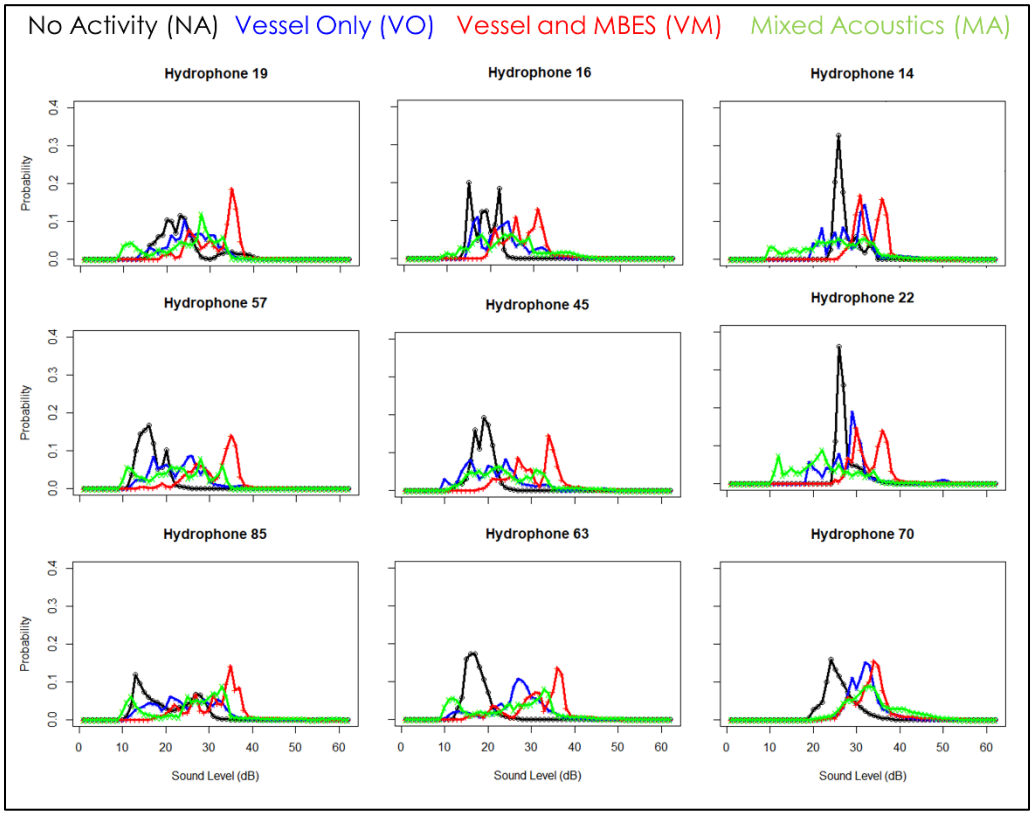

Figure 5.9. 12.5 kHz decidecade band sound level probability distributions by hydrophone for each analysis period, where the NA period is indicated by black lines, the VO period by blue lines, the VM period by red, and the MA period by green. Plot axes are the same in each plot. Sound level bins across the x-axis of each plot range from 0 to 60 dB re 1 µPa^2/Hz and probability of the sound levels being in a bin are shown by the y-axis and range from 0 to 0.4. Hydrophone number is provided above the corresponding plot.

Five of the nine hydrophone probability distributions differed between the NA and VM periods, i.e., hydrophones 16, 45, 57, 63 and 85 (See Table 5.3 for specific results). The decomposition again suggested these two periods largely differed in terms of shape, i.e., 65-78%, and to some extent location i.e., 17-25% (Table 5.3). In each case, the VM period had a left-skewed distribution and was shifted to the right of the symmetrical NA distribution (Figure 5.9). This suggests that the VM period was generally louder with intermittent loud periods in comparison to the more stable and quieter NA period, in terms of the 12.5 kHz decidecade band.

Of note, these hydrophones were all located in the western and central part of the array (Figure 5.9). After a closer inspection of these results, it appeared that this spatial difference in results across hydrophones was due to the NA period being quieter on the central and western hydrophones (i.e., central peak in the distributions around 18 dB re 1 $\mu Pa^2/Hz$) than on the eastern hydrophones (i.e., central peak in the distributions around 23 dB re 1 $\mu Pa^2/Hz$), rather than a difference spatially in the VM period across hydrophones (i.e., central peak in the distributions around 38 dB re 1 $\mu Pa^2/Hz$). Although, no explicit comparisons were made within the same period across hydrophones.

Only one hydrophone, hydrophone 63, differed between the NA and MA periods. In fact, this was the only hydrophone that differed between the NA period and all periods of survey activity. In all three cases the decomposition reveals that this was largely with respect to the shape of the distributions: the NA period distribution was symmetrical, whereas the other periods were left-skewed and multi-modal indicating that there was some noise-generating activity during these other periods that affected the soundscape in the MBES band. Although there are other hydrophones (i.e., hydrophone 16 and 45) that lie on a track line in all three survey periods, hydrophone 63 was the shallowest. By qualitatively comparing the distributions across hydrophones 16, 45, and 63, hydrophone 63 clearly has the most separation between distributions. This may be related in some part to the difference in attenuation of sound in this band because of the difference in depth among these hydrophones.

Only one difference was detected between the VO and VM periods (hydrophone 45), and hydrophones differed between the distribution of sound levels in the 12.5 kHz band between the VM and MA periods (hydrophone 22). This suggests that the EM 122 activity had little noticeable impact above and beyond the other anthropogenic activities in the 12.5 kHz band.

And in fact, it cannot be said with certainty that the EM 122 activity is what was driving these results. Although other bands were not examined, this was anticipated to be the most likely band for which a difference related to the EM 122 activity would be detected among periods. So a lack of difference between the periods of survey activity in this band was surprising.

Interestingly, these differences were the only instances where 10% or more of the difference was attributed to differences in the size term, or the standard deviation of the distributions (Table 5.3). In the case of the VO and VM periods on hydrophone 45, the VO period distribution was much broader and less peaked than the VM period distribution, suggesting it was quite dynamic. During the VO period, the survey vessel was at a constant position within 5 km of hydrophone 45 for 3.5 hours, whereas during the VM period the survey vessel was constantly moving to a close distance and away again and did not sit near the hydrophone for any long period of time. Similarly in the latter case, the MA period distribution of hydrophone 22 was much broader and flatter than the VM period. The survey vessel never went within 7.5 km of hydrophone 22 during the MA period, whereas it did on three occasions during the VM period. However, this was not the only hydrophone for which the survey vessel did not go within about 7 km of a hydrophone (e.g., hydro 19, hydro 57), so there appear to be other important factors at play. For one, there is also biological activity that contributes to the energy in this frequency band.

It is worth noting that despite differences detected, the VM distributions are noticeably more peaked than the MA period distributions, which are generally broader and flat (Figure 5.9). This characteristic distribution makes sense given the activities of the MA period. There were many sources used intermittently and at times no active acoustic sources at all. So the hydrophones were exposed to a range of conditions, resulting in a roughly uniform coverage of

sound levels. The activity during the VM period on the other hand was very systematic and characteristic. The EM 122 was on during the entire period as the survey vessel moved back and forth across the array. This difference in the distributions of the VM and MA periods, therefore, seems to align more with the way the active acoustics were operated, rather than the source levels or propagation characteristics of each of the different acoustic systems that were used. Some of these confounding factors (i.e., spatial coverage, length of time an active acoustic system is on, etc.) would need to be controlled for between various period of operation to fully understand this result.

Array-Wide

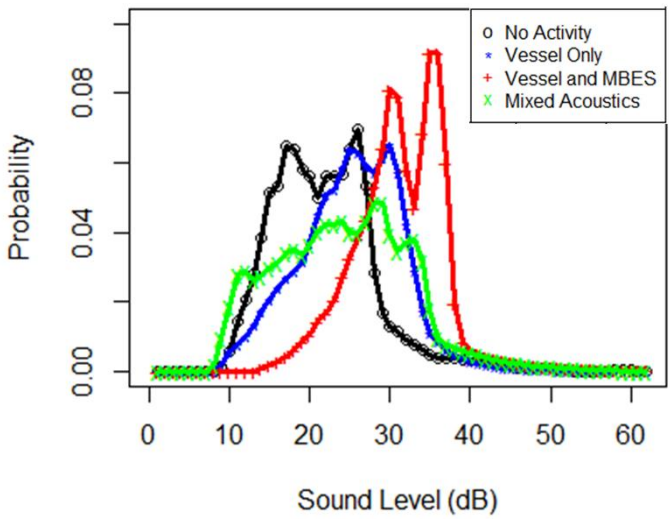

Figure 5.10. Array-wide sound level probability distributions of the 12.5 kHz decidecade band for each analysis period, where the NA period is indicated by black lines, the VO period by blue lines, the VM period by red, and the MA period by green. Sound level bins across the x-axis of each plot range from 0 to 65 dB re 1 $\mu Pa^2/Hz$ and the probability of the sound levels in each bin is shown along the y-axis, range from 0 to 0.1.

Table 5.4. Summary of the array-wide hypothesis test result using the 2-Wasserstein Distance for comparing the 12.5 kHz decidecade band sound level distributions. The two distributions compared are listed, followed by the p-value of the comparison test, the 2-Wasserstein distance (W^2), and its decomposition into location, size, and shape terms.

	P-value	W^2	Location (%)	Size (%)	Shape (%)
NA vs. VO	0.529	0.007	15.8	8.5	75.7
NA vs. VM	0.087	0.042	21.3	9.1	69.6
NA vs. MA	0.661	0.004	15.4	0.1	84.5
VO vs. VM	0.325	0.017	22.3	8.3	69.4
VO vs. MA	0.897	0.001	4.6	32.2	63.2
VM vs. MA	0.210	0.022	23	16.6	60.4

From an array-wide perspective only the comparison between the NA and VM periods resulted in a p-value less than 0.1, suggesting these two periods were distributed most differently (Table 5.4). The decomposition of the 2-Wasserstein Distance suggested that these periods largely differed with respect to shape (75.7%). The VM distribution was more left-skewed, whereas the NA period was more symmetrical (Figure 5.10), suggesting the VM period had intermittent epochs that were loud. The symmetrical distribution of the NA period in comparison to the left-skewed distribution of the VM period suggested that the NA period was quieter in the 12.5 kHz decidecade, and this was consistent across the period. The distributions also differed somewhat with respect to location; the VM distribution was shifted to the right of the NA distribution (Figure 5.10). In the context this meant that the VM period was generally louder than the NA period. There were no other differences detected between periods (i.e., $p>0.1$). This matches the findings of the annotation work of this chapter, the EM 122 signal was most obvious in the sound level time series on a hydrophone when the vessel and MBES were within a close distance to the hydrophone. The result here suggests the VM period was generally

louder with intermittent loud periods, which is likely heavily influenced by the closest passes of the survey vessel and the EM 122 signal at those times.

Major Findings

- The sound level distributions of the 12.5 kHz decidecade band between the NA and VM periods differed on five of nine hydrophones. In each case, the VM distribution was left-skewed and shifted to the right, indicating the VM period was loud, but intermittently so.
    - This result was more widespread on central and western hydrophones, a result that was driven by clear spatial differences in the 12.5 kHz band levels during the NA period, which were quieter on the central and western hydrophones than on the eastern hydrophones.
- The sound level distributions of the 12.5 kHz decidecade band for the nine hydrophones examined were generally normally distributed in the NA period, left-skewed and shifted right of the NA period distribution for the VM period (i.e., loud, but intermittently so), uniformly distributed for the MA period (i.e., dynamic), whereas the VO period distribution looked like an intermediate of the NA period and VM period distributions, i.e., somewhat left-skewed and only slightly shifted to the right of the NA distribution.
- Comparing sound level distributions for assessing changes to a soundscape is a novel approach that provides insight about relative differences between two sound level distributions.

Cumulative Sound Exposure Levels

Analysis-Specific Methodology

Observed $SELcum_{24h}$

Sound exposure level is the time integration of the squared acoustic pressure over a defined period. To align with marine mammal acoustic impact thresholds, cumulative sound exposure levels were calculated for each analysis period of activity extrapolated to a 24-hour period. Therefore, it was assumed that the survey activities defining each analysis period were representative of a 24-hour period of that activity. In the discrete sense, $SELcum_{24h}$ was computed by accumulating the 5-minute *SEL* (SEL_{5min}) time series data for each analysis period. In using a 5 minute on, 10 minute off sampling scheme, it was assumed that *SEL* was stable over a 15-minute period, and therefore that each SEL_{5min} value was representative of its respective 15-minute period. The SEL_{5min} values were multiplied by three to account for the energy in the entire 15-minute period (Equation 5.11). (Note: this step was necessary to most accurately scale the available observations to a 24-hour period. This calculation was built on the assumption that the empirical observations within a 5 minute sample were stable enough to represent the longer 15 minute period it represented. Because there were empirical observations at this 5 minute resolution, this was the smallest unit upon which this assumption could be confidently made. Therefore, this was the basis for extrapolating to a 24-hour period.) *SEL* was then extrapolated to a 24-hour cumulative value representing each analysis period by summing and then appropriately scaling (i.e., multiplying by $24/T_h$) the energy by multiplying by the ratio of 24 hours to the duration (hours) of an analysis period, T_h (Equation 5.11).

$$SELcum_{24h,period,hydro} = \left(\sum_{i=1}^{N}\left(10^{\frac{SEL_{5min,hydro}}{10}} * 3\right) * 24/T_h\right) \qquad \text{(Equation 5.11)}$$

where *N* is the analysis period-specific number of SEL_{5min} observations. Unweighted and weighted $SELcum_{24h}$ were computed for each hydrophone and each analysis period, as were array-wide averages.

Modelled $SELcum_{24h}$

As identified in earlier sections of this work, clipping occurred to some extent over the course of the study period and cannot be ignored. Clipping also occurred in some contexts unrelated to the survey activity. As such, there was no way to recover the missed energy due to clipping. To estimate the effect of clipping related to the survey activity, $SELcum_{24h}$ was modelled by considering various scenarios of receiver, i.e., stationary seafloor hydrophone receiver, exposure to the EM 122 activity. This was done with two goals in mind, 1) to understand the amount of cumulated energy with respect to this type of deep-water mapping survey that would be needed to surpass the marine mammal sound impact thresholds used by U.S. regulators (NMFS 2018), and 2) to realistically estimate what the levels may have been, had they not been clipped.

The basis of this modeling effort follows on the work of Lurton (2016), and Lurton and DeRuiter (2011) who modelled the *SEL* of the signals from deep water (12 kHz) multibeam echosounders. In their work, *SEL* was obtained using Equation 5.12.

$$SEL = RL + 10log(T) = SL - TL + 10log(T), \quad \text{(Equation 5.12)}$$

where *RL* is the receive level, *SL* is the source level, *TL* is the transmission loss, and *T* is the total exposure time. Transmission loss (*TL*) is a function of range (*R* in meters) and was estimated here by considering the spherical spreading loss and frequency-specific attenuation (α), i.e., $TL = 20log(R) + \alpha R$.

To account for clipping in a 24-hour period, the *RL* was further broken down into the portion (*a*) of the acoustic data that was clipped and the portion (*1-a*) that was not (Equation

5.13). The non-clipped level was assumed to be the average observed instantaneous sound pressure level (*SPLav*) during the 24-hour period (*T*), estimated from the equality $SEL_{obs} = SPL_{av} + 10log(T)$. The clipped sound level value and portion of time clipped were determined based on the context. Modifying Equation 5.12 to account for the effect of clipping resulted in Equation 5.13:

$$SELmod = (RL_{obs} + RL_{cl}) + 10log(T) = 10log\left(\left((1-a) \times 10^{\frac{SPLav}{10}}\right) + \left(a \times 10^{\frac{SPLcl}{10}}\right)\right) + 10log(T) \quad \text{(Equation 5.13)}$$

where *a* was the fraction of a day that the hydrophone clipped, *SPLav* was the average SPL over a day, *SPLcl* was the estimated magnitude of the level had it not been clipped during recording, and *T* was the total exposure time, i.e., the number of seconds in a day.

A set of generalized but worst-case scenarios, in terms of the most clipping, were explored by constraining the clipping context to situations where transmission loss would be at a minimum and therefore *RL* would be most similar to *SL*, i.e., when the vessel and EM 122 were positioned directly overhead a receiver (i.e., a hydrophone). Therefore, the values obtained represented conservative, and louder, estimates of the actual received levels. Exposure durations (i.e., time that the EM 122 was on) and whether the received signal came from a main or side lobe transmission beam were also explored within this context (i.e., source transmitting directly overhead a receiver). These scenarios were assessed assuming the same operational conditions of the 2017 mapping survey (i.e., 10 ms pulse lengths, 1 pulse every 5 seconds duty-cycle, 16 transmitting sectors, etc.).

The worst case was assumed to be when the survey vessel was directly overhead of a hydrophone and TL was the lowest. The hydrophones were, on average, at 1300 m depth. To be conservative the EM 122 was considered to be constantly 1000 m away for this exercise. The *SEL* was then modelled by varying the length of operation from zero transmissions to operating

the EM 122, in its typical capacity, for the entire 24-hour period. It is important to note that typical capacity refers to the duty-cycled nature of the operation of the EM 122, which depends on the local water depth. In the deep-water environment at the SOAR, the EM 122 transmitted approximately every 5 s with pulse lengths of 10 ms. Therefore, for continuous operation over a 24-hour period, on the order of 10^4 pulses would be transmitted. The source level of the EM 122 was assumed to be 243 dB re 1 µPa at 1 m, whereas the source level of a sidelobe transmission was assumed to be 30 dB lower, or 213 dB re 1 µPa at 1 m. The EM 122 signal transmits 8 sectors for a single swath and generally operates in *Dual swath* mode, i.e., 16 sectors in total. Accounting for all 16 sector transmissions, the cumulative side lobe source level can be approximated by $213 + 10\log_{10}(16) = 225$ dB re 1 µPa at 1 m. The clipped and non-clipped levels were based on reception at 1000 m from the source and a frequency-specific attenuation coefficient of 1.2 dB/km was assumed based on the 12 kHz center frequency of the EM 122 signal (Francois and Garrison 1982). The main transmission beam received level was therefore 182 dB re 1 µPa and the received level from a single sidelobe transmission was 152 dB re 1 µPa, or 164 dB re 1 µPa when considering all 16 sidelobes together. *SELmod* was estimated for both weighted and unweighted conditions, for both main beam and side lobe assumptions. *SPLav* was assumed to be 90 dB re 1 µPa for the unweighted scenario and 75 dB re 1 µPa for the weighted scenario.

In addition to these worst-case scenarios, a more realistic estimation of the effect of clipping was made using a modified version of Equation 5.13 (Equation 5.14) by considering multiple conditions in which clipping may have occurred:

$$SELmod2 = 10log\left(\left(\left((1-(a+b)) \times 10^{\frac{SPLav}{10}}\right) + \left(a \times 10^{\frac{SPLcl\_a}{10}}\right) + \left(b \times 10^{\frac{SPLcl\_b}{10}}\right)\right) + 10log(T)\right) \qquad \text{(Equation 5.14)}$$

where *a* and *b* refer to the amount of time the signal clipped for two different scenarios in which clipping may have occurred. These values, *a* and *b,* were obtained by computing the fraction of time the EM 122 signal was on over the duration of a day in each context, i.e., $a=n*t_p/24/3600/1000$, where n= the number of pulses, t_p = the duration of a pulse (i.e., 10 ms), and the same formula was used for *b* by varying *n*. All other variables were the same as for Equation 5.13. Though still simplified from reality, this model was used to provide a more realistic illustration of $SELcum_{24}$ had the EM 122 signal not clipped during recording in certain circumstances. The observed and modelled cumulative sound exposure levels were compared to the 24-hour cumulative sound exposure level thresholds (Table 5.5) used by U.S. regulators and the results discussed.

Table 5.5. 24-hour cumulative sound exposure level thresholds for a mid-frequency cetacean used in the United States. Note: all SEL thresholds listed below are weighted to the mid-frequency cetacean hearing group. (Values obtained from NMFS, 2018, Table AE-1.)

Threshold Description	**Threshold Value (dB re 1 µPa^{2}s)**
Temporary threshold shift (TTS) – impulsive sound	170
Permanent threshold shift (PTS)- impulsive sound	185
TTS – non-impulsive sound	178
PTS- non-impulsive sound	198

Results

Observed $SELcum_{24h}$

$SELcum_{24h}$ for each hydrophone and each analysis period were computed and are contained in Appendix 5.6. The unweighted and weighted $SELcum_{24h}$ array-wide average, standard deviations and values for each of the nine select hydrophones are presented in Table 5.6 by analysis period. A boxplot summarizing the unweighted versus weighted $SELcum_{24h}$ by analysis period for all of the array hydrophones is contained in Figure 5.11.

The unweighted *SELcum*$_{24h}$ across analysis periods was no more than 153.3 dB re 1 µPa^2 s (on one hydrophone during the VM period), no less than 134.3 dB re 1 µPa^2 s (on one hydrophone during the MA period), and the average across all periods and hydrophones was 141.7 dB re 1 µPa^2 s. The average *SELcum*$_{24h}$ for the NA period was the highest at 142.5 dB re 1 µPa^2 s, whereas for the VO and MA periods it was 141.0 dB re 1 µPa^2 s, and the VM period was 142.1 dB re 1 µPa^2 s. This varied on individual hydrophones by a similar magnitude in all periods (SD = 2.3-2.8 dB), except the MA period, in which there was more variability across the 89 hydrophones (SD = 3.7 dB). For the weighted *SELcum*$_{24h}$, the VM period had the most energy on average at 137.0 dB re 1 µPa^2 s, followed by the MA period at 131.1 dB re 1 µPa^2 s, which was the most variable period in terms of weighted *SELcum*$_{24h}$ (SD = 8.0 dB). The average weighted *SELcum*$_{24h}$ during the VO period was 126.4 dB re 1 µPa^2 s and for the NA period the average was 118.4 dB re 1 µPa^2 s across the array (Table 5.6). (Figure 5.11)

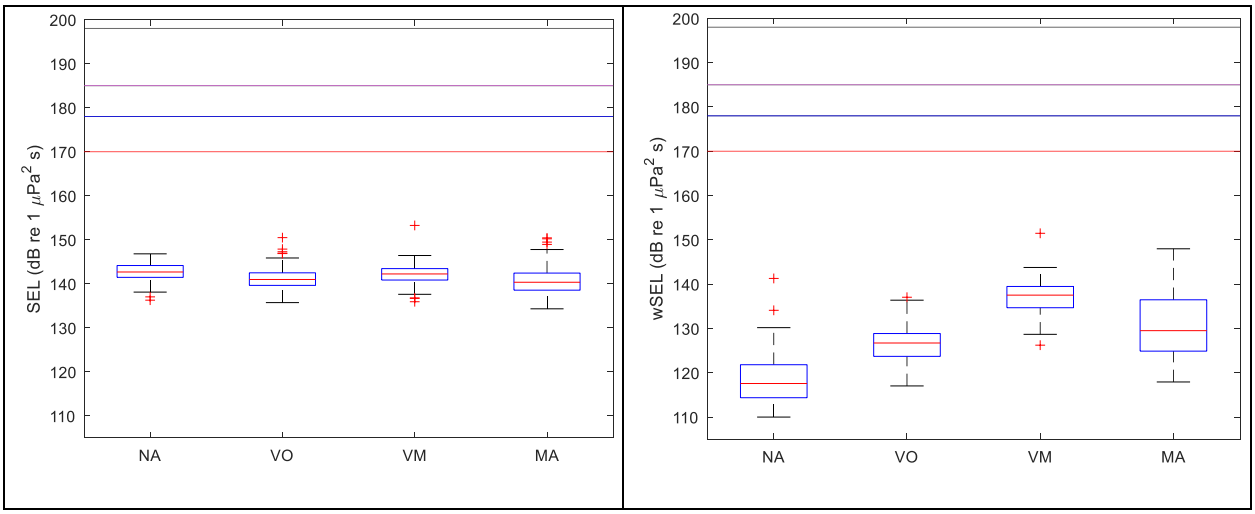

Figure 5.11. Boxplot of observed unweighted *SELcum*$_{24h}$ (left) and weighted SELcum$_{24h}$ (right) across the 89 hydrophones of the SOAR array by analysis period, i.e., NA=No Activity, VO=Vessel Only, VM=Vessel and MBES, MA=Mixed Acoustics. The blue box represents the 25th through 75th quartiles, the red line represents the median, the whiskers extend to the most extreme data points, and the red plus signs indicate outliers, as defined by MATLAB boxplot function. The NMFS acoustic thresholds (2018) are indicated by the horizontal lines across the plots, i.e., black line = PTS, non-impulsive threshold; magenta line = PTS, impulsive threshold; blue line = TTS, non-impulsive threshold; red line=TTS, impulsive threshold.

Table 5.6. Observed weighted and unweighted *SELcum*$_{24h}$ (dB re 1 µPa^2 s) for each of the analysis periods, array-wide and for the nine select hydrophones.

Analysis Period	Hydrophone	24hr-SEL	24hr-wSEL
No Activity	Array-wide	142.5 (2.3)	118.4 (5.3)
	14	146.8	120.7
	16	141.5	112.7
	19	144.8	122.0
	22	144.6	120.7
	45	142.9	113.0
	57	142.1	116.1
	63	142.6	113.3
	70	143.0	119.6
	85	143.2	119.7
Vessel Only	Array-wide	141.0 (2.8)	126.4 (3.8)
	14	145.9	127.0
	16	141.3	122.0
	19	142.3	125.5
	22	143.7	128.8
	45	142.0	124.3
	57	141.2	123.7
	63	140.8	130.9
	70	140.9	132.7
	85	140.2	129.1
Vessel and MBES	Array-wide	142.1 (2.4)	137 (3.8)
	14	142.0	135.9
	16	140.1	135.8
	19	142.9	137.9
	22	144.6	141.3
	45	143.8	140.6
	57	143.7	140.5
	63	143.4	139.7
	70	144.1	140.6
	85	144.0	139.4
Mixed Acoustics	Array-wide	141.0 (3.7)	131.1 (8.0)
	14	145.6	143.0
	16	139.5	132.3
	19	139.9	124.9
	22	137.0	122.9
	45	140.5	133.4
	57	139.0	127.6
	63	141.0	131.3
	70	143.3	136.3
	85	150.4	148.0

Modelled $SELcum_{24h}$

A worst-case scenario

A summary of the results of the worst-case scenario modelling exercise is provided in Figure 5.12, where *SELmod* is shown as a function of the number of EM 122 pulses. All of the impulsive and non-impulsive sound exposure thresholds for a mid-frequency cetacean, as well as the observed unweighted (cyan) and weighted (green) $SELcum_{24h}$ for hydrophone 45 (center of the array) were also plotted as horizontal lines in Figure 5.12 as a reference. Note that the unweighted scenarios were nearly identical to the weighted scenarios because the weighting curve is close to 0 dB at the frequency of the 12 kHz MBES signal. Therefore, there is little difference between unweighted and weighted modelled $SELcum_{24h}$ values.

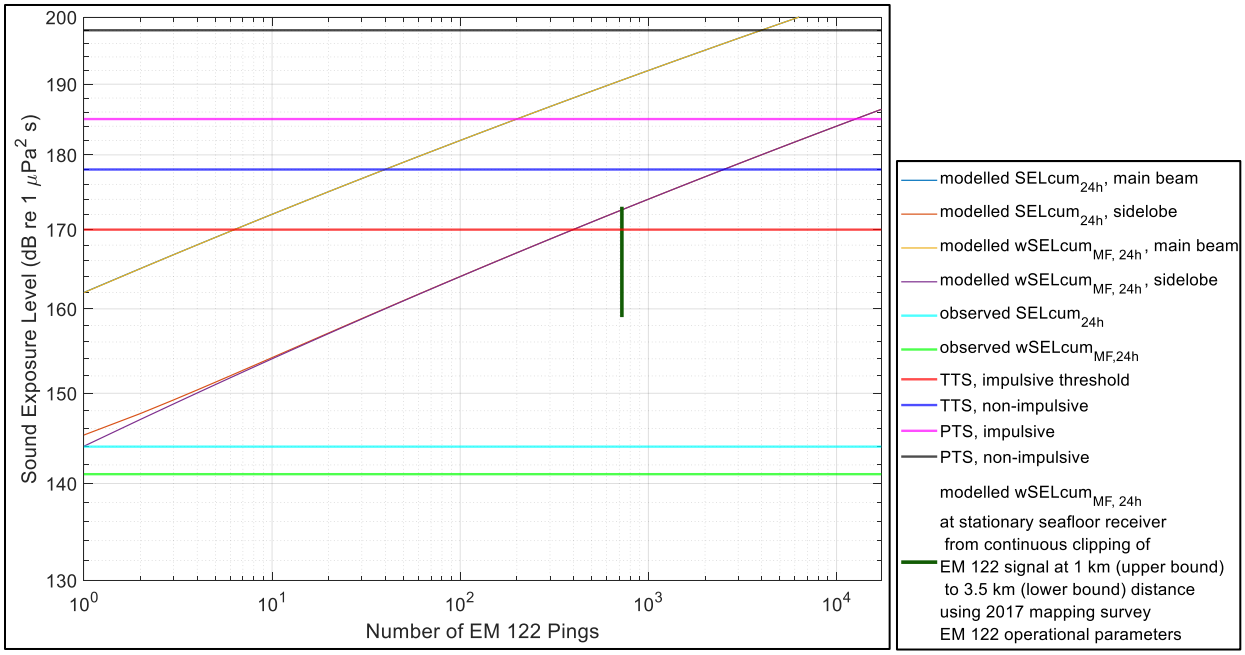

Figure 5.12. Modelled *SELcum*$_{24h}$ plotted as a function of the number of pings (no pings --far left-- up to 24 hours of pinging with the operational parameters of the 2017 mapping survey—far right) received on a stationary bottom-mounted hydrophone from 1 kilometer away for various permutations of the following assumptions: whether the clipped signal received was from the main beam, a sidelobe, weighted or unweighted conditions using *SELmod* equation. Realistic scenario results using *SELmod2* equation, plotted as a single green horizontal line. The lower bound represents the scenario for if clipping occurred from sidelobe transmissions received at a constant distance of 3.5 km from the stationary receiver for one hour, in addition to three main beam transmissions received from a distance of 1 km. The upper bound represents clipping that may have occurred from sidelobe transmissions at a distance 1 km from the stationary receiver for 1 hour in addition to 3 main beam transmissions received from a distance of 1 km.

The worst-case modelling exercise was based on the EM 122 transmitting at a constant distance of 1000 m from the stationary receiver, while the duration of transmission was varied. This again was a conservative illustration exercise that definitely produced levels louder than any realistic scenario since the average depth of the seafloor-mounted hydrophones was 1300 m and the survey vessel and hull-mounted EM 122 were almost never fixed to one location during the study period. It is important to keep in mind that most exposures would be with respect to the sidelobes, and exposure to the main transmission beam would be reserved to times when the survey vessel is directly overhead a receiver. Thus, the results are presented as 1) the number of

pings or temporal duration of exposure to the sidelobes, or 2) pings from the main beam with the notion that the survey vessel would be steaming directly overhead the receiver for an exposure to occur from the main beam.

For the most conservative threshold, i.e., TTS for an impulsive sound, the worst-case modelling exercise revealed that ~404 sidelobe transmission pings (~ 34 min. of operation at the duty cycle of the EM 122 used in the 2017 survey) would be needed to reach the 170 dB re 1 μPa^2 s value; whereas for a main beam transmission, 6 pulses would be needed to reach this same threshold. For the TTS, non-impulsive threshold, 2590 pulses (~3.6 h of operation) would be needed from the sidelobe transmissions to reach the 178 dB re 1 μPa^2 s value, or 40 main beam pulses. To reach the PTS, impulsive threshold of 185 dB re 1 μPa^2 s, 12540 sidelobe pulses (17.4 h of operation) or 201 main beam pulses would be needed. And finally, to reach the PTS, non-impulsive threshold of 198 dB re 1 μPa^2 s, much more than 24 hours of continuous exposure (>>>10^4 pulses) to the sidelobe transmissions would be needed, or 4027 main beam pulses to surpass the 24-h cumulative sound exposure threshold. (Figure 5.12)

Realistic scenario

To provide insight on what a more realistic—albeit simplified—accounting of the clipped levels would do to the $SELcum_{24}$, the geometry of the acoustic transmission as well as a few findings of this study were considered. First, clipping should occur mainly with respect to the transmission of sidelobes, as the main beam very rarely ensonifies the receiver hydrophone. Based on transmission loss, clipping (i.e., a received level of 138 dB re 1 µPa) from a side lobe is estimated to occur when the EM 122 is within 3.5 km. Based on the time series annotation work, the survey vessel, in standard operation (i.e., mowing the lawn configuration and continuously moving), was generally at or within 3.5 km of a hydrophone for no more than an hour, (i.e., 720 pulses in an hour with 10 ms duration each, a=720 *10 /24/3600/1000 $= 8.3 \times 10^{-5}$). For

example, the survey vessel was within 5 km of hydrophone 45 for about an hour of the VM period. But if the vessel runs directly overhead a hydrophone, the main transmission beam will also cause clipping. Thus this also needs to be considered. Based on the typical line plans of a mapping survey, the survey vessel should not go over the same place more than a few times, if at all. Again, drawing on the exposure of hydrophone 45 in the 2017 mapping survey as an example, the survey vessel passed overhead about three times. Thus, the approximate amount of time used for the clipping of condition *b*--related to the main beam-- was 3×10^{-7} of the time (i.e., 3 pulses of 10 ms duration each, *b*=3*10 /24/3600/1000 $= 3 \times 10^{-7}$). Since the received level accounting for clipping will vary between 3.5 km and the closest point of approach, i.e., 1 km, a range of possible $SELcum_{24}$ were obtained (Figure 4.12, green horizontal line). The lower bound of this range represented clipping of the EM 122 signal at a receiver 3.5 km away, and the upper bound represented clipping related to the EM 122 signal detected at a receiver 1 km away. The result of this more realistic modelling exercise was a range of $SELcum_{24}$ from 159-173 dB re 1 μPa^2 s (Figure 5.12). Again, the survey vessel was constantly moving so the actual value was most definitely somewhere in between. The 2017 mapping survey was primarily conducted in *Dual-swath* mode, such that there were 16 sectors active per transmission. If instead it had been operating in *Single-swath* mode with only eight sectors, this would have reduced the reported modelled $SELcum_{24}$ by 3 dB. The upper bound (173 dB re 1 μPa^2 s) of the more realistic estimate surpassed only the most conservative regulatory sound exposure threshold, i.e., TTS for an impulsive sound, by 3 dB.

Discussion

With this modelling exercise it is imperative to keep in mind that this was done to provide insight about the potential difference clipping made to the $SELcum_{24}$, but it is a necessarily simplified accounting of the clipped levels and only an illustration of what the missed

signal may have contributed to the cumulative sound exposure levels at a stationary seafloor receiver. However, there are a few key points to take away from this exercise. First, the difference between observed and modelled levels was not negligible. When accounting for clipping, the modelled *SEL*cum$_{24}$, i.e., 159-173 dB re 1 µPa^2 s, were approximately 19-33 dB higher than the observed values, i.e., ~141 dB re 1 µPa^2 s. So the observed (clipped) values cannot be considered representative of the actual exposure levels. The clipping-modelled levels suggest the actual levels are louder than what was observed with the SOAR receivers, warranting an empirical measurement with a recording system capable of capturing the full signal dynamics. So although the EM 122 transmissions are very short and occur rarely, they are sufficiently loud to contribute significantly, even at the 24-hour scale.

Despite this, the modelled *SELcum$_{24}$* values –accounting for clipping--are well below both PTS regulatory thresholds (i.e., 25-39 dB, below the 198 dB re 1 µPa^2 s PTS non-impulsive threshold, and 12-26 dB below the 185 dB re 1 µPa^2 s PTS impulsive threshold). The modelled *SELcum$_{24}$* values –accounting for clipping--are also clearly below the TTS threshold for a non-impulsive sound (i.e., 5-19 dB below the 178 dB re 1 µPa^2 s TTS threshold). Only the upper bound (173 dB re 1 µPa^2 s) of the modelled *SELcum$_{24}$* values exceeded the threshold for TTS from an impulsive sound (i.e., 170 dB re 1 µPa^2 s), whereas the lower bound of the modelled estimate was 11 dB below the same threshold. The actual *SELcum$_{24}$* was very likely somewhere in between this range. Also, though this modelling exercise was done in order to provide a more realistic range of *SELcum$_{24}$* after accounting for clipping, a conservative approach was taken, such that even the range of values obtained should be higher than in reality.

The worst-case scenario modelling exercise showed that the amount of energy required to exceed the regulatory thresholds for permanent acoustic injury (i.e., PTS) to a mid-frequency

cetacean would necessitate scenarios well outside the typical operation of the EM 122 for a deep-water mapping survey. Such scenarios would have required the use of the EM 122 constantly at 1 km from a receiver for more than 17 hours in a 24-hour period to exceed the impulsive sound PTS threshold, or a duration much longer than 24-hours to exceed the non-impulsive sound PTS threshold. Not only are these totally unrealistic scenarios for which the EM 122 would be operated, but the likelihood that a marine mammal would also be stationary for such periods is also very unlikely. The duration of required exposure of a stationary receiver to the EM 122 signal to exceed the temporary (TTS) acoustic injury thresholds was shorter (i.e., 34 minutes at 1 km for TTS to an impulsive sound, or 3.6 h at 1 km for TTS to a non-impulsive sound), but still unrealistic in the applied context. This is particularly true since neither the survey vessel or a marine mammal are stationary, so neither continuous exposure over even a half an hour or constant exposure at a range of 1 km would be likely.

One point worth reiterating is that $SELcum_{24}$ was calculated based on the sound levels observed at the seafloor and are therefore not valid for any other depth. An assessment of the sound levels at other depths was beyond the scope of this work. The seafloor observations are representative of what foraging beaked whales may be exposed to as they generally forage very close to the seafloor. The results of this exercise suggest that the 2017 mapping survey could not have produced enough energy to cause permanent acoustic injury to a mid-frequency cetacean foraging at the depth of the hydrophones. It is possible that a stationary receiver at 1 km depth could have been exposed to enough acoustic energy to surpass the TTS threshold for an impulsive sound. However, this was a conservative result that was not only based on a simplified approach to addressing the movement of the sound source, but did not consider the mobility of the receiver. To truly understand the sound exposure of a marine mammal, a tagging study would

need to be conducted where the acoustic exposure could be calculated directly from a mobile marine mammal receiver.

It is also worth revisiting the challenge of where the MBES signal fits in terms of sound source type and regulation. In light of this challenge, both impulsive and non-impulsive thresholds were considered. In the current regulatory framework, the results here suggest that a foraging beaked whale would not be exposed to a sound exposure level that exceeds the non-impulsive thresholds, whereas the lower TTS impulsive threshold would be exceeded. Based on these results, the placement of this sound source in one category over another would certainly have repercussions in terms of how this source is regulated.

Major Findings

- Observed (clipped) $SELcum_{24}$ on the array was ~141 dB re 1 μPa^2 s at the stationary seafloor receiver during the MBES mapping survey.
- A modelling exercise accounting for potential clipped signals from the EM 122 when the survey vessel was within 1-3.5 km of a stationary receiver resulted in estimated values for $SELcum_{24}$ of 159-173 dB re 1 μPa^2 s.
- Observed and modelled $SELcum_{24}$ did not exceed regulatory thresholds for a non-impulsive sound. The upper bound of the range of modelled $SELcum_{24}$, accounting for clipping at a stationary seafloor receiver exceeded the impulsive threshold for TTS by up to 3 dB. This was a conservative estimate that does not consider the mobility of a marine mammal receiver.

Frequency Correlation Analysis

Analysis-Specific Methodology

The frequency analysis methodology differed slightly from the amplitude analysis. The voltage data was extracted in a 5 minute on/5 minute off scheme to provide a closer to real-time sampling than the other analyses. The voltage data were then converted to absolute sound pressure levels as previously described by applying the gain and receiver sensitivity, but were then transformed to the frequency domain using the MATLAB function pwelch (MATLAB R2021a) in 1-s windows using a fast Fourier transform length of 1048 (50% overlap and Hamming window, the pwelch default).

A frequency correlation coefficient (r) was calculated using Equation 5.15 from Miksis-Olds and Nichols (2016, Equation 1) for each pair of frequencies (f_1, f_2) from 91 Hz to 39.9 kHz, at a resolution of 91 Hz:

$$r(f_1, f_2) = \frac{\sum_{i=1}^{n}[x(f_1)_i - \overline{(x(f_1)}][x(f_2)_i - \overline{(x(f_2)}]}{\sqrt{\sum_{i=1}^{n}[x(f_1)_i - \overline{(x(f_1)}]^2}\sqrt{\sum_{i=1}^{n}[x(f_2)_i - \overline{(x(f_2)}]^2}} \quad \text{(Equation 5.15)}$$

where *x(f)* are the frequency-specific sound levels in dB re 1 μPa^2. The resulting matrix of correlation coefficients formed a diagonally symmetric matrix, where the diagonal was the autocorrelation of each frequency.

Frequency correlation matrices were computed for each of the four analysis periods previously defined (NA, VO, VM, and MA) for hydrophone 45. Hydrophone 45 was selected because it was closely passed during all three survey activity periods and was central to the activity throughout each analysis period. Therefore, it was expected to be representative of the anthropogenic activities during the study. Frequency correlation difference plots were generated by subtracting one frequency correlation matrix from another. To aid in the interpretation of the

frequency correlation matrices and difference matrices, spectrograms and spectral probability density plots of each period were also generated.

It was hypothesized that within the frequency correlation matrices there would be identifiable features related to the vessel-radiated sound, the EM 122, and potentially other distinguishable sources, like biological activity. In particular, during the NA period, it was expected that there may be a lack of correlation in the very low frequency (10s of Hz) attributed to the very high amplitude sound detected there in earlier parts of this work. For the VO period, it was expected that the lower frequencies would be highly correlated with one another attributed to vessel-radiated sound. For the VM period, it was expected that frequencies between 11-13 kHz, the frequency range of the EM 122 signals, would be highly correlated with one another but not with other frequencies. Since the EM 122 was also used in the MA period, it was expected that any pattern attributed to the EM 122 in the VM correlation matrix would be present in the MA matrix as well. In addition, it was hypothesized that there might be an area of correlation related to the SBP around 3.5 kHz in the MA correlation matrix, but not associated with the other active acoustic sources, which were hardly discernible in other analyses in this chapter.

Results

Frequency correlation matrices were generated for each analysis period and are contained in Figure 5.13. The corresponding spectrograms and spectral probability density plots for each analysis period are contained in Appendix 5.7. The NA period contained a few distinct but small areas of high correlation mostly of frequencies very close to one another in the spectrum (Figure 5.13, A). For example, frequencies roughly between 1-5 kHz, 7-22 kHz, 20-25 kHz, 30-38 kHz, were highly correlated within those ranges. There was very little correlation between the lowest and highest frequencies e.g., 0-5 kHz had near zero correlation with frequencies higher than 30

kHz. And in visually comparing this matrix to the other analysis periods, there was the least correlation between frequencies in this period. This can be attributed to the lack of distinguishable noise sources present on this hydrophone during this period. The sound levels across the broader frequency space generally change randomly with respect to one another.

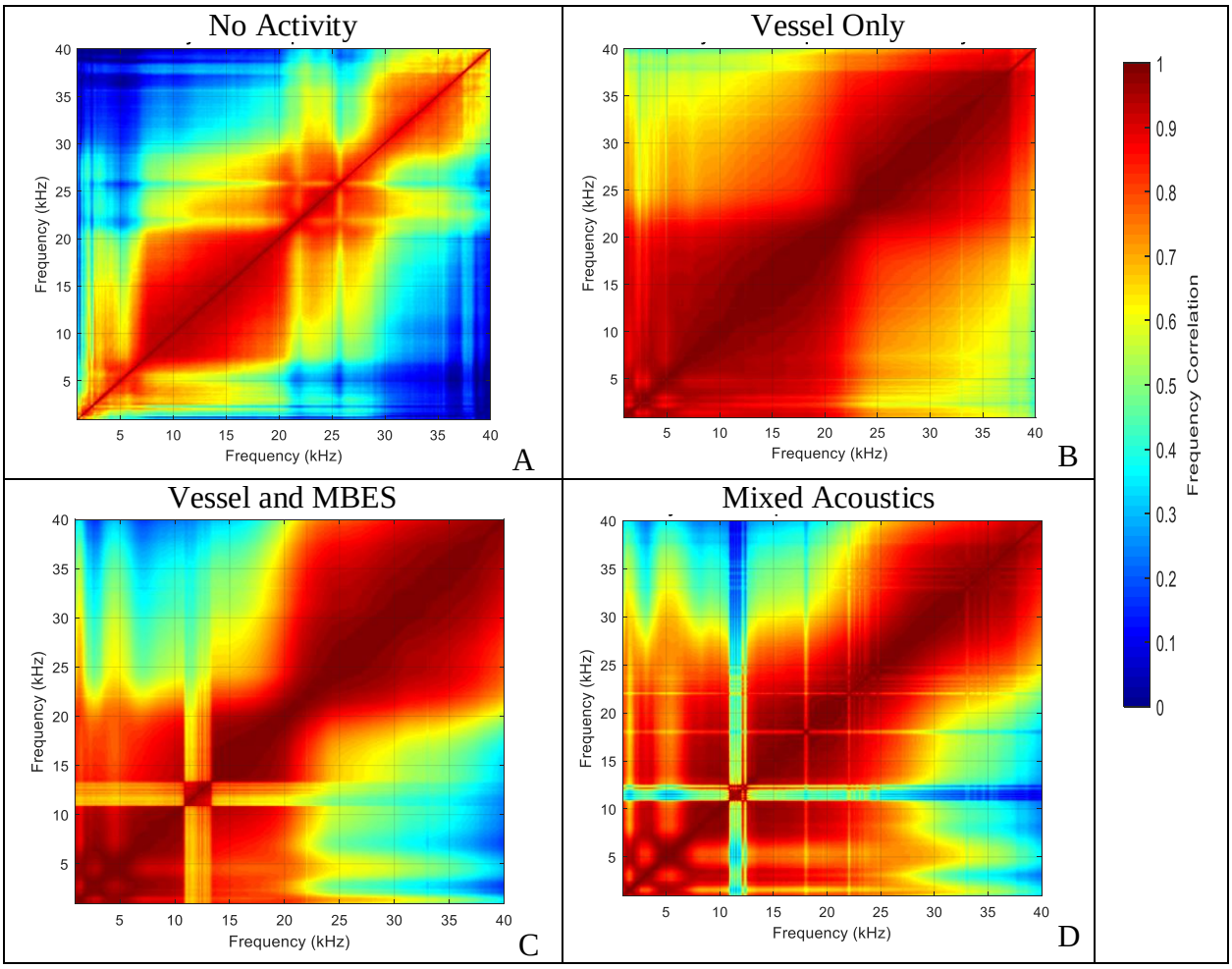

Figure 5.13. Hydrophone 45 – Frequency correlation plots. Each frequency correlation plots contains frequencies from 91 Hz to 40 kHz, at a frequency resolution of 91 Hz, along both axes. The color bar represents the frequency correlation from 0 to 1. A, B, C, D correspond to the No Activity, Vessel Only, Vessel and MBES, and Mixed Acoustic periods, respectively.

The VO period on the other hand was highly correlated in comparison to the other frequency correlation matrices of the other periods (Figure 5.13, B). The sound levels were highly correlated in this period, and there were no distinct pockets of the spectrum lacking correlation. There were two distinct areas of highest correlation: frequencies below ~ 20 kHz

and frequencies greater than about 25 kHz (Figure 5.13, B). In both cases, the further away on the frequency spectrum from a specific frequency, the less correlated it was with other frequencies. This matches well with the known acoustic activity during this period. The presence of the survey vessel increased sound levels broadly, with the most energy concentrated at the lowest frequencies (Appendix 5.7, spectrogram of VO period). The distinguishable small sub-regions from the NA period were no longer visible, masked by the louder broadband acoustic energy of the survey vessel. Although still correlated, there was an area of lower correlation centered around 2 and 5 kHz, within the highly correlated sub-region of frequencies below 20 kHz. This was likely attributed to the vessel activity, as it becomes more prominent in the spectrogram as the vessel gets closer to the hydrophone under consideration, but may be related to a different mechanism than the broader sub-region. As in the NA period, the lowest frequencies and highest frequencies were the least correlated, which makes sense given there is very little acoustic energy in the higher parts of the spectrum, as most of it is concentrated in the lowest frequencies.

The frequency correlation matrix of the VM period had a similar structure to the VO period matrix: generally frequencies lower than 20 kHz were correlated and those higher than 25 kHz were correlated, and the lack of correlation around 2 and 5 kHz was still present (Figure 5.13, C). Although the graded decrease in correlation with increasing distance between two frequencies on the spectrum was even more pronounced. This suggests that the mechanism driving the higher correlation areas was even more pronounced during this period, i.e., present longer during the period. The most distinguishable feature of the VM period frequency correlation matrix, however, was the area of lower correlation between frequencies in the 11-13 kHz band and those either higher or lower and the distinct area of correlation within the range

11-13 kHz. This can be attributed to the EM 122 signal that was distinct in comparison to any other sound source present in the data during this time (Appendix 5.7, spectrogram VM period). Lastly, the second high correlation area from 20-40 kHz, was even more correlated in this time period. One potential explanation for this correlation was the presence of broadband clicks throughout the period. This was likely attributed to the foraging clicks of Cuvier's beaked whales.

The MA period frequency correlation matrix had a very similar structure to the VM period, except there were several small areas of decorrelation across the spectrum (Figure 5.13, D). In particular, some of the areas of local decorrelation that were most prominent were centered around 1.5 kHz, 18 kHz, and 22 kHz. The EK-80 (18 kHz signal) was detected on this hydrophone during this period and is likely the source of decorrelation centered at 18 kHz. A closer inspection of the 1 kHz and 22 kHz suggests there was a continuous sound in a very narrow band around these frequencies across the entire time series likely responsible for the decorrelation at these frequencies. Although the SBP was detected in the time series analysis on this hydrophone there is no clear pattern in the frequency correlation plot with respect to the known frequencies of this system (i.e., 3.5-12 kHz). This may mean the signal was masked by other sources at the same frequency, or that it was not sufficiently strong in the time series to make a substantial impact.

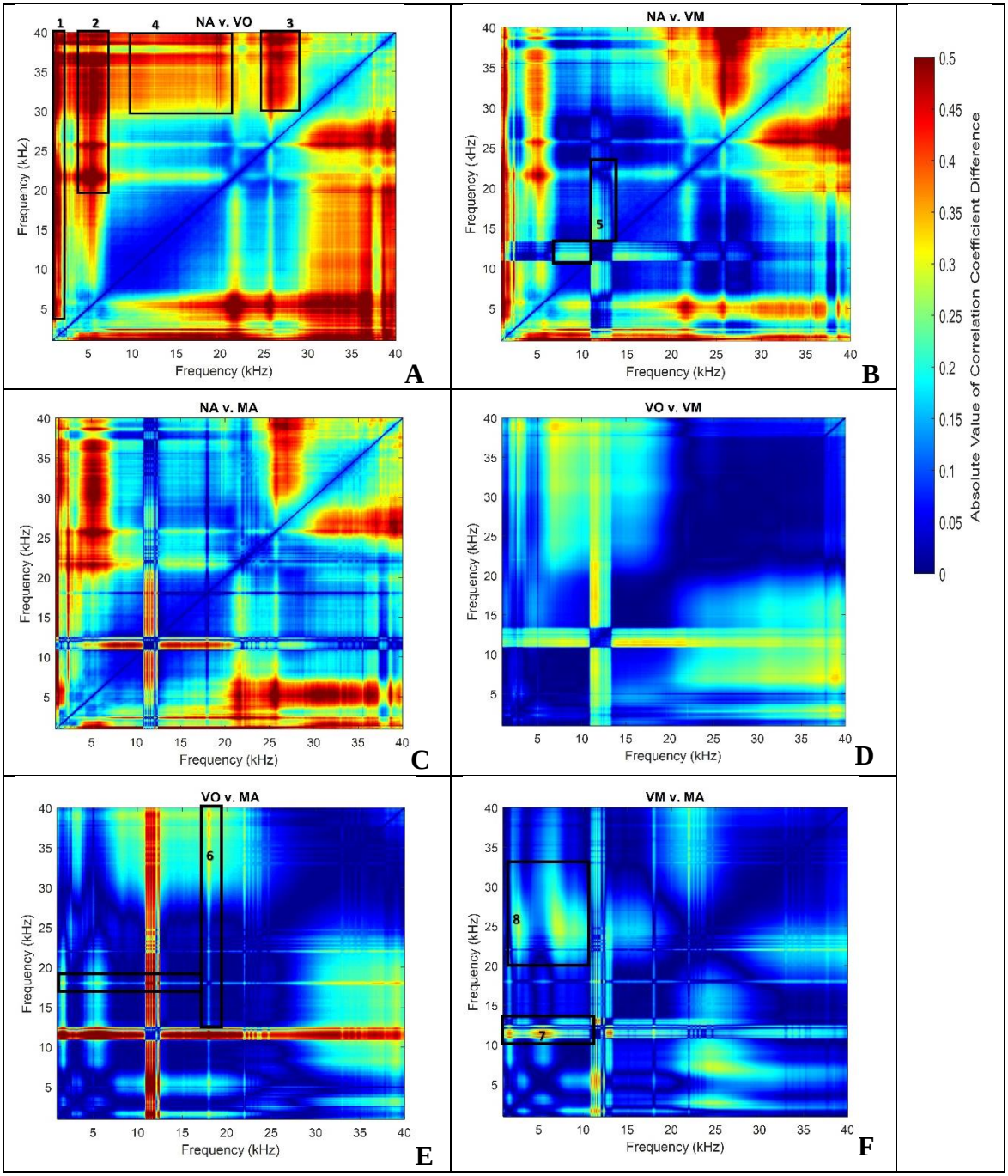

Figure 5.14. Hydrophone 45 frequency correlation difference matrix plots. From top left to right bottom the analysis period comparisons are: A-NA vs VO, B-NA vs VM, C-NA vs MA, D-VO vs VM, E-VO vs MA, F-VM vs MA, where NA = No Activity, VO=Vessel Only, VM=Vessel and MBES, and MA=Mixed Acoustics. Frequency in kHz on both x and y axes. The color bar represents the absolute value of the correlation coefficient difference where blue equals no difference and red equals a difference of 0.5. The black boxes around sub-regions are referenced in the text.

Six difference plots were generated comparing each pair of frequency correlation matrices from the four analysis periods and are contained in Figure 5.14. Red indicates the frequency correlation that most differed between periods, whereas blue indicates areas of the frequency spectrum that were most similar in terms of frequency correlation between periods. In general, the NA period was the most different from the other analysis periods, which is reasonable given there was little activity except at very low frequencies (common in an ambient acoustic environment). The NA period differed from the three survey activity periods in three consistent areas, 1) at very low frequencies, < 1 kHz with respect to all other frequencies, 2) below 5 kHz and at frequencies 20 kHz and above, and 3) frequencies centered around 25 kHz and those 30-40 kHz. The first area can be attributed to the array-wide elevated levels during the NA period that was not present during other periods (Figure 5.14, 1). The second difference (Figure 5.4, 2) appears to be related to the presence of the survey vessel as this difference is absent in the plots comparing different periods of survey activity (i.e., Figure 5.14, D, E, F). And the final difference appears correlated with the high frequency clicks, presumably beaked whale foraging clicks, in all periods of survey activity, but which were mostly absent in the NA period (Figure 5.14, 3).

There was only one area of frequency correlation in the NA vs VO comparison (Figure 5.14, A) that was noticeably different from the other comparisons to survey activity (Figure 5.14, B and C). This was between frequencies of ~7-22 kHz and those 30 kHz and higher. This result suggests that there were very different mechanisms driving the sound levels at these frequencies in each of these periods. The high frequency activity (~30 kHz and higher) appears to be related to the difference in beaked whale activity, whereas the activity in the 7-22 kHz range appears related to the absence of activity in the NA period and the presence of the survey vessel during

the VO period. During the VO period, the survey vessel was stationary near hydrophone 45 for several hours in a row (Figure 5.14), which likely explains this difference. And this was not seen across comparisons with other survey activity because the survey vessel was continually moving throughout those other periods. In the other comparisons (Figure 5.14 B, and C) there was less of a correlation difference in this same area.

Between the NA and VM period, the only obvious difference not previously addressed is the frequency correlation difference around 11-13 kHz (Figure 5.14, 5). This difference is most certainly related to the EM 122 signal which was present frequently in the acoustic data on hydrophone 45. Within this area there are finer lines suggesting frequency correlation differences, which correspond with the sector specific center frequencies of the EM 122 signal. It is worth noting that the magnitude of difference is not as high as some of the other frequency correlation differences already identified. This suggests that the EM 122 signal was not constant and that there were times when the energy in this area of the frequency spectrum matched the NA period (i.e., there were periods of relative quiet during the VM period, even at these frequencies. This is corroborated by inspection of the spectrogram of this period which only shows the EM 122 signal intermittently. The NA vs MA frequency correlation difference plot depicted similar patterns as the NA vs VM comparison. However, the correlation difference in the 11-13 kHz frequencies was even more prominent between these two periods (Figure 5.14, C). Miksis-Olds and Nichols (2016) suggest that although correlation does not perfectly relate to the intensity of a source, a strong correlation can mean that either the sound is frequently occurring or of higher intensity. Based on the time series analysis earlier, the survey activity was detected during just under 50% of the MA period, whereas it was only detected for approximately a third of the time during the VM period. Thus it appears the stronger correlation (in Figure 5.14, B vs

C) is likely due to the difference in presence of the signal in the acoustic record for these two periods. It is worth noting that the two periods were not of the same duration, and the absolute time the signal was present was actually higher in the VM period (11.75 hours) than the MA period (8.75 hours). This difference in duration of source presence across analysis periods also explains the subtle differences in some of the difference areas identified (i.e., broader/narrower area of difference, smaller/larger differences, etc.).

The difference in the VO and VM periods was most obviously related to the presence of the EM 122 signal in the VM period as the 11-13 kHz band was one of the only differences between these two periods (Figure 5.14, D). In addition, the frequency area 2 identified previously (Figure 5.14) was also different between the VO and VM periods. Between the VO and MA periods in this same area, there was even less of a difference. This suggests that this frequency correlation difference is likely attributed to the difference in how the survey activity was conducted in these periods. In both the VO and MA period, the survey vessel was present for several hours in a row within a very close distance to hydrophone 45 at a constant distance (which was not the case during the VM period). During these times there was broadband energy radiating from the ship. This was more pronounced in the VO period when the survey vessel was closer, which appears to be driving the larger difference detected in this area (2) between the VO v VM difference plot (Figure 5.14, D) in comparison to the VO v MA difference plot (Figure 5.14, E).

One obvious difference between the VO and MA periods that was not present in the VO and VM comparison was between 18 kHz and all other frequencies (Figure 5.14, 6), which can be attributed to the EK-80 signal at 18 kHz. In addition, the difference at 22 kHz was also visible as a line of higher correlation difference with respect to all other frequencies. Between the VM

and MA period there are many smaller regions representing a moderate difference between the two periods, but only one area of strong correlation difference (Figure 5.14, 7) centered around 1.5 and 5 kHz with respect to frequencies between 11-12 kHz. This appears to be related to the EM 122 signal and the acoustic activity centered around 1.5 and 5 kHz, the latter which is presumed to be related to the operation of survey vessel. However it is unclear what about the difference in these activities between the VM and MA periods could manifest in this way. The largest region of correlation difference between the VM and MA period was between frequencies of 3-11 kHz and those 20-30 kHz (Figure 5.14, 8). One explanation is that this could be related to the SBP signal which contributes significant energy between 3-11 kHz and was active during this period. There was an area of slight decorrelation in this frequency region in the MA period frequency correlation plot (Figure 5.13). However, it was not as distinguishable as other sources, such as the EM 122. Thus it is unclear whether this is the cause of the correlation difference. The manifestation of the SBP signal in the frequency correlation plot was undoubtedly more subtle than the EM122 signal. The subtle manifestation of the signal would be expected since the SBP has a longer duration and is more broadband than the EM 122 signal. Thus it may be masked more easily by the more continuous ambient acoustic environment at similar frequencies.

Major Findings

- The EM 122 signal contributed to a very narrow frequency band between 11-13 kHz, whereas the vessel-radiated sound manifested most as correlation in the lowest frequencies (<5 kHz).
- The other active acoustic sources contributed more subtly, i.e., lower correlation, to the frequency correlation than the EM 122 signal. The EM 712 was not distinguishable.

These results suggest the EM 122 had the clearest impact in terms of the active acoustic sources and frequency correlation.

- The frequency correlation difference plots provide a useful way to separate the contribution of two or more sources, i.e., such as vessel sound from the EM 122 signal, or the other acoustic sources.

Chapter Discussion and Summary

A comprehensive soundscape assessment was conducted of the 2017 mapping survey, which included 1) a detailed annotation of several sound level metric time series from nine array hydrophones, 2) the calculation and comparison of sound level percentiles across the four analysis periods of survey activity, 3) the calculation and discussion of cumulative sound exposure levels with respect to noise impact thresholds, 4) a probability distribution analysis of the most relevant sound level metrics with respect to the activity of the EM 122, and 5) a detailed frequency analysis examining differences in frequency correlation among the four analysis periods of survey activity. Each analysis contributed to a more thorough understanding of the impact the 2017 mapping survey had on the marine acoustic environment at the SOAR. While the annotation provided the most detailed and localized perspective of what acoustic sources contributed to the changing acoustic environment and how, the other analyses provided a more global perspective of how the natural soundscape was changed by the survey activity.

The acoustic sources contributing to the SOAR soundscape during the 2017 study included more than just the survey vessel and its active acoustic sources. There were other anthropogenic activities on or near the array, very likely including vessels passing by. There was also significant biological activity, particularly, mid-to high frequency (i.e., > 1 kHz) vocalizing marine mammals, and some contributions from unknown sources, mostly low frequency (< 1

kHz), that manifested as acoustic events throughout the time series. However, the acoustic events differed spatially. For example, there were instances in the time series of the western and northern edge hydrophones indicating other vessels passing, unrelated to the survey activity, whereas the time series of hydrophones in the southwest of the array, suggested significant biological activity (i.e., 12.5-kHz and 40-kHz band). These other acoustic sources varied temporally irrespective of the designation of analysis periods. For example, despite the absence of survey activity in the NA period, there were other vessels present in the acoustic data during this period associated with some of the hydrophones.

During the VO period, the presence of the *Sally Ride* at ranges of 6 km or less was typically associated with sound levels 5-15 dB over baseline (i.e., the 50^{th} percentile sound level for a specific analysis period). Beyond about 15 km, the *Sally Ride* alone was not clearly distinguishable in the time series. In the VM period, the presence of the *Sally Ride* and EM 122 at ranges of 6 km or less was typically associated with sound levels of 5-15 dB over baseline for all but the 12.5 kHz, 40 kHz, and *SPLpk* metrics, which were typically more than 20 dB and as high as 40 dB over baseline. Clipping also occurred within this range, though to varying degrees, when the EM 122 was on. From 6-10 km only the 12.5 kHz and *SPLpk* metrics were elevated more than 15 dB, whereas the other *BL*s were about 3-10 dB higher than baseline. Small peaks, i.e., 3-10 dB in these same metrics, were identified in association with the vessel and EM 122 activity to a distance of about 17 km. Due to the nature of the survey, it was not possible to characterize the impact of the other sound sources in a similar way. All of the active acoustic survey sources, with the exception of the SBP, were of higher frequencies than the EM 122, hence subject to a higher attenuation effect in water. Their acoustic contribution to the soundscape is smaller by this fact alone. In addition, none of the other active acoustic sources

were on long enough to characterize their impact in a meaningful way. The time series annotation revealed that the survey activity was, on average, detectable on a hydrophone for about one fourth of the study period, though intermittently. This varied spatially and was even more variable in the MA period consistently with the above remark—from as little as no detection of the survey activity to as much as 50% in the period. Moreover, the higher variability in the amount of time the survey activity was discernible in the MA period was likely because the survey lines were not as spatially comprehensive as in the VM period. The findings of the time-series annotation motivated a more quantified approach and holistic perspective of how the sound levels were changed by the survey activity which led to a series of broader-stroke analyses.

In particular, the sound level percentile comparison partitioned percentile differences into three relative magnitude classes for interpretation, guided by the findings of the time-series annotations. Changes of 20 dB or more corresponded to the most *extreme* changes which were rare in the time series annotation, for example, with respect to the survey activity at very close distances (i.e., under a few kilometers) of a hydrophone. Differences of 10-20 dB were considered *moderate* changes and occurred more often. With respect to survey activity, this corresponded to activity at distances up to10 km, but was also frequently seen with respect to other acoustic sources not related to the survey activity. Changes of 3-10 dB corresponded to the *smallest* changes in the sound levels that were still easily associated with distinct acoustic events, in some cases attributed to the activity of the EM 122 at distances under 17 km. Changes less than 3 dB were not interpreted, as they were not easily associated with distinct acoustic events. One of the most insightful findings of this analysis was that the difference between the NA period and those with survey activity were generally larger with increasing percentile. In other

words, the survey activity appeared to be most impactful on the loudest levels. This also suggests that the survey impacted the soundscape at a local temporal and spatial resolution rather than across the entire SOAR or over the entire study period. The percentile difference magnitudes were larger after weighting, which is reasonable given the EM 122 signal is well within the highest sensitivity frequency band of the hearing range of a mid-frequency cetacean. This implies that the EM122 survey activity is detectable by a mid-frequency cetacean. For the 12.5-kHz band, *extreme* differences were primarily only found in the 99th percentile between the NA period and those with echosounder activity. For w*SPLpk extreme* differences were primarily in the upper 25th percent between the NA period and those with survey activity, although the most numerous *extreme* differences were found between the VO and NA period in this metric. This suggests that 1) even the sounds inherent to the transiting vessel alone can cause extreme change to the soundscape, and 2) that external non-controlled sound sources were prevalent during these periods of observation. There were differences among the periods of anthropogenic activity, but the results varied and depended on the metrics being assessed and the exposure of the hydrophone to the particular survey activity.

The probability distribution analysis focused solely on the 12.5 kHz *BL*s which were deemed the best proxy of the EM 122 activity, of those metrics explored herein. The analysis revealed that largely only the NA and VM periods differed, with the VM period generally louder and intermittently loud in comparison to the NA period. This was really only seen on western and central hydrophones, whereas no difference was detected between these periods on the eastern hydrophones. One explanation for this was that the baseline sound levels on the eastern hydrophones were generally louder because of their proximity to San Clemente Island and their relatively shallower depths in comparison to the rest of the array. The probability distribution of

the MA period sound levels was often flatter than the other periods, suggesting a more uniform distribution of sound levels and thus a more dynamic acoustic environment. However, there were no statistical differences among the three periods of survey activity. Despite only one decidecade band being examined in the probability distribution analysis, the findings corroborated those of the time-series annotation: on a given hydrophone, the survey activity was intermittent and loud. This suggested that the 12.5 kHz band served as a good proxy to assess the impact of the survey activity, particularly because the EM 122 was the primary source used throughout the survey.

The frequency correlation analysis showed that there were several ways the frequency correlation differed among analysis periods. In particular, there were three areas that differed between the NA period and those with survey activity, two of which seemed unrelated to the anthropogenic activity-centric period designations, i.e., 1) the very low frequency array-wide phenomena and 2) the presence of high frequency biological acoustic activity. This left only one broad area of frequency correlation difference, which corresponded with ship-radiated sound. This suggests that the survey activity was among several acoustic events—biological, anthropogenic, and sources unknown-- that caused distinguishable differences in frequency correlation over the course of this study. The VM period was largely only different from the VO period at the frequency range of the EM 122 (i.e., 11-13 kHz). Due to the more interspersed use of the EM 122 in the MA period, the MA and VO periods were even more different in this region than the VM and VO periods, highlighting the fact that increased correlation relates to time rather than intensity. In other words, because the EM 122 was used continuously in the VM period and only intermittently in the MA period, the VM period was more similar in terms of frequency correlation to the VO period than the MA period was. Although it was known from

the onset that it would be difficult to characterize the contribution of specific acoustic sources other than the EM 122, the frequency correlation analysis provided some insight. In particular, the EK-80 signal made a noticeable contribution to the frequency correlation around 18 kHz. The correlation difference associated with this source was about a third of the magnitude in comparison to the correlation difference caused by the EM 122 signal. This suggests the EK-80 contributed even less to the changing sound levels across time than the EM 122 signal, which makes sense given the higher frequency signal of the EK-80 and greater attenuation. There was also an area of higher correlation around the frequencies associated with the SBP, but a discrete area was not clear. This was likely because there were other sources of sound in this part of the frequency spectrum that, at least partially, masked the signal. There were no clear frequency correlation differences associated with the EM 712 signal, suggesting this source did not contribute greatly to this metric.

Although significant insight was gained about deep-water mapping through this soundscape analysis, there are aspects of this particular survey at the SOAR that need to be acknowledged if using this insight more broadly. For one, the survey was not conducted in isolation of the natural acoustic activities that occurred at the SOAR. So although broad stroke trends were gleaned about the survey activity, they were specific to the survey conducted at the SOAR and inclusive of the features that make up the current marine acoustic environment there. If one were to repeat the survey over a different hydrophone array, the local ambient acoustic activity would likely contribute in different and unknown ways. Secondly, although the primary survey offered insight about the typical operation of the EM 122, the more arbitrary and sporadic use of the other acoustic sources in the MA period did not facilitate a clear assessment of these other sources. Finally, by approaching this study holistically as an assessment of how the survey

activity impacted the *entire* SOAR soundscape, there were many confounding factors that necessarily made a clear characterization of all of the acoustic survey activities more difficult. In particular, the various differences in depth, bathymetry, and anthropogenic exposure of each hydrophone largely contributed to the variability seen through each analysis. Nonetheless, identifying and considering these complexities was a necessary part of assessing the contribution of a real mapping survey in a real marine environment. These factors (i.e., depth, bathymetry, exposure) were discussed with respect to the sound level differences identified and were largely satisfactory in explaining the observed variation. Future work could be done to account for these confounding factors in a more directed way, such as through exploring the data by controlling one or more of these factors, e.g., making comparisons across hydrophones of the same depth, or with similar anthropogenic exposure, etc.

Along these lines, it was imperative that the time-series annotation was conducted to provide the detailed understanding of what acoustic sources were present in the SOAR soundscape and in what capacity. Without this it would have been difficult to accurately interpret the results of the other analyses. For example, one of the biggest shortcomings of the percentile analysis was that the mechanism driving the results was not known. The annotation results were relied heavily upon to interpret the findings. However, it was difficult to quantifiably summarize the impact of the survey activity on the soundscape through the annotation alone, thus broader stroke analyses such as the probability distribution and sound level percentile comparisons served this purpose. The calculation of cumulative sound exposure levels and the modelling of clipped signals helped to put the findings into the context of sound exposure regulation, forming an information base upon which regulators could pull to inform policy regulating mapping echosounders such as the 12 kHz multibeam echosounder. The frequency correlation analysis

provided the most detailed frequency assessment helping to summarize the contribution of the other, lesser used, acoustic sources which had been difficult to glean through the other analyses. For these reasons, each of the five analyses were a necessary part of a comprehensive soundscape assessment.

As previously alluded to, there are many analyses that could contribute understanding to an effective soundscape study. The tools used here were selected to specifically understand the contribution of the EM 122 to the soundscape. But not all of the tools used were optimized for a general soundscape assessment and each analysis had its limitations, thus necessitating the use of a comprehensive suite of tools. The probability distribution analysis, for example, identified differences between the VM and NA periods, as was anticipated, but it did not detect differences between the VM and MA periods, despite visually identifiable differences (i.e., flat versus peaked distributions). It was not expected that there would be very significant differences between these two periods given they both contained activity from the EM 122. But future work could be conducted to explore these differences further, making the method more accessible for general use in soundscape studies. In particular, finding a more optimal range of bins for partitioning the data would be a good place to start. Here, the entire data set over the course of the study period was partitioned such that every sound level was considered in the comparison. Thus, the range of bin values were defined by the maximum and minimum over the entire study period, rather than with respect to a single analysis period. This choice--in addition to the assessment of decibel values rather than values on a linear scale-- may have unintentionally led to the distributions seeming more similar to one another. One way to remedy this would be to choose only a subset of the data (e.g., only data between 1st and 99th percentiles) based on a reasonable set of carefully considered assumptions. Additionally, the 'waddR' package is

capable of comparing two distributions with a different set of bins, so an alternative approach would be to compare distributions with bin value range optimized for the specific analysis period. These approaches were not explored here, but may prove useful in being able to more closely match visually identifiable differences to statistically identifiable ones. And finally, only the 12.5-kHz decidecade band was explored here. In applying this approach more generally to soundscape studies, additional sound level metrics--particularly broadband metrics-- should be explored where relevant to the particular research question.

The sound level percentile comparison also has the potential to be used more broadly in soundscape assessments. Again, the relative magnitude classes used here were optimized for this specific application. As was obvious between the individual hydrophone versus array-wide approach, the resolution and scale of the analysis must be carefully considered when using this technique, as well as really any tool. The relative magnitude classes used here were chosen based on the changes identified in the time series annotation conducted on an individual hydrophone basis and with respect to the survey activity. Although the same relative magnitude classes were also applied in the array-wide sound level percentile comparisons, it was less clear that differences of those magnitude classes could be interpreted similarly. For example, a change in 3 dB at a spatial scale of 1000s of kilometers does not likely have the same meaning as a change in 3 dB at a spatial scale of 10s of kilometers. The same can be said about differences of 3 dB at various temporal scales. Careful consideration of scale should be made when adopting or modifying this approach for use in other soundscape studies.

One of the most useful aspects of the frequency correlation analysis is the ability to separate the contribution of two or more simultaneous sources from one another. This was particularly useful in this analysis in separating the ship-radiated sound contribution from the

EM 122 signal. Future work can extend this idea in identifying the distance from a fixed receiver that each source remains detectable, with respect to frequency correlation. For example, frequency correlation matrices could be computed and compared for periods associated with the vessel's fixed distance from the receiver (e.g., 0-2 km, 2-5 km, 5-10 km, 10-20 km) to understand how frequency correlation differs for these two sources (ship-radiated noise versus MBES signal) as a function of distance. With this data set, this could be conducted across time using the acoustic data from a single hydrophone, or across space looking at the acoustic data from the same point of time across a line of hydrophones. Although at face value frequency correlation clearly provides insight about the spectral nature of a changing soundscape, it is a function of time. The strength of a correlation is about the temporal nature of two signals. If one signal is represented in the time series for a different fraction of time than another signal, there will be a difference in their correlation. If one signal has a different duty-cycle (i.e., continuous versus pulsed) than another signal, there will be a difference in their correlation. Thus the effectiveness of this --or any soundscape study-- comparison requires significant *a priori* understanding of the sources contributing to the soundscape. Therefore, this tool is most useful for identifying areas of strong or lacking frequency correlation, and then looking to the data to uncover the contributing source mechanism. Finally, the frequency correlation analysis does not provide information about differences in sound level intensity, providing another reason for a suite of tools to be used for a comprehensive assessment of the soundscape.

By the far the most insightful tool used to observe changes in the SOAR soundscape was the time-series annotation. It not only provided insight about the magnitude, duration, and frequency of changes associated with the survey activity, but it provided insight about other acoustic sources, their magnitude, duration, frequency, and identification. This part of the

assessment provided a clear understanding of the strong time and space dependence of the contribution of the survey activity to the soundscape. In other words, that the deep-water mapping activity impacted a local area of the time (i.e., intermittent), space (i.e., <<area of the SOAR), and frequency (i.e., largely 11-13 kHz) dimensions of the soundscape. However, this was also the most time-intensive analysis. It took over 40 hours of effort for the careful review of hydrophone 45, and there was undoubtedly much more that could be garnered from the acoustic data. This is why automated tools exist for extracting characteristic information from comprehensive data sets. Therefore, the findings from this annotation will provide a resource from which information can be extracted for future efforts to automatically identify and characterize the 12 kHz-MBES signal in acoustic data. In particular, the physical characteristics of the EM 122 signal are reliable parameters that can be used with little if any uncertainty, i.e., 11-13 kHz frequency, pulse length and duty cycle based on ocean depth, etc. These characteristics within a roughly 17 km radius of a hydrophone can be reliably attributed to this acoustic source. This is not new insight, but this study provides empirical support that these characteristics are valid *in situ*.

The modelling exercise revealed that the EM 122 signal did significantly contribute to the cumulative sound exposure levels, as indicated by the 19-33 dB difference between observed and modelled $SELcum_{24}$ (realistic scenario accounting for EM 122-related clipping). This suggests that the energy in the EM 122 signal more than compensates for its infrequent and short duration attributes. One of the most important motivations for this particular piece of the soundscape assessment was to evaluate whether the observed changes would impact marine mammals at the SOAR. In this respect, the modelled 2017 mapping survey $SELcum_{24}$ did not meet or surpass three of the four acoustic injury thresholds (i.e., PTS or TTS, for a non-impulsive sound, or PTS

for an impulsive sound) for mid-frequency cetaceans, thought to be the most vulnerable marine life to mid-frequency sonar sounds and hence to the deep-water MBES (12 kHz) mapping activity. The upper bound of the realistic scenario modelled $SELcum_{24}$ did exceed the TTS impulsive threshold by 3 dB, but again, this was a conservative estimate for a stationary receiver. This result indicates that surpassing this threshold is possible in this specific way but for a mobile foraging marine mammal this is likely an overestimate of the potential exposure. These results indicate that acoustic injury at the depth of the hydrophones would be very unlikely in this group. As there are currently no accepted behavioral impact thresholds for this metric by the scientific community, an interpretation of these results with respect to behavior thresholds was not made here. However, the behavioral impact study results presented in earlier chapters represent the best available assessment of the potential impact that deep-water MBES mapping has on the behavior of foraging beaked whales. The final chapter of this dissertation explores how the results of this soundscape chapter inform and contextualize the results of those earlier chapters on behavioral effects of the EM 122 signal on foraging Cuvier's beaked whales.

CHAPTER 6: SUMMARY AND CONCLUSION

Research Summary

With expanding human advancement and global connectivity, the use of the marine environment for such purposes as commerce, energy production, national security, and the exploitation of marine resources, has been growing for years. With this comes the need to understand the marine environment and for tools like active acoustic systems that provide detailed and comprehensive information about the underwater environment. However, vital information-gathering activities -- using sonar technology-- transmit acoustic energy into the marine environment. One form of sonar, mid-frequency active sonar (MFAS), has been observed to have clear adverse impacts on marine mammals, i.e., stranding events and reduced foraging behavior (McCarthy *et al.* 2011, Ketten 2014, Manzano-Roth *et al.* 2016, DiMarzio *et al.* 2019). The question has arisen whether other sonar types have a similar adverse effect, such as geophysical acoustic sources, like the deep-water multibeam echosounder studied herein. Multibeam echosounders are routinely used for providing critical bathymetric, backscatter, and water column data for a range of important applications, including habitat mapping, search and recover efforts, mapping safe navigational paths, as well as a multitude of scientific research applications. It is not only in our best interest to understand how these activities affect the marine acoustic environment as responsible stewards of the ocean environment, but it is also our obligation by mandate through such legislation as the Marine Mammal Protection Act.

Prior to this work, no empirical studies had been conducted that specifically examined the effect of multibeam echosounder signals on free-ranging wild marine mammals or on the marine acoustic environment, in general. Thus the main goal of this work was to assess, through a dedicated experiment at sea, potential effects of deep-water multibeam echosounder signals on

beaked whales and the marine acoustic environment. This was a novel and important contribution to our understanding of this topic.

The Kongsberg EM 122, a deep-water multibeam echosounder with center frequency of 12 kHz was the primary multibeam echosounder considered in this study. The EM 122 represents the most powerful and lowest frequency echosounders available and thus the worst-case scenario for potential acoustic interactions of echosounders with marine mammals. Two ocean-mapping surveys using an EM 122, one in 2017 and the other in 2019, were conducted over the Southern California Offshore Antisubmarine Warfare Range hydrophone array, during which acoustic observations of marine mammals and the mapping survey were collected. These surveys and their impact on the SOAR acoustic environment and marine life within it were the study system for examining this main goal. Cuvier's beaked whales were the species of interest due to their consistent presence at the SOAR. This and other beaked whale species have repeatedly been sighted in stranding events associated with MFAS across the globe (Ketten 1994), and through dedicated research, have been shown to clearly decrease their foraging effort and leave an area during MFAS exercises (McCarthy *et al.* 2011, Tyack *et al.* 2011, Manzano-Roth *et al.* 2016, DiMarzio *et al.* 2019). Thus this was an ideal species for which to compare the known effect of MFAS on beaked whale foraging with the potential effect of MBES evaluated here.

Therefore, a secondary goal of this research was to compare the behavioral response of foraging beaked whales to MBES mapping activity to the response of beaked whales to MFAS naval activity assessed by other researchers (McCarthy *et al.* 2011, Manzano-Roth *et al.* 2016, DiMarzio *et al.* 2019). Analogous methodologies to those studies were used here to be able to make such comparisons. Specifically, the temporal and spatial foraging behavior of beaked

whales was compared *Before, During,* and *After* MBES mapping activity. Insight about the foraging behavior of beaked whales was gained through the echolocation clicks that beaked whales produce during a foraging event, called a group vocal period (GVP). Echolocation clicks were recorded on a large-scale hydrophone array over which the MBES mapping surveys were conducted and compared in the aforementioned framework. This was the same approach taken by researchers assessing the effect of MFAS naval activity on foraging beaked whales, i.e., GVPs recorded on large-scale hydrophone arrays were used to evaluate beaked whale foraging behavior *Before, During,* and *After* MFAS exercises (McCarthy *et al.* 2011, Manzano-Roth *et al.* 2016, DiMarzio *et al.* 2019). A summary of the research chapters is provided, giving insight on the effect of deep-water mapping activity on beaked whale foraging and the marine acoustic environment. Along the way, the results are compared to analogous studies on the effect of MFAS on beaked whales foraging.

Three of the four research chapters of this dissertation explored potential avenues for which the deep-water multibeam echosounder (EM 122) may have affected the marine system under study. Chapter 2 assessed the effect of the multibeam mapping surveys on the temporal foraging behavior of Cuvier's beaked whales, whereas Chapter 4 examined the effect of the same mapping surveys on the spatial distribution of foraging activity. Chapter 5 characterized the change in sound levels during a deep-water MBES mapping survey over the SOAR array. Although the aim of this work was to assess the effect, or lack thereof, of the multibeam mapping survey activities on beaked whales, wherever possible general findings were described such that the insight gained could be used for other applications, such as with a different species or sound source. Thus Chapter 3 proposed and demonstrated a multi-pronged statistical approach for identifying changes in spatial observations across distinct periods of time from a

large-scale hydrophone array. The approach was used here to assess spatial change in Cuvier's beaked whale behavior with respect to the ocean-mapping surveys (Chapter 4).

The objective of Chapter 2 was to identify, from the experimental data recorded on site, whether the activities of the two ocean-mapping surveys affected foraging behavior of Cuvier's beaked whales. This was assessed by examining four GVP characteristics which were used as proxies of beaked whale foraging activity across distinct time periods with respect to the survey operations. In particular, 1) the number of GVPs, 2) the number of clicks per GVP, 3) the GVP duration, and 4) the click rate per GVP were examined. Nearly 300 hours of data were assessed over the two mapping survey studies (~50 hours of activity for each survey) and several hundred GVPs were identified across both years (575 in 2017, 394 in 2019). There were two levels of temporal assessment undertaken. The first utilized a *Before*, *During*, and *After* design, which revealed that the number of GVPs increased *During* the mapping surveys and remained high *After* in comparison to *Before* (i.e., on average, 2.44 GVPs per hour *Before*, 3.61 *During*, and 3.74 *After*). The GVP click rate also changed but only with respect to the *Before* and *After* periods (i.e., click rate increased from 58 clicks/min. *Before* to 69 clicks/min. *After*). There were no other statistically significant differences detected in the GVP characteristics.

A finer temporal assessment was also conducted separately for each survey year, which showed that the number of GVPs actually fluctuated across the study period, and that the 2017 survey was driving the result presented in the coarse assessment—i.e., the number of GVPs increased *During* the mapping activity, specifically in the 2017 survey. These findings revealed that there was substantial variability in beaked whale foraging behavior even outside of the survey activity, suggesting the changes observed were most likely a response to some other factor, such as prey dynamics, than to the MBES mapping activity itself.

Overall, the temporal behavior study showed that the animals did not stop foraging and did not leave the range during either MBES mapping survey. There were no differences detected between MBES and non-MBES periods in three of the four GVP characteristics assessed. The increase in foraging effort, i.e., in the number of GVPs, detected during one of the two MBES mapping surveys was a stark contrast to the effect that MFAS had on beaked whale foraging, where a monotonic decrease was observed in the number of GVPs during MFAS exercises (McCarthy *et al.* 2011, Manzano-Roth *et al.* 2016, DiMarzio *et al.* 2019). Furthermore, the temporal fluctuation of the number of GVPs across time suggested that the statistical increase observed *During* the 2017 MBES survey was likely a function of some other factor than the MBES surveys, and was most certainly not the clear drawn-out response seen by beaked whales in response to MFAS.

Chapter 3 presented the Global-Local-Comparison (GLC) approach, motivated by the need to analyze the spatial aspects of marine mammal behavior within a *Before-During-After* framework. Chapter 3 was more of a methodological chapter, rather than addressing the main topic itself, but was applied in Chapter 4 to address the primary research question. The three-pronged GLC approach used established spatial autocorrelation statistics — Moran's I and Getis-Ord Gi*-- to 1) identify changes in clustering of observations in a study area, i.e., random, clustered, or dispersed, i.e., the global analysis, and 2) to identify changes in observation hot and cold spot distributions, respectively, i.e., the local analysis. A comparison test, here the Kruskal-Wallis test, was used to assess whether there was an order-of-magnitude difference in the number of observations. The GLC approach was tested on synthetic data of known spatial patterning and exemplar data sets extracted from peer-reviewed studies of marine mammal behavior during noise exposure events. The demonstration with synthetic data revealed that

detection of change was possible, with some fine-tuning based on the study system being considered and with respect to the statistical input parameters used, mainly the neighbor-weighting scheme. The demonstration with exemplar data sets revealed that the approach resulted in similar findings to the original studies, but now backed by a robust statistical analysis. The demonstration also shed light on the importance of combining the three analyses, because any one analysis in isolation was limited. However, when combined the three analyses provided a comprehensive assessment of spatial change.

The GLC approach was applied in Chapter 4 to assess whether there was a change in the spatial distribution of foraging Cuvier's beaked whales *Before, During,* and *After* the same two ocean mapping surveys at the SOAR. This analysis offered a second context upon which to assess whether the mapping surveys affected foraging behavior of Cuvier's beaked whales. The spatial analysis revealed that foraging was consistently clustered throughout both study periods, and within each study year, the magnitude of foraging effort was not different on a per hydrophone basis across analysis periods. In 2017, there was large overlap in the foraging hot spots identified, indicating no obvious change to the spatial distribution of foraging whales at a local level. In 2019, the cluster of foraging hot spots was in the southernmost corner *Before* the survey, in the center *During*, and was split between these two locations *After*. Despite the clear difference in foraging hot spots across 2019 analysis periods, the foraging hot spots remained in the historically well-utilized areas of the SOAR (Falcone *et al*. 2009, Schorr *et al.* 2019) throughout the study. Differences in the *Before* periods between the two years point to the natural variability in the usage of the SOAR by foraging beaked whales, suggesting the cause for the differences *During* the 2019 survey cannot automatically be attributed to the survey activity. Although beyond the scope of this study to test, the most probable reason for the shift in foraging

hot spots in 2019 was that foraging behavior in beaked whales is largely driven by their field of prey, which can be extremely patchy over finite areas.

Overall, the spatial analysis of beaked whale foraging behavior revealed no global, local, or order-of-magnitude change in foraging effort during the 2017 mapping survey. There was also no global or order-of-magnitude change during the 2019 mapping survey. There was a change locally, but it was a shift in foraging effort toward the center of the array which remained in the historically well-utilized area of the array (Falcone *et al.* 2009, Schorr *et al.* 2019). This was unlike the avoidance response seen by beaked whales in response to MFAS, where animals not only stopped foraging on the array (McCarthy *et al.* 2011, Manzano-Roth *et al.* 2016), but left the area of the MFAS exercises entirely (Tyack *et al.* 2011). Here, the animals remained on the range and continued to forage throughout both MBES mapping surveys.

The final research chapter (Chapter 5) provided a third perspective from which to consider the possible effect of deep–water mapping activity on beaked whale foraging, in addition to the effect on the marine acoustic environment. This perspective was gained through a detailed documentation and characterization of the changing sound levels during the 2017 mapping survey, providing a general understanding of the spatial, temporal, and frequency attributes of a typical deep-water MBES mapping survey. The comprehensive soundscape assessment examined four analysis periods with respect to the mapping activity, i.e., No Activity, Vessel Only, Vessel and MBES, and Mixed Acoustics, across nine select hydrophones from the SOAR array. The assessment included:

- A detailed annotation of several sound level metric time series-- *SEL*, *SPLpk*, and five decidecade bands (centered at 50 Hz, 500 Hz, 3.2 kHz, 12.5 kHz, and 40 kHz) --informed by spectrograms, spatio-temporal animations, and spectral-temporal animations.

- A quasi-spatial, relative-magnitude comparison of sound level percentiles across the four analysis periods.
- The calculation of observed and modelled 24-hour cumulative sound exposure levels and comparison to regulatory sound exposure thresholds.
- A comparison of the 12.5 kHz decidecade band sound level probability distributions among the four analysis periods.
- A full-spectrum frequency correlation assessment of the four analysis periods.

The assessment revealed that the sound from the EM 122 was distinguishable within a maximum radius from the *Sally Ride* of about 17 km, which illustrated the expected dependence between the sound pressure level received at a SOAR hydrophone and the propagation range from the sonar to the hydrophone. The sound from the EM 122 was consistently prominent in the acoustic record when the *Sally Ride* was within this finite radius of a hydrophone receiver, but in a very specific capacity. That is, the EM 122 activity manifested most in the loudest levels (i.e., 99^{th} percentile) in the 12.5 kHz band, the operating frequency band of the echosounder. The EM 122 signals were detectable on a given hydrophone for a quarter of the survey period, on average, but intermittently across the study period. Observed 24-h cumulative sound exposure levels were calculated for the various analysis periods of anthropogenic activity, but at very close passes of the *Sally Ride* to a hydrophone the dynamic range of the SOAR receiver was insufficient at capturing the full energy of the MBES signal. To account for this, a modelling exercise was conducted resulting in a conservative estimation of the 24 h-cumulative sound exposure levels at a stationary seafloor receiver of 159-173 dB re 1 μPa^2 s. These values were below three of four of the mid-frequency cetacean acoustic injury thresholds, but the upper bound did exceed the current U.S. regulatory threshold for TTS to a mid-frequency cetacean

exposed to an impulsive sound (i.e., 170 dB re 1 μPa^2 s) (NMFS 2018). This conservative estimate assumed exposure to a stationary seafloor receiver, which serves as an appropriate proxy of what a foraging beaked whale at the seafloor may be exposed to, except that it did not account for the mobility of marine mammals. So, this is likely a conservative overestimation of the potential exposure of a mobile marine mammal receiver. This finding serves as a critical reminder of the ambiguity in how MBES signals are currently classified in the U.S. regulatory framework (NMFS 2018). MBES signals are not clearly defined as being non-impulsive or impulsive signals, and this has important repercussions on how this sound source is regulated. This is an important topic that needs careful consideration by both the scientific and regulatory community. The findings of this chapter confirm that the deep-water survey activity had a very local and well-defined impact on the SOAR soundscape. The deep-water MBES mapping activity was the most recurrent, loud source of sound across the three-day survey, but intermittently present at any specific location. The MBES contributed to the acoustical energy field only within the frequency band of the echosounder and at a finite distance around the *Sally Ride* (~17 km).

The soundscape assessment provided integral insight about the detectability of the MBES mapping survey and therefore the ability to relate any observed behavioral response to the MBES mapping activity. First, the acoustic environment was only impacted by the MBES signal within a finite radius (i.e., ~17 km) around the *Sally Ride*. Although it is not fully known what the auditory performance is of a beaked whale (and this is also an important topic for future work), it is reasonable to expect that if a behavioral response were to occur as a result of the MBES activity, it might begin within a roughly similar radius of detection. However, the *Sally Ride*—and therefore the radius of detection—was constantly moving. In addition, the marine mammals

were most certainly moving, and their movement likely varied on a time scale different than the mapping activity. One might therefore expect any spatial response to the mapping survey would be linked to the mapping survey lines, thereby requiring observations to be made on a scale much smaller than the SOAR hydrophone array. Therefore, it was nearly impossible to reasonably associate any observed changes in behavior with the mapping survey at the temporal and spatial resolution used in the behavior assessments here. Because behavioral responses have been observed for the same and other beaked whale species (McCarthy *et al.* 2011, Manzano-Roth *et al.* 2016, DiMarzio *et al.* 2019) at a similar scale to that studied here in response MFAS, it was a reasonable scale to use.

But there was a local spatial change detected in where the most foraging effort was detected in the 2019 spatial assessment, so this needs to be discussed. Based on 1) the understanding that the MBES signal had a very local spatial and temporal contribution to the soundscape that was constantly shifting around the SOAR, and 2) that *During* the 2017 MBES mapping survey there was no spatial change detected, it seems most unlikely that the shift in foraging activity from the southeast corner of the array *Before* the 2019 mapping survey toward the center of the array *During* the survey was a response to the mapping activity. Furthermore, the foraging activity remained on the array in a historically well-utilized area by foraging beaked whales (Falcone *et al.* 2009, Schorr *et al.* 2019), suggesting this observation was 1) not an adverse response--whatever the cause-- and 2) most likely a response to the animals' prey field.

An important additional notion to consider is that the detectable area of a stressor does not necessarily indicate the potential spatial scale over which a behavioral response may extend. In fact, in cases of clear adverse effect, marine mammals have been observed to respond over great distances to a stressor (Miller *et al.* 2012). Therefore, one of the values of these SOAR-

wide behavior assessments was that they provided the ability to identify whether spatially large and temporally drawn-out responses occurred, which can be indicative of whether the interaction and response came with substantial cost to the animals, and/or elicited a widespread response from a group of animals. The existence or absence of such a response can be helpful in linking observed effects to a clear impact. So, a key result that can be gleaned from the spatial and temporal resolution available from the behavior assessments here is that there were no large and drawn-out changes, either spatially or temporally, that would suggest the survey activity had a clear or lasting effect on foraging behavior at a group or array-wide level. This again, is a stark contrast from the MFAS studies that showed a very clear adverse temporal and spatial change (i.e., animals stopped foraging and left the area) in foraging behavior at the resolution of the large-scale hydrophone arrays used during the MFAS studies (McCarthy *et al.* 2011, Manzano Roth *et al.* 2016, DiMarzio *et al.* 2019).

The difference in behavioral results between these two sonar types is not surprising, given the very different characteristics of the two sources (see Table 1.1), which leads to a very different potential for direct ensonification between the two sources, as well as differences in how the signal propagates into the environment. This includes differences in the radiation geometry of the two systems, i.e., near-horizontal conical beam (MFAS) vs vertical swath (MBES), which is directly linked to the very different purposes for using the two sonar types. MFAS is commonly used for surveillance purposes, which necessitates ensonifying a broad search area, whereas MBES --used here for mapping the seafloor-- requires precise measurements and a narrow aperture. In addition, the frequency differences, i.e., 3-8 kHz (MFAS) vs 12 kHz (MBES), and signal characteristic differences (i.e., shorter duty-cycle and longer pulse lengths for MFAS) also play a role in how much energy is transmitted and how

large an area the signals will propagate. The soundscape assessment of this dissertation very clearly demonstrated the local temporal, spatial, and frequency contribution of the deep-water MBES to the acoustic environment, which is a direct result of how these MBES characteristics manifest in the environment.

As discussed in Chapters 2 and 4, there are other factors that may play an important role in the behavioral results observed, such as prey distribution and behavior, or oceanographic conditions. These data were either not available or not at the resolution needed to fully assess the impact of such factors. In addition, there is most certainly a degree of natural variation in behavior that needs to be considered, such as diel variation or other natural factors in an undisturbed system. An attempt was made to account for such factors by considering longer analysis periods and the same start times from one period to the next. In any opportunistic study, there are limitations in study design. Here, there was a limit in how much data representing undisturbed times could be analyzed because the hydrophone array is part of a naval facility. Thus, extending the GVP time series further before or after the survey to get a better understanding of the natural variability in GVP characteristics was not possible. The time period for these studies was specifically chosen because no other anthropogenic activities were occurring on the array during that time. It seems most certain that there are other important factors, unaccounted for here, which dictated the observed changes in beaked whale foraging behavior.

Past modelling work of MBES radiation (Lurton 2016) has suggested that based on the transmission geometry, duty cycle, signal duration, and frequency content there should be minimal occurrences of interaction between MBES and marine mammals. What sonar modelling efforts cannot predict is whether those infrequent chances of interaction could have

meaningful effects. The empirical work here demonstrated no adverse changes in Cuvier's beaked whale foraging behavior, and no clear response to the deep-water MBES mapping activity.

The work conducted here was on a single species and a single multibeam echosounder during two three-day mapping surveys, meaning any extrapolation of these results, broadly, to other species and echosounders needs to be carefully considered. The scientific community recognizes that there is a myriad of factors that need to be considered on a case-by-case basis in predicting the effect a sound will have on marine life beyond just the physical characteristics of the signal. This includes the behavioral state of the animal, the frequency range of best hearing of an animal, the duration of exposure, the proximity to the source, the perception of the character of a sound by the receiver, and the ambient acoustic conditions of the environment, among other factors (Southall *et al.* 2021). But the results presented from this empirical study assessing the effect of deep-water 12 kHz MBES mapping activity on Cuvier's beaked whale foraging behavior should serve as an upper bound on the potential effect of geophysical echosounders on marine mammals. That is because the deep-water 12 kHz MBES is the loudest and lowest-frequency mapping system available, meaning its signals will have the largest spatial and temporal impact of any current geophysical echosounder. Cuvier's beaked whales have a frequency range of best hearing sensitivity that directly overlaps with the 12 kHz signal. In addition, this species has been shown to be quite vulnerable (i.e., stranding, reduced foraging) to other sonar sources (i.e., MFAS). And finally foraging behavior, studied here, represents a critical life-sustaining behavior of this species. Therefore, based on our current understanding of the myriad of important factors to consider when predicting the effect of anthropogenic sounds on marine life, the assessment of Cuvier's beaked whale foraging behavior during deep-water

MBES mapping should represent the potential worst-case interaction, or upper bound, on the potential behavioral effects on marine mammals related to echosounder signals.

The results here showed that foraging continued and the animals did not leave the area during the deep-water MBES mapping surveys. This suggests there was no clear effect of the mapping surveys on the foraging behavior of Cuvier's beaked whales. Thus, for other less sensitive marine mammal species the expected effect would be negligible. Of course, there is still a lot to be learned about the effect that sounds may have on marine mammals, particularly with regards to perception which is, arguably, impossible to measure for a marine mammal. But this work serves as the best available assessment, backed by empirical evidence, and based on the current state of understanding on the effect of echosounder signals on marine mammals. These findings can be used to help scientists and regulators better evaluate how this anthropogenic sound source fits into the bigger issue of biologically meaningful effects of anthropogenic sounds on marine life.

Future Work Recommendations

A unique and valuable aspect of the behavior studies conducted here was the ability to capitalize on observations from a large-scale hydrophone array of the U.S. Navy representing a subpopulation of beaked whales over an extensive area. This study resolution, broader than individual behavioral assessments, provides a stepping-stone toward our understanding of population level impacts. Studies that focus on individual behavior or that are conducted over finer spatial scales provide important ground-truthing about the results of such larger scale efforts. For example, tagging efforts in this study might have provided important insight into what an increase in the number of foraging events during the 2017 mapping survey meant. Tags exist that include passive acoustic monitoring (PAM), swim speeds, acceleration, dive patterns,

and other relevant information that could be used to better understand what changes in small-scale processes manifest as specific large-scale trends. Tags that include PAM can also provide relevant data to assess individual sound exposure information. Also, to most clearly understand what an increase in the number of foraging events meant for the animals, information about the success rate (i.e., prey captured or not) of those foraging events is needed. It is not clear that tagging information would explicitly provide this, but this is an area ripe for technological advancement. Large-scale hydrophone arrays, such as those of the U.S. Navy, should continue to be used to gain insight toward population level effects of anthropogenic sounds, but where possible, future studies should strongly consider incorporating complementary tagging efforts and other fine-scale monitoring ground-truthing efforts.

The behavioral studies here were opportunistic. Future more controlled studies utilizing PAM to remotely study behavior of marine life during anthropogenic activities should make every effort to include observations of other relevant environmental and ecological factors. For example, the prey field of the whales was hypothesized as the most likely driver of the changes to foraging behavior observed herein, but no observations of the current prey field were available to confirm this in this work. For environmental factors that are temporally and spatially dynamic, it is imperative to sample at the time of the study and with adequate resolution to be able to integrate the observations meaningfully into the analysis. In addition, long-term studies of these factors as well as monitoring studies of foraging characteristics will help to build a better understanding of the natural variability in beaked whale foraging and what drives that variability. Finally, if controlled studies are undertaken in the future, power analyses can help to understand the minimum sample size needed to see a statistically significant effect, should there be one. This would be particularly important for assessing changes in behavior with a similar resolution

(i.e., 2-6 km) but over a smaller overall spatial scale (<<1800 km^2) where the expected number of observations of foraging events would likely be less. Given there were observed effects at the significance level used in the work presented here, this was not an issue in this study, but most certainly can be for similar work where there are fewer observations.

Modelling research exists on the relationship between beaked whale feeding energetics and population level effects (New *et al.* 2013). Although work has been done to characterize the prey field of beaked whales at the SOAR and that was considered in the interpretation of the behavior studies (Southall *et al.* 2018), a complete assessment of the energetics of the whales observed in this study was not made. If those data were collected in future studies alongside foraging behavior data, such energetic models could continue to be refined to obtain a clearer understanding of the energetic expenditure associated with beaked whale foraging and the relationship to population growth. This is important baseline information to have when relating the potential biological meaning of an effect on such a critical life-sustaining behavior.

Localizing and tracking foraging groups is critical, but outside the scope of this work. There is a lot to consider in trying to localize a foraging group beyond designating a central hydrophone to a foraging event. A foraging event may begin with one set of animals and end with another set, and consist of an unknown number of animals that likely do not stay in the same position relative to one another throughout the event. For animals like Cuvier's beaked whales with high site fidelity at the SOAR, continued long-term monitoring studies of group foraging characteristics may prove useful in identifying features that can be used to localize foraging groups or animals within a foraging group and building out appropriate methods for doing so.

The findings of the soundscape study suggested that the contribution of the deep-water MBES to the marine acoustic environment were very clearly characterized by its reported physical signal characteristics (i.e., nominal frequency, pulse length, etc.). Future work should consider developing automated detection algorithms for identifying this sound source in passive acoustic data. This is presumably routine work in naval operations, but less so in the scientific research community, despite its potential usefulness. This can be useful in remote and long-term monitoring studies where there is a need to understand the frequency and prevalence of certain sound sources, such as in longitudinal studies assessing changing ocean soundscapes.

Because the signal of the EM 122 recorded on the SOAR hydrophone receiver clipped at times, sound exposure modeling was done to obtain otherwise irretrievable sound pressure levels from certain times over the 2017 mapping survey. Future work should be done to verify the validity of these modelled estimates. This could be done using the survey work in 2019, which included the deployment of a higher-dynamics receiver, avoiding clipping issues. These data could be used for such a verification effort. The sound pressure levels when the vessel was at various ranges to the wide-dynamics receiver can be used to understand similar distance scenarios (i.e., the received sound pressure levels at various distances) in which clipping occurred on the SOAR hydrophones during the 2017 survey.

A soundscape assessment was conducted for the 2017 mapping survey. An additional soundscape assessment of the 2019 study would provide further insight about the variation that could be expected with different survey plans. For example, the 2019 SOAR survey included a concentrated survey of the southeast corner of the array, within a canyon. A characterization of the soundscape during this part of the survey could provide further insight about how the MBES signal manifests differently when it propagates in the acoustic environment in the presence of

bathymetric features. This would be interesting from both a soundscape perspective, as well as looking at beaked whale foraging behavior in this concentrated area specifically. For the case of beaked whales at SOAR, the southeast corner was not a well-utilized area of the array for foraging, so this may be less insightful to consider retroactively for the behavior data sets examined in this dissertation, which is one reason why it was not explored here.

The emphasis of the soundscape study was on understanding the contribution of the deep-water MBES, the EM 122. As such, the analyses were optimized to identify and characterize its contributions to the soundscape. However, there were several other active acoustic sources that were used. The findings here suggested those sources did not substantially contribute beyond the use of the EM 122. This observation warrants further thought, particularly for those seeking to regulate underwater sound from multiple concurrent acoustic sources. The sound source with the most substantial (temporal and spatial—amplitude and frequency) contribution to the acoustic environment could be used as the worst-case scenario for acoustic effect by assuming that all of the other sound sources would be adequately accounted for if the most substantial source was addressed. Work would need to be done to fully understand the repercussions of such a choice since sounds of various frequency content and with various duty cycles and pulse lengths and other temporal patterning may have unknown and significant biological relevance to an animal receiver that is not captured by the physically relevant characteristics of the signal alone. In this respect, it would be interesting to assess the effect of sub-bottom profilers which work at similar frequencies to MFAS, although they have different operational paradigms.

A valuable applied direction for future work is to explore the various and dynamic signals that state-of-the art MBES use. Depending on the water depth, survey needs, and oceanographic conditions MBES can be operated in several different modes. These modes manifest as different

signals ranging in duration, inter-ping intervals, and even frequency content (i.e., frequency-modulated versus continuous wave). It is unclear what, if any, the effect of these dynamic signals may have on marine mammals, but they could lead to differences in behavioral response. Carefully controlled studies, likely on captive animals would be needed to fully understand if there is any difference in response by marine mammals related to different MBES signals.

Another topic related to the perception of sound by marine mammals that needs better understanding is the detectability of the sonar signals by a marine mammal. This would not only include research to understand the range-dependence of the detectability of the sonar signals by a marine mammal, but would include research to better assess the hearing integration time of a marine mammal receiver, as there are currently a range of unique values being used in the scientific community, including here (i.e., 100 ms). There is also some indication that integration time may vary with species and more specifically depending on the frequency or frequencies of a signal. The question related to the range-dependence of detectability of a signal is, how does a marine mammal extract a signal from ambient noise? We have a good understanding of how this can be done with computer-processing and even based on a human-detector, but less is known about how a marine mammal receiver does this. This is an important question for consideration since to elicit a behavioral change, a signal must first be detected. This is a relevant question when assessing behavioral change at the scale of the SOAR. This could be studied using captive animals and measuring their detection to sonar-like signals mixed with broadband noise at various signal-to-noise ratio (SNR) values. The measured SNR could then be extrapolated to propagation ranges. The topic of signal detection and signal perception in marine mammals has a lot of potential for future research.

As part of the larger MBES characterization project, another radiation pattern characterization experiment was conducted over the U.S. Navy Atlantic Undersea Test and Evaluation Center (AUTEC) hydrophone range off of Andros Island in the Bahamas in December 2018 (Mayer 2019) using the Kongsberg EM 302 (30 kHz) mounted to the Research Vessel, *Okeanos Explorer*. This experiment provides another potential data set with similar structure to the SOAR January 2017 study. Blainville's beaked whales are known to be highly resident on the AUTEC range and could provide insight about the effect of a different MBES on another species (Claridge 2013). During the Mayer (2019) study, a higher-frequency multibeam system with a nominal frequency of 30 kHz was used, in comparison to the studies herein conducted at SOAR. The nominal frequency of the 30 kHz MBES is also in line with the range of best hearing sensitivity of beaked whales, but due to the high-frequency nature of the system the signal is more susceptible to attenuation in the marine environment (i.e., 5-6 dB/km for the 30 kHz system versus 1 dB/km for the 12 kHz MBES). Thus, the resolution of the AUTEC hydrophone array may not be ideal for either a behavioral effect study or a well-resolved soundscape assessment. In addition, the AUTEC mapping survey took place at night during the same period of time when the U.S. Navy was also present and active on the range during the day. This project would provide an opportunity to assess beaked whale behavior during multiple concurrent anthropogenic activities, which may provide insight about cumulative effects of anthropogenic activity on beaked whale foraging. The specifics of the activities and data availability should be considered first.

Another avenue for future research is to test the applicability of the GLC approach to a spatial observation other than beaked whale foraging events, such as a sound pressure level metric. This would not only provide insight into whether the GLC approach is appropriate for

non-behavioral observations, but could serve as an additional tool upon which to understand the contribution of a sound source to a spatially broad soundscape. If conducted in parallel with a behavior assessment using the GLC approach, this could provide further clarity on the relationship between the two sets of observations. In addition, some of the other GVP characteristics assessed in the temporal study, that more intrinsically describe a foraging event, could be examined using the GLC approach. For example, looking at how echolocation click rate changes spatially may indicate something about the quality of the prey field in particular locations, which may serve as a reasonable proxy of the prey field where explicit prey field data are unavailable. It seems reasonable to expect the GLC approach would work for other spatial features but modifications may be necessary (i.e., neighbor-weighting rule) to optimize the approach for other spatial features. The spatial scale that these other features vary on also needs to be considered when determining if this is an appropriate approach.

One final area for recommended future research pertinent to the topic of research here is on the ambiguity of how MBES signals, among some other sound source signals, are classified. Even with the current binary U.S. regulatory delineation of sound sources into either impulsive or non-impulsive sounds it is unclear where this sound source should fall. This is in part due to the dynamic nature of the MBES signal, which can be operated at different pulse lengths, with multiple sectors, and in different depth-dependent modes, and all have repercussions on the actual physical signal that is transmitted into the environment. It is also a challenge to classify types of sound sources because the regulatory framework does not explicitly define the characteristics of an impulsive or non-impulsive sound. This is a challenging task because these designations have very specific meanings for very specific applications. The designation of a sound type for a source with respect to acoustic injury is generally much clearer than with

respect to behavioral impacts. In addition, the impulsiveness of a signal may be species-specific and this is not well understood. Therefore, the first step that is needed is to explicitly define the terms impulsive and non-impulsive with respect to acoustic injury of a marine mammal. With respect to behavioral impacts, the current binary delineation of sound types needs to be revisited and a discussion needs to be had on whether this delineation is appropriate for assessing the effect of a sound on marine mammal behavior. A dialogue needs to be had between both scientific experts and the regulatory community on this topic. Eventually, substantial empirical work will be needed to identify what specific metrics can be used to properly characterize the sound type designations with respect to marine mammal behavior and what appropriate thresholds would be for each of those metrics.

Conclusion

At the resolution of the SOAR hydrophone array, the empirical work here assessing Cuvier's beaked whale foraging behavior during deep-water 12 kHz MBES mapping activity demonstrated:

1) Cuvier's beaked whales did not stop foraging and did not leave the SOAR array during two deep-water MBES mapping surveys of the SOAR.
2) There was no adverse change observed in Cuvier's beaked whale foraging behavior, and no clear response to the deep-water MBES mapping activity.

Deep-water MBES mapping activity contributes substantially to a local marine acoustic environment. The EM 122 signal was only distinguishable at a finite scale (i.e., <17 km) around the *Sally Ride* and the effect on the changing sound levels had a clear range-dependence within this radius (i.e., louder with decreasing distance). This led to a temporally intermittent impact on

the soundscape at any given location. Within these spatio-temporal bounds, deep-water MBES mapping activity has the potential to be detected by a mid-frequency cetacean due to its spectral content and loudness. However, no adverse effects on beaked whale foraging behavior were observed here. This is a stark contrast to the observed adverse behavioral effect of MFAS on beaked whale foraging where a reduction in foraging was observed and animals left the area during MFAS exercises. This stark contrast in results was an unsurprising finding, given the very different physical and operational characteristics of these two sonar types and their impact on the marine acoustic environment. This was the first empirical study of the effect of multibeam echosounder signals on freely ranging wild marine mammals and the results should serve as an upper bound of the potential effect multibeam echosounders have on marine mammals.

LIST OF REFERENCES

Acevedo-Gutierrez, A., and Parker, N. (2000). Surface behavior of bottlenose dolphins is related to spatial arrangement of prey. *Marine Mammal Science* 16(2), 287-298.

Aguilar Soto, N., M. Johnson, P.T. Madsen, P.L. Tyack, A. Bocconcelli and J.F. Borsani. (2006). Does intense ship noise disrupt foraging in deep-diving Cuvier's beaked whales? (*Ziphius cavirostris*). *Marine Mammal Science* 22(3), 690-699.

Ainslie, M.A., Miksis-Olds, J.L., Martin, B., Heaney, K., de Jong, C.A.F., von Benda-Beckman, A.M., and Lyons, A.P. (2017). ADEON Soundscape and Modeling Metadata Standard. Version 2.0 DRAFT. Technical report by TNO for ADEON Prime Contract No. M16PC00003. Available from: https://adeon.unh.edu/sites/default/files/user-uploads/ADEON%20Soundscape%20Specification%20Deliverable%20v1.0%20FINAL%20Submission.pdf

Andre, M., and Natchgill, P.E. (2007). Electrophysiological Measurements of Hearing in Marine Mammals. *Aquatic Mammals* 33(1),1-5. doi: 10.1578/AM.33.1.2007.1

Andrew, R.K., Howe, B.M., Mercer, J.A., and Dzieciuch, M.A. (2002). Ocean ambient sound: Comparing the 1960s with the 1990s for a receiver off the California coast. *Acoustics Research Letters Online* 3(2), 65.

Andrew, R.J., Howe, B.M., and Mercer, J.A. (2011). Long-term trends in ship traffic noise for four sites off the North American West Coast. *The Journal of the Acoustical Society of America* 129(2).

Andrews, F. (1954). Asymptotic behavior of some rank tests for Analysis of Variance. *Annals of Mathematical Statistics* 25, 724-736.

Anselin, L. (1995). Local Indicators of Spatial Association – LISA. *Geographical Analysis* 27(2), 93-115. doi:10.1111/j.1538-4632.1995.tb00338.x

Arranz, P., Aguilar de Soto, N., Madsen, P.T., Brito, A., Bordes, F., Johnson, M.P. (2011). Following a Foraging Fish-Finder: Diel Habitat Use of Blainville's Beaked Whales Revealed by Echolocation. *PLoS ONE* 6(12), e28353. doi:10.1371/journal.pone.0028353

Arveson, P.T., and Vendittis, D.J. (2000). Radiated noise characteristics of a modern cargo ship. *The Journal of the Acoustical Society of America* 107(118). Doi: 10.1121/1.428344.

Baddeley, A., Rubak, E., and Turner, R. (2015). Spatial Point Patterns: Methodology and Applications with R. Chapman & Hall/CRC Press.

Baird, R.W., Webster, D.L., McSweeney, D. J., Ligon, A.D., Schorr, G.S., and Barlow, J. (2006). Diving behavior of Cuvier's (*Ziphius cavirostris)* and Blainville's *(Mesoplodon densirostris)* beaked whales in Hawai'i. *Canadian Journal of Zoology* 84, 1120-1128.

Baird, R.W., Webster, D.L., Schorr, G.S., McSweeney, D.J., and Barlow, J. (2008). Diel variation in beaked whale diving behavior. *Marine Mammal Science* 24(3), 630-642.

Baird, R.W. (2019). “Behavior and ecology of not-so-social odontocetes: Cuvier’s and Blainville’s Beaked Whales,” in *Ethology and Behavioral Ecology of Odontocetes*, ed. B. Wursig (Springer International Publishing), 305-329. doi:10.1007/978-3-030-16663-2_14

Barlow, J., Rankin, S., and Dawson, S. (2008). A guide to constructing hydrophones and hydrophone arrays for monitoring marine mammal vocalizations. NOAA Technical Memorandum. NOAA-TM-NMFS-SWFSC-417.

Barlow, J., Schorr, G.S., Falcone, E.A., and Moretti, D. (2020). Variation in dive behavior of Cuvier’s beaked whales with seafloor depth, time-of-day, and lunar illumination. *Marine Ecology Progress Series* 644, 199-214. doi: 10.3354/meps13350

Battista, T., and O’Brien, K. (2015). Spatially Prioritizing Seafloor Mapping for Coastal and Marine Planning. *Coastal Management* 43(1), 35-51. Doi: 10.1080/089270753.2014.985177

Baumann-Pickering, S., McDonald, M.A., Simonis, A.E., Berga, A.S., Merkens, K., Oleson, E.M., Roch, M.A., Wiggins, S.M., Rankin, S., Yack, T.M., and Hildebrand, J.A. (2013). Species-specific beaked whale echolocation signals. *The Journal of the Acoustical Society of America* 134(3). doi:10.1121/1/4817832

Baumann-Pickering, S., Roch, M.A., Brownell, R.L., Simonis, A.E., McDonald, M.A., Solsona-Berga, A., Oleson, E.M., Wiggins, S.M., and Hildebrand, J.A. (2014). Spatio-Temporal Patterns of Beaked Whale Echolocation Signals in the North Pacific. *PLoS ONE* 9(1).

Baumgartner, M.F., Fratantoni, D.M., Hurst, T.P., Brown, M.W., Cole, T. VSN., van Parijs, S.M., and Johnson, M. (2013). Real-time reporting of baleen whale passive acoustic detections from ocean gliders. *The Journal of the Acoustical Society of America* 134, 1814–1823. doi: 10.1121/1.4816406

Beale, C.M. (2007). The behavioral ecology of disturbance responses. *International Journal of Comparative* Psychology 20, 111-120.

Benoit-Bird, K.J., Battaile, B.C., Heppell, S.A., Hoover, B., Irons, D., Jones, N., Kuletz, K.J., Nordstrom, C.A., Paredes, R., Suryan, R.M., Waluk, C.M., and Trites, A.W. (2013). Prey patch patterns predict habitat use by top marine predators with diverse foraging strategies. *PLoS ONE* 8(1). doi:10.1371/journal.pone.0053348

Benoit-Bird, K.J., Southall, B.L., and Moline, M.A. (2016). Predator-guided sampling reveals biotic structure in the bathypelagic. *Proceedings of the Royal Society B* 283, 20152457. doi: 10.1098/rspb.2015.2457

Benoit-Bird, K.J., Southall, B.L., Moline, M.A., Claridge, D.E., Dunn, C.A., Dolan, K.A., and Moretti, D.J. (2020). Critical threshold identified in the functional relationship between beaked whales and their prey. *Marine Ecology Progress Series* 654, 1-16. doi:10.3354/meps13521

Bertucci, F., Parmentier, E., Berten, L., Brooker, R.M., and Lecchini, D. (2015). Temporal and Spatial Comparisons of Underwater Sound Signatures of Different Reef Habitats in Moorea Island, French Polynesia. *PLoS ONE* 10(9), e0135733. doi.org/10.1371/journal.pone.0135733

Bograd, S.J., Block, B.A., Costa, D.P., and Godley, B.J. (2010). Biologging technologies: new tools for conservation. *Endangered Species Research* 10, 1-7. doi: 10.3354/esr00269

Boyd, I., Frisk, G., Urban, E., Tyack, P., Ausubel, J., Seeyave, S., Cato, D., Southall, B., Weise, M., Andrew, R., Akamatsu, T., Dekeling, R., Erbe, C., Farmer, D., Gentry, R., Gross, T., Hawkins, A., Li, F., Metcalf, K., Miller, J., Moretti, D., Rodrigo, C., and Shinke, T. (2015). An International Quiet Ocean Experiment. *Oceanography* 24(2), 174-181.

Blom, E.L., Kvarnemo, C., Dekhla, I., Schold, S., Andersson, M.H., Svensson, O., Clara, M., and Amorim, P. (2019). Continuous but not intermittent noise has a negative impact on mating success in a marine fish with paternal care. *Nature Scientific Reports* 9, 5494. doi:10.1038/s41598-019-41786-x

Bowen, W.D., Tully, D., Boness, D.J., Bulheier, B.M., and Marshall, G.J. (2002). Prey-dependent foraging tactics and prey profitability in a marine mammal. *Marine Ecology Progress Series* 244, 235-245. doi:10.3354/meps244235

Bradbury, J. and S. Vehrencamp. (1998). *Principles of Animal Communication.* Sinauer Associates, Inc. Sunderland, MA.

Busch-Vishniac, I., and Ryherd, E. (2019). Hospital Soundscapes: Characterization, Impacts, and Interventions. *Acoustics Today* 15(3). doi: 10.1121/AT.2019.15.3.11

Carstensen, J., Henriksen, O.D., and Teilmann, J. (2006). Impacts of offshore wind farm construction on harbor porpoises: acoustic monitoring of echo-location activity using porpoise detectors (T-PODs). *Marine Ecology Progress Series* 321, 295-308.

Caruso, F., Dong, L., Lin, M., Liu, M., Xu, W., and Li, S. (2020). Influence of acoustic habitat variation on Indo-Pacific humpback dolphin (*Sousa chinensis)* in shallow water of Hainan Island, China. *The Journal of the Acoustical Society of America* 147(6), 3871-3882.

Caruso, F., Dong, L., Lin, M., Liu, M., Gong, Z., Xu, W., Alonge, G., and Li, S. (2020). Monitoring of a nearshore small dolphin species using passive acoustic platforms and supervised machine learning techniques. *Frontiers in Marine Science* 7(267). doi: 10.3389/fmars.2020.00267

Castro, J.J., Santiago, J.A., and Santana-Ortega, A.T. (2002). A general theory on fish aggregation to floating objects: An alternative to the meeting point hypothesis. *Reviews in Fish Biology and Fisheries* 11, 255-277. doi: 10.1023/A:1020302414472

Chapman, N.R., and A. Price. (2011). Low frequency deep ocean ambient noise trend in the Northeast Pacific Ocean. *The Journal of the Acoustical Society of America* 129, EL 161.

Chiocci, F.L., Cattaneo, A., and Urgeles, R. (2011). Seafloor mapping for geohazard assessment: state of the art. *Marine Geophysical Research* 32, 1-1. doi: 10.1007/s11001-011-9139-8

Cholewiak, D., DeAngelis, A., Palka, D., Corkeron, P., Van Parijs, S. (2017). Beaked whales demonstrate a marked acoustic response to the use of shipboard echosounders. *Royal Society Open Science* 4, 170940. doi: 10.1098/rsos.170940

Claridge, D.E. (2013). Population ecology of Blainville's beaked whales (*Mesoplodon densirostris*). PhD Thesis. University of St. Andrews. http://hdl.handle.net/10023/3741

Codarin, A., and Picciulin, M. (2015). Underwater noise assessment in the Gulf of Trieste (Northern Adriatic Sea, Italy) using an MSFD approach. *Marine Pollution Bulletin* 101(2), 694-700. doi: 10.1016/j.marpolbul.2015.10.028

Cook, M.L.H., Varela, R.A., Goldstein, J.D., McCulloch, S.D., Bossart, G.D., Finneran, J.J., Houser, D., and Mann, D.A. (2006). Beaked whale auditory evoked potential hearing measurements. *Journal of Comparative Physiology A* 192, 489-495.

Costa, D.P. (1993). The Secret Life of Marine Mammals Novel Tools for Studying Their Behavior and Biology at Sea. *Oceanography* 6(3), 120-128.

Cox, S.L., Embling, C.B., Hosegood, P.J., Votier, S.C., and Ingram, S.N. (2018). Oceanographic drivers of marine mammal and seabird habitat-use across shelf-seas: a guide to key features and recommendations for future research and conservation management. *Estuarine, Coastal and Shelf Science*. 212, 294-310. doi: 10.1016/j.ecss.2018.06.022

Crocker, S.E., Fratantonio, F.D., Hart, P.E., Foster, D.S., O'Brien, T.S., and Labak, S. (2019). Measurement of Sounds Emitted by Certain High-Resolution Geophysical Survey Systems. *Journal of Oceanic Engineering* doi: 10.1109/JOE/2018/2829958

Croll, D.A., Clark, C.W., Calambokidis, J., Ellison, W.T., and Tershy, B.R. (2006). Effect of anthropogenic low-frequency noise on the foraging ecology of *Balaenoptera* whales. *Animal Conservation* 4(1), 13-27. doi: 10.1017/S1367943001001020

Davis, R.W., Fuiman, L.A., Williams, T.M., Collier, S.O., Hagey, W.P., Kanatous, S.B., Kohin, S., and Horning, M. (1999). Hunting Behavior of a Marine Mammal Beneath the Antarctic Fast Ice. *Science* 283(5404), 993-996. doi: 10.1126/science.283.5404.993

Department of the Interior. (2003). Endangered Species Act of 1973. As Amended through the 108th Congress.

Department of the Navy. (2012). Final Supplemental Environmental Impact Statement/Supplemental Overseas Environmental Impact Statement for Surveillance Towed Array Sensor System Low Frequency Active (SURTASS LFA) Sonar. Department of the Navy, Chief of Naval Operations.

D'Amico, A., and Pittenger, R. (2009). A Brief History of Active Sonar. *Aquatic Mammals* 35(4), 426-434.

D'Amico, A., Gisiner, R.C., Ketten, D.R., Hammock, J.A., Johnson, C., Tyack, P.L., and Mead, J. (2009). Beaked whale strandings and naval exercises. *Aquatic Mammals* 35(4), 452-472.

Deng, Z.D., Southall, B.L., Carlson, T.J., Xu, J., Martinez, J.J., Weiland, M.A., Ingraham, J.M. (2014). 200 kHz Commercial Sonar Systems Generate Lower Frequency Side Lobes Audible to Some Marine Mammals. *PLoS ONE* 9(4), e95315.

DeRuiter, S.L. (2010). "Marine Animal Acoustics", in *An Introduction to Underwater Acoustics: Principles and Applications,* X. Lurton, Editor. Praxis Publish-ing Limited: Chichester, UK. p. 425-474.

DeRuiter, S.L., Southall, B.L., Calambokidis, J., Zimmer, W.M.X., Sadykova, D., Falcone, E.A., Friedlaender, A.S., Joseph, J.E., Moretti, D., Schorr, G.S., Thomas, L., and Tyack, P.L. (2013).

First direct measurements of behavioral responses by Cuvier's beaked whales to mid-frequency active sonar. *Biology Letters* 9. doi: 10.1098/rsbl.2013.0223

DiMarzio, N., and Jarvis, S. (2016). Temporal and Spatial Distribution and Habitat Use of Cuvier's Beaked Whales on the U.S. Navy's Southern California Antisubmarine Warfare Range (SOAR): Data Preparation. Naval Undersea Warfare Center. Newport, Rhode Island.

DiMarzio, N., Jones, B., Moretti, D., Thomas, L., and Oedekoven, C. (2018). Marine Mammal Monitoring on Navy Ranges (M3R) on the Southern California Offshore Range (SOAR) and the Pacific Missile Range Facility (PMRF)- 2017. Naval Undersea Warfare Center, Newport R.I.

DiMarzio, N., Watwood, S., Fetherston, T., and Moretti, D. (2019). Marine mammal monitoring on navy ranges (M3R) on the Southern California Anti-Submarine Warfare Range (SOAR) and the Pacific Missile Range Facility (PMRF) 2018. Naval Undersea Warfare Center Newport, Newport, R.I.

Embling, C.B., Illian, J., Armstrong, E., van der Kooij, J., Sharples, J., Camphuysen, K.C.J., and Scott, B.E. (2012). Investigating fine-scale spatio-temporal predator-prey patterns in dynamic marine ecosystems: a functional data analysis approach. *Journal of Applied Ecology* 49(2), 481-492. doi: 10.1111/j.1365-2664.2012.02114.x

Erbe, C., and Farmer, D.M. (2000). Zones of impact around icebreakers affecting beluga whales in the Beaufort Sea. *The Journal of the Acoustical Society of America* 108(3), 1332-1340. doi:10.1121/1.1288938

Erbe, C. (2012). "Effects of underwater noise on marine mammals." in *The Effects of Noise on Aquatic Life II* Advances in Experimental Medicine and Biology, eds. A.N. Popper and A. Hawkins (New York, NY: Springer), 730, 17-22. doi: 10.1007/978-1-4419-7311-5_3.

Erbe, C., Reichmuth, C., Cunningham, K., Lucke, K., Dooling, R. (2015). Communication masking in marine mammals: A review and research strategy. *Marine Pollution Bulletin.*

Erbe, C., McCauley, R., Gavrilov, A., Madhusudhana, S., and Verma, A. The underwater soundscape around Australia. Proceedings of Acoustics 2016. Brisbane, Australia, 9-11 November 2016.

Erbe, C., McCauley, R., Gavrilovs, A. (2016). "Characterizing Marine Soundscapes." In: *The Effects of Noise on Aquatic Life II*. Advances in Experimental Medicine and Biology, eds. A.N. Popper and A. Hawkins (New York, NY: Springer), 730, 17-22. doi: 10.1007/978-1-4419-7311-5_3.

Erbe, C., Dunlop, R., and Dolman, S. (2018). "Effects of Noise on Marine Mammals." In: *Effects of Anthropogenic Noise on Animals*. Springer Handbook of Auditory Research. eds. H. Slabbekoorn, R. Dooling, A. Popper, and R. Fay (New York, NY: Springer), 66, 277-309. doi: 10.1007/978-1-4939-8574-6_10

Evans, D., and England, G. (2001). Joint interim report Bahamas marine mammal stranding event of 15-16 March 2000, Washington, DC: U.S. Department of Commerce and Secretary of the Navy.

Falcone, E.A., Schorr, G.S., Douglas, A.B., Calambokidis, J., Henderson, E., McKenna, M.F., Hildebrand, J., and Moretti, D. (2009). Sighting characteristics and photo-identification of Cuvier's beaked whales (*Ziphius cavirostris*) near San Clemente Island, California: a key area for beaked whales and the military? *Marine Biology* 156(12), 2631-2640. doi: 10.1007/s00227-009-1289-8

Falcone, E.A., Schorr, G.S., Watwood, S.L., DeRuiter, S.L., Zerbini, A.N., Andrews, R.D., Morrissey, R.P., and Moretti, D.J. (2017). Diving behaviour of Cuvier's beaked whales exposed to two types of military sonar. *Royal Society Open Science* 4, 170629. http://dx.doi.org/10.1098/rsos.170629

Faul, F., Erdfelder, E., Lang, A.-G., and Buchner, A. (2007). G*Power3: A flexible statistical power analysis program for the social, behavioral, and biomedical sciences. *Behavior Research Methods* 30(2), 175-191.

Fedak, M., Lovell, P., McConnell, B., and Hunter, C. (2002). Overcoming the constraints of long range radio telemetry from animals: getting more useful data from smaller packages. *Integrative and Comparative Biology* 42, 3-10.

Fernandez, A., Sierra, E., Martin, VS, Mendez, M., Sacchinnin, S., Bernaldo de Quiros, Y., Andrada, M., Rivero, M., Quesada, O., Tejedor, M., and Arbelo, M. (2012). Last "atypical" beaked whales mass stranding in the Canary Islands (July, 2004). *Journal of Marine Science: Research and Development* 2(2), 107. doi:10.4172/2155-9910.1000107

Fewtrell, J.L., and McCauley, R.D. (2012). Impact of air gun noise on the behavior of marine fish and squid. *Marine Pollution Bulletin* 64, 984-993. doi:10.1016/j.marpolbul.2012.02.009

Filadelfo, R., Mintz, J., Michlovich, E., D'Amico, A., Tyack, P.L. and Ketten, D.R. (2009). Correlating Military Sonar Use with Beaked Whale Mass Strandings: What Do the Historical Data Show? *Aquatic Mammals* 35(4), 435-444.

Finneran, J.J., Houser, D.S., Mase-Guthrie, B., Wing, R.Y., and Lingenfelser, R.G. (2009). Auditory evoked potentials in a stranded Gervais' beaked whale *(Mesoplodon europeaus)*. *The Journal of the Acoustical Society of America* 126, 484-490.

Fitzmaurice, M. (2017). International Convention for the Regulation of Whaling. United Nations Audiovisual Library of International Law.

Fleishman, E., Costa, D., Harwood, J., Kraus, S., Moretti, D., New, L.F., Schick, R.S., Schwarz, L.K., Simmons, S.E., Thomas, L., and Wells, R.S. (2016). Monitoring population-level responses of marine mammals to human activities. *Marine Mammal Science* 32(3), 1004-1021. doi: 10.1111/mms.12310

Francois, R.E., and Garrison, G.R. (1982). Sound absorption based on ocean measurements. Part II: Boric acid contribution and equation for total absorption. *The Journal of the Acoustical Society of America* 72. doi: 10.1121/1.388673.

Frantzis, A. (1998). Does acoustic testing strand whales? *Nature* 392(5), 29.

Frantzis, A., Goold, J. C., Skarsoulis, E. K., Taroudakis, M. I., and Kandia, V.S. (2002). Clicks from Cuvier's beaked whales, *Ziphius cavirostris* (L). *The Journal of the Acoustical Society of America* 112(1), 34-37.

Frouin-Mouy, H., Tenoirio-Halle, L., Thode, A., Swartz, S., and Urban, J. (2020). Using two drones to simultaneously monitor visual and acoustic behavior of gray whales (*Eschrichtius robustus*) in Baja California, Mexico. *Journal of Experimental Marine Biology and Ecology* 525. doi: 10.1016/j.jembe.2020.151321.

Gallagher, C.A., Grimm, V.S., Kyhn, L.A., Kinze, C.C., and Nabe-Nielsen, J. (2021). Movement and Seasonal Energetics Mediate Vulnerability to Disturbance in Marine Mammal Populations. *The American Naturalist* 197(3). doi: 10.1086/712798

Gassmann, M., Henderson, E. E., Wiggins, S.M., Roch, M.A., and Hildebrand, J.A. (2013). Offshore killer whale tracking using multiple hydrophone arrays. *The Journal of the Acoustical Society of America* 134, 3513. doi: 10.1121/1.4824162.

Gassmann, M., Wiggins, S.M., and Hildebrand, J.A. (2015). Three-dimensional tracking of Cuvier's beaked whales' echolocation sounds using nested hydrophone arrays. *The Journal of the Acoustical Society of America* 138, 2483.

Gassmann, M., Wiggins, S.M., and Hildebrand, J.A. (2017). Deep-water measurements of container ship radiated noise signatures and directionality. *The Journal of the Acoustical Society of America* 142(3), 1563-1574. doi: 10.1121/1.5001063.

Getis, A., and Ord, J.K. (1992). The analysis of spatial association by use of distance statistics. *Geographical Analysis* 24(3), 189-206.

Geyer, F., Sagen, H., Hope, G., Babiker, M. and Worcester, P.F. (2016). Identification and quantification of soundscape components in the Marginal Ice Zone. *The Journal of the Acoustical Society of America* 139, 1873-1884.

Giorli, G., and Goetz, K.T. (2019). Foraging activity of sperm whales (*Physeter microcephalus*) off the east coast of New Zealand. *Scientific Reports* 9, 12182.

Giraudet, P., and Glotin, H. (2006). Real-time 3D tracking of whales by echo-robust precise TDOA estimates with a widely-spaced hydrophone array. *Applied Acoustics* 67(11-12), 1106-1117.

Gomez, C., Lawson, J.W., Wright, A.J., Buren, A.D., Tollit, D., and Lesage, V.S. (2016). A systematic review on the behavioural responses of wild marine mammals to noise: the disparity between science and policy. *Canadian Journal of Zoology* 94, 801-819.

Goodchild, M. F. (1986). Spatial Autocorrelation (Concepts and techniques in modern geography). Ontario: Geo Books, 13-28.

Gotz, T., and Janik, V.S.M. (2010). Aversiveness of sounds in phocid seals: psycho-physiological factors, learning processes and motivation. *The Journal of Experimental Biology* 213, 1536-1548. doi: 10.1242/jeb.035535

Greenland, S., Senn, S.J., Rothman, K.J., Carlin, J.B., Poole, C., Goodman, S.N., and Altman, D.G. (2016). Statistical tests, P values, confidence intervals, and power: a guide to misinterpretations. *European Journal of Epidemiology* 31, 337-350. doi: 10.1007/s10654-016-0149-3.

Hammond P.S. (2002). "Assessment of Marine Mammal Population Size and Status." In: *Marine Mammals* eds. Evans P.G.H., and Raga J.A. (Springer, Boston, MA). doi: 10.1007/978-1-4615-0529-7_7

Harris, C.M. and Thomas, L. (2015). Status and future of research on the behavioral responses of marine mammals to U.S. Navy sonar. CREEM Technical Report 2015-3, University of St. Andrews.

Harris, S.A., Shears, N.T., and Radford, C.A. (2015). Ecoacoustic indices as proxies for biodiversity on temperate reefs. *Methods in Ecology and Evolution* 7(6), 713-724. doi: 10.1111/2041-210X.12527

Harris, C. M., Thomas, L. Falcone, E.A., Hildebrand, J. Houser, J., Kvadsheim, P.H., Lam, F.P.A., Miller, P.O., Moretti, D.J., Read, A., Slabbekoorn, H., Southall, B.L., Tyack, P.L., Wartzok, D., and Janik, V.S.M. (2017). Marine mammals and sonar: Dose-response studies, the risk-disturbance hypothesis and the role of exposure context. *Journal of Applied Ecology*. 55(1), 396-404. doi: 10.1111/1365-2664.12955

Hart, K.M., and Hyrenbach, K.D. (2009). Satellite telemetry of marine megavertebrates: the coming of age of an experimental science. *Endangered Species Research* 10, 9-20. doi: 10.3354/esr00238

Hastie, G., Donovan, C., Gotz, T. and Janik, V.S. (2014). Behavioral responses by grey seals (*Halichoerus grypus*) to high frequency sonar. *Marine Pollution Bulletin* 79, 205-210.

Hatch, L., Clark, C., Merrick, R., Van Parijs, S., Ponirakis, D., Schwehr, K., Thompson, M., and Wiley, D. (2008). Characterizing the Relative Contributions of Large Vessels to Total Ocean Noise Fields: A Case Study Using the Gerry E. Studds Stellwagen Bank National Marine Sanctuary. *Environmental Management* 42: 735-752.

Haver, S.M., Fournet, M.E.H., Dziak, R.P., Gabriele, C., Gedamke, J., Hatch, L.T., Haxel, J., Heppell, S.A., McKenna, M.F., Mellinger, D.K., and Van Parijs, S.M. (2019). Comparing the Underwater Soundscapes of Four U.S. National Parks and Marine Sanctuaries. *Frontiers in Marine Science* doi: 10.3389/fmars.2019.00500

Hawkins, E.R., Harcourt, R., Bejder, L., Brooks, L.O., Grech, A., Christiansen, F., Marsh, H., and Harrison, P.L. (2017). Best Practice Framework and Principles for Monitoring the Effect of Coastal Development on Marine Mammals. *Frontiers in Marine Science* doi: 10.3389/fmars.2017.00059

Henderson, E.E., Smith, M.H., Gassman, M., Wiggins, S.M., Douglas, A.B., and Hildebrand, J.A. (2014). Delphinid behavioral responses to incidental mid-frequency active sonar. *The Journal of the Acoustical Society of America* 136(4).

Henderson, E.E., Martin, S.W., Manzano-Roth, R., and Matsuyama, B.M. (2016). Occurrence and habitat use of foraging Blainville's beaked whales (*Mesoplodon densirostris*) on a U.S. Navy Range in Hawaii. *Aquatic Mammals* 42(4), 549-562. doi: 10.1578/AM/42/4/2016.549

Henderson, E.E., Aschettino, J., Deakos, M., Alongi, G., and T. Leota. (2019). Blainville's beaked whales reduced foraging dives prior to the onset of hull-mounted MFAS sonar during Navy training events. Conference presentation. 5th International Conference on Effects of Aquatic Noise on Marine Life, Den Haag, Netherlands.

Hermannsen, L., Tougaard, J., Beedholm, K., Nabe-Nielsen, J., Tgelberg, P. Madsen, P. (2015). Characteristics and Propagation of Airgun Pulses in Shallow Water with Implications for Effects on Small Marine Mammals. *PLoS ONE* 10(7), e0133436.

Hertz, O., and F. Kapel. (1986). Commercial and Subsistence Hunting of Marine Mammals. *AMBIO* 15(3), 144-151.

Hildebrand, J. (2005). "Impacts of Anthropogenic Sound." In: *Marine Mammal Research: Conservation Beyond Crisis*, eds. J.E. Reynolds II, W.F. Perrin, R.R. Reeves, S. Montgomery, T. and J. Ragen. (Baltimore, MD: The Johns Hopkins University Press), 101-124.

Hildebrand, J.A. (2009). Anthropogenic and natural sources of ambient noise in the ocean. *Marine Ecology Progress Series* 395, 5-20. Doi: 10.3354/meps08353

Hohn, A.A., D.S. Rotstein, C.A. Harms, B.L. Southall. 2006. Report on Marine Mammal Unusual Mortality Even UMESE0501Sp: Multispecies Mass Stranding of Pilot Whales (*Globicephala macrorhynchus*), Minke Whale (*Balaenoptera acutorostrata*), and Dwarf Sperm Whales (*Kogia sima*) in North Carolina on 15-16 January 2005. *NOAA Technical Memorandum* NMFS-SEFSC-537, 222.

Houser, D.S. (2004). A Method for Modeling Marine Mammal Movement and Behavior for Environmental Impact Assessment. *IEEE Journal of Oceanic Engineering* 31(1), 76-81.

Houser, D.S., Martin, S.W., Finneran, J.J. (2013). Behavioral responses of California sea lions to mid-frequency (3250-2450 Hz) sonar signals. *Marine Environmental Research* 92, 268-278.

Houser, D.S., Yost, W., Burkard, R., Finneran, J.J., Reichmuth, C. and Mulsow, J. (2017). A review of the history, development and application of auditory weighting functions in humans and marine mammals. *The Journal of the Acoustical Society of America* 141(3), 1271-1413.

International Convention for the Regulation of Whaling. 1946.

ISO 18405:2017. Underwater acoustics — Terminology, International Organization for Standardization (ISO), Geneva, Switzerland, April 2017. Available from http://www.iso.org/iso/catalogue_detail.htm?csnumber=62406.

Isojunno, S., Cure, C., Kvadsheim, P.H., Lam, F.P.A., Tyack, P.L., Wensveen, P.J., Miller, P.J.O. (2016). Sperm whales reduce foraging effort during exposure to 1-2 kHz sonar and killer whale sounds. *Ecological Applications* 26(1).

Jacobson, E.K., Henderson, E.E., Oedekoven, C.S., Miller, D.L., Watwood, S.L., Moretti, D.J, and Thomas, L. (2019). Quantifying the response of Blainville's beaked whales to Naval sonar exercises in Hawaii. Conference presentation. World Marine Mammal Conference, Barcelona, Spain.

Jarvis, S.M., Morrissey, R.P., Moretti, D.J., DiMarzio, N.A., and Shaffer, J.A. (2014). Marine mammal monitoring on Navy ranges (M3R): a toolset for automated detection, localization, and monitoring of marine mammals in open ocean environments. *Marine Technology Society Journal* 48(1), 5-20.

Johnson, C. S. (1991). Hearing thresholds for periodic 60-kHz tone pulses in the beluga whale. *The Journal of the Acoustical Society of America* 89(6), 2996-3001.

Johnson, C.E. (2012). "Regulatory Assessments of the Effects of Noise: Moving From Threshold Shift and Injury to Behavior." In: *The Effects of Noise on Aquatic Life*, eds. A.N. Popper, A. Hawkins (New York, NY: Springer), 563-565.

Johnson, M., Madsen, P.T., Zimmer, W.M.X., Aguilar de Soto, N., and Tyack, P.L. (2004). Beaked whales echolocate on prey. *Biology Letters*: S383-S386.

Johnson, M., Aguilar de Soto, N., and Madsen, P.T. (2009). Studying the behavior and sensory ecology of marine mammals using acoustic recording tags: a review. *Marine Ecology Progress Series* 395, 55-73. doi:10.3354/meps08255

Jones, N. (2019). The Quest for Quieter Seas. *Nature* 568, 158-161.

Jossart, J., Theuerkauf, S.J., Wickliffe, L.C., and Morris Jr., J.A. (2020). Applications of Spatial Autocorrelation Analyses for Marine Aquaculture Siting. *Frontiers in Marine Science* 6(806). doi: 10.3389/fmars.2019.00806

Joyce, T.W., Durban, J.W., Claridge, D.E., Dunn, C.A., Hickmott, L.S., Fearnback, H., Dolan, K., and Moretti, D. (2020). Behavioral responses of satellite tracked Blainville's beaked whales (*Mesoplodon densirostris)* to mid-frequency active sonar. *Marine Mammal Science* 36, 29-46. doi: 10.1111/mms.12624

Kastelein, R.A., Hoek, L., de Jong, C.A., and Wensveen, P.J. (2010a). The effect of signal duration on the underwater detection thresholds of a harbor porpoise (*Phocoena phocoena*) for single frequency-modulated tonal signals between 0.25 and 160 kHz. *The Journal of the Acoustical Society of America* 128(5), 3211-3222.

Kastelein, R.A., Hoek, L., Wensveen, P.J., Terhune, J.M., and de Jong, C.A. (2010b). The effect of signal duration on the underwater hearing thresholds of two harbor seals (*Phoca vitulina*) for

single tonal signals between 0.2 and 40 kHz. *The Journal of the Acoustical Society of America*, 127(2), 1135- 1145.

Kastelein, R.A., Helder-Hoek, L., Van de Voorde, S., von Benda-Bechmann, S., Lam, F.P.A., Jansen, E., de Jong, C.A.F., and Ainslie, M. (2017). Temporary hearing threshold shift in a harbor porpoise (*Phocoena phocoena)* after exposure to multiple airgun sounds. *The Journal of the Acoustical Society of America* 142(4), 2430-2442. doi: 10.1121/1/5007720

Kates Varghese, H., Smith, M.J., Miksis-Olds, J.L., and Mayer, L. (2019a). Regulation Consideration of Ocean Mapping Multibeam Echo Sounders: A Square Peg in a Round Hole. *Journal of Ocean Technology* 14(3), 40-46.

Kates Varghese, H., Smith M.J., Miksis-Olds, J.L., and Mayer, L. (2019b). The contribution of 12 kHz multibeam sonar to a southern California marine soundscape. *The Journal of the Acoustical Society of America* 145, 1671. doi: 10.1121/1.5101132

Kates Varghese, H., Miksis-Olds, J., DiMarzio, N., Lowell, K., Linder, E., and Mayer, L. (2020) The effect of two 12 kHz multibeam mapping surveys on the foraging behavior of Cuvier's beaked whales off of southern California. *The Journal of the Acoustical Society of America* 147(6), 3849-3858. Doi:10.1121/10.0001385.

Kates Varghese, H., Lowell K. and Miksis-Olds J. (2021a). Global-Local-Comparison Approach: Understanding Marine Mammal Spatial Behavior by Applying Spatial Statistics and Hypothesis Testing to Passive Acoustic Data. *Frontiers in Marine Science* 8, 625322. doi: 10.3389/fmars.2021.625322

Kates Varghese, H., Lowell, K., Miksis-Olds, J., DiMarzio, N., Moretti, D., and Mayer, L. (2021b). Spatial Analysis of Beaked Whale Foraging During Two 12 kHz Multibeam Echosounder Surveys. *Frontiers in Marine Science* 8, 654184. doi: 10.3389/fmars.2021.654184

Kellar, N.M., Catelani, K.N., Robbins, M.N., Trego, M.L., Allen, C.D., Danil, K., Chivers, S.J. (2015). Blubber Cortisol: A Potential Tool for Assessing Stress Response in Free-Ranging Dolphins without Effects due to Sampling. *PLOS One* 10(2).

Ketten, D.R. (1998). Marine Mammal Auditory Systems: A Summary of audiometric and anatomical data and its implications for underwater acoustic impacts. NOAA-TM-NMFS-SWFSC-256.

Ketten, D.R. (2014). Sonars and Strandings: Are Beaked Whales the Aquatic Acoustic Canary? *Acoustics Today* 10(3), 45-55.

Kowarski, K., Gaudet, B.J., Cole, AJ., Maxner, E.E., Turner, S.P., Martin, S.B., Johnson, H.D., and Moloney, J.E. (2020). Near real-time marine mammal monitoring from gliders: practical challenges, system development, and management implications. *The Journal of the Acoustical Society of America* 148, 1215. doi: 10.1121/10.0001811

Krause, B. (2008). Anatomy of the Soundscape: Evolving Perspectives. *Journal of the Audio Engineering Society* 56(1-2), 73-80.

Kruskal, W.H., and Wallis, W.A. (1952). Use of Ranks in One-Criterion Variance Analysis. *Journal of the American Statistical Association* 47(260), 583-621. doi: 10.1080/01621459.1952.10483441

Landeo-Yauri, S.S., Ramos, E.A., Castelblanco-Martínez, D.N., Niño-Torres, C.A., and Searle, L. (2020). Using small drones to photo-identify Antillean manatees: a novel method for monitoring an endangered marine mammal in the Caribbean Sea. *Endangered Species Research* 41, 79-90. https://doi.org/10.3354/esr01007

Li, W., Osher, S., and Gangbo, W. (2016). A fast algorithm for Earth Mover's Distance based on optimal transport and L1 type Regularization. Retrieved from: https://arxivsorg/pdf/1609.07092.pdf.

Lillis, A., Eggleston, D.B., and Bohnenstiehl, D.R. (2014). Estuarine soundscapes: Distinct acoustic characteristics of oyster reefs compared to soft-bottom habitats. *Marine Ecology Progress Series* 505, 1-17.

Lin, T., and Tsao, Y. (2018). Listening to the Deep: Exploring Marine Soundscape Variability by Information Retrieval Techniques, *2018 OCEANS - MTS/IEEE Kobe Techno-Oceans (OTO)*, Kobe. doi: 10.1109/OCEANSKOBE.2018.8559307

Lindseth, A.V.S., and Lobel, P.S. (2018). Underwater Soundscape Monitoring and Fish Bioacoustics: A Review. *Fishes* 3(36). doi: 10.3390/fishes3030036.

Lucke, K. (2008). Auditory studies on marine mammals. Christian-Albrechts-University Kiel, PhD Dissertation. Accessed from: https://d-nb.info/1019811455/34 Last accessed: 10/28/2021.

Lurton, X. (2002). An Introduction to Underwater Acoustics: Principles and Applications. (Springer-Verlag, New York, NY).

Lurton, X. and DeRuiter, S. (2011). Sound radiation of seafloor-mapping echosounders in the water column, in relation to the risks posed to marine mammals. *International Hydrographic Review* 7-17.

Lurton, X. (2016). Modelling of the sound field radiated by multibeam echosounders for acoustical impact assessment. *Applied Acoustics* 101, 201-211.

Maclean, I.M.D., Inger, R., Benson, D., Booth, C.G., Embling, C.B., Grecian, W.J., Heymans, J.J., Plummer, K.E., Shackshaft, M., Sparling, C.E., Wilson, B., Wright, L.J., Bradbury, G., Christen, N., Godley, B.J., Jackson, A.C., McCluskie, A., Nicholls-Lee, R., and Bearhop, S. (2014). Resolving issues with environmental impact assessment of marine renewable energy installations. *Frontiers in Marine Science* doi: 10.3389/fmars.2014.00075

MacKenzie, M.L., Scott-Hayward, L.A.S., Paxton, C.G.M., and Burt, M.L. (2017). Quantifying the Power to Detect Change: methodological development and implementation using the R package MRSeaPower. In Quantifying the Power to Detect Change: methodological development and implementation using the R package MRSeaPower. (pp. 1). [CREEM-13804-2016-1. Provided to the Scottish Government and Marine Scotland Science (USA/012/15] The

Scottish Government.
http://www.govsscot/Topics/marine/marineenergy/Research/SB9/MRSeamethod.

MacLeod, C.D. and Zuur, A.F. (2005). Habitat utilization by Blainville's beaked whales off Great Abaco, northern Bahamas, in relation to seabed topography. *Marine Biology* 147, 1-11.

MacLeod, C.D., Perrin, W.F., Pitman, R., Barlow, J., Balance, L., D'Amico, A., Gerrodette, T., Joyce, G., Mullin, K.D., Palka, D.L., and Waring, G.T. (2006). Known and inferred distributions of beaked whale species (Cetacea: Ziphiidae). *Journal of Cetacean Research and Management* 7(3), 271-286.

Madsen, P.T. (2005). Marine mammals and noise: Problems with root mean square sound pressure levels for transients. *The Journal of the Acoustical Society of America* 117(6), 3952-3956.

Madsen, P.T., Johnson, M., Miller, P.J.O., Aguilar Soto, N., Lynch, J., and Tyack, P. (2006). Quantitative measures of air-gun pulses recorded on sperm whales (*Physeter microcephalus)* using acoustic tags during controlled exposure experiments. *The Journal of the Acoustical Society of America* 120, 2366-2379. doi: 10.1121/1.2229287

Madsen, P.T., Anguilar de Soto, N., Arranz, P. and Johnson, M. (2013). Echolocation in Blainville's beaked whales (*Mesoplodon densirostris)*. *Journal of Comparative Physiology A* 199, 451-469.

Malinka, C.E, Atkins, J., Johnson, M.P., Tonnesen, P., Dunn, C.A., Claridge, D.E., Aguilar de Soto, N., and Madsen, P.T. (2020). An autonomous hydrophone array to study the acoustic ecology of deep-water toothed whales. *Deep-Sea Research Part I* 158, 103233. doi: 10/1016/j.dsr.2020.103233

Malme, C.I., Miles, P.R., Clark, C.W., Tyack, P., and Bird, J.E. (1984). Investigations of the potential effects of underwater noise from petroleum-industry activities on migrating gray-whale behavior. Phase 2: January 1984 migration. U.S. Department of Energy Office of Scientific and Technical Information, Report Number: PB-86-218377/XAB; BBN-5586.

Mann, J. (1999). Behavioral sampling methods for cetaceans: a review and critique. *Marine Mammal Science*. 15(1), 102-122.

Manzano-Roth, R., Henderson, E., Martin, S., Martin, C., and Matsuyama, B. (2016). Impacts of U.S. Navy Training Events on Blainville's Beaked Whale (*Mesoplodon densirostris)* Foraging Dives in Hawaiian Waters. *Aquatic Mammals* 42(4), 507-528. doi: 10.1578/AM.42.4.2016.507

Marine Mammal Commission. (2015). The Marine Mammal Protection Act of 1972 As Amended. NOAA National Marine Fisheries Service.

Martin, S., Martin, C. R., Matsuyama, B. M., and Henderson, E. E. (2015). Minke whales (*Balaenoptera acutorostrata)* respond to navy training. *The Journal of the Acoustical Society of America* 137(5), 2533-2541.

Martin, S.B. (2019). One Minute at a time: advancing our ability to estimate effects of human sound on marine life. PhD Dissertation, Dalhousie University.

Martin, S.B., Morris, C., Broker, K., and O'Neill, C. (2019). Sound exposure level as a metric for analyzing and managing underwater soundscapes. *The Journal of the Acoustical Society of America* 146(135). doi: 10.1121/1.5113578

Masson, D.G. (2003). "Summary of Geophysical Techniques." In: *European Margin Sediment Dynamics.* eds. Mienert, J., and Weaver P. (Springer, Berlin, Heidelberg). doi: 10.1007/978-3-642-55846-7_2

Mate, B.R., Irvine, L.M., and Palacios D.M. (2016). The development of an intermediate-duration tag to characterize the diving behavior of large whales. *Ecology and Evolution* 7, 585-595. doi: 10.1002/ece3.2649

MathWorks. (R2021a). Generalized Pareto Distribution. Retrieved from: www.mathworks.com/help/stats/generalized-pareto-distribution.html (Last viewed: 9/4/2021).

Maxwell, S.M., Frank, J.J., Breed, G.A., Robinson, P.W., Simmons, S.E., Crocker, D.E., Gallo-Reynoso, J.P., and Costa, D.P. (2011). Benthic foraging on seamounts: A specialized foraging behavior in a deep-diving pinniped. *Marine Mammal Science* doi: 10.1111/j.1748-7692.2011.00527.x

Mayer, L.A. (2006). Frontiers in seafloor mapping and visualization. *Marine Geophysical Research* 27, 7-17. doi: 10.1007/s11001-05-0267-x

Mayer, L. (2017). Performance and Progress Report University of New Hampshire/National Oceanic and Atmospheric Administration Joint Hydrographic Center 2017. NOAA Grant No. NA15NOS4000200, Retrieved from: https://ccom.unh.edu/sites/default/files/progress_reports/2017-jhc-ccom-progress-report-web.pdf (Last viewed 12/23/2020).

Mayer, L. (2018). University of New Hampshire/National Oceanic and Atmospheric Administration Joint Hydrographic Center Performance and Progress Report 2018. NOAA Grant No. NA15NOS4000200, Retrieved from: https://ccom.unh.edu/sites/default/files/progress_reports/2018_jhc-ccom_full_annual_report_0.pdf (Last viewed 10/28/2021)

Mayer, L. (2019). University of New Hampshire/National Oceanic and Atmospheric Administration Joint Hydrographic Center 2019 Performance and Progress Report. NOAA Grant No. NA15NOS4000200, Retrieved from: https://ccom.unh.edu/sites/default/files/progress_reports/2019-jhc-ccom-full-annual-report.pdf (Last viewed 12/23/2020).

Mayer, L., Jakobsson, M., Allen, G., Dorschel, B., Falconer, R., Ferrini, VS, Lamarche, G., Snaith, H., and Weatherall, P. (2018). The Nippon Foundation-GEBCO Seabed 2030 Project: The Quest to See the World's Oceans Completely Mapped by 2030. *Geosciences* 8(63). Doi: 10/3390/geosciences8020063.

McCarthy, E., Moretti, D., Thomas, L., DiMarzio, N., Morrissey, R., Jarvis, S., Ward, J., Izzi, A. and Dilley, A. (2011). Changes in spatial and temporal distribution and vocal behavior of Blainville's beaked whales (*Mesoplodon densirostris*) during multiship exercises with mid-frequency sonar. *Marine Mammal Science* 27(3), E206-E226.

McDonald, M.A. (2006). Increases in deep ocean ambient noise in the Northeast Pacific west of San Nicolas Island, California. *The Journal of the Acoustical Society of America* 120, 711.

Mcintyre, T. (2014). Trends in tagging of marine mammals: a review of marine mammal biologging studies. *African Journal of Marine Science* 36(4), 409-422.

McKenna, M.F., Ross, D., Wiggins, S.M., and Hildebrand, J.A. (2011). Underwater radiated noise from modern commercial ships. *The Journal of the Acoustical Society of America* 131(1), 92-103. doi: 10.1121/1.3664100

McSweeney, D.J., Baird, R.W., Mahaffy, S.D. (2007). Site fidelity, associations, and movements of Cuvier's (*Ziphius cavirostris)* and Blainville's *(Mesoplodon densirostris)* beaked whales off the island of Hawai'i. *Marine Mammal Science* 23(3), 666-687.

Mead, J.G. (2009). Survey of Reproductive Data for the Beaked Whales (Ziphiidae). *Report of the International Whaling Commission,* Special Issue 6.

Merchant, N.D., Blondel, P., Dakin, D.T., and Dorocicz, J. (2012). Averaging underwater noise levels for environmental assessment of shipping. *The Journal of the Acoustical Society of America Express Letters*. doi: 10.1121.1.4754429

Merchant, N.D., Barton, T.R., Thompson, P.M., Pirotta, E., Dakin, D.T., and Dorocicz, J. (2013). Spectral probability density as a tool for ambient noise analysis. *The Journal of the Acoustical Society of America* 133, EL262-EL267.

Miksis-Olds, J.L., Bradley, D.L. and Niu, X.M. (2013). Decadal trends in Indian Ocean ambient sound. *The Journal of the Acoustical Society of America* 134(5).

Miksis-Olds, J.L., and Nichols, S.M. (2016). Is low frequency ocean sound increasing globally? *The Journal of the Acoustical Society of America* 139(1), 501-511. doi: 10.1121/1.4938237.

Mikkelsen, L., Hermannsen, L., Beedholm, K., Madsen, P.T., and Tougaard, J. (2017). Simulated seal scarer sounds scare porpoises, but not seals: species-specific responses to 12 kHz deterrence sounds. *Royal Society Open Science* 4, 170286. doi:10.1098/rsos.170286.

Miller, P.J., and Tyack, P.L. (1998). A small towed beamforming array to identify vocalizing resident killer whales (*Orcinus orca)* concurrent with focal behavioral observations. *Deep Sea Research Part II: Topical Studies in Oceanography* 45(7), 1389-1405.

Miller, P.J.O., Johnson, M.P., Madsen, P.T., Biassoni, N., Quero, M., and Tyack, P.L. (2008). Using at-sea experiments to study the effects of airguns on the foraging behavior of sperm

whales in the Gulf of Mexico. *Deep Sea Research Part I* 56, 1168-1181. doi: 10.1016/j.dsr.2009.02.008

Miller, P.J.O., Kvadsheim, P.H., Lam, F.P.A., Wensveen, P.J., Antunes, R., Alves, A.C., Visser, F., Kleivane, L., Tyack, P.L., and Sivle, L.D. (2012). The severity of behavioral changes observed during experimental exposures of Killer (*Orcinus orca*), Long-Finned Pilot (*Globicephala melas*), and Sperm (*Physeter microcephalus*) Whales to naval sonar. *Aquatic Mammals* 38(4), 362-401. doi: 10.1578/AM.38.4.2012.362

Miller, P. (2014). A Study to Interpret the Biological Significance of Behavior Associated with 3S Experimental Sonar Exposures. University of St. Andrews, UK.

Mitson, R.B. (1993). Underwater noise radiated by research vessels. *ICES Marine Science Symposium* 196, 147-152.

Moline, M.A., and Benoit-Bird, K. (2016). Sensor fusion and autonomy as a powerful combination for biological assessment in the marine environment. *Robotics* 5(1), 4.

Mooney, T.A., Hanlon, R.T., Christensen-Dalsgaard, J., Madsen, P.T., Ketten, D.R., and Nachtigall, P. (2010). Sound detection by the longfin squid (*Loligo pealeii*) studied with auditory evoked potentials: sensitivity to low-frequency particle motion and not pressure. *Journal of Experimental Biology* 213, 3748-3759. doi:10.1242/jeb.048348

Moran, P.A.P. (1948). The interpretation of statistical maps. *Journal of the Royal Statistical Society: Series B* 10(2), 243-251.

Moretti, D., Thomas, L., Marques, T., Harwood, J., Dilley, A., Neales, B., Shaffer, J., McCarthy, E., New, L., Jarvis, S., and Morrissey, R. (2014). A risk function for behavioral disruption of Blainville's beaked whales (*Mesoplodon densirostris*) from mid-frequency active sonar. *PLOS One* 9(1), e85064. doi:10.1371/journal.pone.0085064

Moretti, D., Morrissey, R., Jarvis, S., and Shaffer, J. (2016). "Findings from U.S. Navy Hydrophone Ranges." In: *Listening in the Ocean*, eds. W.W.L. Au, and M.O. Landers. (Springer, New York, NY), 239-256.

Moretti, D.J. (2019). Estimating the effect of mid-frequency active sonar on the population health of Blainville's beaked whale (*Mesoplodon densirostris*) in the Tongue of the Ocean. PhD Dissertation. University of St. Andrews. http://hdl.handle.net/10023/19250

Moulins, A., Rosso, M., Nani, B., and Wurtz, M. (2007). Aspects of the distribution of Cuvier's beaked whale (*Ziphius cavirostris*) in relation to topographic features in the Pelagos Sanctuary (north-western Mediterranean Sea). *Journal of the Marine Biological Association of the United Kingdom* 87, 177-186. doi: 10.1017/S0025315407055002

Natchigall, P.E., Mooney, T.A., Taylor, K.A., Yuen, M.M.L. (2007). Hearing and Auditory Evoked Potential Methods Applied to Odontocete Cetaceans. *Aquatic Mammals* 33(1), 6-13. doi: 10.1578/AM.33.1.2007.6

National Academies of Sciences, Engineering, and Medicine. (2017). *Approaches to Understanding the Cumulative Effects of Stressors on Marine Mammals*. (The National Academies Press, Washington, D. C.). https://doi.org/10.17226/23479.

National Marine Fisheries Service. (2016). Technical Guidance for Assessing the Effects of Anthropogenic Sound on Marine Mammal Hearing: Underwater Acoustic Thresholds for Onset of Permanent and Temporary Threshold Shifts. U.S. Dept. of Commerce, NOAA. NOAA Technical Memorandum NMFS-OPR-55, 178 p.

National Marine Fisheries Service. (2018). 2018 Revisions to: Technical Guidance for Assessing the Effects of Anthropogenic Sound on Marine Mammal Hearing (Version 2.0): Underwater Thresholds for Onset of Permanent and Temporary Threshold Shifts. U.S. Dept. of Commerce, NOAA. NOAA Technical Memorandum NMFS-OPR-59, 167 p.

National Research Council. (2005). Marine Mammal Populations and Ocean Noise: Determining When Noise Causes Biologically Significant Effects. (Washington, DC: The National Academies Press) doi:10.17226/11147

National Environmental Policy Act of 1969. § 102, 42 U.S.C. § 4332 (1994).

Nedelec, S.L., Campbell, J., Radford, A.N., Simpson, S.D., and Merchant, N.D. (2016). Particle motion: the missing link in underwater acoustic ecology. *Methods in Ecology and Evolution* 7, 836-842.

Nedwell, J.R., Edwards, B., Turnpenny, A.W.H., and Gordon, J. (2004). Fish and Marine Mammal Audiograms: A summary of available information. *Subacoustech Report* 534R0214.

New, L.F., Harwood, J., Thomas, L., Donovan, C., Clark, J.S., Hastie, G., Thompson, P.M., Cheney, B., Scott-Hayward, L., and Lusseau, D. (2013). Modelling the biological significance of behavioural change in coastal bottlenose dolphins in response to disturbance. *Functional Ecology* 27, 314-322. doi: 10.1111/1365-2435.12052

Nichols, S.M., and Bradley, D.L. (2019). Use of noise correlation matrices to interpret ocean ambient noise. *The Journal of the Acoustical Society of America* 145(4), 2337-2349. doi: 10.1121/1/5096846

Odland, J. (1988). "Spatial Autocorrelation." In: *Scientific Geography Series*, eds. G.I. Thrall (Beverly Hills, California: Sage Publications, Inc.), 9.

Ord, J.K., and Getis, A. (1995). Local Spatial Autocorrelation Statistics: Distributional Issues and an Application. *Geographical Analysis* 27(4), 286-306.

Pacini, A.F., Nachtigall, P.E., Quintos, C.T., Schofield, T.D., Look, D.A., Levine, G.A., Turner, J.P. (2011). Audiogram of a stranded Blainville's beaked whale (*Mesoplodon densirostris)* measured using auditory evoked potentials. *The Journal of Experimental Biology* 214, 2409-2415.

Parks, S.E., and Clark, C.W. (2007). Short- and long-term changes in right whale calling behavior: The potential effects of noise on acoustic communication. *The Journal of the Acoustical Society of America* 122(6), 3725-3731. doi: 10.1121/1.2799904

Parks, S.E., Miksis-Olds, J.L., and Denes, S.L. (2014). Assessing marine ecosystem acoustic diversity across ocean basins. *Ecological Informatics* 21, 81-88. doi:10.1016/j.ecoinf.2013.11.003

Piatt, J.F., and Methven, D.A. (1992). Threshold foraging behavior of baleen whales. *Marine Ecology Progress Series* 84, 205-210.

Pijanowski, B.C., Farina, A., Gage, S.H., Dumyahn, S.L., and Krause, B.L. (2011). What is soundscape ecology? An introduction and overview of an emerging new science. *Landscape Ecology* 26(9), 1213-1232.

Pirotta, E., Booth, C.G., Costa, D.P., Flesishman, E., Kraus, S.D., Lusseau, D., Moretti, D., New, L.F., Schick, R.S., Schwarz, L.K., Simmons, S.E., Thomas, L., Tyack, P.L., Weise, M.J., Wells, R.S., and Harwood, J. (2018). Understanding the population consequences of disturbance. *Ecology and Evolution* 8, 9934–9946. doi: 10.1002/ece3.4458

Piwetz, S., Gailey, G., Munger, L., Lammers, M.O., Jefferson, T.A., and Wursig, B. (2018). Theodolite Tracking in Marine Mammal Research: From Roger Payne to the Present. *Aquatic Mammals* 44(6). doi: 10.1578/AM.44.6.2018.683

Popper, A.N., Hawkins, A.D., and Thomsen, F. (2020). Taking the animals' perspective regarding anthropogenic underwater sound. *Trends in Ecology and Evolution*. 35(9), 787-794. doi:10.1016/j.tree.2020.05.002

Putland, R.L., Constantine, R., and Radford, C.A. (2017). Exploring spatial and temporal trends in the soundscape of an ecologically significant embayment. *Nature: Scientific Reports* 7, 5713. doi: 10.1038/s41598-017-06347-0

Putland, R.L., Merchant, N.D., Farcas, A., and Radford, C.A. (2017). Vessel noise cuts down communication space for vocalizing fish and marine mammals. *Global Change Biology*, 1-14.

Quetin, L.B., Ross, R.M., Frazer, T.K., and Haberman, K.L. (1996). Factors affecting distribution and abundance of zooplankton, with an emphasis on Antarctic krill, *Euphausia superba. Foundations for Ecological Research West of the Antarctic Peninsula Antarctic Research Series* 70, 357-371.

Quick, N., Scott-Hayward, L., Sadykova, D., Nowacek, D., and Read, A. (2017). Effects of a scientific echo sounder on the behavior of short finned pilot whales (*Globicephala macrorhynchus*). *Canadian Journal of Fisheries and Aquatic Sciences* 74(5), 716-726.

R Core Team. (2018). Version 3.5.1. R: A language and environment for statistical computing. (R Foundation for Statistical Computing, Vienna, Austria).

Redfern, J.V.S., McKenna, M.F., Moore, T.J., Calambokidis, J., Deangelis, M.L., Becker, E.A., Barlow, J., Forney, K.A., Fiedler, P.C., and Chivers, S.J. (2013). Assessing the Risk of Ships Striking Large Whales in Marine Spatial Planning. *Conservation Biology*. 27(2), 292-302. doi: 10.1111/cobi.12029

Rettig, S., Boebel, O., Menze, S., Kindermann, I., Thomisch, K., and van Opzeeland, I. (2013). Local to basin scale arrays for passive acoustic monitoring in the Atlantic sector of the Southern

Ocean. Conference presentation. Proceedings of the 1st International Conference and Exhibition on Underwater Acoustics, Corfu Island, Greece.

Richardson, W.J., Davis, R.A., Evans, C.R., Ljungblad, D.K., and Norton, P. (1987). Summer Distribution of Bowhead Whales, *Balaena mysticetes*, Relative to Oil Industry Activities in the Canadian Beaufort Sea, 1980-84. *Arctic* 40(2), 93-104.

Richardson, W.J., Green Jr., C.R., Malme, C.I., and Thomson, D.H. (1991). Effects of Noise on Marine Mammals. USDI/MMA/OCS study 90-0093, (Bryan, Texas: LGL Ecological Research Associates).

Richardson, W., J. Malme, C. Green, and D. Thomson. (1995). *Marine Mammals and Noise.* (Academic Press, San Diego, California).

Rolland, R.M., Parks, S.E., Hunt, K.E., Castellote, M., Corkeron, P.J., Nowacek, D.P., Wasser, S.K., and Kraus, S.D. (2017). Evidence that ship noise increases stress in right whales. *Proceedings of the Royal Society* 279.

Rubner, Y., Tomasi, C., and Guibas L.J. (2000). The Earth Mover's Distance as a Metric for Image Retrieval. *International Journal of Computer Vision* 40(2), 99-121.

Sahrhage, D., and Lundbeck, J. (1992). "Hunting of Marine Mammals." In: *A History of Fishing*. (Springer, Berlin, Heidelberg).

Sanchez-Gendriz, I., and Padovese, L.R. (2016). Underwater soundscape of marine protected areas in the south Brazilian coast. *Marine Pollution Bulletin* 105(1), 65-72. doi: 10.1016/j.marpolbul.2016.02.055

Santora, J.A., Schroeder, I.D., Field, J.C., Wells, B.K., and Sydeman, W.J. (2014). Spatio-temporal dynamics of ocean conditions and forage taxa reveal regional structuring of seabird-prey relationships. *Ecological Applications* 24(7), 1730-1747.

Santos, M.B., Pierce, G.J., Herman, J., Lopez, A., Guerra, A., Mente, E., and Clarke, M.R. (2001). Feeding ecology of Cuvier's beaked whale (*Ziphius cavirostris*): a review with new information on the diet of this species. *Journal of the Marine Biological Association of the United Kingdom* 81, 687-694. doi.org/10.1017/S0025315401004386

Schafer, R.M. (1969). *The New Soundscape.* Associated Music Publishers, Inc., New York.

Schefzik, R., Flesch, J., and Goncalves, A. (2021). Fast identification of differential distributions in single-cell RNA-sequencing data with waddR. *Bioinformatics* doi: 10.1093/bioinformatics/btab226

Schefzik, R. (2020). waddR: Statistical tests for detecting differential distributions based on the 2-Wasserstein distance. R package version 1.4.0. Last accessed: 12/12/2021 from https://github.com/goncalves-lab/waddR.git.

Schorr, G.S., Falcone, E.A., Moretti, D.J., and Andrews, R.D. (2014). First Long-Term Behavioral Records from Cuvier's Beaked Whales (*Ziphius cavirostris)* Reveal Record-Breaking Dives. *PLOS One* 9(3), e92633.

Schorr, G.S., Falcone, E.A., Rone, B.K., and Keene, E.L. (2019). Distribution and demographics of Cuvier's beaked whales and fin whales in the Southern California Bight. U.S. Navy's 2018 Annual Marine Species Monitoring Report for the Pacific.

Scott-Hayward, L., Oedekoven, C., Mackenzie, M., and Rexstad, E. (2013). MRSea Package (version 0.0.1): Statistical Modelling of Bird and Cetacean Distributions in Offshore Renewables Development Areas (Report No. CR/2012/05). Report by University of St Andrews. Report for Marine Scotland Science.

Scott-Hayward, L., Mackenzie, M., and Oedekoven, C. (2014). Modelling impact assessment in renewables development areas using the new R package. Proceedings: 2nd International Conference on Environment Interactions of Marine Renewable Energy Technologies (EIMR2014), 3 pp., 28 April-02 May 2014. Stornoway, Isle of Lewis, Outer Hebrides, Scotland.

Schuster, M., Fisher, M., Muller, M., and Wittekind, D. (2020). Modelling Cumulative Sound Exposure Around Hydroacoustic Sources. *Journal of Ocean Technology* 15(1), 44-66.

Shearer, J.M., Quick, N.J., Cioffi, W.R., Baird, R.W., Webster, D.L., Foley, H.J., Swaim, Z.T., Waples, D.M., Bell, J.T., and Read, A.J. (2019). Diving behavior of Cuvier's beaked whales (*Ziphius cavirostris*) off Cape Hatteras, North Carolina. *Royal Society Open Science* 6, 181728. doi: 10.1098/rsos181728

Sims, D.W., Witt, M.J., Richardson, A.J., Southall, E.J., and Metcalf, J.D. (2006). Encounter success of free-ranging marine predator movements across a dynamic prey landscape. *Proceedings of the Royal Society B* 273, 1195-1201. doi:10.1098/rspb.2005.3444

Sirovic, A., and Hildebrand, J.A. (2016). Ocean ambient sound south of Bermuda and Panama Canal traffic. *The Journal of the Acoustical Society of America* 139, 2417.

Sivle, L.D., Kvadsheim, P.H., Cure, C., Isojunno, S., Wensveen, P.J., Lam, F.P.A., Visser, F., Kleivane, L., Tyack, P.L., Harris, C.M., and Miller, P.J.O. (2015). Severity of Expert-Identified Behavioural Responses of Humpback Whale, Minke Whale, and Northern Bottlenose Whale to Naval Sonar. *Aquatic Mammals* 41(4).

Smith, M.J. (2019). Analysis of the radiated sound field of a deep-water multibeam echo sounder using a navy hydrophone array. M.S. thesis, University of New Hampshire, https://unh.idm.oclc.org/login?url=https://search.proquest.com/docview/2273838102?accountid=14612.

Smith, M., Kates Varghese, H., Lurton, X., Mayer L.A., and Miksis-Olds, J. (2021). Exploring visualization techniques to enhance and inform soundscape analysis. Conference Presentation. *Acoustical Society of America* 149, A99. doi: 10.1121/10.0004635

Sorensen, P.M., Wisniewska, D.M., Jensen, F.H., Johnson, M., Teilmann, J., and Madsen, P.T. (2018). Click communication in wild harbor porpoises (*Phocoena phocoena)*. *Nature: Scientific Reports* 8, 9702.

Sousa-Lima, R., Fernandes, D.P., Norris, T., and Oswald, J. (2013). A review and inventory of fixed autonomous recorders for passive acoustic monitoring of marine mammals: 2013 state-of-the-industry. Conference presentation. 2013 IEEE/OES Acoustics in Underwater Geosciences Symposium, Rio de Janeiro, Brazil. doi: 10.1109/RIOAcoustics.2013.6683984

Southall, B., Bowles, A., Ellison, W., Finneran, J., Gentry, R., Greene Jr., C., Kastak, D., Ketten, D., Miller, J., Nachtigall, P., Richardson, W., Thomas, J., and Tyack, P. (2007). Marine Mammal Noise Exposure Criteria: Initial Scientific Recommendations. *Aquatic Mammals* 33(4).

Southall, B., Berkson, J., Bowen, D., Brake, R., Eckman, J., Field, J., Gisiner, R., Gregerson, S., Lang, W., Lewandoski, J., Wilson, J., and Winokur, R. (2009). Addressing the Effects of Human-Generated Sound on Marine Life: An Integrated Research Plan for U.S. federal agencies. Interagency Task Force on Anthropogenic Sound and the Marine Environment of the Joint Subcommittee on Ocean Science and Technology. Washington, DC.

Southall, B., Boyd, I., Tyack, P., and Wartzok, D. (2012). Deep-Diving Odontocetes Behavioral Response Study (BRS). *Bioacoustics* 17(1-3), 185-188. doi: 10.1080/09524622.2008.9753811

Southall, B.L., Rowles, T., Gulland, F., Baird, R.W., and Jepson, P.D. (2013). Final report of the Independent Scientific Review Panel investigating potential contributing factors to a 2008 mass stranding of melon-headed whales in Antsohihy, Madagascar. Retrieved from: https://www.cascadiaresearch.org/Hawaii/Madagascar_ISRP_Final_report.pdf (Last viewed 12/1/19).

Southall, B.L., Benoit-Bird, K.J., Moline, M.A., and Moretti, D. (2019). Quantifying deep-sea predator-prey dynamics: Implications of biological heterogeneity for beaked whale conservation. *Journal of Applied Ecology* 56, 1040-1049. doi: 10.1111/1365-2664.13334

Southall, B.L., Finneran, J.J., Reichmuth, C., Nachtigall, P.E., Ketten, D.R., Bowles, A.E., Ellison, W.T., Nowacek, D.P., and Tyack, P.L. (2019). Marine mammal noise exposure criteria: updated scientific recommendations for residual hearing effects. *Aquatic Mammals* 45(2), 125-230. doi: 10.1578/AM.45.2.2019.125

Southall, B.L., Nowacek, D.P., Bowles, A.E., Senigaglia, VS, Bejder, L., and Tyack P.L. (2021). Marine Mammal Noise Exposure Criteria: Assessing the Severity of Marine Mammal Behavioral Responses to Human Noise. *Aquatic Mammals* 47(5), 421-464. Doi: 10.1578/AM.47.5.2021.421

Tanha, K., Mohammadi, N., and Janani, L. (2017). P-value: What is and what is not. *Medical Journal of the Islamic Republic of Iran* 31(65). doi: 10.14196/mjiri.31.65

Thayer, J.A., and Sydeman, W.J. (2007). Spatio-temporal variability in prey harvest and reproductive ecology of a piscivorous seabird, *Cerorhinca monocerata,* in an upwelling system. *Marine Ecology Progress Series* 329, 253-265. doi: 10.3354/meps329253

The MathWorks, Inc. 2020. *Multiple Comparisons (R2020a).* Retrieved July 6, 2021 from https://www.mathworks.com/help/stats/multiple-comparisons.html?s_tid=srchtitle

Thompson, P.M., Brookes, K.L., Graham, I.M., Barton, T.R., Needham, K., Bradbury, G., and Merchant, N.D. (2013). Short-term disturbance by a commercial two-dimensional seismic survey does not lead to long-term displacement of harbor porpoises. *Proceedings of the Royal Society B* 280(1771), 20132001. doi: 10.1098/rspb.2013.2001

Tolimieri, N., Jeffs, A. and Montgomery, J.C. (2000). Ambient sound as a cue for navigation by the pelagic larvae of reef fishes. *Marine Ecology Progress Series.* 207, 219-224.

Torres, L.G., Nieukirk, S.L., Lemos, L., and Chandler, T.E. (2018). Drone Up! Quantifying Whale Behavior From a New Perspective Improves Observational Capacity. *Frontiers in Marine Science* doi: 10.3389/fmars.2018.00319.

Tougaard, J., Wright, A.J., and Madsen, P.T. (2015). Cetacean noise criteria revisted in the light of proposed exposure limits for harbor porpoises. *Marine Pollution Bulletin* 90(1-2), 196-208. doi:10.1016/j.marpolbul.2014.10.051

Tyack, P. (1986). Population biology, social behavior and communication in whales and dolphins. *Trends in Ecology and Evolution* 1(6), 144-150.

Tyack, P., Johnson, M., Aguilar Soto, N., Sturlese, A., and Madsen, P.T. (2006). Extreme diving of beaked whales. *Journal of Experimental Biology* 209, 4238-4253.

Tyack, P., Zimmer, W., Moretti, D., Southall, B., Claridge, D., Durban, J., Clark, C., D'Amico A., DiMarzio, N., Jarvis, S., McCarthy, E., Morrissey, R., Ward, J., and Boyd I. (2011). Beaked Whales Respond to Simulated and Actual Navy Sonar. *PLOS One* 6(3), e17009. doi: 10.1371/journal.pone.0017009.

Tyack, P.L., and Thomas, L. (2019). Using dose-response functions to improve calculations of the impact of anthropogenic noise. *Aquatic Conservation* 29(S1), 242-253. doi:10.1002/aqc.3149

Van Opzeeland, I. and O. Boebel. (2018). Marine soundscape planning: Seeking acoustic niches for anthropogenic sound. *Journal of Ecoacoustics* 2, 5GSNT8.

Vires, G. (2011). Echosounder effects on beaked whales in the Tongue of the Ocean, Bahamas. Master's Thesis. Duke University, Durham, N.C.

Wahlberg, M. (2002). The acoustic behavior of diving sperm whales observed with a hydrophone array. *Journal of Experimental Marine Biology and Ecology* 281, 53-62.

Wall Bell, C.C., Rountree, R.A., and Juanes F. (2016). "Mapping the Acoustic Soundscape off Vancouver Island Using the NEPTUNE Canada Ocean Observatory." In: *The Effects of Noise on Aquatic Life II* eds. Popper A., and Hawkins A. Advances in Experimental Medicine and Biology, 875. (Springer, New York, NY).

Ward, J., Fitzpatrick, M., DiMarzio, N., Moretti, D., and Morrissey, R. (2000). New algorithms for open ocean marine mammal monitoring. Conference presentation. OCEANS 2000 MTS/IEEE Conference and Exhibition, Providence, RI, United States. doi: 10.1109/OCEANS.2000.882193

Ward, J., Morrissey, R., Moretti, D., DiMarzio, N., Jarvis, S., Johnson, M., Tyack, P., and White, C. (2008a). Passive acoustic detection and localization of *Mesoplodon densirostris* (Blainville's beaked whale) vocalizations using distributed bottom-mounted hydrophones in conjunction with a digital tag (dtag) recording. *Canadian Acoustics* 36(1), 60-66.

Ward, J., Moretti, D., Morrissey, R. P., DiMarzio, N. A., Tyack, P., and Johnson, M. (2008b). *Mesoplodon densirostris* transmission beam pattern estimated from passive acoustic bottom mounted hydrophones and a DTag record. *The Journal of the Acoustical Society of America* 123, 3619.

Ward, J., Jarvis, S., Moretti, D., Morrissey, R., DiMarzio, N., Thomas, L. and Marques, T. A. (2011). Beaked whale (*Mesoplodon densirostris*) passive acoustic detection with increasing ambient noise. *The Journal of the Acoustical Society of America* 129, 662– 669.

Weilgart, L.S. (2007). A brief review of known effects of noise on marine mammals. *International Journal of Comparative Psychology* 20(2), 159-168.

Wenz, G.M. (1962). Acoustic Ambient Noise in the Ocean: Spectra and Sources. *The Journal of the Acoustical Society of America* 1936-1956. doi:10.1121/1/1909155

Wiggins, S.M., and Hildebrand, J.A. (2007). High-frequency Acoustic Recording Package (HARP) for broad-band, long-term marine mammal monitoring. Conference presentation. Symposium on Underwater Technology and Workshop on Scientific Use of Submarine Cables and Related Technologies, Tokyo, Japan. doi: 10.1109/UT.2007.370760

Wilford, D.C., Miksis-Olds, J.L., Martin, S.B., Howard, D.R., Lowell, K., Lyons, A.P., and Smith, M.J. (2021). Quantitative Soundscape Analysis to Understand Multidimensional Features. *Frontiers in Marine Science* 8, 672336. doi: 10.3389/fmars.2021.672336

Williams, R., Wright, A., Ashe, E., Blight, L., Bruintjes, R., Canessa, R., Clark, C., Cullis-Suzuki, S., Dakin, D., Erbe, C., Hammond, P., Merchant, N., O'Hara, P., Purser, J., Radford, A., Simpson, S., Thomas, L., Wale, M. (2015). Impacts of anthropogenic noise on marine life: Publication patterns, new discoveries, and future directions in research and management. *Ocean and Coastal Management* 115, 17-24.

Wright, A.J., Soto, N.A., Baldwin, A.L., Bateson, M., Beale, C.M., Clark, C., Deak, T., Edwards, E.F., Fernandez, A., Godinho, A., Hatch, L.T., Kakuschke, A., Lusseau, D., Martineau, D., Romero, M.L., Weilgart, L.S., Wintle, B.A., Notarbartolo-di-Sciara, G., and Martin, V.S. (2007). Do marine mammals experience stress related to anthropogenic noise? *International Journal of Comparative Psychology* 20(2), 274-316.

Yost, W.A. (2015). Pyschoacoustics: A Brief Historical Overview. *Acoustics Today* 11(3).

Zimmer, W.M.X., Johnson, M.P., Madsen, P.T., and Tyack, P.L. (2005). Echolocation clicks of free-ranging Cuvier's beaked whales (*Ziphius cavirostris*). *The Journal of the Acoustical Society of America* 117, 3919–3927.

Zimmer, W.M.X. (2011). *Passive Acoustic Monitoring of Cetaceans*. (Cambridge University Press, Cambridge, United Kingdom).

APPENDICES

Appendix 2.1. Finer temporal results of beaked whale foraging behavior during the two MBES mapping surveys.

INTRODUCTION

There are many confounding factors that can be eliminated from coarse-scale (e.g., *Before*, *During*, and *After*) impact studies through a finer temporal analysis (e.g. *Before, After, Control, Impact*). Response differences related to noise source operational use, including length of time, spatial distribution of the activity, or use of multiple versus single sources are not necessarily considered in coarse-scale impact studies. For example, though the trend of decreasing foraging activity during MFAS exercises was the same in the three MFAS studies, there were different degrees of response by foraging beaked whales (McCarthy *et al.* 2011, Manzano-Roth *et al.* 2016, DiMarzio *et al.* 2019). In particular, at the SOAR, the number of GVPs *After* was no different than the number of GVPs *Before,* whereas at AUTEC the recovery to pre-MFAS GVP numbers lagged by several days. The SOAR Naval exercises (DiMarzio *et al.* 2019) were considerably shorter than the AUTEC Naval exercises (McCarthy *et al.* 2011), which could be a contributing factor as to why the response at AUTEC was stronger. And even within the SOAR MFAS study there were differences with regards to the type of MFAS source used. For example, the decline in GVPs was larger during MFAS exercises with hull-mounted sonar in comparison to helicopter-deployed dipping sonar (DiMarzio *et al.* 2019). A similar distinction was made in the MFAS study on the Hawaii range, where only Naval exercises with MFAS, versus Naval exercises without, had a clear impact on the spatial use of the Hawaii range by foraging beaked whales (Manzano-Roth *et al.* 2016). These results highlight the importance and relevance of examining the finer details of a noise-generating activity. Taking a careful look at

operational differences in how certain anthropogenic activities are conducted, including MBES surveys, may provide insight into what factors contribute most when there is an exhibited effect.

METHODS

In addition to the *Before-During-After* analysis, a finer temporal analysis was conducted for each year in order to elucidate potential changes in foraging behavior as it relates to the different spatial mapping configurations and/or source frequencies that were used. This analysis followed a *Before-After-Control-Impact* (BACI) design. Work in both years started with a control survey of the range, where the vessel was present but the MBES was inactive. There were differences in the '*Impact*' periods between the two years. In particular, in 2017, there were two distinct periods of MBES activity, one where only the EM 122 was active and another where the EM 122, as well as several other active acoustic sources including another MBES were also active (Table A2.1). In 2019, only the EM 122 was used. However, various spatial mapping configurations, as well as single versus dual swath modes were used (Table A2.1). This included a survey confined to a small portion of the range, repeat lines over the same area, and a traditional 'mowing-the-lawn' configuration. The results of the BACI comparison for beaked whale foraging behavior during each survey year are described here.

Table A2.1. Descriptions of MBES settings during the exposure periods from 2017 (left) and 2019 (right), including duration of exposure period, acoustic systems that were active, and other operator inputs. The vessel was on the range during all periods where vessel location is not noted explicitly.

2017			2019		
Exposure Period	**Date and Time (UTC)**	**Description**	**Exposure Period**	**Date and Time (UTC)**	**Description**
Before	1/3/17 17:51:00 -1/4/17 23:51:00	30 hours, immediately preceding control survey, MBES	*Before*	1/3/19 07:11:00 -1/4/19 07:11:00	24 hours, immediately preceding control survey; MBES

		inactive, vessel off-range			inactive; vessel off-range
Control Survey	1/4/17 23:51:00 -1/5/17 08:51:00	~9 hours, MBES inactive	*Control Survey*	1/4/19 07:11:00 -1/4/19 12:11:00	~5 hours; MBES inactive
EM 122 Survey	1/5/17 08:16- 1/6/17 13:48:00	~30 hours, EM 122 active in dual swath CW only mode, motion compensation on	*Corner Survey*	1/4/19 12:19:00 -1/5/19 12:19:00	~24 hours; EM 122 active in single swath CW only mode for 1st 19 hours, final hours forced tilt between 2°-10°; motion compensation off throughout
Mixed Active Acoustics	1/6/17 13:48- 1/7/17 06:55:00	~ 18 hours, EM 122 active as in EM 122 Survey; other sources active intermittently including Kongsberg EM 712 (40 kHz), Simrad EK 80 wide-band echo sounder (18, 38, 70, 120, 200 kHz), Knudsen sub-bottom profiler (3.5 kHz)	*Across Range Survey*	1/5/19 14:58:00 -1/5/19 22:58:00	~ 8 hours; EM 122 active 1st-2nd lines: single swath CW only mode, motion compensation on; 3rd-4th lines: dual swath FM-enabled mode, motion compensation on
Immediately After	1/7/17 06:55:00 -1/7/17 21:30:00	~15 hours, EM 122 active off-range	*Traditional Survey*	1/6/19 02:00:00 -1/6/19 16:00:00	~ 14 hours, EM 122 active in dual swath FM-enabled mode, motion compensation on
After	1/7/17 21:30- 1/9/17 03:30:00	30 hours, immediately following MBES activity off-range, MBES inactive, vessel off-range	*After*	1/6/19 16:00:00 -1/7/19 16:00:00	24 hours, immediately following vessel leaving the range, MBES inactive, vessel off-range

For each mapping survey, a comparison of each of the four GVP characteristics was made across the six exposure categories described in Table A2.1 using the same methodology discussed in the main text of Chapter 2. See Figure A2.1-Left for the lines driven during the

different exposure periods of the 2017 mapping survey and Figures A2.1-Right for the lines of the 2019 survey.

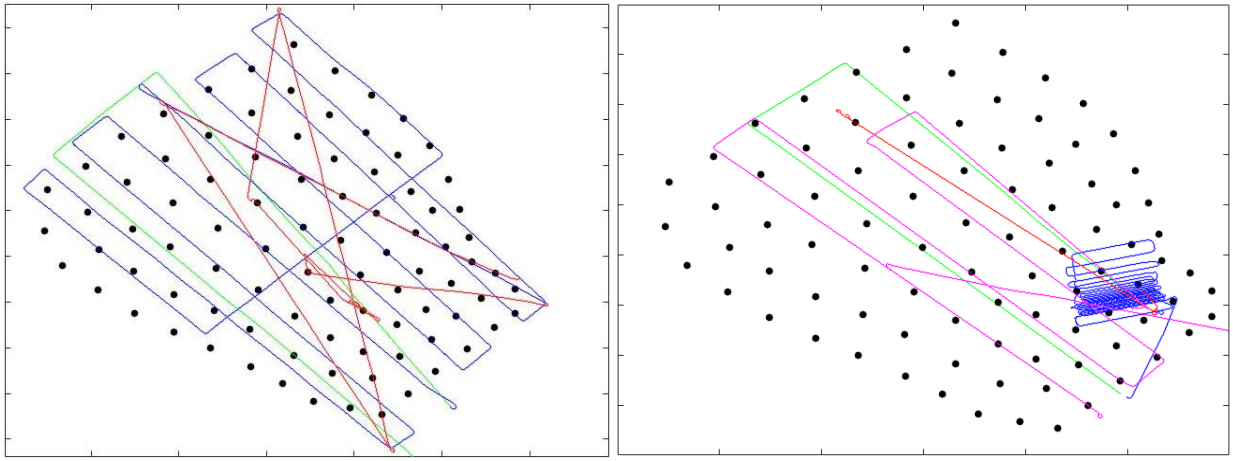

Figure A2.1. Left: Track lines of the 2017 study when the vessel was on the range during the *Control Survey*, *EM 122 Survey*, and *Mixed Active Acoustics* periods. Right: Track lines of the 2019 study when the vessel was on the range during the *Control Survey*, *Corner Survey*, *Across Range Survey*, and *Traditional Survey*.

2017 SURVEY

Predictions

By looking at the survey over a finer time-scale it was possible to evaluate differences in effect due to the presence of the vessel itself on the range versus the vessel plus the MBES, and differences between the various periods of MBES activity. It was hypothesized that if there was an effect due to just the presence of the vessel there would be a difference in the *Control Survey* GVP characteristics with respect to the *Before* and *After* time periods, but no difference in comparison to the MBES periods (*EM 122 Survey* and *Mixed Active Acoustics*). If there was an effect due to the use of the MBES, there should be a difference in the GVP characteristics between the *Control Survey* and the MBES periods. Further, if there was an effect on foraging behavior due to the MBES, it was hypothesized that the trend would be exacerbated during the *Mixed Active Acoustic* period. Multiple acoustic sources may be louder and span a broader

frequency range than one active source. Therefore the *Mixed Active Acoustic* period may be more disruptive to foraging whales, resulting in a larger effect than one active source alone.

Results

Number of GVPs per hour

A Kruskal-Wallis test was used to examine the number of GVP per hour across the six exposure periods since the data failed to satisfy the normality assumption required for an ANOVA test. There was a statistically significant difference between the exposure periods [H (5) =29.79, p=0.000017]. There were fewer GVPs *Before* the mapping survey compared with both during the *EM 122 Survey* (p=0.0037) and *After* (p=0.0000339). See Table A2.2 for descriptive statistics on this metric and Figure A2.2, which shows the hourly GVP data across the six exposure periods.

Table A2.2. Descriptive statistics for the four GVP characteristics during the 2017 MBES study, including the mean and standard deviation for each exposure period and number of samples used to compute those values in parentheses.

	Before	***Control Survey***	***EM 122 Survey***	***Mixed Active Acoustics***	***Immediately After***	***After***
Number of GVP per hour	2.47 ± 1.55 (n=30)	2.94 ± 2.15 (n=9)	4.56 ± 2.24 (n=30)	4.17 ± 2.46 (n=18)	3.03 ± 2.02 (n=15)	5.23 ± 2.16 (n=30)
Number of clicks per GVP	3267 ± 1745 (n=27)	2558 ± 2095 (n=9)	2011 ±1286 (n=30)	3934 ± 2262 (n=17)	3396 ± 2675 (n=15)	3138 ± 1273 (n=30)
GVP duration (min)	47.15 ± 12.9 (n=27)	35.2 ± 12.49 (n=9)	39.02 ± 13.26 (n=30)	44.58 ± 9.95 (n=17)	38.74 ± 17.03 (n=15)	44.82 ± 9.26 (n=30)
Click rate (clicks/min)	68.67 ± 26.96 (n=27)	72.59 ± 62.66 (n=9)	49.3 ± 20.32 (n=30)	83.81 ± 44.75 (n=17)	96.21 ± 74.71 (n=15)	71.92 ± 27.25 (n=30)

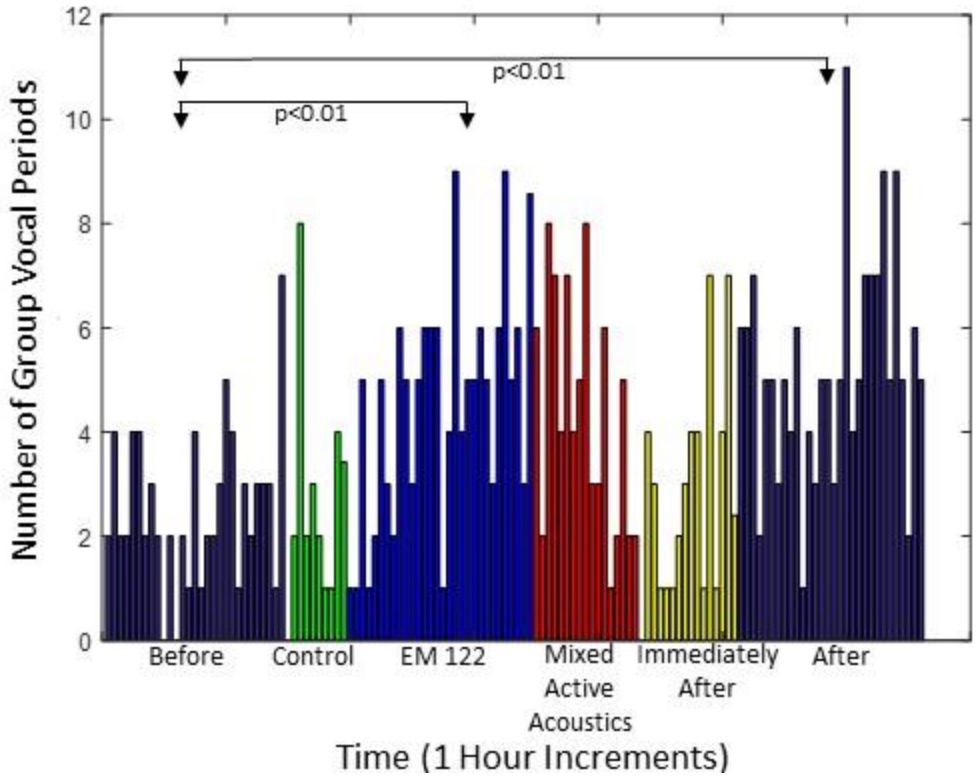

Figure A2.2. Bar graph showing the number of GVPs per hour during each exposure period for the 2017 survey. The arrows indicate statistically significant differences at the p-value indicated between the two exposure periods with which the arrows correspond.

Number of clicks per GVP

A Kruskal-Wallis test was used to compare the exposure periods for the number of clicks per GVP since the data failed to satisfy the normality assumption required for an ANOVA test. There was a difference in the exposure periods [H (5) =18.95, p=0.002]; there were more (p=0.0047) clicks per GVP during the *Mixed Active Acoustics* than there were during the *EM 122 Survey* period. See Table A2.2 for descriptive statistics and Figure A2.3, which shows the hourly averages across the six exposure periods for this metric.

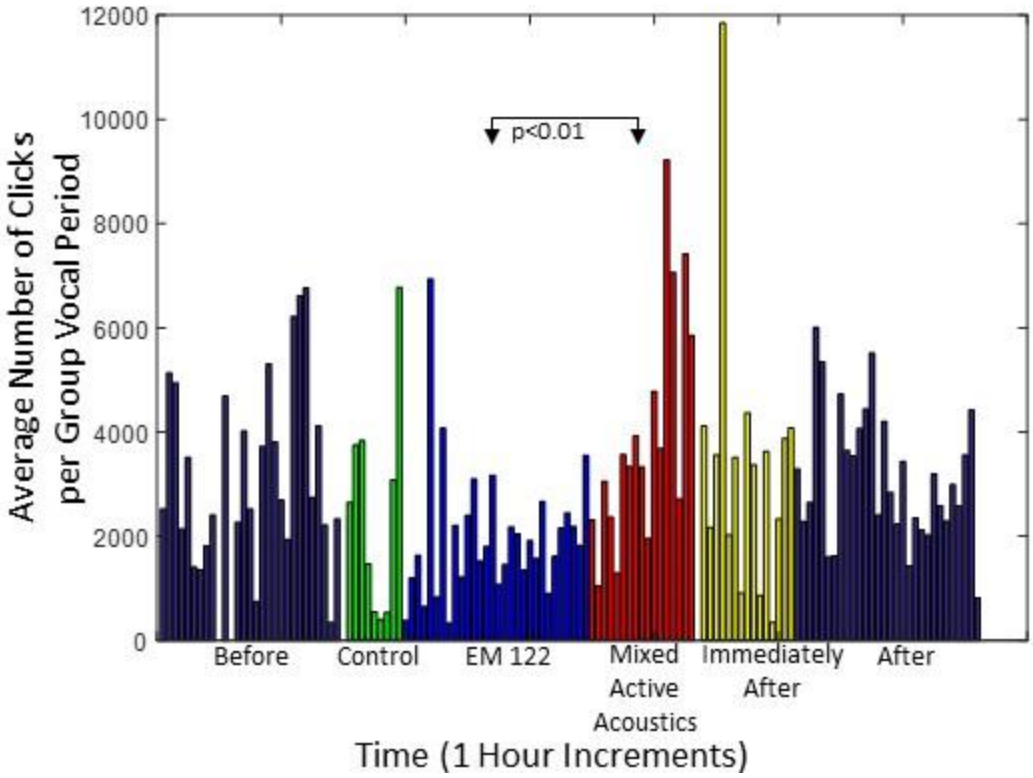

Figure A2.3. Bar graph showing the number of GVPs per hour during each exposure period for the 2017 survey. The arrows indicate statistically significant differences between the two exposure periods the arrows correspond with at the p-value indicated.

GVP duration

Since all of the assumptions of the ANOVA were met, a one-way ANOVA was used to compare the exposure periods for GVP duration. There were no statistically significant differences between exposure periods for this metric [$F(5, 122) = 2.43$, $p = 0.0388$]. See Table A2.2 for descriptive statistics and Figure A2.4, which shows the hourly averages of this metric across the six exposure periods.

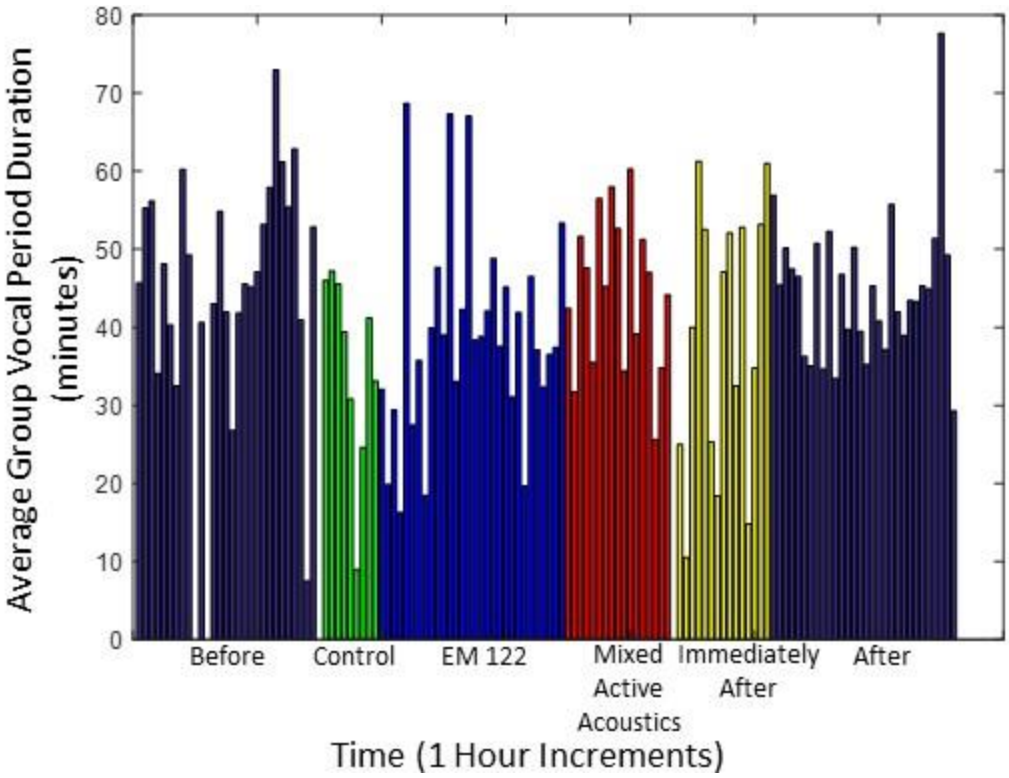

Figure A2.4. Bar graph showing the average GVP duration (minutes) per hour of each exposure period for the 2017 survey.

Click rate

The click rate data failed the normality assumption of an ANOVA, so a Kruskal-Wallis test was used to compare exposure periods for this metric. There was a statistically significant difference between the exposure periods [H (5) =15.84, p=0.0073]. However, the post-hoc multiple comparison test showed no difference between any of the exposure periods at a 99% significance level. See Table A2.2 for descriptive statistics and Figure A2.5, which shows the hourly averages of this metric across the six exposure periods.

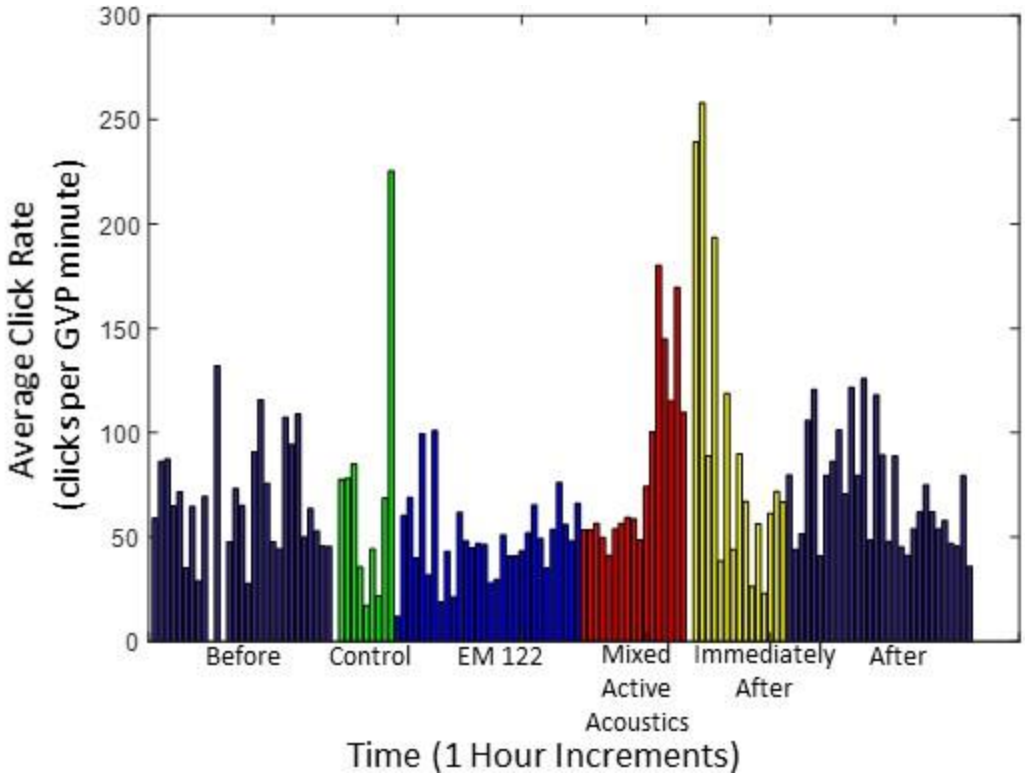

Figure A2.5. Bar graph showing the average GVP duration (minutes) per hour of each exposure period for the 2017 survey.

Discussion

There were no statistically significant differences among any of the exposure periods and the *Control Survey* for any of the GVP characteristics, which suggests the presence of the vessel alone did not affect the foraging metrics examined in this study.

The only metric where there was a difference between non-MBES periods and MBES periods was in the number of GVP per hour. There were fewer GVP per hour *Before* than during the *EM 122 Survey*, but there were also fewer GVP per hour *Before* compared with *After*. This was the same general result seen in the main study. However, the finer temporal analysis shows that between these three periods the number of GVP fluctuated. In particular, during the *Control Survey* and *EM 122 Survey* the number of GVPs increased and then during the *Mixed Active Acoustic* and *Immediately After* periods the number of GVPs decreased before increasing again *After* (Figure A2.2). This result differs from the monotonic decrease seen in the number of

GVPs during and immediately after exposure to MFAS sonar in the McCarthy study (2011). Therefore, it appears more likely that the mechanism driving the number of GVPs per hour is something other than what was tested for in this study (i.e., MBES activity), rather than a lagged response to MBES activity. The fluctuations observed in this GVP characteristic may be better described by variability in oceanographic conditions or prey behavior during the study period.

There were no GVP characteristics with an exacerbated effect from the *EM 122 Survey* to the *Mixed Active Acoustics* period. For the number of GVPs per hour where there was a statistically significant increase between *Before* and the *EM 122 Survey,* there was a decrease from the *EM 122 Survey* to the *Mixed Active Acoustic* period (Figure S2), though this was not statistically significant. The trend in the number of clicks per GVP was the opposite: a decrease between the *Before* period through the *EM 122 Survey,* and a significant increase into the *Mixed Active Acoustics* period (Figure S3). And there were no differences across any of the exposure periods for both GVP duration and click rate (Figure S4 and Figure S5). In general, there was not a clear and consistent relationship in the change of foraging behavior between the periods using a single MBES versus multiple acoustic sources.

However, there were more clicks per GVP during the *Mixed Active Acoustic* period than during the *EM 122 Survey*. This might suggest that having multiple active acoustic sources on at a time has a noticeable effect on foraging in a way that a single MBES source does not. The scientific community is now recognizing the need to examine the effect of aggregate (e.g., multiple noise sources) and cumulative stressors on marine mammal behavior (NASEM 2017). This may have been a contributing factor for why Naval exercises, which commonly use multiple active acoustic sources, have often been associated with significant reactions from beaked whales. However, neither the *EM 122 Survey* nor the *Mixed Active Acoustics* periods

were significantly different from the non-MBES periods for this metric; this does not provide strong support that this finding is a result of aggregate stressors. Nevertheless, this result may be worth further exploration, especially if multiple MBES are used in spatiotemporal proximity in the future.

2019 SURVEY

Predictions

By looking at the 2019 survey on a finer time-scale it was possible to evaluate potential differences in effect due to 1) presence of the vessel alone versus presence of vessel and MBES, and 2) the various spatial configurations that were run during the MBES survey. It was expected that if the presence of the vessel alone had an effect on foraging behavior there would be a difference in GVP characteristics between the *Control Survey,* and the *Before* and *After* periods, and there would be no difference between the *Control Survey* and MBES periods (*Corner Survey*, *Across Range Survey,* and *Traditional Survey*). If the presence of the vessel plus the actively transmitting MBES had an effect, significant differences in the GVP characteristics during the MBES periods compared to non-MBES periods would be expected. Of the three MBES periods, it was hypothesized that the survey restricted to the corner location might elicit the largest effect on foraging since animals in that area would be in the vicinity of the MBES for several hours at a time. However, based on where this species primarily forages, the area for that survey (*Corner Survey*) was not a heavily used area by these animals (DiMarzio *et al.* 2019). Both the *Across Range* and *Traditional Surveys* went into deeper water where the animals are more commonly found. As such, it was hypothesized that foraging behavior during these surveys would be most likely to significantly differ from non-MBES periods.

Results

Kruskal-Wallis tests were used to compare exposure periods for each of the GVP characteristics since none of the variables satisfied the normality assumption of an ANOVA. There were no statistically significant differences across the exposure periods for the number of GVP per hour [H (5) =5.77, p=0.3292]; the number of clicks per GVP [H (5) =2.82, p=0.7276], or click rate [H (5) =3.54, p=0.6169]. See Table A2.3 for descriptive statistics and Figure A2.6, which shows the hourly binned data across the six exposure periods for each of these three GVP characteristics.

Table A2.3. Descriptive statistics for the four GVP characteristics during the 2019 MBES study, including the mean and standard deviation for each exposure period and number of samples used to compute those values in parentheses.

	Before	***Control Survey***	***Corner Survey***	***Across Range Survey***	***Traditional Survey***	***After***
Number of GVP per hour	2.46 ± 2.43 (n=24)	3.6 ± 1.52 (n=5)	2.67 ± 2.06 (n=24)	4.38 ± 2.77 (n=8)	2.57 ± 1.34 (n=14)	2.42 ± 1.93 (n=24)
Number of clicks per GVP	3002.3 ± 2042.18 (n=17)	2975.85 ± 1289.52 (n=5)	2424.13 ± 1510.87 (n=21)	2248.53 ± 923.14 (n=8)	2287.23 ± 1226.76 (n=13)	2478.17 ± 1229.01 (n=20)
GVP duration (min)	49.53 ± 12.42 (n=17)	40.54 ± 14.65 (n=5)	40.41 ± 11.46 (n=21)	36.60 ± 12.29 (n=8)	31.83 ± 11.91 (n=13)	42.88 ± 9.54 (n=20)
Click rate (clicks/min)	63.19 ± 39.82 (n=17)	69.96 ± 14.35 (n=5)	56.12 ± 29.11 (n=21)	59.59 ± 19.93 (n=8)	65.48 ± 31.66 (n=13)	56.19 ± 34.34 (n=20)

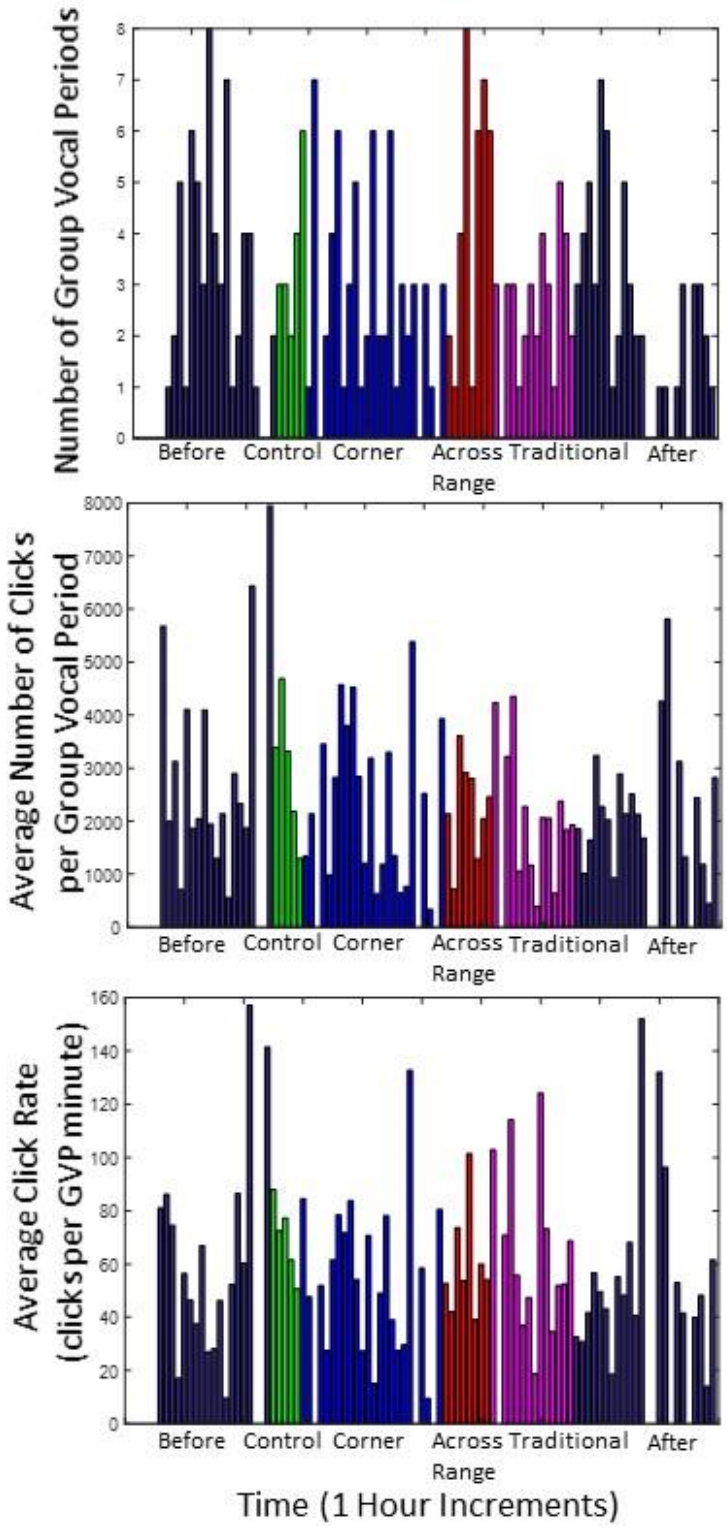

Figure A2.6. Bar graphs of the three GVP characteristics where no differences were found across exposure periods in the 2019 survey. Each graph shows the data binned into hour increments for each of the six exposure periods. Top: the number of group vocal periods; Middle: the average number of clicks per GVP; Bottom: the average click rate. From left to right: *Before, Control Survey, Corner Survey, Across Range Survey, Traditional Survey,* and *After.*

There was a statistically significant difference among exposure periods for GVP duration [H (5) =14.53, p=0.0126]. GVPs were shorter in duration during the *Traditional Survey* than *Before* (p=0.004). See Table A2.3 for descriptive statistics and Figure A2.7, which shows the hourly averaged data across the six exposure periods for this metric.

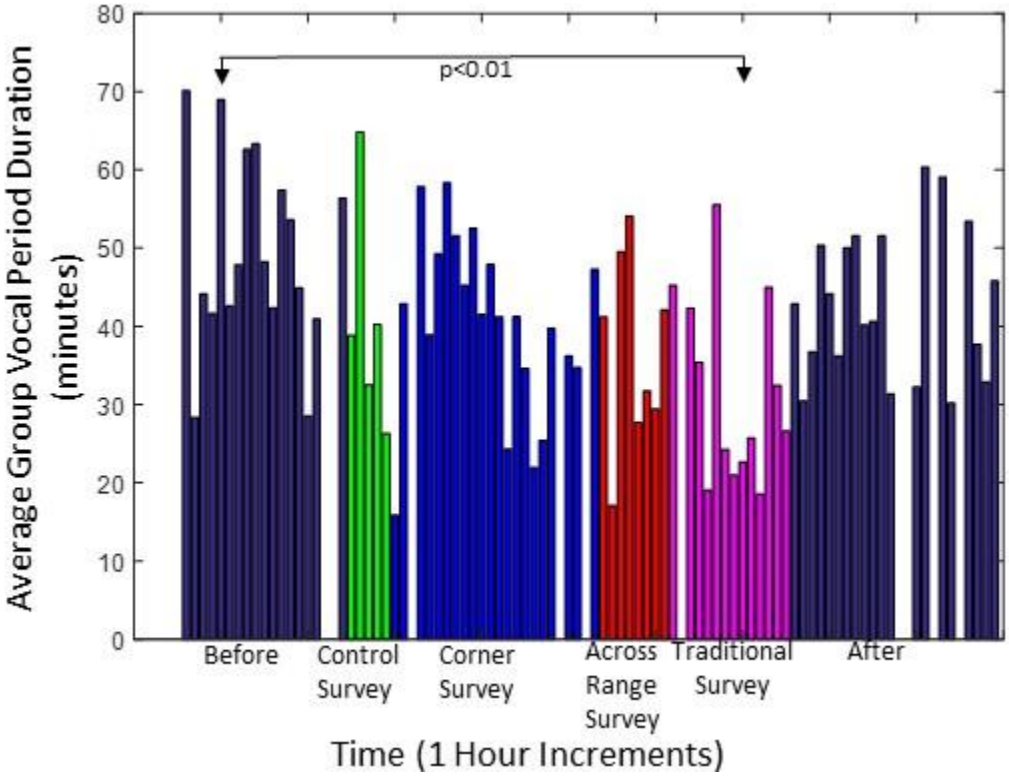

Figure A2.7. Bar graph showing the average GVP duration in minutes for each hour during the six exposure periods of the 2019 survey. The arrows indicate statistically significant differences at the p-value indicated between the two exposure periods corresponding with the arrows. From left to right: *Before*, *Control Survey*, *Corner Survey*, *Across Range Survey*, *Traditional Survey*, and *After*.

Discussion

The only significant difference observed in any of the GVP characteristics during the 2019 survey was in GVP duration. The GVP duration steadily shortened from the *Before* period through the *Traditional Survey* and then increased again *After* (Table A2.7). The only significant difference in this trend was between the *Before* period and the *Traditional Survey* (Figure A2.7). One interpretation of this is that the particular lines run may have affected this foraging behavior

metric in line with predictions. The C*orner Survey*, which was confined to a small part of the range where animals are not as commonly observed, had no effect on this characteristic. But during the *Across Range* and *Traditional Surveys*, which were run over larger and deeper portions of the range, there was a decreasing trend in GVP duration. The *Traditional Survey* covered the broadest area on the range, potentially leading to the interaction of MBES with more foraging groups. Alternatively, this decreasing trend in GVP duration could be explained by some variable(s) not examined in this study, such as a change in prey behavior that consequently impacted foraging behavior, or an underlying bias in the time of day for foraging. Without tagging data and/or studying prey dynamics it is difficult to say whether this decrease over time is biologically meaningful. The anticipated spatial analysis of this same data set should provide insight into this result and its interpretation.

There were no differences between the *Control Survey* and the *Before* and *After* periods, which was a similar finding to that of 2017. This suggests that the presence of the vessel alone did not elicit a change in the GVP characteristics examined in this study.

CONCLUSION

There were no consistent changes in GVP characteristics exhibited in both years. The finer scale analysis of the two years reveals that the difference observed in the main study between the number of GVPs per hour *Before* and *During* MBES activity is largely driven by the 2017 study. There, the same trend was observed between the *Before* and *EM 122 Survey* periods in the finer-scale analysis, while in 2019, there were no differences in the exposure periods for this GVP characteristic. In 2019, the only significant result was seen in GVP duration between the *Before* and *Traditional Survey* periods. The *Traditional Survey* of 2019 was conducted similarly to the *EM 122 Survey* in the 2017 study, where there was no difference in GVP

duration. The only difference between these two surveys was that during the *Traditional Survey* FM signals were enabled, versus CW only signals during the *EM 122 Survey*. This may be an important consideration in the detection and reaction of this noise source by a receiver (Kates Varghese *et al.* 2019), but as of yet, it is unclear whether this difference in signal type has an effect on beaked whales. Additionally, part of the *Across Range Survey* was also run in FM-enabled mode which was not statistically different from any other exposure period for this metric. Thus these differences in results between the two years are likely an effect of the large underlying temporal variability seen in foraging behavior that exists regardless of outside factors such as anthropogenic activity.

Of the four GVP characteristics, there were only one (2019) or two (2017) that had significant differences between exposure periods. It was expected that if there was an effect of MBES on beaked whale foraging that there would be widespread change in all of the GVP characteristics. Additionally, it was expected that there would be a monotonic change across the various MBES periods, rather than fluctuations, as was primarily seen here. This suggests that there is not a clear relationship between the MBES activity of these surveys and the changes exhibited in beaked whale foraging behavior at the SOAR.

Overall, the BACI analysis provided insight into beaked whale foraging behavior during two MBES surveys at a finer temporal scale. There was no change in foraging behavior due to vessel presence alone. There were differences in foraging behavior during various periods of MBES activity in the two years. But, as these results were not widespread across GVP characteristics, and not in line with expectations of behavioral changes during similar types of noise exposure, the results may be better explained by factors other than MBES activity. Future work related to MBES activity should consider 1) examining differences in MBES surveys using

multiple sources versus a single source, as well as 2) taking a holistic approach when assessing beaked whale foraging behavior by incorporating prey dynamic information. The overall trend remains clear from the main study, the animals continued to forage during both years of MBES mapping work and did not leave the SOAR range.

Appendix 5.1. Spectrograms associated with acoustic events described in the time series annotation.

All spectrograms made in Audacity ® with the following settings: window size, 4096; Hanning window; 20 dB gain; 80 dB range. The default, 20dB gain, corresponds to a -20 dB signal at a particular frequency being displayed as "white". Affects the range of signal sizes that will be displayed as colors. The default, 80 dB range, means that you will not see anything for signals 80 dB below the value set for "gain". Note the default spectrogram in Audacity does not have a visual color map, but with the default settings of Gain = 20 dB and Range = 80 dB used here, the colors correspond to the following levels:

- anything above -20 dB is indistinguishably white
- levels from -40 dB to -20 dB transition from red to white
- levels from -60 dB to -40 dB transition from magenta to red
- levels from -80 dB to -60 dB transition from dark blue to magenta
- levels from -100 dB to -80 dB transition from light blue to dark blue
- anything below -100 dB is gray.

Hydro 45

Event 1: 1/4/17 21:26

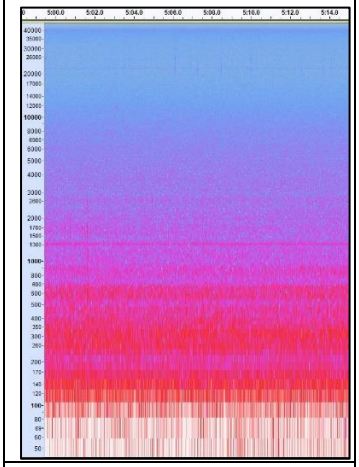

Event 2: 1/4/17 23:27

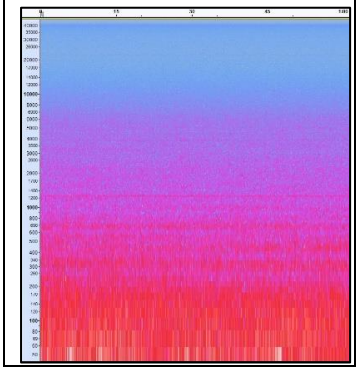

Pre-Event 3:

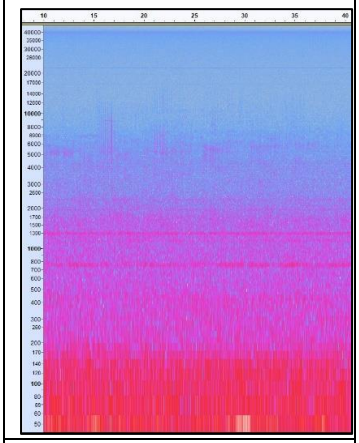

Event 3: 1/5/17 02:42

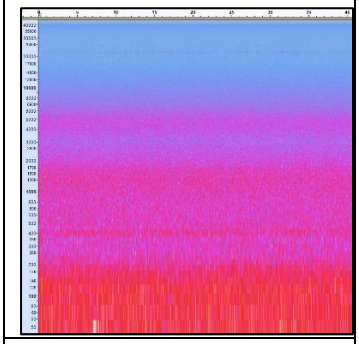

Event 4: 1/5/17 05:12

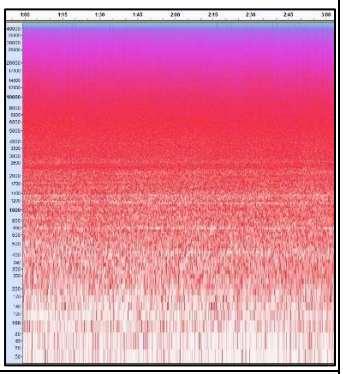

Event 5: 1/5/17 08:57

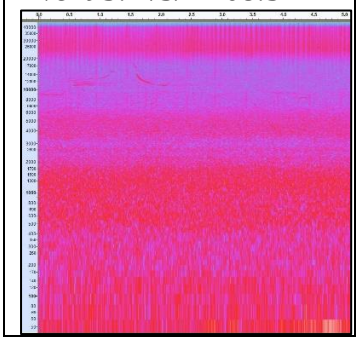

Event 6: 1/5/17 09:42

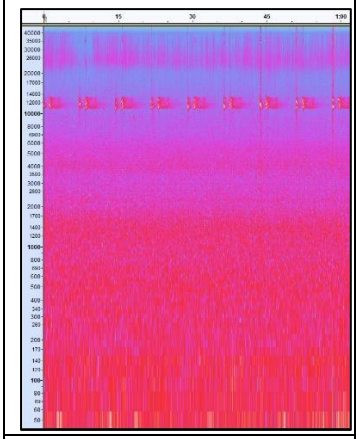

Event 7: 1/5/17 11:41

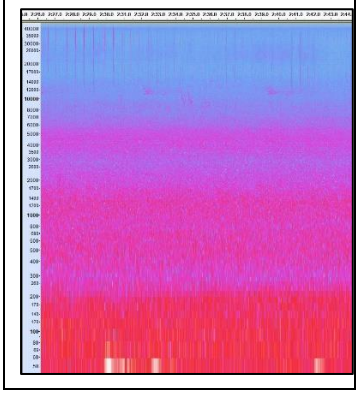

Event 8: 1/5/17 12:26

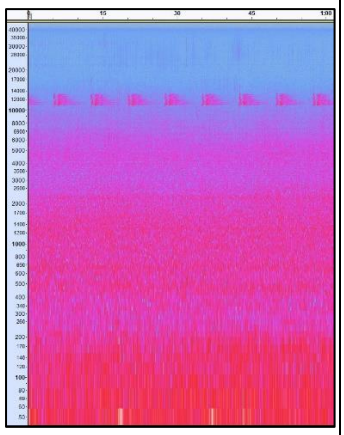

Event 9: 1/5/17 14:12

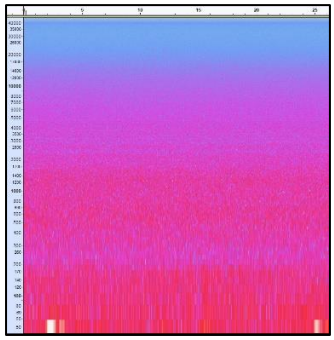

Event 10: 1/5/17 15:26

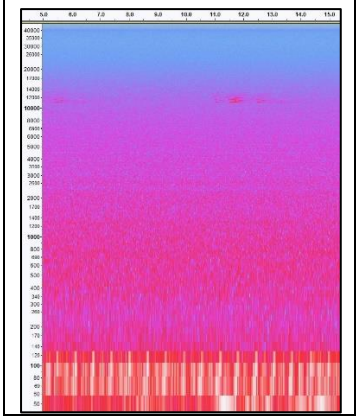

Event 11: 1/5/17 17:12

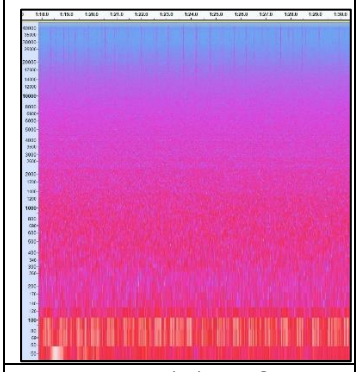

Event 12: 1/5/17 19:11

Event 13: 1/5/17 22:42

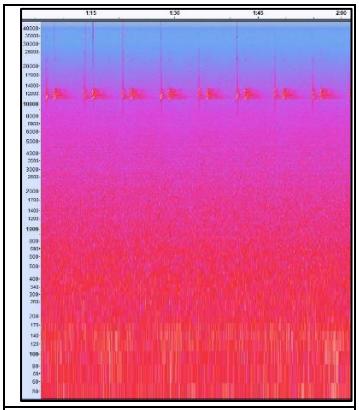

Event 14: 1/6/17 1:42

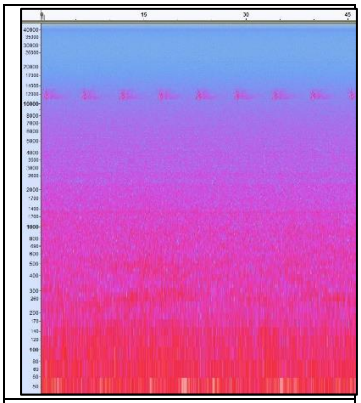

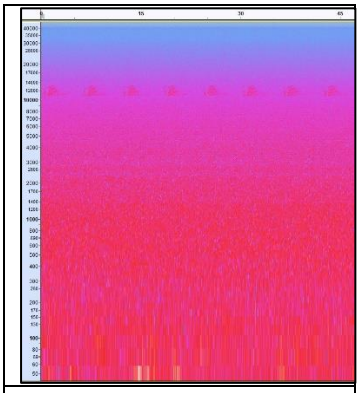

Event 15: 1/6/17 4:11

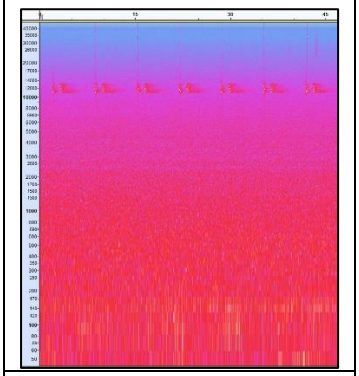

Event 16: 1/6/17 6:57

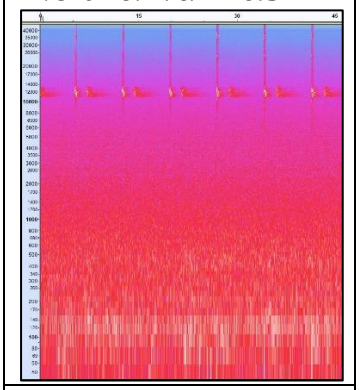

Event 17: 1/6/17 10:57

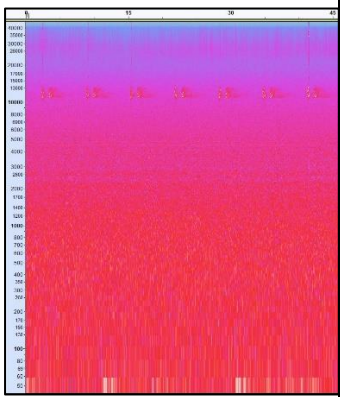

Event 17: grating lobes?

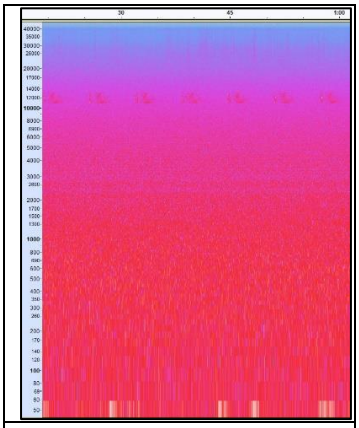

Event 18: 1/6/17 12:12

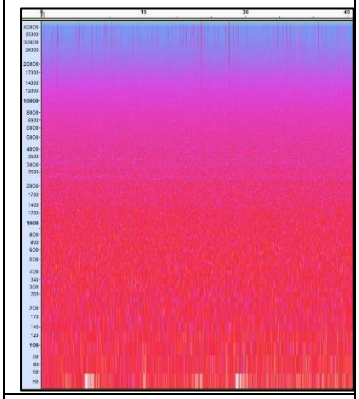

Event 19: 1/6/17 13:27

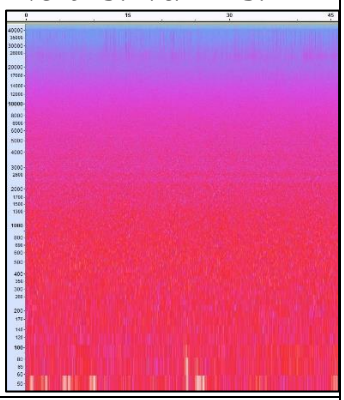

Event 20: 1/6/17 13:57

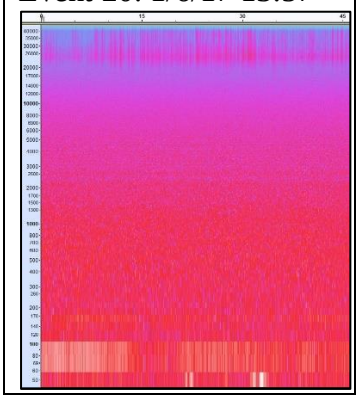

Event 21: 1/6/17 14:27

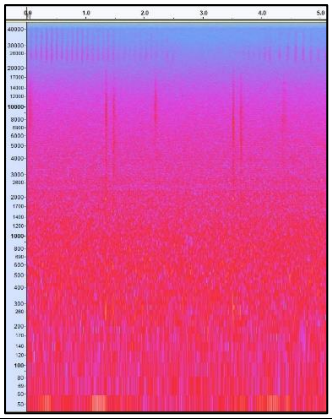

Event 22: 1/6/17 15:42

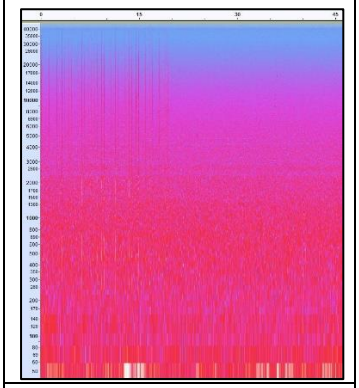

Event 23: 16:42

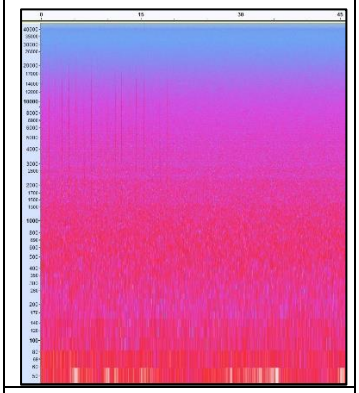

Event 24: 1/6/17 19:56

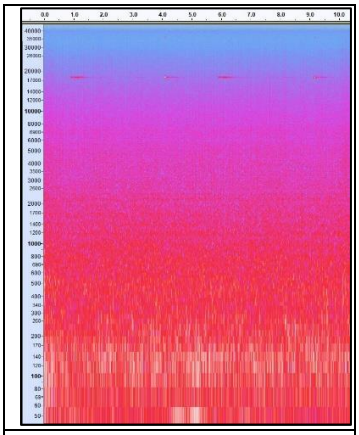

Event 25: 1/6/17 20:57

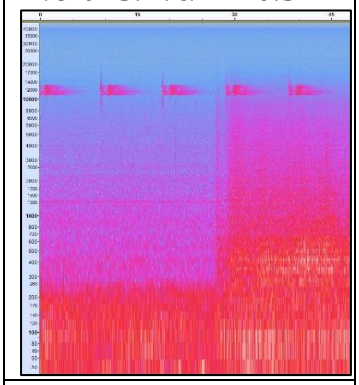

Event 26: 1/6/17 23:57

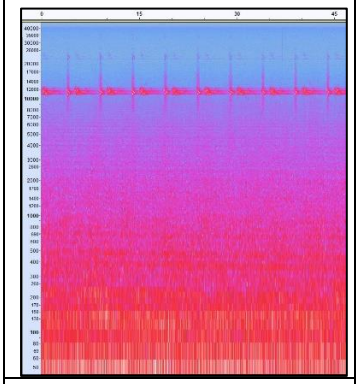

Event 27: 1/7/17 03:12

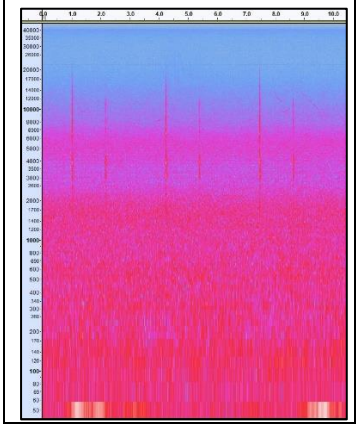

Event 28: 1/7/17 03:57

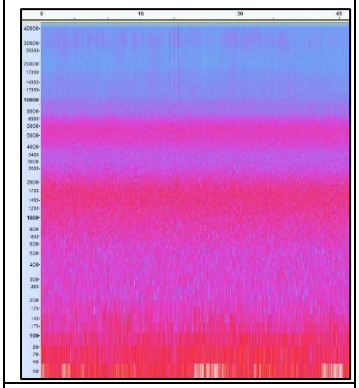

Event 29: 1/7/17 05:38

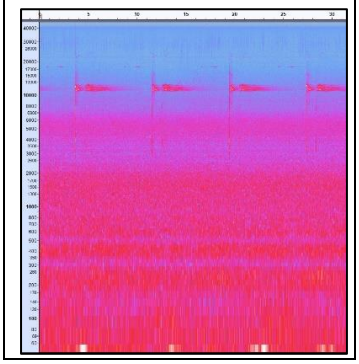

Hydro 14

Event 1: 1/4/17 21:30

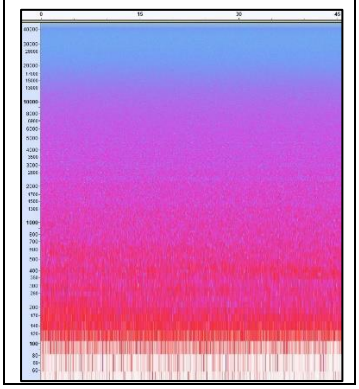

Event 2: 1/4/17 23:30

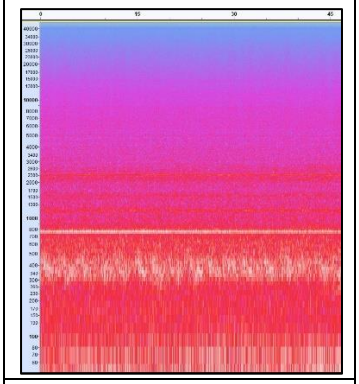

Event 3: 1/5/17 3:45

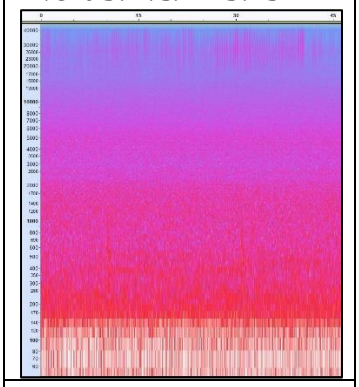

Event 4: 1/5/17 5:30

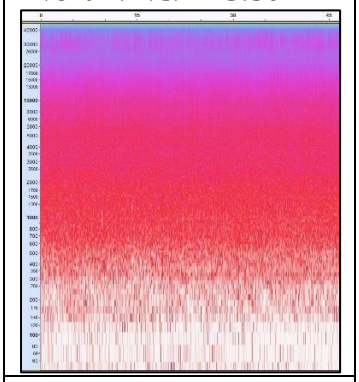

Event 12: 1/6/17 23:45

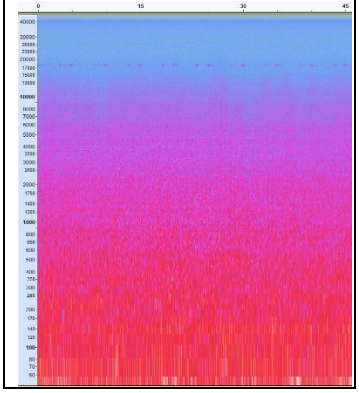

Hydro 16

Event 7: 1/5/17 15:45

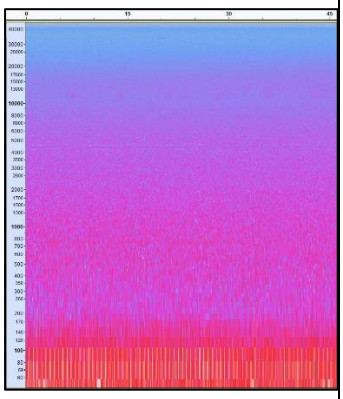

1/5/17 17:15

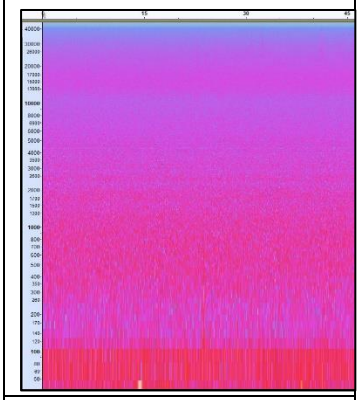

Event 11: 1/6/17 17:00

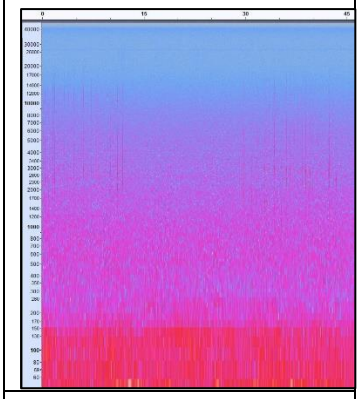

Event 12: 1/6/17 20:45

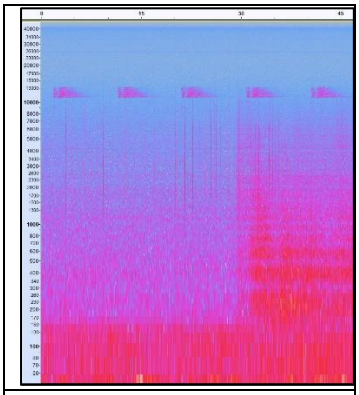

Event 13: 1/7/17 1:00

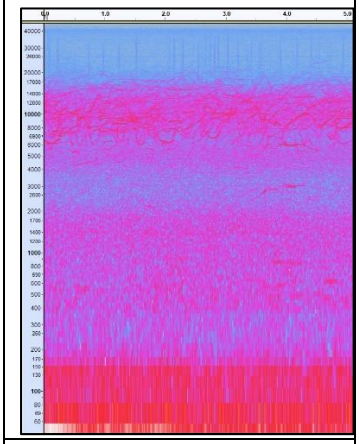

Event 14: 1/7/17 4:00

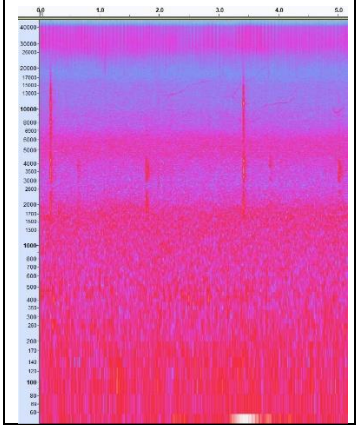

Event 15: 1/7/17 4:27

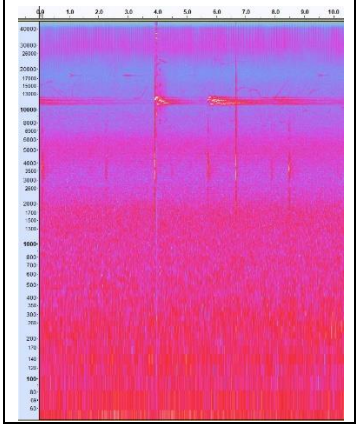

Hydro 19

Event 8: 1/6/17 20:57

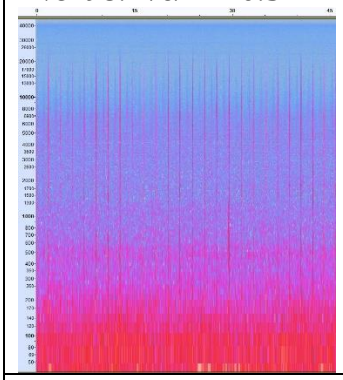

Event 9: 1/6/17 23:57

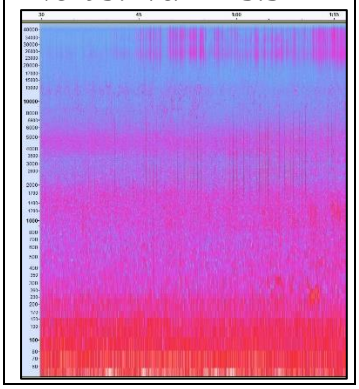

Hydro 22

Event 1: 1/5/17 3:57

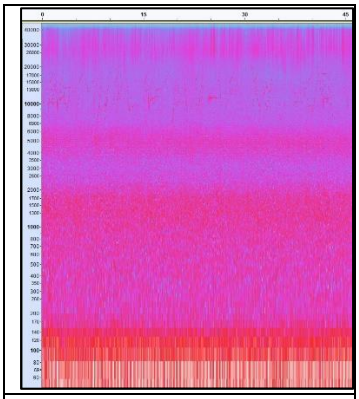

Event 2: 1/5/17 6:00

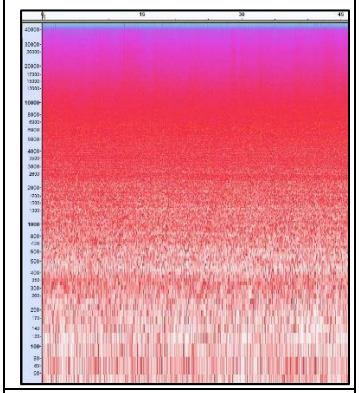

Event 3: 1/5/17 9:00

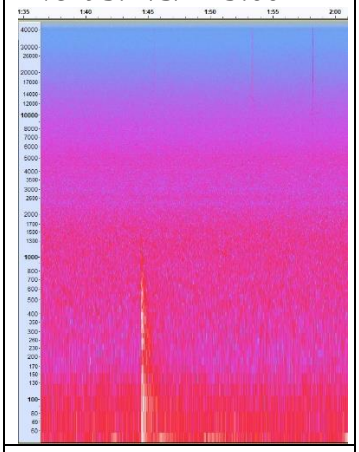

Event 7: 1/6/17 4:00

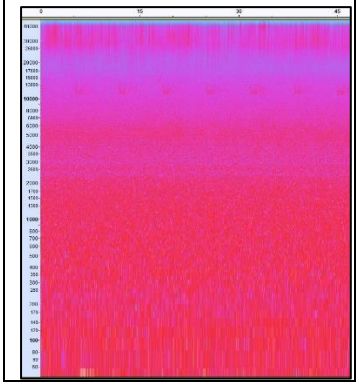

Event 8: 1/6/17 6:00

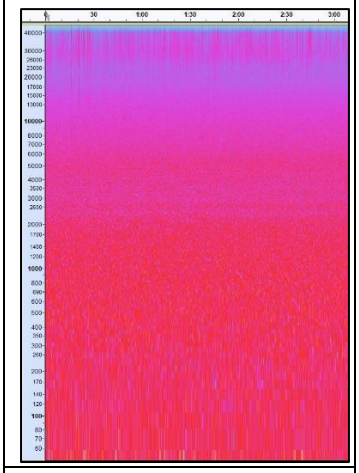

Event 10: 1/6/17 23:30

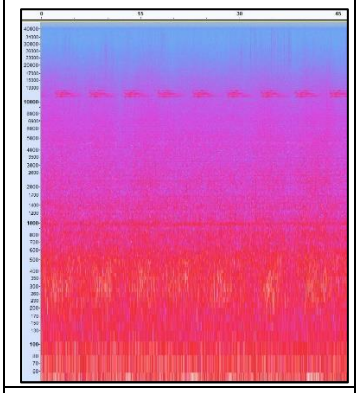

Event 11: 1/7/17 5:40

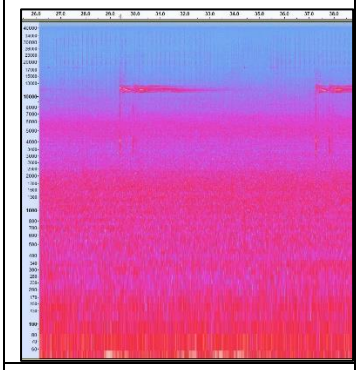

Hydro 57

Event 1: 1/4/17 21:00

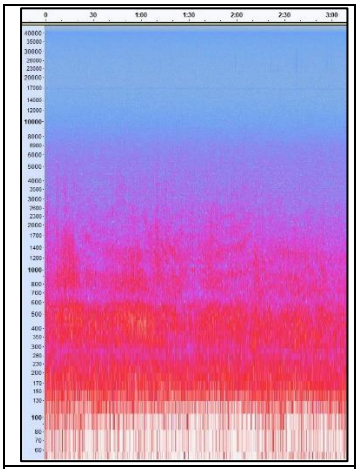

Event 9: 1/5/17 19:45

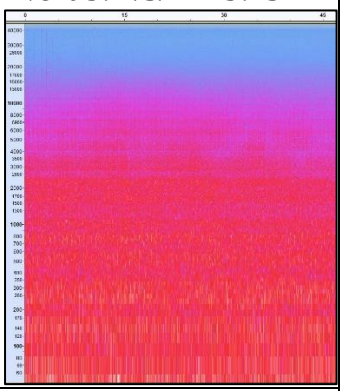

Event 10: 1/5/17 21:50

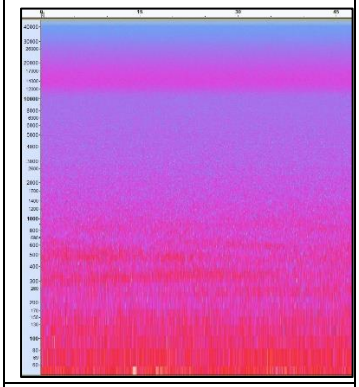

Event 11: 1/6/17 19:40

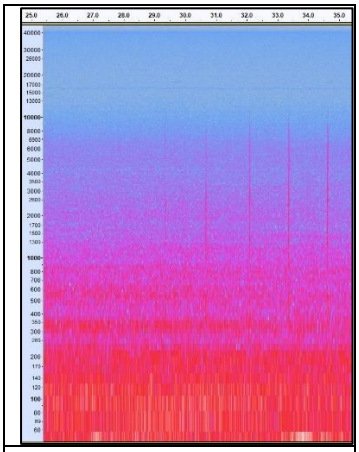

Event 12: 1/6/17 21:15

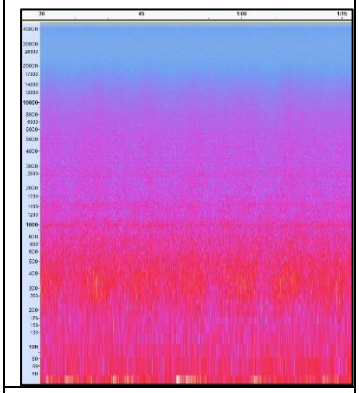

Event 13: 1/7/17 2:45

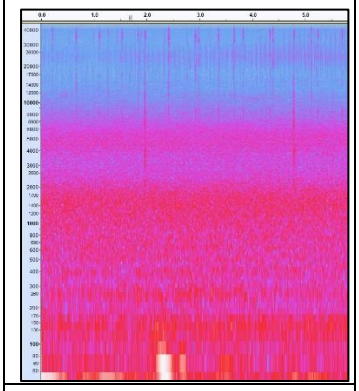

Event 14: 1/7/17 5:15

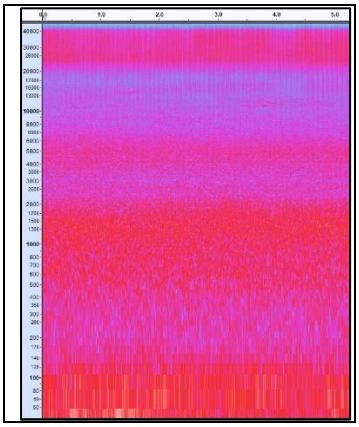

Hydro 63

Event 1: 1/5/17 5:15

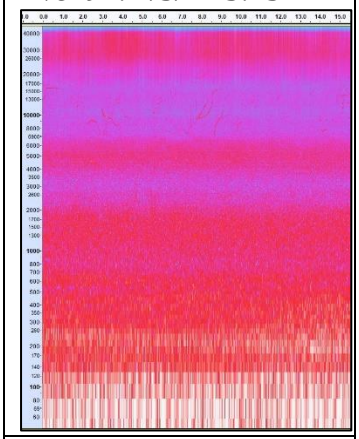

Event 2: 1/5/17 7:30

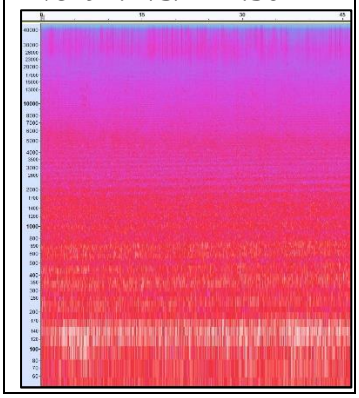

Event 12: 1/6/17 12:15

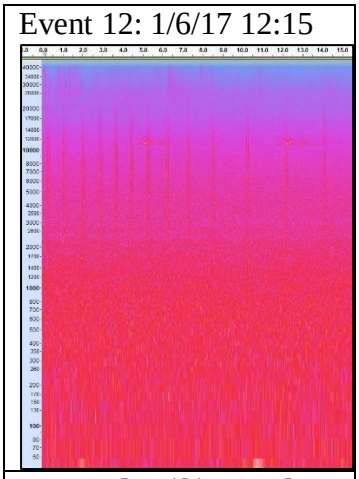

Event 13: 1/6/17 14:31

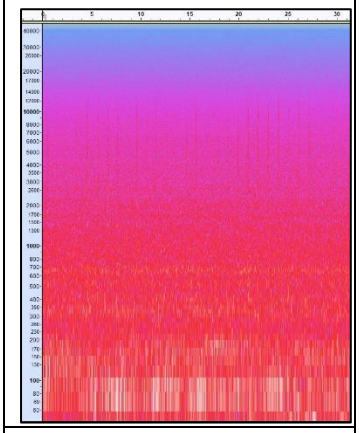

Event 14: 1/6/17 19:00

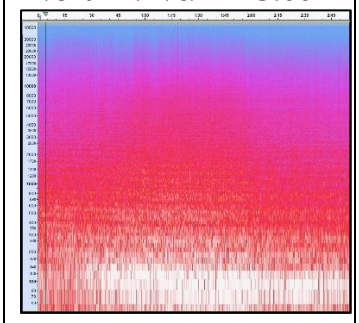

Event 16: 1/7/17 2:16

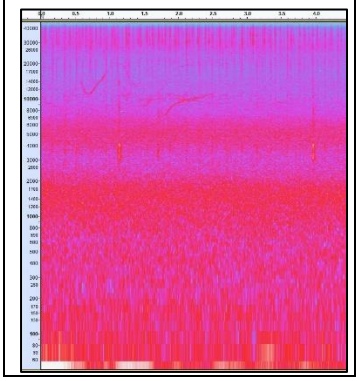

Event 17: 1/7/17 06:15

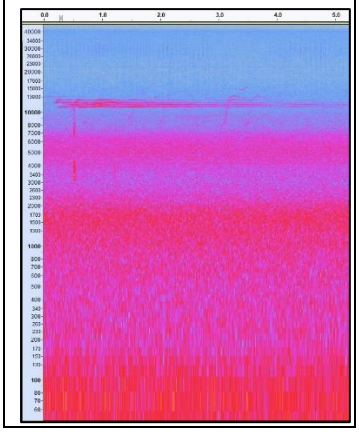

Hydro 70

Event 1: 1/4/17 22:12

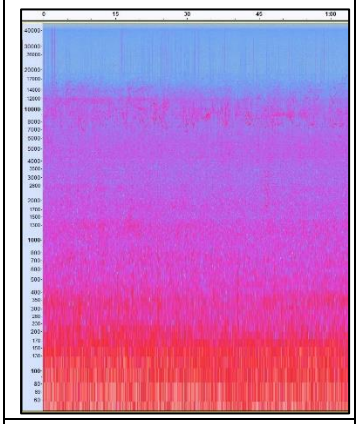

Event 2: 1/5/17 3:42

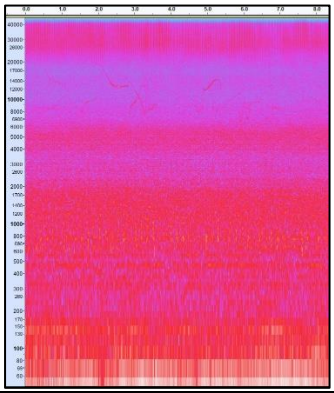

Event 3: 1/5/17 6:15

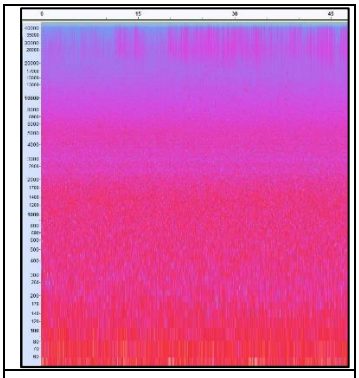

Event 4: 1/5/17 8:30

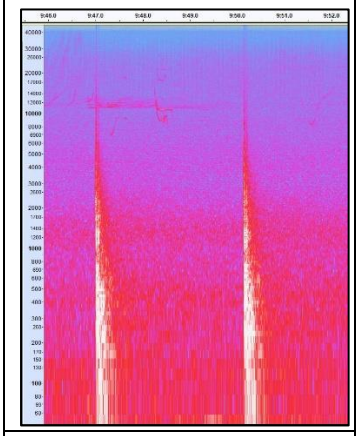

Event 5: 1/5/17 17:30

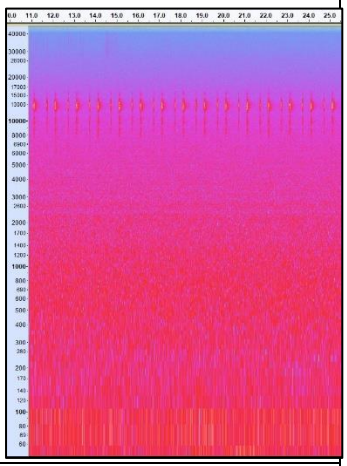

Event 6: 1/5/17 22:55

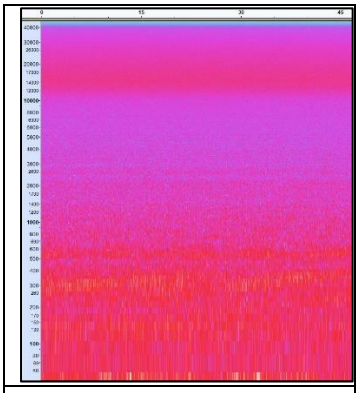

Event 10: 1/6/17 14:00

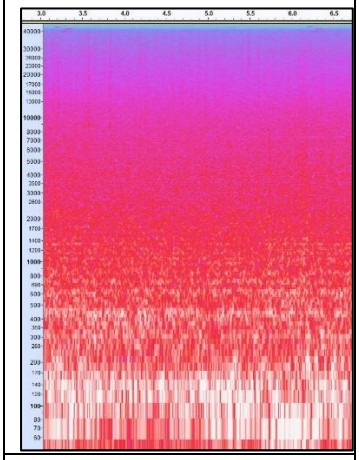

Event 11: 1/6/17 18:15

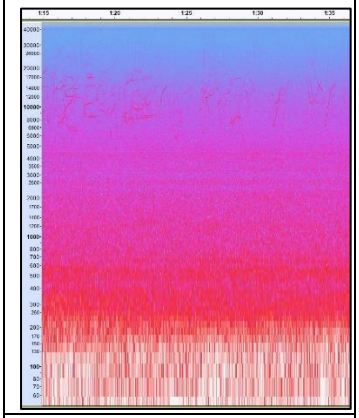

Event 12: 17/17 00:30

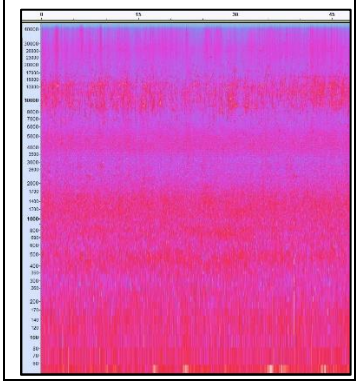

Event 13: 1/7/17 6:30

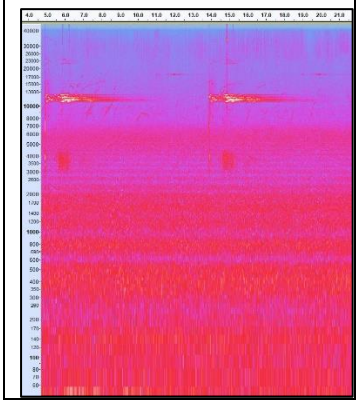

Event 9: 1/6/17 00:15

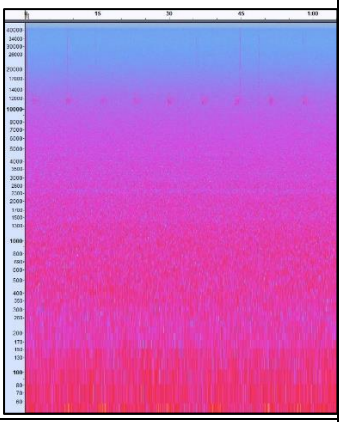

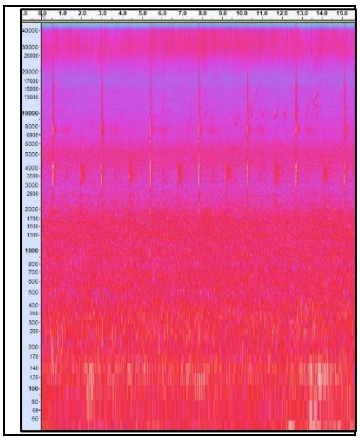

Hydro 85

Event 1: 1/4/17 22:44

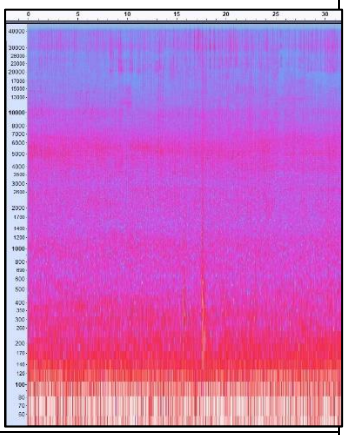

Event 8: 1/5/17 18:50

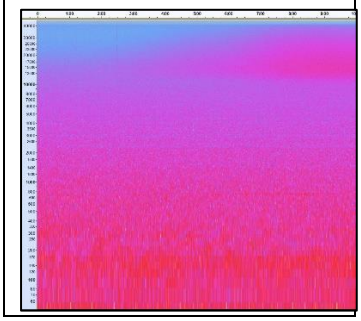

Event 12: 1/6/17 19:00

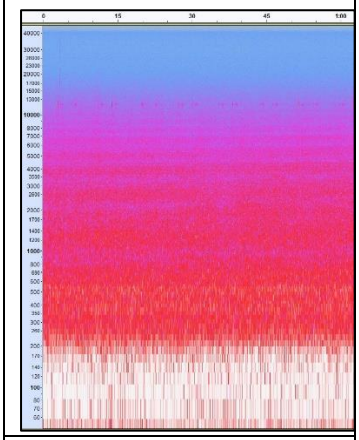

Event 13: 1/7/17 1:00

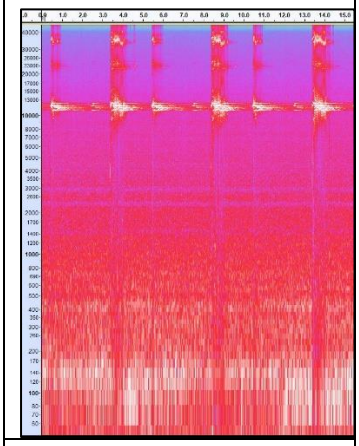

Event 14: 1/7/17 2:00

Appendix 5.2. Period-specific weighted and unweighted sound level metric percentiles array-wide and by hydrophone for the total study period, and each of the four distinct analysis periods: No Activity, Vessel Only, Vessel and MBES, and Mixed Acoustics.

Metrics included: *SPLpk*, *wSPLpk*, *SEL*, *wSEL*, 12.5 kHz BL, 50 Hz BL, and 40 kHz BL
Percentiles included: 1, 5, 10, 25, 50, 75, 90, 95, 99th.
Hydrophones included: 14, 16, 19, 22, 45, 57, 63, 70, 85, and array-averaged.

Peak sound pressure level (*SPLpk*)

Total Study Period										
Percentiles	**Array-wide**	**14**	**16**	**19**	**22**	**45**	**57**	**63**	**70**	**85**
1	92.9	95.1	92.4	94.4	94.2	93.4	94.7	94.6	98.0	93.9
5	95.1	97.7	93.8	96.3	96.0	95.2	96.7	96.2	99.3	95.9
10	96.5	99.2	94.7	97.3	97.1	96.3	97.8	97.3	100.3	97.1
25	99.1	101.3	96.7	99.5	99.0	98.5	100.2	99.7	102.3	100.1
50	102.5	104.3	99.6	103.0	101.8	102.3	103.5	103.5	104.9	103.5
75	106.1	106.9	102.9	105.9	105.7	105.4	106.5	107.4	108.9	107.1
90	110.3	110.3	107.0	109.7	110.4	109.3	110.8	112.1	113.9	111.6
95	113.2	112.7	109.9	112.0	113.4	112.7	113.8	114.6	116.3	114.1
99	119.6	119.3	118.0	118.2	119.7	120.8	120.4	119.1	120.0	120.4
No Activity (NA)										
Percentiles	**Array-wide**	**14**	**16**	**19**	**22**	**45**	**57**	**63**	**70**	**85**
1	93.1	98.0	92.2	97.2	97.1	93.4	94.7	95.4	97.1	97.6
5	95.3	99.4	93.1	98.3	98.3	94.4	95.8	96.1	97.9	99.1
10	96.7	100.2	93.9	99.6	99.1	95.5	96.9	96.6	98.6	100.0
25	99.3	101.6	95.6	102.4	100.5	98.3	99.6	98.3	100.4	102.0
50	102.8	106.2	98.3	105.4	103.1	101.0	103.2	102.2	103.6	104.7
75	106.9	110.0	106.0	109.5	108.6	106.9	106.3	105.5	107.0	107.9
90	110.3	114.2	108.5	114.0	111.5	109.7	108.8	109.1	109.6	110.2
95	112.2	115.4	109.5	117.8	112.9	110.9	110.3	110.9	110.6	111.3
99	116.3	117.0	111.1	121.7	114.6	112.9	116.7	113.1	112.0	113.7
Vessel Only (VO)										
Percentiles	**Array-wide**	**14**	**16**	**19**	**22**	**45**	**57**	**63**	**70**	**85**
1	92.9	95.7	92.0	95.4	95.0	93.7	96.1	95.4	99.1	93.5
5	95.2	96.8	92.8	96.7	96.0	94.8	97.0	96.8	100.2	95.4
10	96.4	97.6	93.4	97.5	97.0	95.4	97.8	98.1	101.1	97.1
25	99.1	99.8	94.7	99.7	99.1	96.6	99.7	100.8	104.1	99.2
50	103.1	103.5	98.3	104.8	101.7	99.2	103.4	106.3	108.1	101.7

75	108.1	108.7	106.0	109.7	106.9	104.6	107.0	110.8	112.9	106.4
90	112.2	112.6	109.7	112.6	110.7	110.5	109.9	114.5	116.0	112.0
95	114.7	119.3	113.7	114.9	113.3	112.7	111.8	116.3	117.3	114.2
99	119.8	124.9	117.3	120.4	121.7	118.5	115.8	118.9	119.4	118.1
Vessel and MBES (VM)										
Percentiles	**Array-wide**	**14**	**16**	**19**	**22**	**45**	**57**	**63**	**70**	**85**
1	93.5	99.1	93.2	95.8	97.1	94.2	94.9	94.8	98.1	94.7
5	95.7	100.0	94.5	97.0	98.1	96.0	96.8	96.4	99.3	95.9
10	97.1	100.6	95.3	97.9	98.9	97.0	97.9	97.4	100.2	96.7
25	99.6	102.1	97.0	99.8	100.4	98.9	100.4	99.5	102.0	99.3
50	102.8	104.5	99.7	103.6	103.9	103.0	104.0	103.7	104.1	103.6
75	105.7	106.1	102.1	105.4	106.7	105.2	106.2	106.3	106.6	106.0
90	109.2	107.6	104.3	107.5	111.6	108.0	110.6	110.4	111.8	109.6
95	112.4	109.2	107.1	109.8	114.2	111.5	113.7	113.4	114.9	112.9
99	120.1	114.8	116.8	116.7	119.8	120.8	120.3	119.4	121.7	120.1
Mixed Acoustics (MA)										
Percentiles	**Array-wide**	**14**	**16**	**19**	**22**	**45**	**57**	**63**	**70**	**85**
1	91.9	93.5	91.9	92.8	92.8	92.0	93.9	93.9	97.8	92.8
5	94.3	95.7	93.7	96.4	94.6	94.7	95.8	95.6	99.2	94.9
10	95.7	97.2	94.8	97.9	95.6	96.1	97.3	97.1	100.2	96.8
25	98.4	99.5	97.1	99.9	97.5	98.6	100.0	99.7	102.3	100.9
50	101.7	102.5	100.0	102.5	100.3	101.7	102.6	102.9	105.7	104.5
75	105.7	106.4	104.7	106.3	102.9	105.6	106.1	108.0	110.1	110.1
90	110.4	110.8	109.1	110.0	105.7	111.8	111.8	112.9	115.4	113.5
95	113.5	113.0	113.9	111.6	108.3	116.6	115.6	115.3	117.4	115.3
99	120.0	116.3	121.2	114.8	117.3	123.0	121.8	121.4	120.2	123.5

Weighted peak sound pressure level (w*SPLpk*)

Total Study Period										
Percentiles	**Array-wide**	**14**	**16**	**19**	**22**	**45**	**57**	**63**	**70**	**85**
1	73.4	74.9	73.2	74.4	75.0	74.8	74.9	73.6	80.6	74.3
5	77.7	79.2	75.8	77.9	79.0	77.1	78.4	77.4	84.5	79.1
10	80.5	82.4	77.6	80.8	82.1	78.8	81.2	80.4	86.8	81.3
25	85.5	87.2	82.5	84.8	86.2	83.4	86.6	85.7	91.2	86.4
50	91.9	93.2	88.7	91.3	89.7	90.0	93.9	92.5	98.2	92.1
75	101.0	102.7	97.8	97.3	97.3	96.6	103.3	103.3	107.2	100.5
90	108.7	108.8	104.3	105.7	108.0	105.5	110.3	111.5	113.7	109.0
95	112.3	111.5	106.9	109.4	113.0	109.5	114.2	114.5	116.3	112.2
99	118.8	115.4	114.1	114.7	118.4	117.7	120.8	118.8	119.6	118.2
No Activity (NA)										

Percentiles	Array-wide	14	16	19	22	45	57	63	70	85
1	71.9	80.6	73.2	74.2	81.6	74.8	73.7	73.7	78.1	72.8
5	74.0	81.3	74.0	75.2	82.0	75.5	74.6	74.6	79.3	73.7
10	75.4	81.6	74.6	76.1	82.3	75.8	75.5	75.3	80.0	74.7
25	78.5	82.2	75.5	77.7	83.1	76.6	78.0	77.3	82.2	78.6
50	82.5	83.1	76.9	80.6	85.9	78.7	82.8	81.7	84.6	89.6
75	88.6	86.4	79.2	91.5	89.1	83.5	90.9	86.0	87.9	97.3
90	96.2	97.7	82.6	103.9	95.1	89.7	98.1	90.9	93.4	102.3
95	101.5	100.3	85.3	108.0	99.8	93.1	103.7	93.9	97.6	106.4
99	112.7	104.5	92.4	112.7	105.8	96.7	117.5	101.1	104.3	113.7
Vessel Only (VO)										
Percentiles	**Array-wide**	**14**	**16**	**19**	**22**	**45**	**57**	**63**	**70**	**85**
1	74.6	77.3	75.0	75.1	78.1	73.1	79.1	77.8	87.2	77.1
5	78.4	78.4	76.1	77.9	80.0	76.2	80.9	83.3	92.0	79.1
10	80.9	79.4	77.1	82.8	83.0	77.8	82.7	85.8	94.1	80.8
25	86.4	83.9	80.2	88.2	86.7	80.0	88.4	92.4	98.3	84.1
50	94.9	96.1	89.0	96.2	89.4	84.8	95.1	102.9	107.0	90.1
75	104.2	103.2	100.1	105.7	96.7	93.0	101.8	110.7	113.3	102.0
90	110.9	109.1	105.1	110.1	102.6	99.6	106.5	114.9	116.5	111.0
95	114.1	112.3	106.9	112.4	108.3	103.9	109.0	116.6	118.0	114.3
99	118.7	115.9	109.5	119.5	116.9	111.6	114.9	118.8	119.7	118.6
Vessel and MBES (VM)										
Percentiles	**Array-wide**	**14**	**16**	**19**	**22**	**45**	**57**	**63**	**70**	**85**
1	77.2	83.5	77.2	77.3	84.2	77.5	76.4	77.7	82.3	78.8
5	80.7	85.1	79.2	81.0	85.5	79.3	80.7	80.0	84.8	80.6
10	82.9	86.4	81.2	82.0	86.1	82.6	83.4	81.9	86.7	82.2
25	86.6	88.2	83.4	84.8	87.2	85.2	88.3	86.4	89.9	86.9
50	91.7	92.3	87.5	90.9	92.0	90.6	93.7	91.6	95.0	91.6
75	98.8	96.7	92.7	92.8	101.3	94.6	102.6	99.1	103.2	97.8
90	107.3	103.5	100.3	97.7	111.0	104.7	110.0	108.9	110.6	105.3
95	111.5	106.7	104.9	102.5	114.2	109.7	114.0	112.6	114.2	109.1
99	119.1	112.2	115.4	112.4	119.0	118.8	120.5	118.2	119.5	117.3
Mixed Acoustics (MA)										
Percentiles	**Array-wide**	**14**	**16**	**19**	**22**	**45**	**57**	**63**	**70**	**85**
1	71.7	72.9	71.8	72.8	73.9	73.9	74.1	72.3	84.1	73.0
5	74.9	75.5	73.7	75.6	75.3	76.3	76.6	74.1	86.6	76.7
10	77.7	77.4	75.4	80.3	76.8	78.3	78.7	76.3	89.2	79.7
25	83.0	83.3	80.6	85.8	80.2	82.1	84.0	83.0	93.0	85.1
50	89.9	92.9	89.8	92.3	87.8	87.5	90.0	90.4	98.2	91.4
75	99.9	103.7	101.9	101.7	94.0	95.7	103.3	101.3	108.3	105.6
90	108.7	110.5	106.5	108.4	101.2	105.9	112.2	111.8	115.1	111.8

95	112.4	113.1	108.7	110.7	107.4	111.9	116.1	115.0	117.4	113.9
99	118.9	116.4	117.0	113.4	118.1	119.8	122.4	120.7	120.0	121.6

Sound exposure level (*SEL*)

Total Study Period										
Percentiles	**Array-wide**	**14**	**16**	**19**	**22**	**45**	**57**	**63**	**70**	**85**
1	71.0	73.0	71.8	72.9	71.1	71.6	72.9	72.9	74.9	71.5
5	72.5	74.5	72.3	73.8	72.3	72.6	74.0	73.7	75.8	72.8
10	73.4	75.4	72.7	74.3	73.3	73.3	74.7	74.3	76.5	73.6
25	75.2	77.0	73.5	75.6	74.9	74.8	76.0	76.0	77.8	76.0
50	77.5	78.8	75.1	78.1	77.4	77.2	78.3	78.2	79.8	78.9
75	80.5	81.6	77.6	81.0	81.0	80.4	80.6	81.3	81.5	81.5
90	82.9	83.6	80.4	83.4	83.2	82.8	82.6	82.9	83.6	84.8
95	85.1	86.2	83.4	86.2	85.7	85.6	84.8	84.7	85.5	88.1
99	90.4	94.0	89.5	91.3	91.9	91.0	88.6	90.2	90.6	92.9
No Activity (NA)										
Percentiles	**Array-wide**	**14**	**16**	**19**	**22**	**45**	**57**	**63**	**70**	**85**
1	71.3	75.0	71.8	74.8	73.6	71.4	72.9	73.1	74.6	72.6
5	72.9	76.2	72.2	75.7	74.5	72.2	73.5	73.6	75.1	73.2
10	73.9	76.8	72.6	76.8	75.3	72.9	74.2	74.0	75.6	73.6
25	76.0	78.5	73.6	78.9	76.8	75.5	76.6	75.3	77.2	76.8
50	79.6	82.5	75.8	82.2	79.6	78.5	80.3	79.4	80.8	81.3
75	83.9	87.5	83.6	86.0	86.3	84.7	83.7	83.4	84.6	84.8
90	87.7	92.2	86.7	89.3	89.6	87.9	86.4	87.3	87.5	87.7
95	89.6	93.7	88.0	91.5	91.1	89.4	87.7	89.0	88.8	89.0
99	92.6	96.0	90.1	93.3	93.4	91.8	89.8	91.8	90.7	91.0
Vessel Only (VO)										
Percentiles	**Array-wide**	**14**	**16**	**19**	**22**	**45**	**57**	**63**	**70**	**85**
1	71.1	73.3	71.8	73.6	71.8	71.7	73.6	72.8	75.9	71.1
5	72.5	74.0	72.0	74.1	72.6	72.4	74.0	73.8	76.4	72.5
10	73.4	74.4	72.3	74.5	73.2	72.7	74.4	74.9	77.0	73.8
25	75.1	75.9	72.9	75.7	75.1	73.6	76.0	76.8	78.5	75.6
50	77.6	78.6	75.5	78.8	77.4	75.4	78.4	78.5	80.2	77.7
75	81.3	84.4	81.3	83.3	82.5	81.0	81.9	81.5	82.1	81.0
90	85.2	88.3	85.4	87.1	87.1	86.6	85.4	84.5	84.2	84.0
95	87.5	94.1	88.7	88.7	90.6	89.2	87.0	86.9	85.4	85.9
99	92.5	98.4	92.9	91.8	96.4	94.1	89.4	90.7	87.7	89.8
Vessel and MBES (VM)										

Percentiles	Array-wide	14	16	19	22	45	57	63	70	85
1	71.5	75.7	72.2	73.9	73.6	72.0	73.1	73.0	74.9	72.0
5	72.9	76.5	72.8	74.6	74.5	73.2	74.2	73.8	75.7	72.8
10	73.9	76.9	73.2	75.1	75.1	73.9	74.9	74.4	76.3	73.4
25	75.8	77.9	74.0	76.3	76.4	75.2	76.2	76.2	77.6	75.4
50	78.1	80.2	76.0	79.8	79.5	79.0	79.1	79.5	79.8	79.3
75	80.9	82.0	77.9	81.3	81.5	80.7	80.9	81.7	81.1	81.5
90	82.5	82.8	79.2	82.5	82.9	82.1	82.1	82.7	82.3	83.3
95	83.5	83.8	80.5	83.8	84.3	83.3	83.0	83.5	83.6	85.7
99	88.6	87.4	85.3	89.2	90.0	88.7	87.8	88.5	89.7	92.1
Mixed Acoustics (MA)										
Percentiles	**Array-wide**	**14**	**16**	**19**	**22**	**45**	**57**	**63**	**70**	**85**
1	70.4	72.2	71.6	72.1	70.3	71.0	72.5	72.5	74.5	70.8
5	72.0	73.2	72.2	73.2	71.3	72.3	73.5	73.6	75.8	72.3
10	73.0	74.2	72.6	74.3	72.0	73.0	74.5	74.5	76.6	73.8
25	74.7	75.7	73.7	75.7	73.5	74.8	76.2	76.2	78.1	77.1
50	77.0	77.6	75.1	77.4	75.5	76.9	77.7	78.2	80.0	79.2
75	79.6	79.5	76.7	79.2	78.4	79.9	79.7	80.5	82.1	82.0
90	82.3	81.5	79.4	81.8	80.5	82.9	82.1	82.6	84.6	88.0
95	84.6	83.5	82.0	84.4	82.1	84.7	83.9	84.5	86.8	90.3
99	89.9	88.6	88.7	90.7	85.7	88.8	87.9	91.5	93.0	95.8

Weighted sound exposure level (*wSEL*)

Total Study Period										
Percentiles	**Array-wide**	**14**	**16**	**19**	**22**	**45**	**57**	**63**	**70**	**85**
1	48.7	49.6	48.9	49.1	50.6	50.0	49.6	49.1	56.9	49.0
5	51.3	53.3	51.0	51.1	54.0	52.3	50.8	50.6	59.7	50.3
10	53.7	56.6	52.4	54.1	55.5	53.6	52.7	52.8	61.3	53.5
25	58.3	61.6	56.0	58.6	59.6	56.6	58.0	58.5	64.7	58.7
50	63.3	66.0	60.2	62.2	63.3	61.2	62.8	64.7	68.1	64.2
75	68.0	69.5	64.6	67.9	68.1	67.2	68.2	69.6	71.8	68.7
90	71.0	71.0	66.7	69.5	71.8	69.3	70.4	73.4	76.1	72.3
95	73.7	73.2	68.5	70.3	74.5	71.0	72.8	75.8	78.1	74.7
99	79.6	77.9	73.8	74.3	81.5	78.2	78.7	81.2	82.0	82.1
No Activity (NA)										
Percentiles	**Array-wide**	**14**	**16**	**19**	**22**	**45**	**57**	**63**	**70**	**85**
1	48.4	58.0	50.1	51.4	59.0	51.5	50.1	50.6	54.8	49.4
5	49.8	58.4	50.3	52.1	59.2	51.8	50.4	51.0	55.6	49.9
10	50.9	58.7	50.4	52.7	59.4	52.1	50.6	51.3	56.4	50.1
25	52.8	59.1	51.3	54.5	59.8	52.6	51.6	52.1	57.6	51.0

50	56.1	59.8	52.8	56.8	60.5	53.6	52.9	53.2	59.4	55.1
75	59.7	61.5	55.3	59.9	61.7	54.7	54.2	54.9	60.9	62.3
90	63.1	64.4	55.9	67.5	63.5	55.8	55.1	56.3	62.4	64.6
95	66.9	66.3	56.1	70.1	64.4	56.6	56.3	57.2	63.7	65.5
99	75.0	67.0	57.6	73.2	66.2	58.9	62.0	60.4	66.3	67.8
Vessel Only (VO)										
Percentiles	**Array-wide**	**14**	**16**	**19**	**22**	**45**	**57**	**63**	**70**	**85**
1	49.2	54.4	50.6	50.9	54.8	49.1	52.1	50.9	59.9	50.7
5	52.0	54.9	51.0	52.1	55.6	51.0	53.7	51.9	62.6	51.9
10	53.8	55.9	51.8	54.7	56.4	53.0	55.0	53.3	63.5	53.4
25	57.5	58.6	53.2	58.6	59.5	54.1	56.1	61.0	65.7	56.3
50	62.1	64.9	57.5	61.6	63.4	56.6	60.1	66.7	70.5	60.4
75	67.0	67.3	63.9	67.5	64.9	60.2	63.8	71.6	74.7	66.5
90	71.7	70.4	67.0	70.1	67.7	66.3	67.4	75.3	77.3	73.9
95	74.5	74.5	68.4	71.5	70.3	68.6	69.9	77.4	78.8	76.9
99	79.0	77.9	72.0	74.0	83.8	79.1	73.0	82.3	81.1	81.0
Vessel and MBES (VM)										
Percentiles	**Array-wide**	**14**	**16**	**19**	**22**	**45**	**57**	**63**	**70**	**85**
1	52.7	60.6	54.0	54.1	59.9	54.3	51.6	53.2	59.1	53.4
5	56.0	62.0	54.8	57.8	61.7	55.5	56.2	54.8	61.2	55.4
10	57.9	63.1	56.0	58.7	62.2	56.9	58.0	56.3	62.3	56.3
25	61.7	64.1	58.3	60.4	63.5	60.3	61.5	61.8	65.5	60.3
50	65.2	67.2	61.6	66.5	66.5	65.8	67.3	65.7	67.9	66.7
75	69.0	69.7	64.9	68.8	70.5	68.4	69.5	70.1	70.1	69.2
90	71.0	70.3	66.3	69.7	73.6	70.2	71.3	73.1	73.3	70.9
95	73.2	70.8	68.0	70.1	75.8	72.6	73.5	75.5	76.2	72.6
99	79.8	75.5	76.0	74.1	82.8	79.1	79.5	81.8	83.8	81.2
Mixed Acoustics (MA)										
Percentiles	**Array-wide**	**14**	**16**	**19**	**22**	**45**	**57**	**63**	**70**	**85**
1	47.7	49.3	47.6	48.8	50.4	49.2	49.3	48.7	57.4	48.6
5	49.2	49.7	49.1	49.2	50.7	50.8	49.7	49.2	59.9	49.1
10	50.4	51.0	50.5	49.7	51.0	51.9	50.1	49.8	61.1	49.5
25	54.3	55.2	53.0	55.8	54.7	55.0	52.5	52.8	64.0	56.2
50	60.3	60.6	60.2	61.8	57.9	59.6	61.2	62.8	68.1	64.4
75	65.8	67.9	65.1	66.1	61.8	63.6	65.7	67.8	73.7	69.9
90	70.6	72.3	68.1	69.6	66.5	66.4	69.1	73.5	77.3	74.8
95	73.9	75.6	69.5	71.8	68.0	68.9	73.5	75.9	79.0	77.5
99	80.0	80.4	75.1	75.0	73.6	78.5	81.3	81.0	82.1	88.3

12.5 kHz band level (12.5 kHz *BL*)

Total Study Period

Percentiles	Array-wide	14	16	19	22	45	57	63	70	85
1	10.6	10.6	12.5	10.4	11.6	11.8	10.8	10.6	22.5	10.9
5	14.4	18.0	15.5	14.3	15.5	15.0	13.2	13.0	25.6	13.1
10	17.3	21.9	17.2	18.1	18.9	16.8	15.7	16.0	27.2	16.6
25	22.6	27.1	21.3	23.2	24.0	21.3	21.1	22.8	29.9	23.8
50	28.2	30.8	24.8	27.3	29.4	26.5	26.4	29.3	33.2	28.7
75	32.9	34.5	29.6	33.5	34.2	33.2	32.8	34.3	35.8	33.9
90	36.2	36.7	32.4	35.6	36.8	35.7	35.4	37.0	40.8	36.6
95	38.0	38.1	36.0	36.4	38.6	38.5	36.4	38.8	44.6	38.3
99	48.9	48.4	45.8	42.0	51.5	48.6	45.4	49.7	53.4	54.5
No Activity (NA)										
Percentiles	**Array-wide**	**14**	**16**	**19**	**22**	**45**	**57**	**63**	**70**	**85**
1	10.7	24.2	14.3	15.7	24.9	12.8	11.9	12.8	19.7	11.5
5	12.8	24.6	14.7	16.8	25.2	14.6	12.6	13.7	21.0	12.6
10	14.3	24.9	14.9	17.7	25.5	15.7	13.1	14.5	22.2	13.0
25	17.1	25.5	15.6	19.8	25.9	17.1	14.3	15.5	23.7	14.4
50	21.4	26.3	18.4	22.6	26.6	19.0	15.9	16.9	25.4	18.8
75	25.6	27.7	21.2	25.0	27.7	20.1	17.8	18.6	27.9	26.1
90	29.0	30.8	22.0	33.6	30.9	21.4	20.1	20.2	30.7	28.4
95	33.6	33.0	22.3	36.2	32.5	22.1	20.7	21.6	32.5	29.5
99	44.7	33.9	23.3	39.4	35.7	24.5	23.2	25.5	36.4	31.8
Vessel Only (VO)										
Percentiles	**Array-wide**	**14**	**16**	**19**	**22**	**45**	**57**	**63**	**70**	**85**
1	10.8	19.9	15.0	14.2	18.7	9.8	12.5	11.3	24.2	12.1
5	14.1	20.7	15.6	16.1	19.3	11.2	14.2	13.2	27.1	13.7
10	16.4	21.8	16.2	18.1	20.5	13.7	16.1	15.8	28.0	15.2
25	21.0	24.7	17.7	21.8	24.9	15.9	18.3	23.5	29.5	18.8
50	25.5	29.3	22.4	25.4	28.9	20.9	23.2	27.3	31.9	24.2
75	29.7	32.2	25.5	29.4	30.3	25.0	26.4	30.2	33.6	29.7
90	32.4	33.7	30.8	32.0	32.4	30.6	29.3	33.2	36.3	33.0
95	34.6	38.7	32.5	33.6	37.0	34.2	32.7	35.3	38.8	34.5
99	41.5	44.0	35.7	36.2	50.4	45.8	38.2	40.6	43.6	40.2
Vessel and MBES (VM)										
Percentiles	**Array-wide**	**14**	**16**	**19**	**22**	**45**	**57**	**63**	**70**	**85**
1	17.4	27.0	19.6	19.5	25.5	19.2	15.6	15.8	25.2	18.1
5	21.5	28.4	20.6	23.4	27.8	21.2	22.0	19.8	27.1	21.0
10	24.0	29.5	21.1	24.6	28.4	22.9	24.1	21.4	28.0	22.2
25	27.9	30.7	24.3	26.7	30.1	26.9	27.2	28.7	31.1	27.0
50	31.4	33.4	28.1	33.5	33.8	31.3	32.8	32.6	33.8	33.4
75	35.3	36.2	31.1	35.4	36.3	34.8	35.1	36.2	35.4	35.6
90	37.0	37.0	32.9	36.4	37.8	36.9	36.4	37.5	38.6	37.4

95	39.2	38.5	36.8	37.0	41.8	40.5	38.1	41.1	44.0	40.4
99	51.8	48.8	50.1	47.8	57.0	52.5	52.8	53.4	58.1	55.0
Mixed Acoustics (MA)										
Percentiles	**Array-wide**	**14**	**16**	**19**	**22**	**45**	**57**	**63**	**70**	**85**
1	9.4	9.9	9.8	9.6	11.2	11.9	10.2	9.9	22.3	10.1
5	11.3	11.0	12.9	10.7	11.7	14.4	11.0	10.8	25.6	11.2
10	13.0	13.9	14.8	11.8	12.5	15.6	11.9	11.8	27.1	12.0
25	17.9	20.1	18.0	18.8	17.5	18.8	16.9	16.8	30.0	19.8
50	24.3	25.8	23.6	26.4	21.9	23.5	22.6	27.2	33.2	27.9
75	30.0	31.5	28.4	29.5	27.1	30.6	28.0	32.6	37.6	32.2
90	34.1	34.7	35.3	32.6	32.7	33.7	32.2	34.9	43.3	34.0
95	38.0	39.1	38.5	33.4	34.4	39.4	33.2	39.8	46.3	39.9
99	49.4	54.4	46.9	36.4	41.9	49.9	34.0	51.3	52.1	61.9

50 Hz band level (50 Hz *BL*)

Total Study Period										
Percentiles	**Array-wide**	**14**	**16**	**19**	**22**	**45**	**57**	**63**	**70**	**85**
1	36.3	39.3	32.6	36.8	38.0	36.3	38.4	37.1	39.0	38.9
5	43.5	46.5	39.7	43.9	45.2	43.4	45.6	44.2	46.1	46.1
10	46.8	49.8	42.9	47.1	48.4	46.6	48.8	47.4	49.3	49.3
25	51.7	54.5	47.6	51.8	53.1	51.3	53.6	52.1	53.9	54.1
50	56.7	59.1	52.4	56.6	57.7	56.0	58.3	56.6	58.5	59.0
75	61.8	63.7	57.7	61.5	62.6	61.1	63.2	61.3	63.3	64.0
90	67.4	68.7	64.0	67.2	68.2	66.8	68.4	66.7	68.8	69.8
95	71.7	73.2	69.3	72.2	72.8	71.3	72.2	71.3	72.6	73.9
99	80.7	84.2	80.3	81.7	82.4	82.1	80.3	80.9	80.1	81.1
No Activity (NA)										
Percentiles	**Array-wide**	**14**	**16**	**19**	**22**	**45**	**57**	**63**	**70**	**85**
1	43.9	48.1	40.7	44.9	48.2	44.9	44.6	45.1	46.3	43.8
5	51.3	55.3	47.9	52.3	55.5	52.0	52.1	52.2	53.6	51.3
10	54.8	58.6	51.5	55.6	58.8	55.5	55.7	55.7	56.9	55.0
25	60.7	63.5	57.1	60.7	63.8	60.9	61.8	61.1	62.2	61.9
50	67.4	69.2	64.2	66.8	69.7	67.5	68.9	67.8	68.5	70.1
75	74.2	77.8	73.6	73.6	77.1	75.3	74.6	74.8	74.9	75.4
90	79.8	84.1	79.8	79.5	82.1	81.1	78.9	80.0	79.8	79.7
95	82.5	86.8	82.3	82.5	84.5	83.6	81.3	82.7	82.2	82.2
99	86.9	90.5	85.8	86.4	87.9	87.6	85.1	86.9	85.7	86.1
Vessel Only (VO)										
Percentiles	**Array-wide**	**14**	**16**	**19**	**22**	**45**	**57**	**63**	**70**	**85**
1	38.5	40.9	33.8	39.6	40.4	38.0	40.9	39.7	42.5	40.3

5	45.8	48.1	41.3	46.8	47.6	45.2	48.0	46.9	49.6	47.4
10	49.3	51.5	44.7	50.2	51.0	48.5	51.3	50.1	52.9	50.7
25	54.7	56.7	50.4	55.4	56.2	53.8	56.7	55.3	57.9	55.6
50	60.9	63.4	58.0	62.1	62.5	60.1	62.8	61.5	63.2	60.8
75	68.2	71.4	67.1	70.7	70.6	68.2	69.3	68.6	69.1	67.1
90	75.5	78.5	75.2	77.8	77.6	76.7	76.0	75.5	75.3	75.4
95	79.6	82.6	79.1	81.7	81.3	81.3	80.0	79.7	78.6	79.9
99	85.9	88.3	85.0	87.8	86.8	86.9	85.1	85.1	83.0	85.8
Vessel and MBES (VM)										
Percentiles	**Array-wide**	**14**	**16**	**19**	**22**	**45**	**57**	**63**	**70**	**85**
1	35.5	38.5	31.9	36.4	37.4	35.5	37.5	36.2	37.7	37.8
5	42.7	45.7	39.0	43.5	44.5	42.7	44.6	43.3	44.8	44.9
10	45.9	48.8	42.2	46.8	47.6	45.9	47.9	46.5	47.9	48.2
25	50.6	53.4	46.8	51.4	52.1	50.4	52.5	51.0	52.5	52.8
50	55.2	57.7	51.1	55.8	56.3	54.7	56.8	55.2	56.6	57.3
75	59.3	61.6	55.1	59.8	60.1	58.5	60.7	58.8	60.3	61.4
90	63.0	64.9	58.6	63.1	63.5	61.8	64.2	62.0	63.6	64.9
95	65.2	66.9	60.8	65.1	65.6	63.8	66.2	64.0	65.7	67.0
99	69.6	70.6	65.0	68.9	69.8	67.8	70.2	68.1	70.3	71.1
Mixed Acoustics (MA)										
Percentiles	**Array-wide**	**14**	**16**	**19**	**22**	**45**	**57**	**63**	**70**	**85**
1	36.4	39.4	32.9	36.1	38.1	36.2	38.5	37.3	39.1	39.2
5	43.6	46.7	40.0	43.3	45.3	43.4	45.6	44.3	46.1	46.4
10	46.9	50.0	43.2	46.5	48.5	46.5	48.9	47.5	49.4	49.7
25	51.9	54.8	48.1	51.3	53.2	51.3	53.8	52.2	54.1	54.5
50	56.9	59.5	53.1	56.1	57.8	56.3	58.6	56.7	58.7	59.5
75	61.8	63.8	58.4	60.9	62.1	61.3	63.2	61.1	63.2	64.5
90	66.2	67.3	63.2	65.6	65.9	65.6	67.0	65.1	67.6	69.6
95	68.8	69.4	65.8	68.7	68.1	67.9	69.2	67.6	70.3	73.0
99	73.7	73.2	70.8	74.3	72.1	71.8	73.0	73.8	75.7	78.2

40 kHz band level (40 kHz *BL*)

Total Study Period										
Percentiles	**Array-wide**	**14**	**16**	**19**	**22**	**45**	**57**	**63**	**70**	**85**
1	11.9	14.3	12.1	12.9	13.0	13.7	12.7	12.5	13.2	13.0
5	12.5	14.6	12.2	13.1	13.2	13.9	12.9	12.7	13.6	13.2
10	13.0	14.7	12.3	13.2	13.4	14.0	13.1	12.8	14.1	13.3
25	13.8	15.4	12.6	13.6	14.1	14.2	13.6	13.2	16.2	13.8
50	15.5	17.2	13.4	14.9	15.3	14.9	15.8	15.6	19.3	15.7
75	20.2	22.2	16.3	16.9	18.6	16.5	20.7	22.7	28.5	19.9
90	29.7	30.9	25.3	24.2	28.4	22.1	29.1	33.7	37.3	31.4

95	34.4	34.3	28.9	30.4	34.4	27.4	33.4	37.5	40.9	36.2
99	41.2	39.6	33.7	37.0	41.4	34.8	40.1	43.7	45.4	42.4
No Activity (NA)										
Percentiles	**Array-wide**	**14**	**16**	**19**	**22**	**45**	**57**	**63**	**70**	**85**
1	11.7	14.5	12.0	12.9	13.6	13.6	12.7	12.4	13.0	12.9
5	12.1	14.7	12.1	13.1	13.8	13.8	12.8	12.5	13.1	13.1
10	12.4	14.8	12.2	13.2	13.9	13.9	12.9	12.6	13.2	13.2
25	13.2	15.0	12.3	13.3	14.1	14.0	13.1	12.7	13.4	13.5
50	13.8	15.2	12.5	13.6	14.3	14.2	13.3	13.0	13.6	14.6
75	14.6	16.0	12.8	14.3	15.0	14.6	13.9	13.6	14.0	18.0
90	16.4	17.3	13.8	16.0	16.8	15.8	15.3	15.0	15.1	21.7
95	18.9	18.7	14.8	17.5	18.6	16.9	17.0	16.4	16.3	24.0
99	30.2	21.9	17.0	20.7	24.3	19.2	26.2	20.1	19.8	30.3
Vessel Only (VO)										
Percentiles	**Array-wide**	**14**	**16**	**19**	**22**	**45**	**57**	**63**	**70**	**85**
1	11.9	14.4	12.0	12.9	13.1	13.7	12.8	12.5	13.3	12.9
5	12.5	14.6	12.2	13.1	13.3	13.8	12.9	12.7	14.9	13.1
10	13.0	14.7	12.3	13.2	13.4	13.9	13.0	12.9	16.1	13.2
25	13.7	14.9	12.5	13.7	13.9	14.0	13.3	13.9	19.8	13.4
50	16.0	17.9	13.0	16.8	15.4	14.3	14.7	25.2	29.9	14.2
75	24.8	23.9	18.3	25.8	18.2	14.9	18.7	33.5	37.5	23.7
90	33.2	29.1	27.2	31.8	23.1	17.5	24.4	38.5	41.2	35.8
95	37.0	32.5	30.2	34.2	28.3	19.7	28.3	41.4	43.1	40.0
99	42.7	38.2	34.8	37.8	33.9	24.8	33.9	47.0	45.9	44.9
Vessel and MBES (VM)										
Percentiles	**Array-wide**	**14**	**16**	**19**	**22**	**45**	**57**	**63**	**70**	**85**
1	12.1	15.0	12.2	13.1	14.0	13.9	12.9	12.6	13.8	13.1
5	12.9	15.3	12.4	13.3	14.4	14.1	13.1	12.8	14.3	13.3
10	13.4	15.5	12.5	13.4	14.6	14.2	13.3	12.9	14.7	13.5
25	14.3	15.9	12.8	13.7	15.1	14.5	13.9	13.9	16.5	13.9
50	16.0	17.3	13.5	15.2	16.7	15.7	16.7	15.6	18.1	15.7
75	19.0	18.4	14.4	16.5	21.3	16.5	20.6	19.3	23.7	17.8
90	26.1	22.0	17.2	17.2	32.3	20.2	29.3	28.6	30.5	22.7
95	31.3	25.8	20.8	18.4	36.5	25.7	33.4	34.4	35.6	27.9
99	38.9	31.9	28.4	24.8	41.9	36.5	39.0	41.4	41.9	34.5
Mixed Acoustics (MA)										
Percentiles	**Array-wide**	**14**	**16**	**19**	**22**	**45**	**57**	**63**	**70**	**85**
1	11.8	14.2	12.0	12.8	12.9	13.7	12.7	12.4	13.2	12.9
5	12.3	14.4	12.1	13.0	13.0	13.8	12.8	12.6	13.6	13.1
10	12.7	14.5	12.2	13.1	13.1	13.9	12.9	12.7	13.9	13.2
25	13.4	14.7	12.4	13.5	13.3	14.1	13.2	12.9	14.9	13.6

50	14.3	15.3	12.7	14.7	13.8	14.4	14.4	14.0	18.1	15.6
75	17.9	23.1	20.9	19.7	15.4	15.3	19.5	17.5	30.2	27.4
90	30.3	33.1	28.9	31.4	19.2	16.8	30.1	34.2	40.0	37.0
95	35.4	37.3	31.5	35.0	25.9	19.4	35.6	37.9	43.0	39.7
99	42.2	42.0	35.0	39.6	35.9	25.0	45.0	43.7	46.9	44.8

Appendix 5.3. Focused time series annotation.

In the hydrophone 45 annotation, the 12.5 kHz *BL*s were reliably indicative of the survey activity. Thus distinct peaks in the 12.5 kHz *BL*s were used to guide a more directed annotation of the other eight hydrophones with respect to the mapping activity. In addition, peaks in the other sound level metrics that were indicative of anthropogenic activity were also annotated, i.e., asterisked events of the hydrophone 45 time series annotation. For example, simultaneously elevated levels in all *BL*s were considered to be indicative of a vessel passing nearby and were therefore examined further. In a few instances other acoustic events (i.e., high amplitude or extensively elevated sound levels in other metrics than the 12.5 kHz band) were identified on each hydrophone, which served as a check that the survey activity was not missed with this focused approach. The annotations for a given hydrophone are relative to the figure contained within each of the following specific hydrophone sections. Thus, the associated figure number is only referred to in the first mention of the annotation events for a specific hydrophone, but pertains to all subsequent events discussed in a specific hydrophone section. Sound level percentiles were calculated for each of the remaining eight hydrophones for *SPLpk*, 50 Hz, 12.5 kHz and 40 kHz *BL*s. These values were used as a reference to discuss the change in sound levels during each analysis period (i.e., NA, VO, VM, and MA). As with hydrophone 45, baseline was defined as the 50^{th} percentile value for a specific metric, for a specific analysis period, on a given hydrophone. The sound level percentile values are contained in Appendix 5.2.

Hydro 14

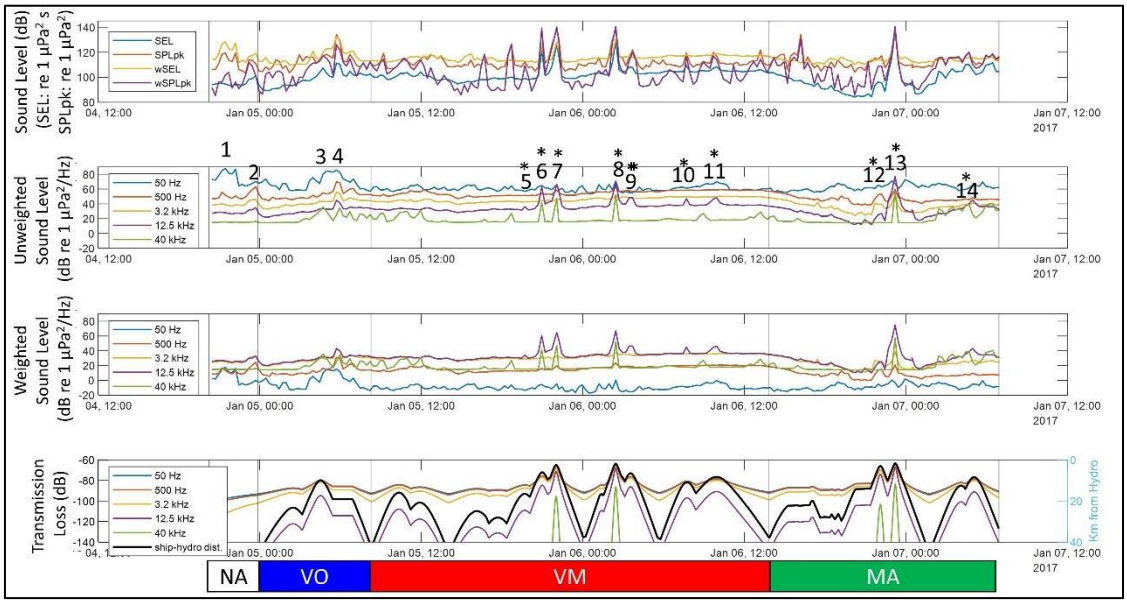

Figure 5.3.1. Sound level time series for hydrophone 14. *First plot*- Broadband sound level time series: *SEL* (blue), *SPLpk* (orange), *wSEL* (yellow), and *wSPLpk* (purple). Numbers indicate acoustic events identified in annotation. Asterisks indicate that the acoustic event was most likely attributed to the survey activity. Perpendicular lines on all graphs delineate the four analysis periods, NA, VO, VM, and MA, shown at the bottom of the figure, respectively. *Second plot*- Select unweighted BL time series: 50 Hz (blue), 500 Hz (orange), 3.2 kHz (yellow), 12.5 kHz (purple), and 40 kHz (green). *Third plot*- Weighted decidecade *BL* time series. Line colors and frequencies are the same as in the second plot. *Fourth plot*-Time series of modelled frequency-specific transmission loss (left axis) and range from hydrophone in kilometers (black line, right axis). Color of frequency-specific transmission loss corresponds to colors of frequencies described for the second plot.

Similar to hydrophone 45, there was an extended time of elevated *SPLpk* during the NA period on hydrophone 14 (event 1, Figure 5.3.1), largely driven by very low frequency sound as indicated by the elevated 50 Hz *BL*. At the end of the NA period (event 2), there was a broadband sound source that elevated sound levels on this hydrophone, likely another passing vessel on the northern edge of the array (the *Sally Ride* was >40 km away). Inspection of this event in the spatiotemporal sound level animation revealed a spatial pattern of elevated sound levels moving from east to west with increasing time.

During the VO period sound levels were generally stable (except again in the 50 Hz band) until the vessel was ~15 km away from the hydrophone about halfway through the period (event 3). At this time there was another loud, very low frequency and continuous sound (10's of Hz), as well as marine mammal clicks around 40 kHz (Appendix 5.1, hydro 14, event 3). The presence of this very low frequency source on this and hydrophone 45 corroborates the hypothesis that this event was not isolated to a single hydrophone. Also in this period, there was another broadband sound source, visible as simultaneous peaks in the time series across all of the select *BL*s (event 4), indicative of a close pass of a vessel near the hydrophone. This does not appear to be the *Sally Ride*, as at this time it was stationary in the middle of the array (19 km from hydro 14) for an hour and a half. Review of the spatiotemporal sound level animation suggests this was another vessel which made its way from east to west across the northern part of the array. The *Sally Ride* made its closest point of approach at ~10 km just before this event, which was not clearly distinguishable as this other, likely closer vessel pass-by (i.e., event 4).

During the VM period, the *Sally Ride* remained greater than 16 km away for the first third of the period and there was no clear detection of the survey vessel on this hydrophone during this time. The next time the vessel was within 17 km of the hydrophone was the first time (event 5) the EM 122 signal was briefly (~30 minutes) detectable above baseline (i.e., baseline was 33 dB re 1 μPa^2/Hz in 12.5 kHz band, Appendix 5.2) on this hydrophone. Peaks in the sound level time series also occurred at RCPAs of 6 (event 6) and 2.5 km (event 7). *SPLpk* increased by more than 30 dB at these RCPAs (note both times it clipped at the closest point of approach so absolute sound levels were not obtained) and did not return to baseline levels (i.e., baseline in *SPLpk* was 104 dB re 1 μPa) until the *Sally Ride* was about 13 km away. The 12.5 kHz and 40 kHz *BL*'s also increased by 25 or more dB when the vessel was closest to the hydrophone. The

survey vessel made another RCPA (2 km) to the hydrophone (event 8), which manifested as a similar signature in the sound levels as event 6 and 7. At each of these three closest approaches (events 6, 7, 8) the 12.5 kHz band increased by as much as 35 dB over baseline (i.e., 33 dB re 1 μPa^2/Hz baseline, peaks in the band of 63, 66, 68 dB re 1 μPa^2/Hz, respectively) and the 40 kHz band increased similarly. The maximum increase in the 50 Hz band was between 7-11 dB (65, 66, 69 dB re 1 μPa^2/Hz, respectively) over baseline (i.e., 58 dB re 1 μPa^2/Hz), corresponding with the closest point of approach. The last three RCPA for this period (events 9, 10, 11) were to 6.4, 10.7 and 8.2 km of hydrophone 14, with maximum peak values in the 12.5 kHz band of 48, 47, and 48 dB re 1 μPa^2/Hz, respectively (about 10 dB over baseline, Appendix 5.2). The peaks in *SPLpk* at these times were 122, 119, and 120 dB re 1 μPa, about 15 dB over baseline (i.e., 105 dB re 1 μPa, Appendix 5.2) for this metric. These RCPAs were not distinguishable as clear peaks on the other select frequency bands. Overall the survey activity during the VM period was distinguishable in the time series for 7 hours (i.e., about one quarter of the period).

The *Sally Ride* was more than 20 km away from hydrophone 14 during the first 8 hours of the MA period. During the middle of this period, there were two RCPAs under 5 km (3.5 and 1.8 km-- events 12, 13, respectively). At the earlier approach (event 12) the EM 122 and the EK-80 were on, while only the EM 122 was on for the later and closer approach (event 13). Interestingly, during the first RCPA (event 12) the signal from the EM 122 was not as pronounced as it had been during similarly close approaches (i.e., event 7) during the VM period, although the second RCPA did have a similar signature to the close passes of the *Sally Ride* during the VM period. Instead the sound level signature of event 12 looked more like the vessel-only RCPAs, where the *BL* peaks scaled similarly with one another. Upon inspecting a spectrogram of this event (Appendix 5.1, hydro 14, event 12), clipped signals were not observed,

which may partly account for the difference in the sound level signature of this event compared to others when the EM 122 was active. Finally, when the vessel came within 8 km of the hydrophone and all the active acoustic sources were on, there were small peaks visible in the select *BL* time series (3-9 dB over the local baseline) and *SPLpk* (10 dB over local baseline) corresponding with this activity (event 14). The survey activity during the MA period was distinguishable intermittently for approximately 4.5 hours (i.e., one quarter of the period).

From the weighted analysis, the entire broadband w*SPLpk* time series on this hydrophone were quite variable, even during the NA period. During the NA period, the peak in w*SPLpk* related to event 2 was presumably associated with ship radiated noise of another passing vessel (Figure 5.3.1, *first plot*). *wSEL* increased most during event 2 in the NA period (associated with another passing vessel), event 3 and 4 in the VO period (associated with the *Sally Ride* and another passing vessel, respectively), events 6, 7, 8 (associated with the *Sally Ride* passing under 5 km of the hydrophone), and event 13 of the MA period (when the *Sally Ride* was under 2 km of the hydrophone). In both the NA and VO periods there were small peaks in the select *wBL*s associated with ship-radiated sound, though in neither case were these related to the *Sally Ride*. The most distinguishable *BL*s were the 12.5 kHz band, but only associated with events identified and tied to the vessel and EM 122 activity. From the weighted perspective, the 50 Hz band was the least distinguishable, though there was much more variability in this band than any of the other select *BL*s (Figure 5.3.1, *third plot*).

Hydro 16

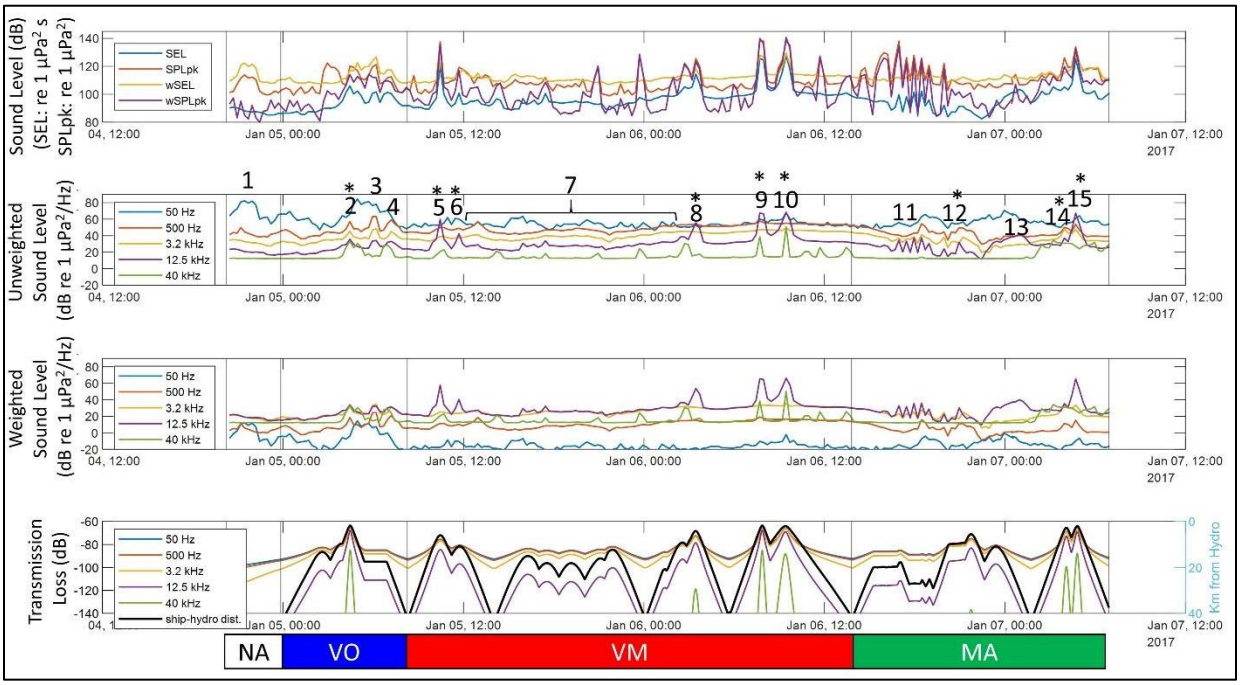

Figure 5.3.2. Sound level time series for hydrophone 16. *First plot*- Broadband sound level time series: *SEL* (blue), *SPLpk* (orange), *wSEL* (yellow), and *wSPLpk* (purple). Numbers indicate acoustic events identified in annotation. Asterisks indicate that the acoustic event was most likely attributed to the survey activity. Perpendicular lines on all graphs delineate the four analysis periods, NA, VO, VM, and MA, shown at the bottom of the figure, respectively. *Second plot*- Select unweighted BL time series: 50 Hz (blue), 500 Hz (orange), 3.2 kHz (yellow), 12.5 kHz (purple), and 40 kHz (green). *Third plot*- Weighted decidecade *BL* time series. Line colors and frequencies are the same as in the second plot. *Fourth plot*-Time series of modelled frequency-specific transmission loss (left axis) and range from hydrophone in kilometers (black line, right axis). Color of frequency-specific transmission loss corresponds to colors of frequencies described for the second plot.

The high-amplitude, low-frequency phenomenon detected on hydrophones 45 and 14 during the NA period was also visible on hydrophone 16 (event 1, Figure 5.3.2), as well as the extended time of elevated very low frequency in the VO period. As these events have consistently been visible on all of the hydrophones they will not be specifically identified and discussed further. There were three events (2, 3, and 4) in the VO period that appeared related to a close approach from a vessel, due to the simultaneous *BL* peaks at each of these times. Event 2 was very likely related to the *Sally Ride* which passed within 2 km of the hydrophone at this

time. At the CPA, *SPLpk* was 121 dB re 1 µPa (23 dB over baseline) and returned to baseline (Appendix 5.2) when the survey vessel was around 13 km away. Event 3 had a similar sound level signature to event 2. However, the *Sally Ride* was stationary at this time, ~17 km away. It is unlikely that the same sound level signature could be produced from a stationary vessel, thus event 3 was likely another vessel passing by the northern edge of the array at this time. This event also occurred only a few minutes after a similar event on hydrophone 14, which further indicates that another vessel was moving by the northern edge of the array from east to west around this time. Similarly, event 4-- which also appeared to be a close pass of a vessel--was unlikely to be the *Sally Ride* which was moving away from hydrophone 16 at this time. Overall the specific activity of the *Sally Ride* in this period was distinguishable for about an hour and fifteen minutes, while vessel activity in general was distinguishable for 3.5 hours.

During the VM period, the *Sally Ride* made a RCPA to hydrophone 16 at ~6 km (event 5) and 11 km (event 6) that were visible in the time series. The sound in the 12.5 kHz band increased starting when the survey vessel was ~16 km away and did not flatten out again until the survey vessel was 13 km from the hydrophone. For the next ~14 hours (event 7) the *Sally Ride* remained 12 km or more from hydrophone 16. During this time, the survey vessel made several RCPAs (i.e., 12- 18 km), some of which the EM 122 signals were faintly visible in a spectrogram. But the small peaks in the 12.5 kHz band (about 3-6 dB) during this time appeared related to some other more continuous energy in this frequency range (Appendix 5.1, hydro 16, event 7). Otherwise, there was no obvious signature of the EM 122 in the sound level time series until the *Sally Ride* was within 15 km of the hydrophone again. At this point the 12.5 kHz *BL* increased as the survey vessel made its next RCPA to 4.5 km (event 8). Once the *Sally Ride* was beyond 11 km, the EM 122 signal was no longer distinguishable in the time series until the

survey vessel was within 16 km of the hydrophone. After the last two RCPAs (events 9 and 10) of the period that were both around 2 km, the signal from the EM 122 was still detectable out to about 12 km from the hydrophone. In total, the survey activity was distinguishable in the sound level time series for approximately 7 hours and 45 minutes during the VM period.

The MA period sound levels were dynamic on hydrophone 16. There was no obvious change in the sound levels with respect to the first calibration event, which occurred about 20 km from the hydrophone. About the time of the second calibration event, the *SPLpk*, 12.5 kHz, and 3.2 kHz *BL*s fluctuated rapidly (event 11). A closer inspection of a spectrogram of the event (Appendix 5.1, hydro 16, event 11) revealed pulses spaced ~300 ms apart extending from 2 to 10 kHz; the source of the pulses is unknown. However, this did not seem related to the calibration event as the *Sally Ride* was more than 25 km away and signals were detected in the acoustic data outside of the time when calibration signals were transmitted. After the calibration testing, the vessel made the next RCPA to within 5.5 km, though it was an hour before this when the vessel was around 9.5 km from the hydrophone that the EM 122 signal was most prominent (event 12). After this, the vessel transited to more than 40 km away from hydrophone 16 during which time the 12.5 kHz *BL*s steadily increased (event 13). A closer inspection of this event on a spectrogram revealed what was clearly biological activity, consisting of frequency upsweeps from 4-14 kHz (Appendix 5.1, hydro 16 event 13).

The two closest points of approach (2.7 km and 2 km, respectively) during this period occurred at the end of the period. The first was when only the SBP was on (event 14), and the second was when all of the active acoustic sources were on (event 15). Event 14 corresponded to an increase over the local baseline of approximately 10 dB in the 500 Hz band, 14 dB in the 3.2 kHz band, and 10 dB in the 12.5 kHz band. Event 15 corresponded with the time when all active

acoustic sources were on, manifesting as an increase over the local baseline of 15 dB in the 500 Hz band, 13 dB in the 3.2 kHz band, and 49 dB in the 12.5 kHz band. The EK-80, EM 122, SBP signals were all visible in the spectrogram for event 15. Although EM 712 was on at this time, it was not visible in the 40 kHz band levels or in the spectrogram (Appendix 5.1, hydro 16, event 15). Even at 2 km the transmission loss for the EM 712 signal is about 87 dB, which likely accounts for why the signal was not readily visible. The elevated 3.2 kHz *BL* corresponding to these events began when the *Sally Ride* was 12 km away and flattened again when the vessel was beyond 7 km away, roughly 1 hour and 45 minutes of the MA period (~ 1/3 the MA period).

From a weighted perspective, the *wSEL* in the NA period was largely stable, while the w*SPLpk* in the same period was highly variable, suggesting the energy in the period was the same throughout but the source mechanism varied. During the VO period, peaks in both broadband metrics correlated with the three vessel approaches identified in the annotation (events 2, 3, and 4). During the VM period, the largest peaks in the *wSEL* and w*SPLpk* correlated with the peaks associated with survey activity, though smaller peaks of undetermined origin were also present. In the MA period, the weighted broadband levels fluctuated rapidly, with the highest and most numerous peaks corresponding to what appeared to be biological activity. Although the final closest approach of the *Sally Ride* when all active acoustic sources were on was equally prominent (Figure 5.3.2, first plot). The weighted 12.5 kHz and 3.2 kHz *BL*s were equally dominant throughout the study, except mainly at times when the survey activities were within 18 km of the hydrophone (i.e, events 5, 6, 8, 9, 10, 12, 14), as well as when there was significant biological activity near the hydrophone (event 13). At these times the 12.5 kHz *BL*s were most dominant. Similarly, there were a few instances where the weighted 40 kHz band was slightly higher (i.e., in the VO and MA periods), which coincided with times when there were 40

kHz clicks present in the acoustic data, presumably from marine mammals, such as foraging beaked whales. (Figure 5.3.2, *third plot*)

Hydro 19

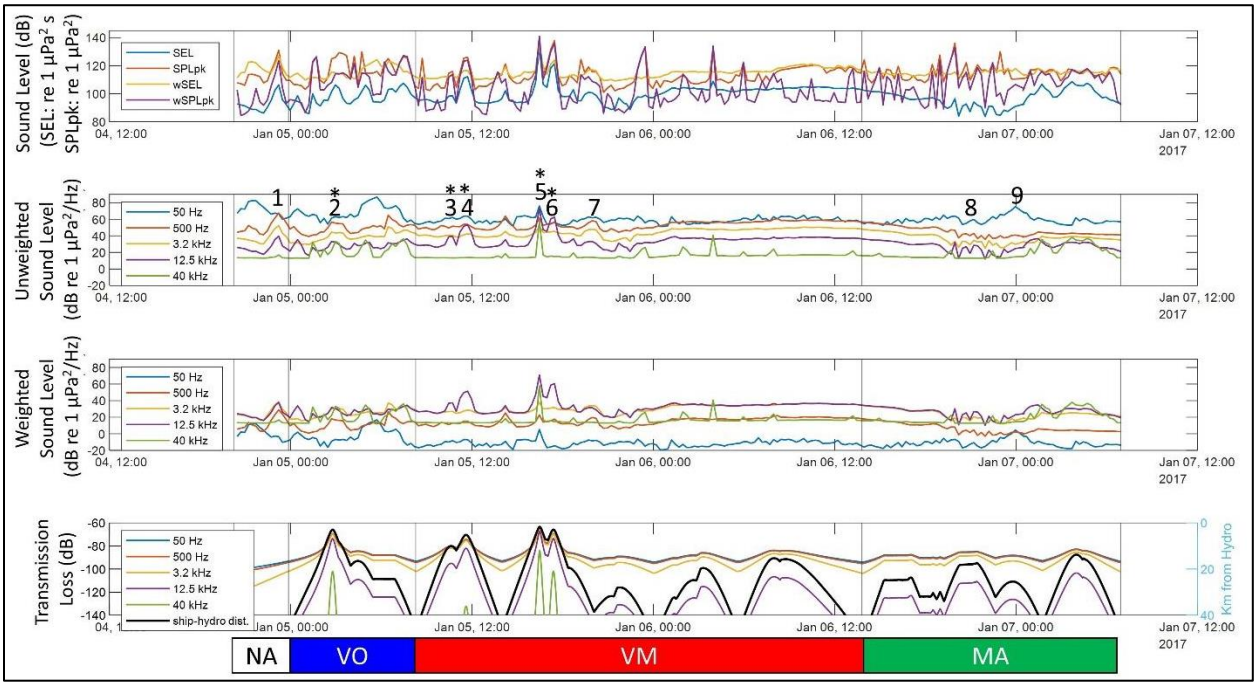

Figure 5.3.3. Sound level time series for hydrophone 19. *First plot*- Broadband sound level time series: *SEL* (blue), *SPLpk* (orange), *wSEL* (yellow), and *wSPLpk* (purple). Numbers indicate acoustic events identified in annotation. Asterisks indicate that the acoustic event was most likely attributed to the survey activity. Perpendicular lines on all graphs delineate the four analysis periods, NA, VO, VM, and MA, shown at the bottom of the figure, respectively. *Second plot*- Select unweighted BL time series: 50 Hz (blue), 500 Hz (orange), 3.2 kHz (yellow), 12.5 kHz (purple), and 40 kHz (green). *Third plot*- Weighted decidecade *BL* time series. Line colors and frequencies are the same as in the second plot. *Fourth plot*-Time series of modelled frequency-specific transmission loss (left axis) and range from hydrophone in kilometers (black line, right axis). Color of frequency-specific transmission loss corresponds to colors of frequencies described for the second plot.

The sound level time series on this hydrophone suggested there was a close approach by a vessel (event 1, Figure 5.3.3) during the NA period. This was not the *Sally Ride* which was beyond 40 km at the time. During the VO period the sound levels were dynamic, corresponding to multiple instances of what appeared to be biological activity and/or vessels passing nearby. The *Sally Ride* closely approached this hydrophone to within ~3.1 km, at which time there was

also biological activity in the 40 kHz band (event 2). This corresponded with local increases in the 500 Hz band of 13 dB, 5 dB in the 3.2 kHz band, and 10 dB in the 12.5 kHz band. The close pass of the *Sally Ride* was distinguishable for about an hour and a half during this period. During the VM period the vessel passed to within 10 km (event 3), 5.3 km (event 4), 2.2 km (event 5), and 2.9 km (event 6) of hydrophone 19, corresponding to peaks in the 12.5 kHz band of 10, 26, 40, and 31 dB over the local baseline. The vessel then transited away from hydrophone 19, at which time there was another event (event 7) characterized by a similar magnitude increase in the 50 Hz-12.5 kHz *BL*s, indicative of a vessel passing nearby. At the peak levels of this event, the *Sally Ride* was over 35 km away, thus related to a different vessel passing near the hydrophone. For the remainder of the period the survey vessel was more than 15 km away from this hydrophone and there was no obvious change in the sound level time series related to its activity. In total, the survey activity was distinguishable in the sound level time series for approximately 5 hours of the VM period. Similarly during the MA period, the *Sally Ride* was almost always beyond 14 km from hydrophone 19 with no obvious contributions of its acoustic sources to the sound levels on this hydrophone during the MA period. Similar sound level fluctuations detected on hydrophone 16 (events 11 and 12) were visible in the hydrophone 19 time series (events 8 and 9). Event 8 was characterized by broadband clicks, whereas event 9 had broadband clicks and significant biological activity (Appendix 5.1, hydro 19, event 8 and 9).

The weighted broadband sound level metrics (*wSEL*, w*SPLpk*) in all four periods were noticeably variable. However, the second half of the VM period and first third of the MA period were fairly stable in terms of *wSEL*. The peaks in w*SPLpk* of the NA and VO periods seemed to be driven by a few close passes of vessels, as indicated by peaks in all *BL*s 12.5 kHz or less. Only one of these instances (event 2) in the VO period appeared related to the *Sally Ride*. In the

weighted frequency *BL* time series, the 12.5 kHz, 40 kHz, and 3.2 kHz bands fluctuated similarly, alternating as the most dominant of the *BL*s examined. In each case the dominant band was generally <5 dB more than the other *BL*s. During the VM period, there was consistently separation between the select *BL*s, with the 50 Hz band being significantly quieter than the other *BL*s (i.e., 50 Hz time series did not intersect the other time series). The 3.2 kHz and 12.5 kHz were generally most dominant, while the 40 kHz and 500 Hz were intermediate out of the five select *BL*s. During events 3, 4, 5, and 6 –all linked to the close approach of the *Sally Ride* when the EM 122 was active—the 12.5 kHz band was the most dominant, i.e., large peaks distinguishable over the other *BL* time series. During the MA period, the levels were generally stable until the two annotated events which appeared to be related to biological activity and a broadband and pulsed signal from an undetermined source. At these times the *BL* time series were much more unstable--more like the VO period—with the 12.5 kHz and 40 kHz bands alternating as the most dominant but only by a few decibels (i.e., <5 dB).

Hydro 22

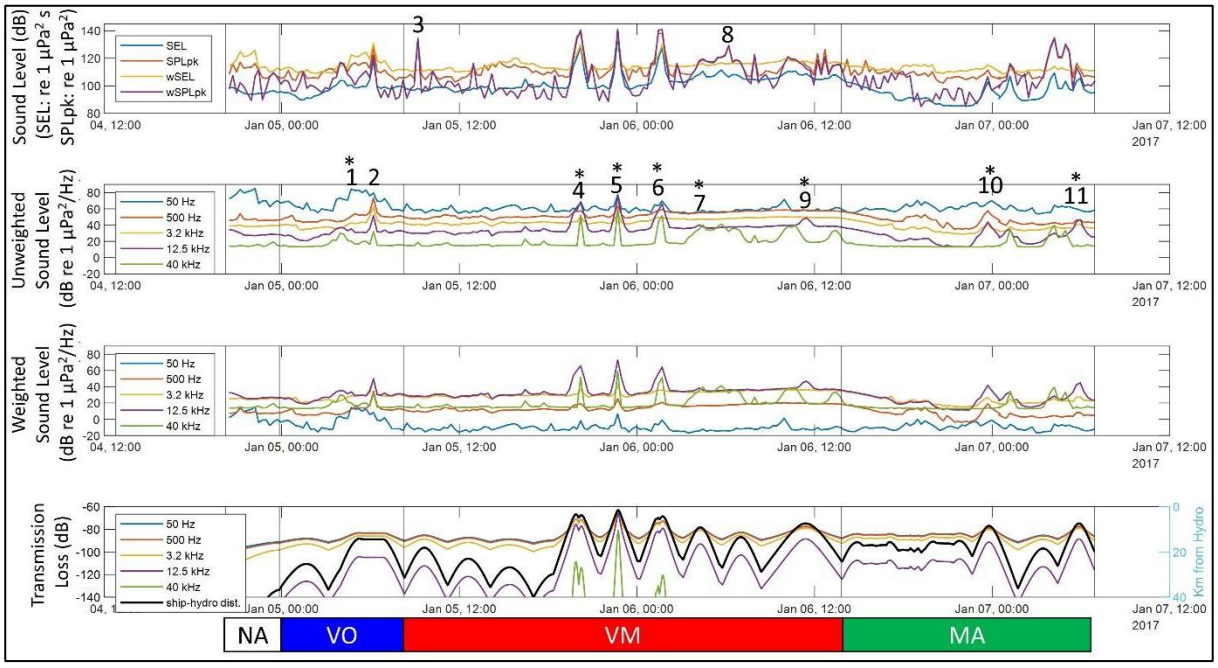

Figure 5.3.4. Sound level time series for hydrophone 22. *First plot*- Broadband sound level time series: *SEL* (blue), *SPLpk* (orange), *wSEL* (yellow), and *wSPLpk* (purple). Numbers indicate acoustic events identified in annotation. Asterisks indicate that the acoustic event was most likely attributed to the survey activity. Perpendicular lines on all graphs delineate the four analysis periods, NA, VO, VM, and MA, shown at the bottom of the figure, respectively. *Second plot*- Select unweighted BL time series: 50 Hz (blue), 500 Hz (orange), 3.2 kHz (yellow), 12.5 kHz (purple), and 40 kHz (green). *Third plot*- Weighted decidecade *BL* time series. Line colors and frequencies are the same as in the second plot. *Fourth plot*-Time series of modelled frequency-specific transmission loss (left axis) and range from hydrophone in kilometers (black line, right axis). Color of frequency-specific transmission loss corresponds to colors of frequencies described for the second plot.

Aside from the elevated very low frequency array-wide phenomenon, the NA period sound levels were fairly stable, suggesting there was little activity recorded on this hydrophone. In the VO period, the close pass of the *Sally Ride* (event 1, Figure 5.3.4) manifested as a subtle increase in the sound levels, likely because the survey vessel remained about 14 km away from the hydrophone for about two hours before transiting away (this was noticeable as a small decrease in the *BL*s). This event also occurred at a time of significant biological activity

(Appendix 5.1, hydro 22, event 1). During this period, there was a clear signature in the sound levels of a vessel passing nearby (event 2), which was unlikely the *Sally Ride* which was stationary at this time. The presence of the survey vessel in the sound level time series of the VO period was distinguishable, but hardly, for approximately 2 hours. It was overshadowed by the louder activity of event 2 which was not attributed to the *Sally Ride*.

During the VM period the *Sally Ride* was over 18 km away from hydrophone 22 for the first 10 hours of the survey and there was no obvious change in the sound levels on this hydrophone due to its activity. However there was a very loud pulse at frequencies of 1 kHz and lower, as well as some short clicks between 10-40 kHz, that correlated with the peak in the *SPLpk* of event 3 (Appendix 5.1, hydro 22, event 3). Once the *Sally Ride* came within 14 km of the hydrophone the 12.5 kHz band levels increased again, during which time the survey vessel made three RCPAs (events 4, 5, and 6) in 7 hours to within 3.5, 2, and 4.3 km, respectively, of the hydrophone. Between each RCPA the vessel moved far enough away again that the signal of the EM 122 was no longer distinguishable in the sound level time series, which was at about 13.5 km from the hydrophone. During each of these events, the signal from the EM 122 was visible for about an hour. Because of the very close approaches to the hydrophone the signal clipped and the maximum *SPLpk* value was not recovered. The maximum sound level recorded for the 12.5 kHz band were 34, 41, and 32 dB, respectively, over baseline (Appendix 5.2). But again, due to the clipped signal the actual levels may have been higher. After these very close approaches, the *Sally Ride* continued to run lines further and further away from hydrophone 22. The next RCPA (event 7) was to 9 km from the hydrophone. This corresponded with an increase of 6 dB in the 12.5 kHz band, and 15 dB in *SPLpk* over the respective baseline (Appendix 5.2) for the analysis period, as well as an elevated 40 kHz band (Figure 5.3.4, *second plot*, event 7).

Upon inspection of the spectrogram related to this event, the mechanism driving the elevated *SPLpk* was likely the prominent biological clicks in the 40 kHz band, rather than the EM 122 signal which was faintly visible at this time (Appendix 5.1, hydro 22, event 7). Marine mammal clicks appeared to be the same mechanism driving the peak in *SPLpk* at event 8, and in this case the EM 122 signals were not distinguishable (Appendix 5.1, hydro 22, event 8). The signal of the EM 122 at the next RCPA of 13.4 km was not visible in the time series. The last RCPA (event 9) for the period was within 7.5 km of the hydrophone with a peak in the 12.5 kHz band and *SPLpk* that at its maximum was 15 and 10 dB, respectively, over the respective baselines (Appendix 5.2). Overall the survey activity was distinguishable in the sound level time series for 6 hours during the VM period.

The *Sally Ride* was over 15 km away during the calibration tests of the MA period and there was no obvious impact on the sound levels on hydrophone 22 related to the distant activity of the survey vessel. The *Sally Ride* made its first RCPA during this period at 8.5 km when the EM 122 was actively transmitting (event 10). The 12.5 kHz band was not as peaked as in the close passes during the VM period, likely because the EM 122 signal was not close for clipping to occur (Appendix 5.1, hydro 22, event 10). Elevated levels in the other lower frequency *BL*s were also visible during this event, likely because the ambient conditions were low prior to and after this event such that the signature of the closely passing vessel was not masked. At maximum, there was a 7 dB increase in *SPLpk*, 22 dB increase in the 12.5 kHz band over baseline and local increase of 5-10 dB in the 500 Hz and the 3.2 kHz *BL*s related to this event. The *Sally Ride* made another RCPA to within 18 km of the hydrophone that was not distinguishable in the time series. The final RCPA was to within 7.3 km of hydrophone 22 (event 11) when all of the acoustic sources were transmitting. During event 11, there was a maximum

increase over baseline in *SPLpk* of 16 dB and of 25 dB in the 12.5 kHz band, and a local increase of 6 dB in the 3.2 kHz band. The peaks in the 3.2 kHz band related to events 10 and 11 were of similar magnitude (~41 dB re 1µPa^2/Hz), despite the SBP active only during event 11. This suggested that the signal of the SBP did not make a significant contribution to the changing sound levels in this band beyond that of the vessel radiated sound associated with the close passage of the *Sally Ride* near the hydrophone. The EM 712 was the only signal not visible in a spectrogram of event 11 (Appendix 5.1, hydro 22, event 11). The activities related to the mapping activity were distinguishable in the sound level time series for approximately 4 hours.

The w*SPLpk* fluctuated throughout the entire study with similar variability across periods—i.e., at most, changes of about 25 dB. There were exceptions however, which were related to the close pass of another vessel during the VO period, the three close passes of the *Sally Ride* during the VM period, and some biological activity during the VM and MA periods. *wSEL* fluctuated less, but the most obvious fluctuations were also generally associated with the survey activity. Of the weighted *BL*s examined, the 12.5 kHz and 3.2 kHz *BL*s were consistently most dominant, while the 12.5 kHz band dominated during times linked to the survey activities. There were a few times when the 40 kHz band was higher than the 12.5 kHz band levels, but generally by less than 10 dB. These events included times when clicks were detected in the acoustic data, presumably from marine mammals.

Hydro 57

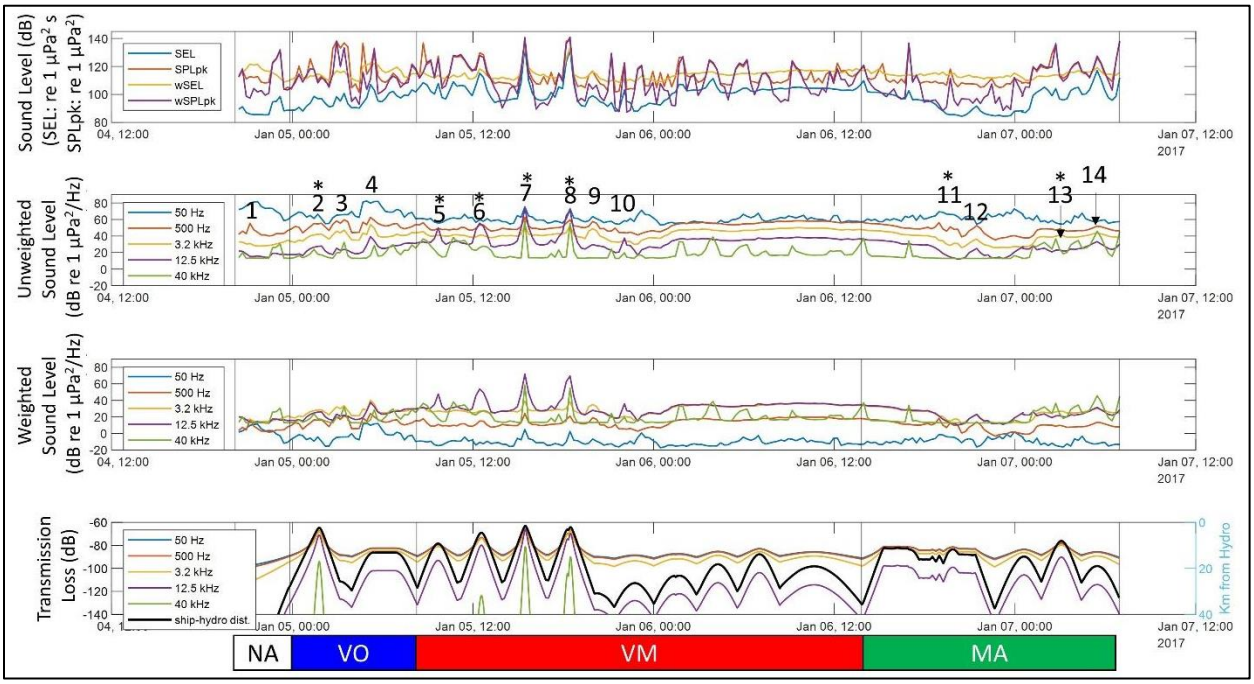

Figure 5.3.5. Sound level time series from hydrophone 57. *First plot*- Broadband sound level time series: *SEL* (blue), *SPLpk* (orange), *wSEL* (yellow), and *wSPLpk* (purple). Numbers indicate acoustic events identified in annotation. Asterisks indicate that the acoustic event was most likely attributed to the survey activity. Perpendicular lines on all graphs delineate the four analysis periods, NA, VO, VM, and MA, shown at the bottom of the figure, respectively. *Second plot*- Select unweighted BL time series: 50 Hz (blue), 500 Hz (orange), 3.2 kHz (yellow), 12.5 kHz (purple), and 40 kHz (green). *Third plot*- Weighted decidecade *BL* time series. Line colors and frequencies are the same as in the second plot. *Fourth plot*-Time series of modelled frequency-specific transmission loss (left axis) and range from hydrophone in kilometers (black line, right axis). Color of frequency-specific transmission loss corresponds to colors of frequencies described for the second plot.

Aside from the array-wide elevated levels in the 50 Hz band during the NA period, there was a peak in the 500 Hz band on hydrophone 57 (event 1, Figure 5.3.5). Upon inspection of the spectrogram of the event it appeared to be related to ship radiated sound from some vessel other than the *Sally Ride* which was over 40 km away at the time (Appendix 5.1, hydro 57, event 1). During the VO period there were three events that appeared to be related to a close pass of a vessel (event 2, 3, and 4). Only one of these corresponded to the *Sally Ride* (event 2), as the increase in *BL*s corresponded with the RCPA of the survey vessel to 2.5 kilometers of

hydrophone 57 during this period. This event was distinguishable for approximately 1 hour and 45 minutes in the time series, while the vessel was within about 15 km of the hydrophone. The other two events occurred when the *Sally Ride* was transiting further away from hydrophone 57 (event 3) and when the survey vessel was approaching but remained at a stable distance of 13 km from the hydrophone (event 4). Neither of the survey activities at these times intuitively match the peaks in the sound level time series, suggesting these events (3 and 4) were likely linked to some other vessel transiting near hydrophone 57 along the western edge of the array. Hydrophone 57 is located on the western edge and deeper side of the array, where many vessels may pass, thereby avoiding the navy range.

During the VM period the *Sally Ride* made several RCPAs by hydrophone 57 within the first half of the period (events 5, 6, 7, and 8). These were at 9, 4.6, 1.5, and 2 km, respectively. At maximum, the sound levels associated with these events were 23, 23, 41, and 38 dB, respectively, over baseline in the 12.5 kHz band, and 23, 26, 34, and 32 dB, respectively, over baseline for *SPLpk* (Appendix 5.2). During each of these events, the EM 122 signal was visible in the 12.5 kHz band time series as elevated sound levels for about 1-1.5 hours including approach and departure from the RCPA. After event 8, the vessel transited to more than 30 km away from hydrophone 57 during which there was another signature in the time series indicating the close approach and departure of another vessel (Figure 5.3.5, event 9). The *Sally Ride* remained more than 13.5 km away from the hydrophone for the remainder of the VM period and was not discernible in the sound level time series of hydrophone 57 during this time. There was one other peak in the 12.5 kHz band while the *Sally Ride* was 30 km away, and this appeared to be a continuous sound of undetermined origin (Appendix 5.1, hydro 57, event 10). Overall, the

activity of the survey vessel was distinguishable for about 6 hours and 15 minutes in the time series of hydrophone 57.

During the calibration testing at the beginning of the MA period, the distance of the *Sally Ride* to the hydrophone ranged from 12 to 18 km. There was no obvious change in the sound levels with respect to this activity. During this period, the survey vessel made a close approach to within 12 km of the hydrophone when the EM 122 and the EK-80 were on. Though the ship-radiated sound was visible in the time series (*SPLpk*, 50 Hz, and 500 Hz *BL*s) and a spectrogram, neither echosounder signal was visible at this distance. There was also a repetitive pulse present in the spectrogram, which was likely responsible for the peaks present in the time series, which had a center frequency of 400 Hz but bandwidth up to 10 kHz (Appendix 5.1, hydro 57, event 11). It is unclear what the source of this repetitive pulse was. Just after this RCPA, there was a clear signature in the *BL*s indicating a nearby passing vessel (Figure 5.3.5, event 12; Appendix 5.1, hydro 57, event 12). This occurred when the *Sally Ride* was holding steady 12 km from hydrophone 57, which suggests the event was most likely attributed to another passing vessel. The CPA of the survey vessel to hydrophone 57 during this period was 8 km and was hardly distinguishable in the sound level time series (event 13). The 3.2 kHz and 500 Hz bands had very small increases at this time. It is worth noting that the SBP was also on during this CPA, and the pulses were visible in the spectrogram of this event (Appendix 5.1, hydro 57, event 13). The peak in *SPLpk* seemed to correlate with the peak in the 40 kHz band just prior to event 13. The 40 kHz peak appeared to correspond with marine mammal clicks at this frequency. The acoustic sources of the survey during the final RCPA of the period to within 18 km were not distinguishable in the spectrogram of this event (14). The peak in *SPLpk* was again likely related to marine mammal clicks as the EM 712 signal at the distance the ship was to the hydrophone,

i.e., 19 km, was much more than 140 dB (Figure 5.3.5, *fourth plot*, event 14). During this event there also appeared to be another vessel passing nearby at the same time (Appendix 5.1, hydro 57, event 14). Examining the spatiotemporal animation verified this was not associated with the *Sally Ride* (only the sound levels on hydrophones directly surrounding the vessel appeared correlated with its presence at this instance). Overall, the survey activity during the MA period was distinguishable for approximately 1.5 hours.

From a weighted perspective the broadband levels appeared equally variable with both moderate fluctuations throughout all four periods (Figure 5.3.5, *first plot*). The 3.2, 12.5, and 40 kHz weighted *BL*s (Figure 5.3.5, *third plot*) were similarly distinguishable in the NA period, though there was one particular time when the 40 kHz band was clearly more dominant (i.e., up to 8 dB over the other *BL*s). All but the 50 Hz bands were similarly distinguishable during the VO period. The overlap of these bands was likely attributed to the numerous close approaches of ship-radiated sound during this period, which really elevated the lower frequency bands. During the VM period the pattern was consistent with other hydrophones: the 3.2 kHz and 12.5 kHz bands were consistently the most dominant, but the 12.5 kHz dominated when the *Sally Ride* was close to the hydrophone during events 5, 6, 7, and 8. This was similar in the first half of the MA period, whereas during the later half of the MA period the 40 kHz band was at times more dominant than the other *BL*s. In some cases, this was attributable to marine mammal clicks, while in other cases the signals were more pulse-like and the source was unclear.

Hydro 63

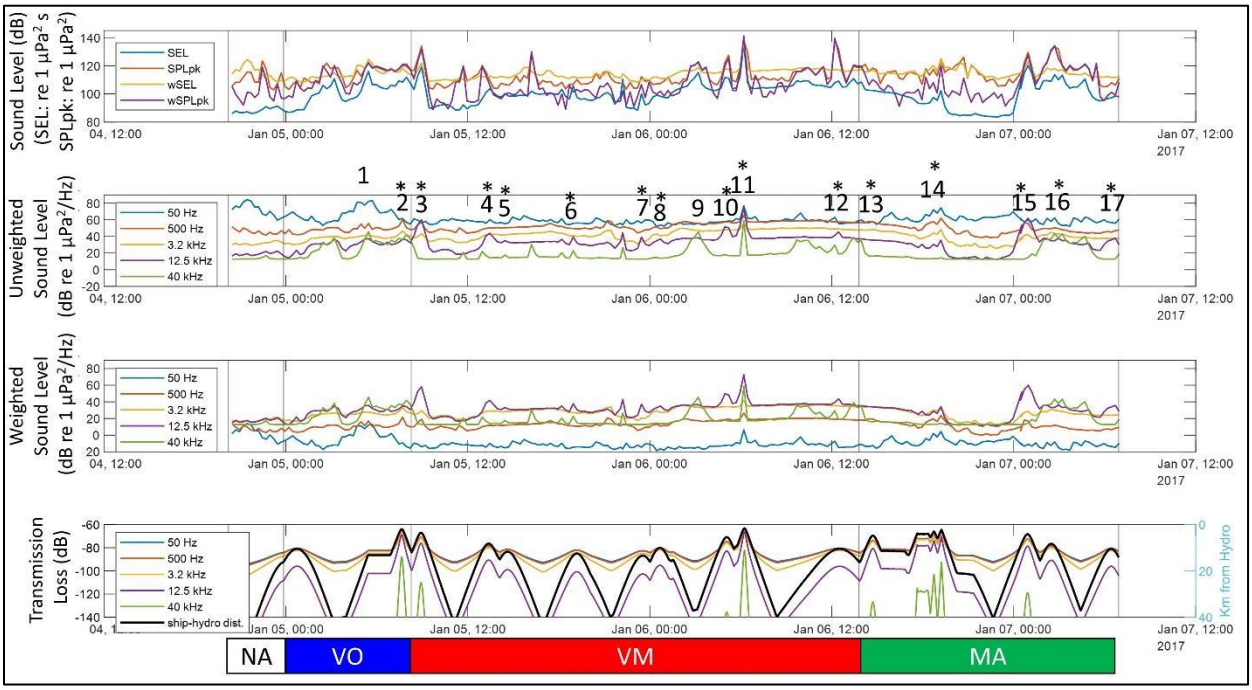

Figure 5.3.6. Sound level time series for hydrophone 63. *First plot*- Broadband sound level time series: *SEL* (blue), *SPLpk* (orange), *wSEL* (yellow), and *wSPLpk* (purple). Numbers indicate acoustic events identified in annotation. Asterisks indicate that the acoustic event was most likely attributed to the survey activity. Perpendicular lines on all graphs delineate the four analysis periods, NA, VO, VM, and MA, shown at the bottom of the figure, respectively. *Second plot*- Select unweighted BL time series: 50 Hz (blue), 500 Hz (orange), 3.2 kHz (yellow), 12.5 kHz (purple), and 40 kHz (green). *Third plot*- Weighted decidecade *BL* time series. Line colors and frequencies are the same as in the second plot. *Fourth plot*-Time series of modelled frequency-specific transmission loss (left axis) and range from hydrophone in kilometers (black line, right axis). Color of frequency-specific transmission loss corresponds to colors of frequencies described for the second plot.

The sound levels of the NA period of hydrophone 63 were relatively stable in comparison to some of the other hydrophones (i.e., western edge hydrophones). There was a lot of biological activity in the 7-15 kHz, and 20-40 kHz ranges during the VO period (event 1, Figure 5.3.6). The *Sally Ride* was 13 km away at this time and may have contributed to some of the low frequency background noise, though the elevated 50 Hz band was largely related to the array-wide phenomenon identified on other hydrophones. The activity of the *Sally Ride* was distinguishable

in the sound level time series during event 2 when it made its closest approach to 2 km away, distinguishable in the time series for roughly an hour (Appendix 5.1, hydro 63, event 2).

During the VM period the *Sally Ride* made its first RCPA at 3.5 kilometers which was most visible in the 12.5 kHz band and *SPLpk* while the survey vessel was within 15.5 km of the hydrophone (event 3). At its maximum, the sound levels were 27 dB (12.5 kHz band) and 30 dB (*SPLpk*) over baseline (Appendix 5.2). Over the next 20 hours the vessel made five RCPAs between 8-12 km from hydrophone 63, which were visible as small peaks in the 12.5 kHz band time series (events 4, 5, 6, 7, and 8) at their maximum, approximately 2-11 dB over baseline (Appendix 5.2). *SPLpk*, at corresponding times, was between 3-16 dB over baseline, with the greatest change occurring when the vessel was 8 km away, although the increase in *SPLpk* was not necessarily solely attributed to the survey activity proximity. For each of these events the 12.5 kHz band began to steadily increase when the vessel was within 14-19 km of the hydrophone. Later, the *Sally Ride* came within 5.6 km (event 10) and 1.8 km (event 11) of the hydrophone within the same hour, after which the vessel ran another line across to the other end of the range and back before the final RCPA at 10.4 km at the end of the VM period (event 12). These events (10, 11, and 12) corresponded to increases in the 12.5 kHz band over baseline (Appendix 5.2) of 19, 42, and 12 dB with increases in *SPLpk* of 24, and more than 34 dB as the hydrophone clipped (events 11 and 12). There was also other acoustic activity present (i.e., clicks between 3-20 kHz) that seemed to account for the clipping during event 12 (Appendix 5.1, hydro 63, event 12). There was one particularly loud period in the 40 kHz band, which can be attributed to marine mammal clicks (Appendix 5.1, hydro 63, event 9). At maximum the levels were 28 dB over the local baseline which was associated with a maximum *SPLpk* of 122 dB re 1 µPa.

Overall the survey activity was distinguishable in the time series for 9 hours and 30 minutes of the VM period.

During the MA period the vessel made its first RCPA to within 5 km (event 13). At this time the EM 712 (40 kHz) was on although it was not visible in the time series or spectrogram of this event, as the transmission of this MBES is both directional and would incur a transmission loss of about 130 dB at this distance. There was also no obvious change in sound levels at this time related to the proximity of the survey vessel to the hydrophone. During the calibration testing over hydrophone 65, the *Sally Ride* was within 4 km of hydrophone 63. The sound level signature related to the ship-radiated sound from the close proximity of the vessel to hydrophone 63 was visible in event 14 (Appendix 5.1, hydro 63, event 14). Although a few signals that may have been the test signals of the calibration test were visible in spectrograms around the time of testing, they unlikely impacted the sound level time series as there were very few (<20) signals transmitted. After this RCPA, the *Sally Ride* transited to nearly 40 km away from hydrophone 63 before coming back again. The survey vessel then made three RCPAs to 4.4, 8.3, and 10.4 km of hydrophone 63 (events 15, 16, and 17). During the closest pass (event 15) only the EM 122 was on, visible as peaks in the 12.5 kHz band and *SPLpk* that were 39 dB and 25 dB over baseline (Appendix 5.2), respectively. During event 16 1.5 hours later, only the SBP was on (Appendix 5.1, hydro 63, event 16). At this time the 3.2 kHz band peak was 3 dB higher than during event 15 when the SBP was off, although the vessel was twice as far away. During the final pass near the hydrophone all acoustic systems were on (event 17), and the contribution of the EM 122 manifested in the time series as a peak in the 12.5 kHz band 13 dB over baseline (Appendix 5.2). However, there was no visible peak present in the 3.2 kHz band associated with the SBP (although the signal was visible in the spectrogram of the event—Appendix 5.1, hydro 63, event

17). The activity of the survey vessel during the MA period was distinguishable on hydrophone 63 for roughly 5 hours and 45 minutes.

The weighted broadband levels on hydrophone 63 had some moderate fluctuations throughout the entire time series, with several larger fluctuations, in most cases, associated with the survey activity. In some cases, larger fluctuations were related to marine mammal clicks. The weighted *BL*s in the NA period were fairly stable in comparison to the other periods. During the VO period the weighted 3.2, 12.5, and 40 kHz bands were similarly distinguishable, with a few instances when the 40 kHz *BL*s were most dominant by no more than 10 dB over other *BL*s. In the VM period, the 3.2 and 12.5 kHz bands were generally most dominant, except during the events closely associated with the vessel and EM 122 activity (i.e., events 3, 4, 10, 11, and 12) when the 12.5 kHz *BL*s dominated. During the MA period, event 15 was particularly distinguishable, likely because it followed a sub-period on the hydrophone that was extremely quiet. Here the 12.5 kHz band increased by as much as 45 dB at its maximum over the local baseline. This event, which was distinguishable for 2 hours, was associated with the survey activity. Otherwise the weighted 3.2, 12.5, and 40 kHz bands were roughly similarly distinguishable during the MA period (Figure 5.3.6, *third plot*).

Hydro 70

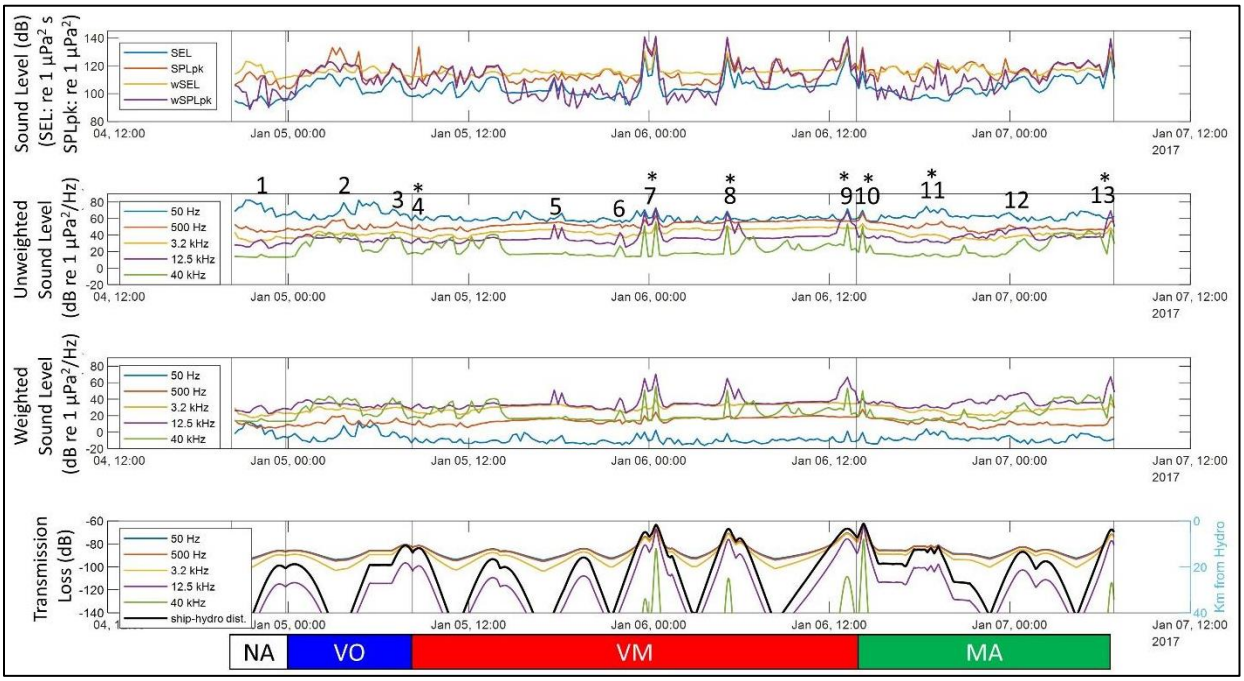

Figure 5.3.7. Sound level time series for hydrophone 70. *First plot*- Broadband sound level time series: *SEL* (blue), *SPLpk* (orange), *wSEL* (yellow), and *wSPLpk* (purple). Numbers indicate acoustic events identified in annotation. Asterisks indicate that the acoustic event was most likely attributed to the survey activity. Perpendicular lines on all graphs delineate the four analysis periods, NA, VO, VM, and MA, shown at the bottom of the figure, respectively. *Second plot*- Select unweighted BL time series: 50 Hz (blue), 500 Hz (orange), 3.2 kHz (yellow), 12.5 kHz (purple), and 40 kHz (green). *Third plot*- Weighted decidecade *BL* time series. Line colors and frequencies are the same as in the second plot. *Fourth plot*-Time series of modelled frequency-specific transmission loss (left axis) and range from hydrophone in kilometers (black line, right axis). Color of frequency-specific transmission loss corresponds to colors of frequencies described for the second plot.

It is worth noting that hydrophone 70 is on the eastern, and also shallower, side of the array close to San Clemente Island, a U.S. Navy base. During the NA period, there was a one hour-long epoch with elevated levels (9 dB above baseline) in the 12.5 kHz band (event 1, Figure 5.3.7). A close inspection of this revealed lots of whistles and signals from vocalizing marine mammals in the 10-15 kHz range (Appendix 5.1, hydro 70, event 1). Aside from the elevated 50 Hz band, the select *BL*s were relatively stable during this period. The VO period had fluctuating sound levels, except the 3.2, and 12.5 kHz band which were rather stable in comparison to the

other bands. A closer inspection of one point (event 2) that had elevated levels in both low frequency (50 and 500 Hz) and high frequency (40 kHz) *BL*s revealed a substantial amount of biological activity and a nearby vessel (Appendix 5.1, hydro 70, event 2). The *Sally Ride* was more than 40 km away at this time, so was unlikely to be the source. Near the end of this period, the *Sally Ride* came within 10.6 km from the hydrophone. However this was not obvious in the sound level time series or the spectrogram of the event (marine mammal clicks in the 40 kHz band were prominent) (Figure 5.3.7, event 3; Appendix 5.1, hydro 70, event 3).

The *Sally Ride* was within 12 km of hydrophone 70 when the EM 122 mapping survey began (event 4). There was a small peak (2 dB more than baseline) in the 12.5 kHz band related to the survey vessel's proximity to the hydrophone while the EM 122 was on and a large peak in *SPLpk* (29 dB more than baseline) at the same time. However, the peak in *SPLpk* was related to a loud signal present at the same time (i.e., broadband pulses 0.5s with energy mostly below 2 kHz—Appendix 5.1, hydro 70, event 4). The *Sally Ride* then remained more than 15 km away for the next 13.5 hours. During this time there were a few RCPAs to 16, 20, and 17 km of the hydrophone, none of which were readily distinguishable in the 12.5 kHz *BL* time series (Figure 5.3.7, *second plot*). The signals that caused the peaks in the 12.5 kHz band of event 5 (i.e., the pulse consisted of two 10 ms pulses, 200 ms apart, repeated every 0.5 s between 9-15 kHz; Appendix 5.1, hydro 70, event 5) and event 6 (i.e., continuous energy between 10-20 kHz; Appendix 5.1, hydro 70, event 6) were not the related to the survey vessel and EM 122, which was over 25 km away during both events. At this range, transmission loss in the 12.5 kHz band is greater than 140 dB (Figure 5.3.7, *fourth plot*). The peaks associated with these events were 19, 14, and 10 dB over baseline, respectively, in the 12.5 kHz band and were all 10 dB over baseline (Appendix 5.2) with respect to *SPLpk*. The signal from the *Sally Ride* and EM 122 became

discernible again in the sound level time series when the survey vessel was within 15.5 km. At this time, the *Sally Ride* made two RCPAs to 4.9 and 2 km within an hour of one another (event 7). The maximum level in the 12.5 kHz band at these RCPAs were 33 and 39 dB more than baseline (Appendix 5.2), respectively, while the *SPLpk* levels clipped. The *Sally Ride* transited across the array and back again before making two more RCPAs to 3.5 and 7.5 km of the hydrophone, again within an hour of one another (event 8). Preceding these events, the EM 122 signal was not visible in the time series until the vessel was within 15 km and was not visible again after the vessel was beyond 11 km from the hydrophone. A final RCPA was made to hydrophone 70 in the VM period to 3.5 km (event 9). At its maximum, the *SPLpk* clipped and the 12.5 kHz band was 35 dB over baseline (Appendix 5.2). Overall the activity of the survey vessel was distinguishable in the time series for 6.5 hours.

The EM 712 was first turned on in the MA period when the *Sally Ride* was less than 1.5 km away from hydrophone 70 (event 10). This manifested as a 50 dB re 1 μPa^2/Hz peak in the 40 kHz band, *SPLpk* of 131 dB re 1 µPa (at its maximum more than 29 dB over baseline), as well as smaller peaks in every other frequency band (Figure 5.3.7, event 10). The EM 712 was only visible (Appendix 5.1, hydro 70, event 10) in the time series for half an hour while the vessel was within 5 km of the hydrophone, beyond which transmission loss of the signal was more than 80 dB. After this, the calibration tests occurred while the vessel was 18 km and then 12 km away from hydrophone 70. Although the test signals were not readily distinguishable in the sound level time series or the spectrograms at either time, the presence of the *Sally Ride* stationary at 12 km during the second calibration test seemed correlated with slightly elevated levels in the 50 Hz, 500 Hz, and 3.2 kHz bands at the same time (Figure 5.3.7, event 11; Appendix 5.1, hydro 70, event 11). At one point during the MA period there was a slow but noticeable increase of up to

15 dB in the 12.5 kHz *BL* (event 12). This approximately 5-hour period appeared correlated with biological activity (Appendix 5.1, hydro 70, event 13). The *Sally Ride* made a final RCPA to 4 km at the end of the period when all of the acoustic sources were active (event 12). This manifested as peaks in the 500 Hz (56 dB re 1 μPa^2/Hz), 12.5 kHz (69 dB re 1 μPa^2/Hz, 35 dB over baseline), 40 kHz (46 dB re 1 μPa^2/Hz) bands, and *SPLpk*, which clipped (>138 dB re 1 µPa). All but the EM 712 signal were easily distinguishable in the spectrogram of the event (Appendix 5.1, hydro 70, event 12). The survey activity was distinguishable for approximately 3 hours and 45 minutes during the MA period.

From a weighted perspective, all periods had similar magnitude fluctuations in the broadband and *BL* metrics, except during the RCPA events under 5 km in the VM and MA period, which were much more dynamic (i.e., peaks up to 138 dB re 1 µPa versus around 120 dB re 1 µPa). The 12.5 kHz band was generally most dominant across the study period (Figure 5.3.7, *third plot*). However, during the VO period, the 40 kHz band alternated in dominance with the 12.5 kHz band, but generally they were within 5 dB of each other. This was also the case during the first half of the VM period and the last quarter of the MA period, when the survey vessel was not near the hydrophone and not likely contributing to this pattern. The 12.5 kHz band was particularly dominant during the closest passes of the survey vessel to the hydrophone (i.e., events 7, 8, 9, 10, and 13), but also with respect to some other signals—often biological-- that were not the EM 122 (i.e., events 5, 6, and 12). The acoustic events in the 40 kHz band were also most often attributed to biological activity.

Hydro 85

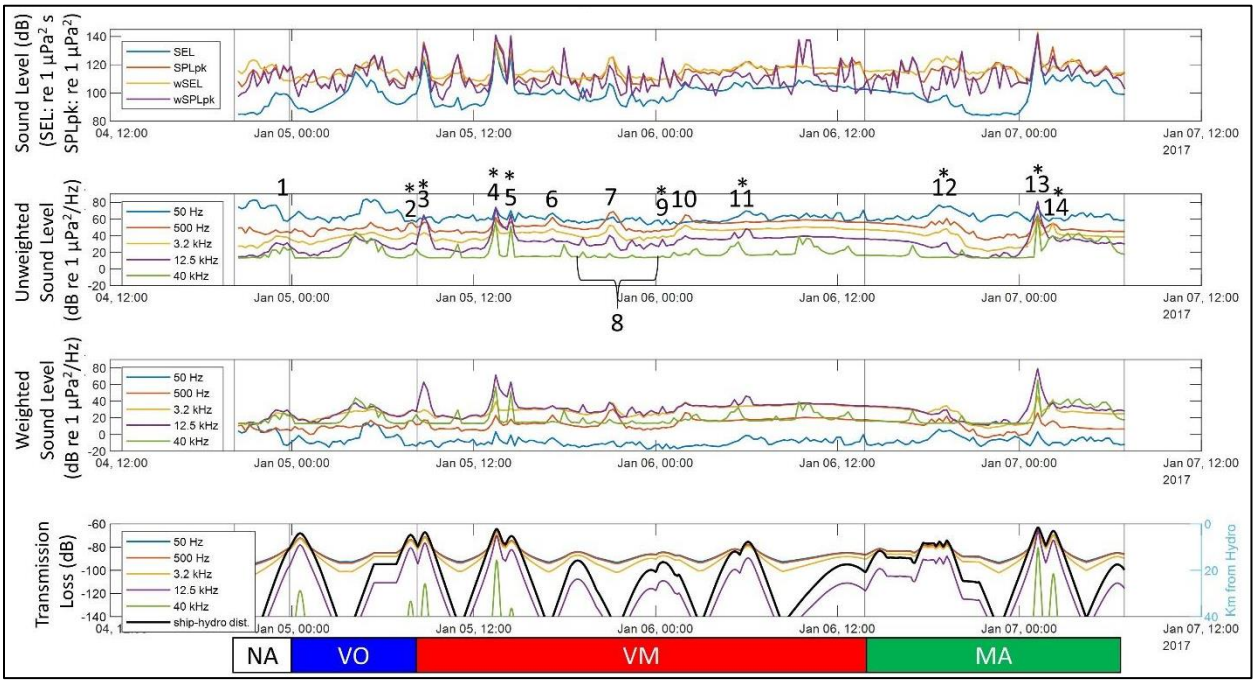

Figure 5.3.8. Sound level time series for hydrophone 85. *First plot*- Broadband sound level time series: *SEL* (blue), *SPLpk* (orange), *wSEL* (yellow), and *wSPLpk* (purple). Numbers indicate acoustic events identified in annotation. Asterisks indicate that the acoustic event was most likely attributed to the survey activity. Perpendicular lines on all graphs delineate the four analysis periods, NA, VO, VM, and MA, shown at the bottom of the figure, respectively. *Second plot*- Select unweighted BL time series: 50 Hz (blue), 500 Hz (orange), 3.2 kHz (yellow), 12.5 kHz (purple), and 40 kHz (green). *Third plot*- Weighted decidecade *BL* time series. Line colors and frequencies are the same as in the second plot. *Fourth plot*-Time series of modelled frequency-specific transmission loss (left axis) and range from hydrophone in kilometers (black line, right axis). Color of frequency-specific transmission loss corresponds to colors of frequencies described for the second plot.

During the second half of the NA period, all of the *BL*s increased (event 1, Figure 5.3.8). Although this seemed to correlate with the *Sally Ride*'s approach to hydrophone 85, the *BL*s began to increase while the vessel was more than 40 km away and decreased again when the vessel was actual at its closest point, suggesting there was another vessel that passed near hydrophone 85 associated with this event (Appendix 5.1, hydro 85, event 1). The first RCPA of the *Sally Ride* (4.2 km) was not distinguishable in the sound level time series. At the end of the VO period the *Sally Ride* was within 4.8 km of hydrophone 85, which was distinguishable in the

time series as elevated levels in the 500 Hz, 3.2 kHz, and 12.5 kHz bands between 5-10 dB above local baseline levels and about 13 dB above baseline (Appendix 5.2) for *SPLpk* (event 2). Prior to this RCPA, the sound levels began to increase when the vessel was about 12.5 km away.

Immediately following event 2, the EM 122 was turned on when the vessel was within 10 kilometers of hydrophone 85 as it made its next RCPA to 3.7 km (event 3). At maximum, the levels of this event were 32 dB and 30 dB over baseline in the 12.5 kHz bands and *SPLpk*, respectively (Appendix 5.2). The next two RCPAs were about an hour apart to 2.3 (event 4) and 5.3 km (event 5) away from the hydrophone. Prior to this event, the 12.5 kHz *BL* began to increase when the *Sally Ride* was 15 km from the hydrophone and flattened out again when the survey vessel was beyond 10 km. At maximum levels during both events, the *SPLpk* clipped at 34 dB over baseline, and the 12.5 kHz band peaked at 40 and 32 dB, respectively, over baseline (Appendix 5.2). There were several events (6, 7, and 10) during the VM period that appeared to be close approaches from a vessel, but since these events occurred when the *Sally Ride* was more than 30 km away they were unlikely related to the survey vessel. The presence of other vessel sound in the time series was not surprising since hydrophone 85 is on the western edge of the array. Amidst these close approaches of other vessels to the hydrophone, the *Sally Ride* did make two RCPAs to 15.7 and 20 km. While there were instances when the 12.5 kHz band level was elevated, they do not align with the RCPAs of the survey vessel (event 8). Closer inspection of these peaks in the 12.5 kHz band revealed high amplitude continuous energy between 10-20 kHz (Appendix 5.1, hydro 85, event 8). Given the more broadband nature of this continuous energy, and that transmission loss at these ranges was over 100 dB for the EM 122 signal, it seems unlikely that the survey activity was responsible for the small peaks in the 12.5 kHz *BL*s. However, the next RCPA of the *Sally Ride* to 16.4 km of the hydrophone correlated with the next

peak in the 12.5 kHz band (event 9; Appendix 5.1, hydro 85, event 9), which was 2 dB over baseline. Therefore, it seems likely that at ranges of 15-20 km the EM 122 signal contributes somewhat (i.e., only a few dB) to the elevated levels in the 12.5 kHz band. Two final RCPAs occurred in the VM period, one to 12.3 km and the other to 8 km within an hour of one another (event 11). These were visible as peaks in the 12.5 kHz band that were over baseline by 11 and 15 dB at their maximum, respectively. These events were visible in the time series when the vessel was within 13 km until it was again beyond 11 km away. The final RCPA in this period was not visible in the time series when the vessel was 17.4 km away. Overall the survey activity during the VM period was distinguishable for 5 hours and 45 minutes.

During the MA period there was no clear sign of the survey activities until the vessel was within 8 km of the hydrophone around the time of the second calibration event (event 12). Upon closer inspection of this event (Appendix 5.1, hydro 85, event 12), an undetermined pulsed signal in the same frequency band as the EM 122 was identified, although with a different temporal structure. According to the survey log, the EM 122 was not on at this time. In addition, the low frequency levels indicative of ship-radiated sound were louder than in instances when the vessel was much closer to the hydrophone (e.g., event 2), so it remains unclear whether this response in the sound levels was attributed to the survey activity or some other source. One explanation for the louder low frequency levels could be that the *Sally Ride* was trying to hold position, requiring dynamic positioning, which can be quite loud. The survey vessel made its closest RCPAs at 1.5 (event 13) and 3.3 km (event 14) within an hour of one another. During event 13, only the EM 122 was on, while during event 14, only the SBP was on. These two events had very different sound level signatures. During event 13, the peak in the 12.5 kHz band was 81 dB re 1 $\mu Pa^2/Hz$ (48 dB over baseline) and there were increases of 20 or more dB in the other *BL*s, while *SPLpk*

clipped. During event 14, the 3.2 kHz band was at most 55 dB re 1 µPa^2/Hz, with a similar magnitude peak in the 500 Hz band, and *SPLpk* at its maximum was 133 dB re 1 µPa. The final RCPA of the period at 17 km was not distinguishable in the time series. Overall the survey activity was clearly discernible for about 3 hours and 15 minutes in the MA period.

From a weighted perspective, the w*SPLpk* fluctuated randomly during the NA period, whereas the *wSEL* appeared correlated with the loud array-wide phenomenon during the period. During the VO period, w*SPLpk* fluctuated with the largest peaks correlated with the 40 kHz band, whereas the *wSEL* seemed to correlate with the loud array-wide low frequency phenomenon. As such, the 40 kHz band was the most dominant *BL* during the VO period, though only by a few dB with respect to the 12.5 and 3.2 kHz bands (Figure 5.3.8, *fourth plot*). During the VM period the fluctuations in w*SPLpk* that were beyond the variability seen in the NA and VO periods, all corresponded to the vessel and EM 122, except for the final peak in the period that corresponded to the 40 kHz band. Throughout the VM period the 12.5 kHz and 3.2 kHz band levels were most distinguishable, with the 40 kHz band intermittently more dominant. During the MA period, the w*SPLpk* fluctuated similarly to the VM period, with the largest fluctuations in the sound levels, attributed to the survey activity. The *wSEL* was most variable during the MA period, decreasing to NA period levels (i.e., quiet) before immediately increasing to its maximum during event 13 (i.e., the closest pass of the *Sally Ride* during this period). During the MA period the 3.2 kHz band was most dominant during event 12, the 12.5 kHz band during event 13, and the 40 kHz band for a period after event 13. These acoustic events seemed to be attributed to ship-radiated sound, the EM 122 and acoustically active marine mammals, respectively.

Appendix 5.4. Heat map tables of sound level metric percentile differences.

Each cell represents the specific percentile (grey row headings) difference by hydrophone (grey columns headings) between two analysis periods (white column headings): VO (Vessel Only), NA (No Activity), VM (Vessel and MBES), MA (Mixed Acoustics). Differences were identified in four classes: 1) < 3dB (white), 2) 3-10 dB (yellow), 3) 10-20 dB (orange), 4) >20 dB (red). Where differences were identified, the color (green/purple) of the value represents which analysis period was louder, corresponding with the color of the two specific analysis periods being compared.

By Hydrophone

VO v. NA				VM v. NA				MA v. NA			
	19	16	14		19	16	14		19	16	14
1	-5.3	-6.9	-7.3	1	-8.5	-8.7	-9.7	1	-8.8	-8.7	-9.7
5	-5.4	-6.6	-7.2	5	-8.7	-8.9	-9.6	5	-9.0	-8.9	-9.6
10	-5.4	-6.8	-7.1	10	-8.8	-9.2	-9.7	10	-9.1	-8.2	-8.6
25	-5.3	-6.8	-6.8	25	-9.3	-10.3	-10.1	25	-9.5	-9.0	-8.8
50	-4.7	-6.2	-5.8	50	-11.0	-13.0	-11.5	50	-10.7	-11.1	-9.7
75	-2.9	-6.6	-6.5	75	-13.8	-18.6	-16.2	75	-12.7	-15.3	-14.0
90	-1.7	-4.5	-5.6	90	-16.4	-21.2	-19.1	90	-13.9	-16.6	-16.7
95	-0.8	-3	-4	95	-17	-22	-20	95	-14	-16	-17
99	1.4	-0.8	-2.2	99	-17.5	-20.8	-19.9	99	-12.1	-15.0	-17.4
	57	45	22		57	45	22		57	45	22
1	-3.7	-6.9	-7.8	1	-7.2	-9.4	-10.8	1	-6.1	-8.7	-10.1
5	-4.1	-6.9	-7.9	5	-7.5	-9.4	-11.0	5	-6.5	-8.7	-10.1
10	-4.4	-7.0	-7.8	10	-7.8	-9.6	-11.2	10	-6.8	-8.9	-10.3
25	-5.1	-7.2	-7.7	25	-9.3	-10.5	-11.7	25	-8.0	-9.6	-10.7
50	-6.1	-7.4	-7.1	50	-12.1	-12.8	-13.3	50	-10.3	-11.2	-11.9
75	-5	-7	-6	75	-14	-17	-17	75	-11	-14	-15
90	-2.9	-4.4	-4.6	90	-14.7	-19.3	-18.7	90	-11.9	-15.5	-16.2
95	-1.4	-2.3	-3.2	95	-15.1	-19.8	-18.9	95	-12.1	-15.7	-16.4
99	0.0	-0.7	-1.2	99	-14.9	-19.8	-18.2	99	-12.1	-15.7	-15.8
	85	63	70		85	63	70		85	63	70
1	-3.6	-5.4	-3.9	1	-6.0	-9.0	-8.6	1	-4.7	-8.7	-7.3
5	-3.9	-5.3	-4.1	5	-6.4	-8.9	-8.8	5	-4.9	-8.7	-7.5
10	-4.3	-5.6	-4.0	10	-6.8	-9.2	-9.0	10	-5.3	-8.2	-7.5
25	-6.3	-5.7	-4.3	25	-9.1	-10.1	-9.8	25	-7.4	-8.9	-8.2
50	-9.3	-6.3	-5.3	50	-12.9	-12.6	-11.8	50	-10.6	-11.0	-9.8
75	-8.3	-6.2	-5.8	75	-14.0	-16.0	-14.6	75	-10.9	-13.7	-11.7
90	-4.4	-4.5	-4.5	90	-14.8	-18.0	-16.2	90	-10.1	-14.9	-12.2
95	-2.3	-3.0	-3.6	95	-15.2	-18.7	-16.5	95	-9.2	-15.1	-11.9
99	-0.3	-1.8	-2.7	99	-15.0	-18.8	-15.5	99	-7.9	-13.1	-10.1

VM v. VO				MA v. VO				MA v. VM			
	19	16	14		19	16	14		19	16	14
1	-3.2	-1.9	-2.4	1	-3.4	-0.9	-1.5	1	-0.3	-0.9	-1.5
5	-3.3	-2.3	-2.4	5	-3.6	-1.3	-1.4	5	-0.3	-1.3	-1.4
10	-3.4	-2.5	-2.7	10	-3.7	-1.4	-1.5	10	-0.3	1.0	1.2
25	-4.0	-3.5	-3.3	25	-4.2	-2.3	-1.9	25	-0.1	1.3	1.4
50	-6.3	-6.9	-5.7	50	-6.0	-4.9	-3.9	50	0.3	2.0	1.8
75	-10.9	-12.0	-9.8	75	-9.8	-8.7	-7.6	75	1.1	3.3	2.2
90	-14.7	-16.6	-13.5	90	-12.2	-12.0	-11.1	90	2.5	4.6	2.4
95	-17	-18	-16	95	-13	-13	-13	95	4	5	2
99	-18.9	-20.0	-17.7	99	-13.6	-14.2	-15.1	99	5.4	5.8	2.6
	57	45	22		57	45	22		57	45	22
1	-3.4	-2.5	-3.0	1	-2.4	-1.8	-2.3	1	1.0	0.7	0.7
5	-3.4	-2.5	-3.1	5	-2.4	-1.8	-2.2	5	1.0	0.7	0.9
10	-3.4	-2.6	-3.4	10	-2.4	-2.0	-2.5	10	1.0	0.7	0.9
25	-4.2	-3.4	-4.0	25	-2.9	-2.4	-3.0	25	1.3	0.9	1.0
50	-6.0	-5.4	-6.2	50	-4.2	-3.8	-4.8	50	1.8	1.6	1.4
75	-9	-10	-10	75	-6	-7	-9	75	2	3	2
90	-11.8	-14.9	-14.1	90	-9.0	-11.1	-11.7	90	2.9	3.8	2.4
95	-13.7	-17.5	-15.7	95	-10.7	-13.4	-13.1	95	3.0	4.1	2.5
99	-14.9	-19.1	-17.0	99	-12.1	-15.1	-14.7	99	2.8	4.0	2.3
	85	63	70		85	63	70		85	63	70
1	-2.5	-3.5	-4.8	1	-1.1	-2.4	-3.4	1	1.4	1.1	1.4
5	-2.5	-3.5	-4.8	5	-1.0	-2.6	-3.4	5	1.5	1.0	1.3
10	-2.5	-3.7	-5.0	10	-0.9	-2.7	-3.6	10	1.5	1.0	1.4
25	-2.8	-4.3	-5.4	25	-1.0	-3.1	-3.8	25	1.7	1.2	1.6
50	-3.5	-6.3	-6.6	50	-1.3	-4.8	-4.5	50	2.2	1.6	2.0
75	-5.7	-9.8	-8.7	75	-2.6	-7.6	-5.9	75	3.1	2.2	2.8
90	-10.4	-13.5	-11.7	90	-5.7	-10.4	-7.7	90	4.7	3.0	4.0
95	-12.9	-15.7	-12.9	95	-6.9	-12.1	-8.3	95	6.0	3.6	4.6
99	-14.7	-17.0	-12.7	99	-7.6	-11.4	-7.3	99	7.0	5.7	5.4

Figure 5.4.1. Sound level percentile differences (dB) for the 50 Hz *BL* across analysis periods.

VO v. NA				VM v. NA				MA v. NA			
	19	16	14		19	16	14		19	16	14
1	0.0	0.0	-0.2	1	0.2	0.2	0.4	1	-0.1	0.2	0.4
5	0.0	0.1	-0.2	5	0.2	0.3	0.6	5	-0.1	0.3	0.6
10	0.1	0.1	-0.1	10	0.3	0.3	0.7	10	0.0	0.0	-0.3
25	0.4	0.1	0.0	25	0.4	0.5	0.9	25	0.1	0.0	-0.3
50	3.2	0.5	2.6	50	1.6	1.0	2.1	50	1.1	0.2	0.1
75	11.5	5.5	7.9	75	2.3	1.5	2.5	75	5.4	8.1	7.1
90	15.8	13.4	11.8	90	1.2	3.4	4.7	90	15.5	15.1	15.8
95	16.6	15	14	95	1	6	7	95	18	17	19
99	17.1	17.8	16.2	99	4.0	11.3	10.0	99	18.9	18.0	20.1
	57	45	22		57	45	22		57	45	22
1	0.1	0.0	-0.5	1	0.2	0.2	0.4	1	0.0	0.0	-0.7
5	0.1	0.0	-0.5	5	0.3	0.3	0.6	5	0.0	0.1	-0.8
10	0.1	0.0	-0.5	10	0.4	0.3	0.7	10	0.0	0.1	-0.8
25	0.3	0.0	-0.2	25	0.9	0.5	1.1	25	0.1	0.1	-0.7
50	1.4	0.1	1.1	50	3.4	1.5	2.3	50	1.1	0.2	-0.6
75	5	0	3	75	7	2	6	75	6	1	0
90	9.1	1.7	6.3	90	14.0	4.3	15.5	90	14.8	1.0	2.4
95	11.2	2.8	9.7	95	16.4	8.8	17.9	95	18.6	2.4	7.3
99	7.7	5.6	9.6	99	12.9	17.3	17.7	99	18.8	5.8	11.6
	85	63	70		85	63	70		85	63	70
1	0.0	0.2	0.3	1	0.2	0.2	0.8	1	0.0	0.0	0.3
5	0.0	0.2	1.8	5	0.2	0.2	1.2	5	0.0	0.1	0.5
10	-0.1	0.3	2.9	10	0.3	0.3	1.5	10	0.0	0.1	0.7
25	-0.1	1.2	6.5	25	0.4	1.2	3.2	25	0.2	0.2	1.5
50	-0.3	12.2	16.4	50	1.2	2.6	4.5	50	1.1	1.0	4.5
75	5.8	19.9	23.4	75	-0.2	5.7	9.7	75	9.5	3.9	16.2
90	14.1	23.5	26.1	90	1.0	13.6	15.4	90	15.3	19.2	24.8
95	16.0	25.1	26.8	95	3.9	18.0	19.4	95	15.7	21.5	26.7
99	14.6	27.0	26.2	99	4.2	21.4	22.1	99	14.5	23.7	27.1

VM v. VO				MA v. VO				MA v. VM			
	19	16	14		19	16	14		19	16	14
1	0.2	0.2	0.6	1	-0.1	-0.1	-0.2	1	-0.2	-0.1	-0.2
5	0.2	0.2	0.8	5	-0.1	-0.1	-0.2	5	-0.3	-0.1	-0.2
10	0.2	0.3	0.8	10	-0.1	-0.1	-0.2	10	-0.3	-0.3	-1.0
25	0.0	0.3	1.0	25	-0.3	-0.1	-0.3	25	-0.3	-0.4	-1.2
50	-1.5	0.4	-0.6	50	-2.1	-0.3	-2.6	50	-0.5	-0.8	-2.0
75	-9.2	-3.9	-5.5	75	-6.1	2.7	-0.8	75	3.2	6.6	4.6
90	-14.6	-9.9	-7.1	90	-0.3	1.7	4.0	90	14.3	11.7	11.1
95	-16	-9	-7	95	1	1	5	95	17	11	12
99	-13.1	-6.5	-6.2	99	1.8	0.2	3.8	99	14.9	6.7	10.1
	57	45	22		57	45	22		57	45	22
1	0.1	0.2	0.9	1	-0.1	0.0	-0.2	1	-0.2	-0.2	-1.1
5	0.2	0.2	1.1	5	-0.1	0.0	-0.2	5	-0.3	-0.2	-1.4
10	0.3	0.3	1.2	10	-0.1	0.0	-0.3	10	-0.4	-0.3	-1.5
25	0.6	0.5	1.3	25	-0.2	0.0	-0.5	25	-0.7	-0.4	-1.8
50	2.0	1.4	1.2	50	-0.4	0.2	-1.7	50	-2.4	-1.2	-2.9
75	2	2	3	75	1	0	-3	75	-1	-1	-6
90	4.9	2.7	9.1	90	5.7	-0.7	-3.9	90	0.8	-3.3	-13.1
95	5.2	5.9	8.2	95	7.4	-0.4	-2.4	95	2.2	-6.3	-10.6
99	5.2	11.7	8.0	99	11.1	0.2	2.0	99	6.0	-11.5	-6.1
	85	63	70		85	63	70		85	63	70
1	0.2	0.0	0.5	1	0.0	-0.1	-0.1	1	-0.2	-0.2	-0.5
5	0.3	0.0	-0.6	5	0.0	-0.2	-1.3	5	-0.2	-0.2	-0.7
10	0.3	0.0	-1.3	10	0.1	-0.2	-2.2	10	-0.2	-0.3	-0.8
25	0.5	0.0	-3.3	25	0.3	-1.0	-4.9	25	-0.3	-1.0	-1.7
50	1.5	-9.7	-11.9	50	1.4	-11.2	-11.9	50	-0.1	-1.5	0.0
75	-6.0	-14.2	-13.8	75	3.7	-15.9	-7.2	75	9.7	-1.7	6.6
90	-13.0	-9.9	-10.7	90	1.2	-4.3	-1.3	90	14.2	5.5	9.5
95	-12.1	-7.0	-7.5	95	-0.3	-3.5	-0.1	95	11.8	3.5	7.3
99	-10.4	-5.6	-4.0	99	-0.1	-3.3	0.9	99	10.3	2.3	5.0

Figure 5.4.2. Sound level percentile differences (dB) for the 40 kHz *BL* across analysis periods.

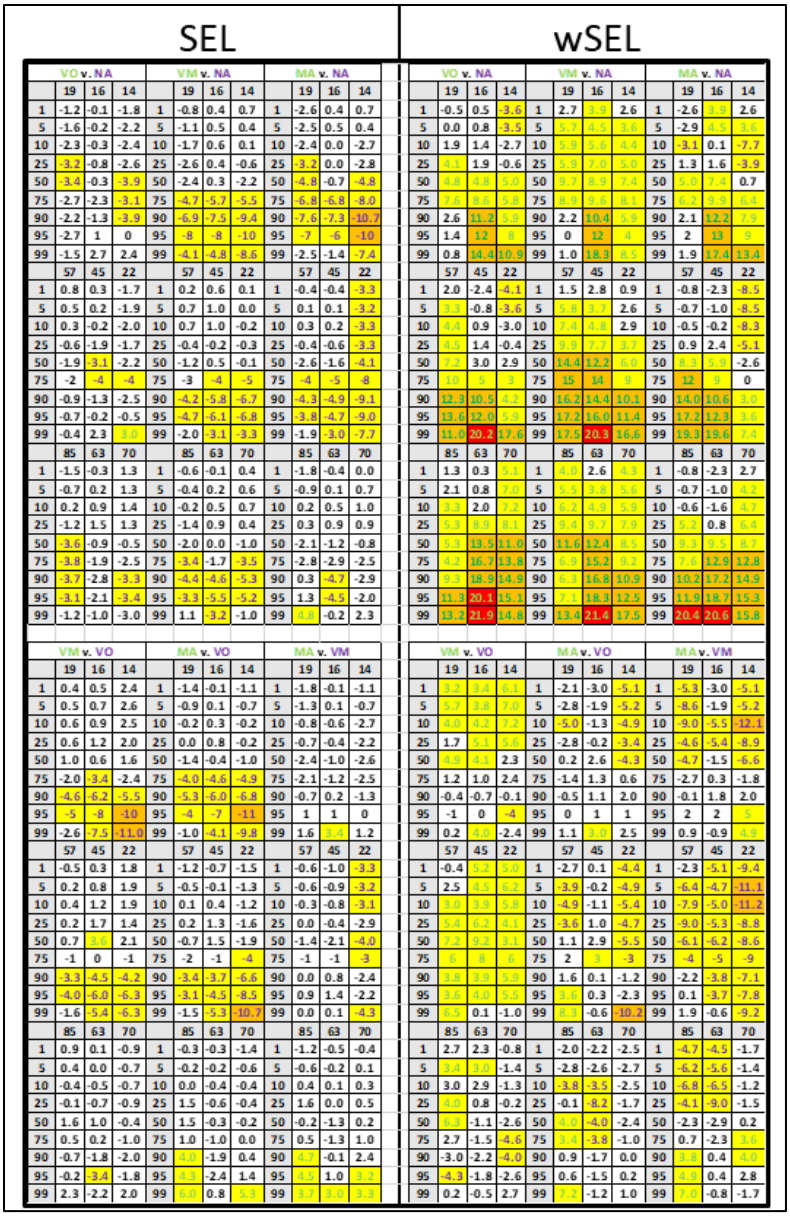

Figure 5.4.3. Sound level percentile differences (dB) for *SEL* (left) and *wSEL* (right) across analysis periods.

Array-wide

Percentiles	VO v NA	VM v NA	MA v NA	VM v VO	MA v VO	MA v VM
1	-5.4	-8.4	-7.5	-3.0	-2.1	0.9
5	-5.4	-8.6	-7.7	-3.1	-2.2	0.9
10	-5.6	-8.9	-7.9	-3.3	-2.3	1.0
25	-6.0	-10.0	-8.8	-4.0	-2.8	1.3
50	-6.5	-12.2	-10.5	-5.7	-4.0	1.7
75	-6.0	-14.9	-12.4	-8.9	-6.4	2.5
90	-4.2	-16.8	-13.6	-12.5	-9.3	3.2
95	-3.0	-17.4	-13.8	-14.4	-10.8	3.6
99	-1.0	-17.3	-13.1	-16.3	-12.1	4.1

Figure 5.4.5. Array-wide sound level percentile comparison for the 50 Hz *BL*.

Percentiles	VO v NA	VM v NA	MA v NA	VM v VO	MA v VO	MA v VM
1	0.2	0.4	0.1	0.2	-0.1	-0.3
5	0.4	0.7	0.2	0.3	-0.3	-0.6
10	0.6	0.9	0.3	0.3	-0.3	-0.6
25	0.6	1.2	0.2	0.6	-0.3	-1.0
50	2.2	2.2	0.4	0.0	-1.7	-1.8
75	10.3	4.4	3.3	-5.9	-7.0	-1.1
90	16.8	9.8	13.9	-7.0	-2.9	4.1
95	18.1	12.4	16.5	-5.7	-1.6	4.1
99	12.4	8.7	12.0	-3.7	-0.4	3.3

Figure 5.4.6. Array-wide sound level percentile comparison for the 40 kHz *BL*.

SEL						
Percentiles	VO v NA	VM v NA	MA v NA	VM v VO	MA v VO	MA v VM
1	-0.2	0.2	-0.9	0.4	-0.7	-1.1
5	-0.4	0.0	-0.9	0.4	-0.4	-0.9
10	-0.6	0.0	-1.0	0.5	-0.4	-1.0
25	-1.0	-0.3	-1.4	0.7	-0.4	-1.1
50	-2.0	-1.5	-2.6	0.5	-0.6	-1.1
75	-2.7	-3.0	-4.4	-0.4	-1.7	-1.4
90	-2.5	-5.2	-5.3	-2.7	-2.8	-0.1
95	-2.1	-6.1	-5.0	-4.0	-3.0	1.0
99	-0.1	-4.0	-2.7	-3.9	-2.6	1.3

wSEL						
Percentiles	VO v NA	VM v NA	MA v NA	VM v VO	MA v VO	MA v VM
1	0.9	4.3	-0.7	3.5	-1.6	-5.0
5	2.1	6.1	-0.6	4.0	-2.8	-6.8
10	2.9	7.1	-0.5	4.2	-3.4	-7.6
25	4.7	8.9	1.5	4.3	-3.1	-7.4
50	6.0	9.1	4.2	3.1	-1.9	-5.0
75	7.3	9.4	6.2	2.1	-1.2	-3.2
90	8.6	7.9	7.5	-0.8	-1.1	-0.4
95	7.6	6.3	7.1	-1.3	-0.5	0.8
99	3.9	4.8	5.0	0.8	1.1	0.2

Figure 5.4.7. Array-wide sound level percentile comparison for *SEL* (left) and *wSEL* (right).

Appendix 5.5. Results of the probability distribution comparisons between each pair of analysis periods, presented by hydrophone.

Columns of table from left to right are: hydrophone number, analysis periods compared, p-value of the statistical comparison test, 2-Wasserstein Distance, location term, size term, and shape term as a percentage.

Hydro	Comparison	P-value	W^2	Location (%)	Size (%)	Shape (%)
14	NA vs. VO	0.6569	0.0069	4.26	1.66	94.08
	NA vs. VM	0.3067	0.03458	12.13	1.15	86.72
	NA vs. MA	0.4551	0.01107	1.78	26.72	71.51
	VO vs. VM	0.4552	0.01488	15.19	6.33	78.48
	VO vs. MA	0.5586	0.00654	14.93	29.21	55.86
	VM vs. MA	0.1592	0.03172	19.58	17.45	62.97
16	NA vs. VO	0.4538	0.01142	15.12	2.01	82.88
	NA vs. VM	0.0842	0.0524	17.79	4.73	77.48
	NA vs. MA	0.2762	0.01785	17.45	0.25	82.3
	VO vs. VM	0.3529	0.016	18.91	7.51	73.58
	VO vs. MA	0.8803	0.0018	11.26	3.93	84.81
	VM vs. MA	0.4424	0.0102	16.24	18.16	65.59
19	NA vs. VO	0.6761	0.00469	7.06	2.78	90.16
	NA vs. VM	0.1519	0.0359	17.68	5.4	76.92
	NA vs. MA	0.5473	0.00675	0.44	2.2	97.36
	VO vs. VM	0.311	0.01987	19.06	5.36	75.58
	VO vs. MA	0.862	0.00206	7.88	27.03	65.09
	VM vs. MA	0.2513	0.02236	24.7	14.17	61.12
22	NA vs. VO	0.7471	0.00491	1.19	5.97	92.84
	NA vs. VM	0.3316	0.03093	13.6	0.45	85.95
	NA vs. MA	0.2909	0.02308	10.34	20.18	69.58
	VO vs. VM	0.3082	0.0168	19.01	15.55	65.44
	VO vs. MA	0.3082	0.0168	19.01	15.55	65.44
	VM vs. MA	0.0512	0.05549	23.33	11.58	65.09
45	NA vs. VO	0.53	0.00835	8.79	2.04	89.16
	NA vs. VM	0.0328	0.07727	19.77	3.63	76.6
	NA vs. MA	0.254	0.02112	17.82	0.14	82.03
	VO vs. VM	0.0803	0.04077	22.84	10.69	66.47
	VO vs. MA	0.618	0.00459	25.55	7.54	66.91
	VM vs. MA	0.2541	0.01893	20.45	11.87	67.68
57	NA vs. VO	0.209	0.02724	15.83	4.01	80.17

	NA vs. VM	0.0063	0.10444	21.82	6.36	71.82
	NA vs. MA	0.172	0.02484	14.49	1.19	84.32
	VO vs. VM	0.1447	0.03453	21.06	6.8	72.14
	VO vs. MA	0.9165	0.00143	2.22	17.42	80.36
	VM vs. MA	0.1185	0.03298	25.08	12.54	62.38
63	NA vs. VO	0.0711	0.0529	15.62	3.32	81.06
	NA vs. VM	0.0079	0.0974	22.04	4.58	73.37
	NA vs. MA	0.0613	0.04046	16.77	0.25	82.98
	VO vs. VM	0.3863	0.01492	20.72	4.16	75.13
	VO vs. MA	0.6764	0.00379	1.92	26.92	71.16
	VM vs. MA	0.2838	0.01591	25.87	20.33	53.8
70	NA vs. VO	0.3288	0.02775	12.87	3.19	83.94
	NA vs. VM	0.2233	0.0385	16.58	2.16	81.26
	NA vs. MA	0.1961	0.03502	19.11	1.21	79.68
	VO vs. VM	0.8565	0.00264	15.26	0.04	84.7
	VO vs. MA	0.7783	0.00356	13.61	2.37	84.02
	VM vs. MA	0.9502	0.00119	0.31	5.64	94.05
85	NA vs. VO	0.4567	0.00852	21.66	8.94	69.4
	NA vs. VM	0.0373	0.0552	24.93	9.56	65.52
	NA vs. MA	0.2108	0.01737	23.41	2.77	73.82
	VO vs. VM	0.2141	0.02279	24.23	8.89	66.88
	VO vs. MA	0.7156	0.00356	12.15	0.9	86.95
	VM vs. MA	0.3882	0.01276	22.44	20.12	57.44

Appendix 5.6. 24-h cumulative sound exposure levels (dB re 1 µPa^{2}s) by hydrophone and analysis period.

NA=No Activity, VO=Vessel Only, VM=Vessel and MBES, MA=Mixed Acoustics. Also included are the average, minimum and maximum per period. Weighted levels imply the mid-frequency cetacean weighting function (NMFS 2018) was applied in the calculation.

	Unweighted					Weighted			
hydro ID	**NA**	**VO**	**VM**	**MA**		**NA**	**VO**	**VM**	**MA**
1	145.4	144.0	141.6	136.6		120.1	127.3	136.2	121.0
2	141.5	143.7	138.2	134.3		116.9	123.6	132.8	125.5
3	146.1	146.9	142.6	146.7		120.5	126.5	134.8	144.2
4	146.4	147.9	143.3	139.7		118.6	126.7	139.2	133.5
5	146.5	147.3	143.2	141.1		118.7	125.8	138.6	130.5
6	145.8	150.5	143.1	146.5		118.9	129.0	138.6	143.3
7	141.6	142.6	138.6	138.3		115.1	122.3	133.7	124.7
8	146.4	145.9	141.4	141.2		122.5	127.7	134.6	128.2
9	143.5	142.1	142.2	140.3		122.1	126.7	136.8	126.2
10	143.5	141.9	141.3	139.3		121.7	124.7	131.7	126.7
11	144.3	141.5	143.1	136.1		119.9	128.7	139.6	119.6
12	145.2	142.2	143.9	137.3		119.5	129.3	139.9	124.3
13	140.9	139.5	139.7	137.2		115.3	121.9	135.5	132.3
14	146.8	145.9	142.0	145.6		120.7	127.0	135.9	143.0
15	146.3	146.9	143.4	140.2		119.1	124.9	138.9	131.9
16	141.5	141.3	140.1	139.5		112.7	122.0	135.8	132.3
17	145.5	144.0	141.7	143.0		115.9	123.3	135.1	128.2
18	140.2	139.6	138.4	139.3		113.7	121.1	132.8	122.0
19	144.8	142.3	142.9	139.9		122.0	125.5	137.9	124.9
20	143.7	141.1	141.4	138.5		122.9	126.2	132.0	124.7
21	144.0	141.4	143.1	136.8		122.0	127.1	139.5	119.4
22	144.6	143.7	144.6	137.0		120.7	128.8	141.3	122.9
23	141.9	138.3	142.3	135.0		114.6	120.4	139.3	124.5
24	144.4	141.8	143.6	146.5		117.6	124.0	139.4	144.1
25	145.0	142.8	142.6	147.5		119.0	122.3	138.0	145.1
26	141.0	139.3	142.1	141.8		114.4	117.0	139.2	138.8
27	144.4	143.7	143.2	141.2		114.5	122.6	138.3	129.9
28	143.3	142.5	140.8	141.8		115.8	123.5	133.3	123.9
29	139.1	138.1	139.5	137.9		113.3	118.6	134.7	117.9
30	144.7	141.9	144.4	139.5		122.3	126.3	140.8	123.8

31	144.3	140.9	141.6	136.6		130.2	123.5	136.2	119.7
32	144.9	141.4	145.5	138.5		124.3	127.9	142.7	128.0
33	144.6	141.5	146.4	145.8		117.4	127.5	143.8	143.2
34	143.8	143.6	145.2	148.9		115.0	127.7	142.0	146.9
35	144.1	142.3	143.7	145.2		114.8	120.6	139.9	142.2
36	138.9	137.7	137.7	140.4		110.0	121.5	132.4	136.9
37	142.1	142.1	141.3	139.5		113.0	127.2	135.7	123.0
38	143.1	142.5	142.3	142.3		116.4	125.5	137.1	120.5
39	143.2	142.6	142.9	141.3		119.0	126.8	137.9	126.7
40	144.8	142.2	140.6	139.9		124.6	127.0	132.4	122.4
41	139.8	136.3	137.6	135.6		125.5	123.1	131.9	128.2
42	143.7	141.0	145.0	146.7		125.0	129.7	141.9	144.2
43	142.3	139.6	142.8	140.9		115.5	126.1	138.0	131.4
44	142.9	140.1	142.1	140.2		113.0	121.2	137.5	131.3
45	142.9	142.0	143.8	140.5		113.0	124.3	140.6	133.4
46	139.1	138.4	140.7	137.3		110.1	124.3	137.2	122.0
47	142.7	142.8	142.2	140.5		113.2	130.6	137.0	125.5
48	142.7	142.5	142.6	140.1		116.9	128.7	138.0	125.8
49	143.1	142.9	140.8	138.8		122.0	125.7	133.3	125.9
50	146.5	141.0	143.8	138.2		141.3	127.5	140.2	126.0
51	140.4	137.3	142.9	143.9		124.0	124.8	140.0	141.2
52	142.0	139.6	141.3	140.3		117.5	129.4	134.9	129.8
53	142.2	140.9	141.1	141.4		114.1	128.5	134.0	130.1
54	142.5	140.8	143.5	149.5		113.7	120.5	139.9	147.2
55	138.3	136.9	139.6	138.7		110.4	118.4	135.5	127.6
56	141.9	142.6	143.0	140.1		112.4	129.1	139.1	125.6
57	142.1	141.2	143.7	139.0		116.1	123.7	140.5	127.6
58	136.3	137.0	138.0	134.6		111.5	118.1	132.9	123.7
59	142.7	139.3	142.2	141.8		134.1	131.0	138.2	138.3
60	142.3	139.0	145.3	147.8		116.5	129.7	142.6	145.5
61	138.2	135.7	136.8	137.8		114.2	127.7	130.7	128.2
62	142.6	140.3	141.1	141.3		113.7	131.8	134.7	130.5
63	142.6	140.8	143.4	141.0		113.3	130.9	139.7	131.3
64	138.1	136.4	136.7	145.8		110.8	121.4	128.7	143.2
65	142.0	140.1	141.6	144.3		113.0	124.2	136.4	139.4
66	142.0	140.1	140.7	140.2		116.9	124.3	134.6	127.7
67	141.4	140.7	142.3	138.6		118.2	126.5	138.5	121.8
68	141.5	143.1	139.7	138.0		114.3	128.8	130.3	125.2
69	142.9	140.2	145.0	150.2		126.7	129.6	142.0	148.0

70	143.0	140.9	144.1	143.3		119.6	132.7	140.6	136.3
71	143.5	141.2	144.3	141.7		115.3	133.1	140.6	130.1
72	142.5	140.6	143.3	141.2		115.1	131.8	139.2	129.9
73	140.6	140.6	143.8	140.8		116.9	129.6	138.9	132.5
74	138.9	136.4	139.6	146.0		117.6	122.9	134.7	143.3
75	142.5	140.0	141.0	141.6		118.7	125.0	134.0	133.7
76	141.5	139.7	140.9	139.5		124.8	128.0	134.7	127.2
77	137.0	136.2	135.9	134.8		117.5	126.7	126.2	119.7
78	141.4	139.9	141.0	139.1		123.2	130.4	130.7	124.8
79	140.3	139.5	145.4	142.5		125.4	131.1	142.8	137.9
80	138.6	136.3	153.3	136.9		119.8	128.3	151.5	128.3
81	142.2	140.0	143.1	140.1		119.4	132.0	139.2	131.0
82	138.3	136.8	139.1	136.5		118.1	129.4	134.8	124.2
83	142.0	142.0	141.2	142.0		119.3	136.4	133.2	129.5
84	143.2	141.9	142.0	143.7		113.2	137.0	136.5	135.0
85	143.2	140.2	144.0	150.4		119.7	129.1	139.4	148.0
86	142.7	139.7	142.4	141.6		125.3	127.0	136.0	132.6
87	141.2	139.0	139.7	139.1		127.3	127.8	131.9	128.3
88	143.5	139.8	143.7	142.4		125.2	128.2	139.5	133.9
89	139.0	135.8	140.8	147.3		112.2	125.1	137.6	145.1
avg	**142.5**	**141.0**	**142.1**	**141.0**		**118.4**	**126.4**	**137.0**	**131.1**
min	**136.3**	**135.7**	**135.9**	**134.3**		**110.0**	**117.0**	**126.2**	**117.9**
max	**146.8**	**150.5**	**153.3**	**150.4**		**141.3**	**137.0**	**151.5**	**148.0**

Appendix 5.7. Frequency correlation analysis spectrograms and spectral probability density plots.

No Activity	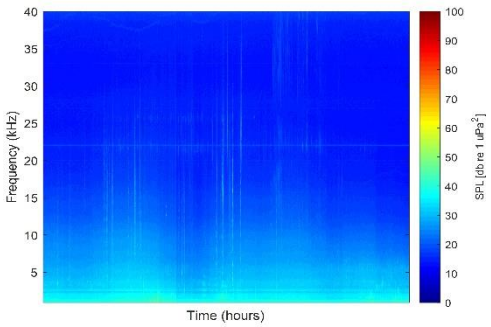
Vessel Only	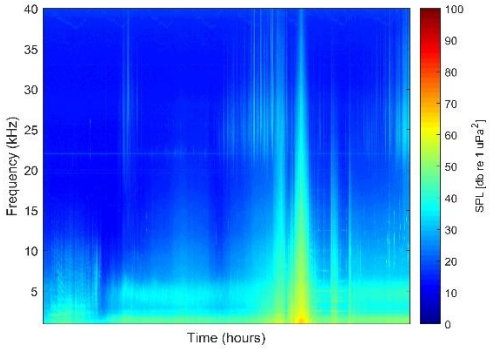
Vessel and MBES	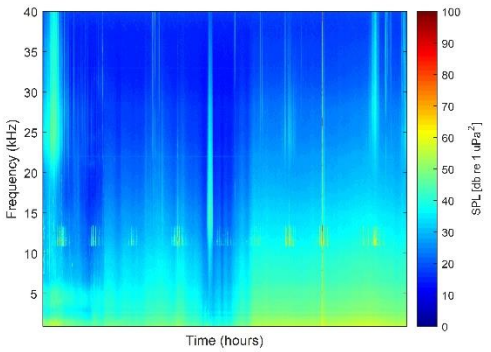
Mixed Acoustics	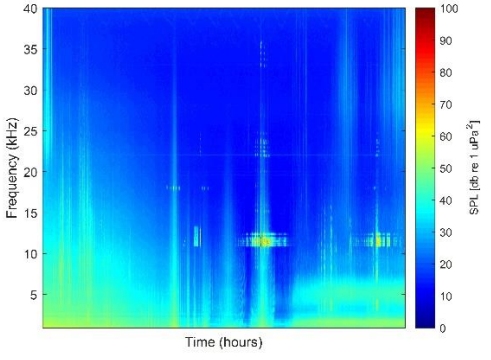

Spectral probability density plots associated with the frequency correlation analysis.

No Activity	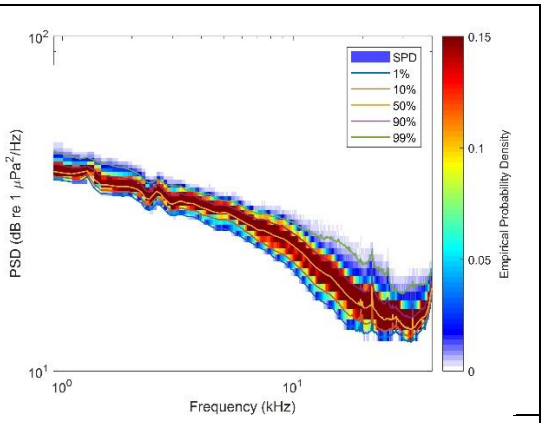
Vessel Only	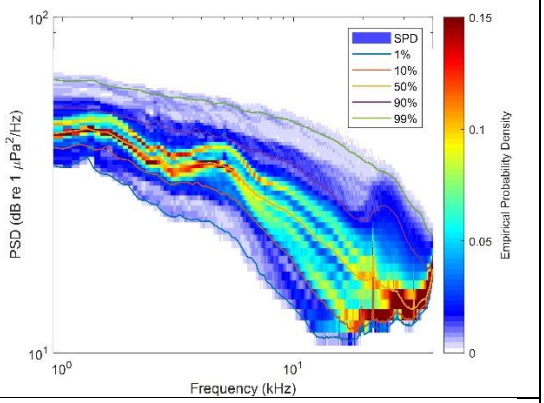
Vessel and MBES	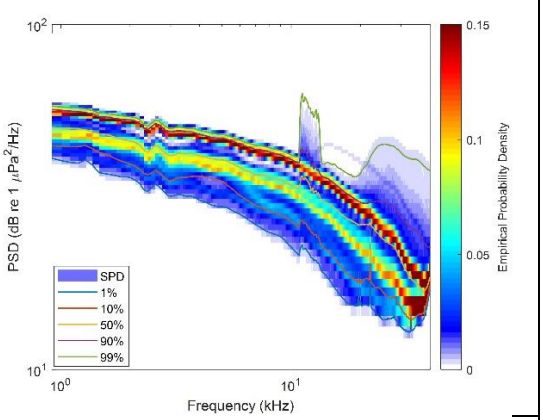
Mixed Acoustics